IDAHO TRANSPORTATION DEPARTMENT

RESEARCH REPORT

Simplified Analysis Methods of TSD and FWD Data for Effective Asphalt Pavement Preservation Program

RP 294

By

Emad Kassem
Ahmed Muftah
Abu Sufian
Natalie Mikels
University of Idaho

Prepared for

Idaho Transportation Department

ITD Research Program, Contracting Services

Highways Construction and Operations

June 2023

Disclaimer

This document is disseminated under the sponsorship of the Idaho Transportation Department and the United States Department of Transportation in the interest of information exchange. The State of Idaho and the United States Government assume no liability of its contents or use thereof.

The contents of this report reflect the view of the authors, who are responsible for the facts and accuracy of the data presented herein. The contents do not necessarily reflect the official policies of the Idaho Transportation Department or the United States Department of Transportation.

The State of Idaho and the United States Government do not endorse products or manufacturers. Trademarks or manufacturers' names appear herein only because they are considered essential to the object of this document.

This report does not constitute a standard, specification or regulation.

Technical Report Documentation Page

1. Report No. FHWA-ID-23-294	2. Government Accession No.	3. Recipient's Catalog No.
4. Title and Subtitle Simplified Analysis Methods of TSD and FWD Data for Effective Pavement Preservation Program		5. Report Date June 2023 6. Performing Organization Code
7. Author(s) Emad Kassem, https://orcid.org/0000-0002-4331-6692 Ahmed Muftah, Abu Sufian, Natalie Mikels		8. Performing Organization Report No. [Billing code]
9. Performing Organization Name and Address University of Idaho 875 Perimeter Drive MS 1022, Moscow, ID 83844-1022		10. Work Unit No. (TRAIS) 11. Contract or Grant No.
12. Sponsoring Agency Name and Address Idaho Transportation Department (SPR) Highways Construction and Operations, Contracting Services, Research Program PO Box 7129 Boise, ID 83707-7129		13. Type of Report and Period Covered [Final or Interim] Report [09/01/2020 - 3/30/2023] 14. Sponsoring Agency Code RP 294
15. Supplementary Notes Project performed in cooperation with the Idaho Transportation Department and Federal Highway Administration.		

Pavement evaluation is critical for determining proper and cost-effective surface treatments and allocation of limited funds and resources to maintain, rehabilitate and reconstruct flexible pavements. This study examined two nondestructive testing devices that are used to evaluate the structural capacity and integrity of highway pavements including the Falling Weight Deflectometer (FWD) and Traffic Speed deflectometer (TSD). The researchers conducted a theoretical parametric study to simulate the FWD and TSD loading and predict pavement performance. In addition, they examined and analyzed FWD and TSD deflection data from various test sections in Idaho. Furthermore, they explored the use of Artificial Intelligence (AI) to predict pavement performance and layers' moduli using the FWD and TSD deflection measurements. The results demonstrated that there was a good correlation between pavement mechanical responses (e.g., vertical compressive strain at top of subgrade and tensile strain at the bottom of asphalt layer) and FWD and TSD deflection parameters. Furthermore, the predicted pavement distresses had a good correlation with the deflection basin parameters. The analysis of FWD and TSD field deflection data demonstrated a strong correlation between FWD and TSD field deflections and effective structural number for the field sections. There was a good agreement between the assessment of pavement conditions using FWD and TSD for most of field sections. The AI was found to be a powerful technique to model pavement performance and response. Based on the comprehensive analysis conducted in this study, the TSD can be effectively used at the network level to identify hot spots or sections with potential structural deficiency for further FWD analysis at the project level. This can optimize the time and resources of employing the FWD crew and reduce traffic interruption and improve the safety of FWD crew and motorists.

17. Key Words FWD, TSD, Pavement Preservation, Deflection, Deflection Basin Parameters, Pavement Performance		18. Distribution Statement Copies available from the ITD Research Program	
19. Security Classification (of this report) Unclassified	20. Security Classification (of this page) Unclassified	21. No. of Pages 281	22. Price None

Acknowledgments

This project is funded by Idaho Transportation Department (ITD) from SPR funds. It is performed in cooperation with ITD. The authors would like to acknowledge all members of the research project Technical Advisory Committee (TAC) for their valuable feedback and cooperation all over the project tasks. The authors would like also to acknowledge support from the National Institute for Advanced Transportation Technology (NIATT) and the Department of Civil and Environmental Engineering at the University of Idaho.

Technical Advisory Committee

Each research project is overseen by a Technical Advisory Committee (TAC), which is led by an ITD project sponsor and project manager. The TAC is responsible for monitoring project progress, reviewing deliverables, ensuring that study objectives are met, and facilitating implementation of research recommendations, as appropriate. ITD's Research Program Manager appreciates the work of the following TAC members in guiding this research study.

- Project Sponsor: Mark Snyder
- Project Manager: John Arambarri
- TAC Members: John Arambarri, Tyler Coy, Mir Tamim, Jerome Daleiden
- FHWA-Idaho Advisor: Kyle Holman

Table of Contents

List of Tables

List of Figures

List of Abbreviations and Acronyms

FWD……Falling Weight Deflectometer

TSD …… Traffic Speed Deflectometer

FHWA ……Federal Highway Administration

ITD ……Idaho Transportation Department

TAC ……Technical Advisory Committee

D0……Deflection Measured at 0-inch Distance from the Applied Load Center

D8……Deflection Measured at 8-inch Distance from the Applied Load Center

D12……Deflection Measured at 12-inch Distance from the Applied Load Center

D18……Deflection Measured at 18-inch Distance from the Applied Load Center

D24……Deflection Measured at 24-inch Distance from the Applied Load Center

D36……Deflection Measured at 36-inch Distance from the Applied Load Center

D48……Deflection Measured at 48-inch Distance from the Applied Load Center

D60……Deflection Measured at 60-inch Distance from the Applied Load Center

D72……Deflection Measured at 72-inch Distance from the Applied Load Center

SCI……Surface Curvature Index

LLI……Lower Layer Index

BDI……Base Damage Index

MLI……Middle Layer Index

CAR_{nor}……Normalized Comprehensive Area Ratio

Executive Summary

Pavement evaluation is critical for determining proper and cost-effective surface treatments and allocation of limited funds and resources to maintain, rehabilitate and reconstruct flexible pavements. State highway agencies use the Pavement Management System (PMS) to make decisions on applying preventive and corrective treatments based on proper assessment of the present status and accurate prediction of pavement future performance. Nondestructive Testing (NDT) is one of most well-recognized tools for evaluating the structural capacity and integrity of highway pavements. The NDT includes Falling Weight Deflectomter (FWD) and Traffic Speed Deflectomter (TSD) among others. The FWD measures deflection with high accuracy; however, it requires lane closures causing traffic delays and posing safety concerns for both operators and motorists. The drawbacks have limited the use of FWD to project level applications only and paved the way for the introduction of TSD. TSD can measure pavement deflection at traffic speeds, which enables large spatial coverage and can generate continuous deflection profiles rather than measuring deflection at discrete points.

This study had three phases. In the first phase, the team conducted a theoretical parametric study to simulate the FWD and TSD loading using the 3D Move software. The theoretical parametric study included 243 different pavement structures with different layer thickness and modulus. The 3D-Move software was used to predict the pavement response including stresses, strains, and deflections. The researchers examined the correlation between TSD and FWD deflections obtained using the 3D-Move. Furthermore, they used the AASHTOWare Pavement ME software to predict the performance of all sections included in the parametric study. The second phase of this study analyzed the deflection data collected using FWD and TSD for field sections across Idaho. The team calculated various Deflection Basin Parameters (DBPs), Effective Structural Number (SN_{eff}) using three different methods (i.e., deflection value, Rohde's Equation, and iterative AASHTO method) and calculated the overlay requirements and remaining service life. The team conducted a comparison between the FWD and TSD results. Also, an Excel-based utility was developed to facilitate the analysis of FWD and TSD deflection data and evaluate the pavement conditions. The third phase of this study explored the use of Artificial Intelligence (AI) to predict pavement performance and layers' moduli using the FWD and TSD deflection measurements.

Key Findings

The key findings of this study are summarized below:

- The results of the parametric study demonstrated that there was a good correlation between the TSD pavement responses and deflection parameters. Both Surface Curvature Index (SCI) and the Area Under Pavement Profile (AUPP) were found to be highly correlated with the tensile strain (ε_t) at the bottom of asphalt layer. In addition, there was a strong correlation between the vertical compressive strain (ε_v) at top of subgrade and $SN_{eff.}$ The vertical compressive strain (ε_v) at the top of subgrade is a parameter that is used to predict the rutting life of flexible pavements, while the tensile strain (ε_t) is used to determine the allowable number of load repetitions before cracking

in flexible pavement design. These relationships can be used as a simple approach to estimate the pavement response without the need for complicated analysis methods.

- There was a strong correlation between the FWD and TSD deflection measurements, with an R^2 of 0.88. Also, the results indicated a strong correlation between the maximum deflection (D_o) from both FWD and TSD.

- The results demonstrated that there are good correlations between the Structural Condition Index (SCI) and maximum deflection (D_0) from the FWD data with the terminal International Roughness Index (IRI) and rutting calculated from the AASHTOWare. Furthermore, there was a trend between bottom-up cracking and both SCI and D_0. However, there was no correlation with these indices (i.e., SCI and D_0) and top-down cracking.

- Both SCI_8 and SCI_{12} calculated from the TSD data were found to correlate with the tensile strain (ε_t) at the bottom of asphalt layer. In addition, higher vertical compressive strain (ε_v) at top of subgrade was associated with lower SN_{eff} and normalized comprehensive area ratio (CAr') calculated from the TSD data.

- There was a good correlation between the Surface Curvature Index (SCI) from the TSD data and the terminal International Roughness Index (IRI) and a fair correlation with rutting. In addition, there was a trend between bottom-up cracking and both TSD SCI and D_0; however, and similar to FWD, there was no correlation with these indices (i.e., SCI and D_0) and top-down cracking.

- There was a strong correlation between the FWD and TSD field deflections before and after temperature correction. However, the correlation between FWD and TSD based on uncorrected deflection data is better than the one based on temperature-corrected deflection data. Furthermore, there was a good correlation between the maximum deflection (Do) from both FWD and TSD.

- The results demonstrated that there is a strong correlation between FWD SN_{eff} and TSD SN_{eff} with R^2 of 0.91 for the uncorrected deflection data and R^2 of 0.87 for the corrected deflection data. In addition, the SN_{eff} values were close to the quality line with higher R^2 using the uncorrected deflection data.

- The overlay requirements showed that there was good agreement between the two data sets (i.e., FWD and TSD); however, the FWD demonstrated that eight sections don't need an overlay while the TSD demonstrated that only six of those eight sections would need an overlay. Furthermore, the remaining service life of the examined test sections exhibited a good agreement between both methods (i.e., FWD and TSD); however, there are two sections where there were conflicting calculations in assessing the remaining service life.

- The researchers developed a Microsoft Excel-based tool to streamline the processing of FWD and TSD data. This tool can handle up to 500 deflection measurements in one run and provides

outputs such as the calculation of DBPs, a rating of the pavement conditions based on the DBPs values, the effective and required structural numbers, and the required overlay thickness.

- The results of the AI models demonstrated a strong correlation between the predicted and calculated performance indicators including IRI, rutting of asphalt layer, total rutting, bottom-up cracking, and top-down cracking. Furthermore, AI models were developed to predict layers' moduli as a function of layer thickness and deflection data. The results clearly indicate the AI is a very powerful technique to model pavement performance and response.

- Based on the comprehensive analysis of the three different phases of this study, and the good correlations between the FWD and TSD, the TSD can be effectively used at the network level to identify hot spots or sections with potential structural deficiency for further FWD analysis at the project level. This can optimize the time and resources of employing the FWD crew and reduce traffic interruption and improve the safety of FWD crew and motorists.

1. Introduction

Pavement evaluation is critical for determining proper and cost-effective surface treatments and allocation of limited funds and resources to maintain, rehabilitate and reconstruct flexible pavements. State highway agencies use PMS to make decisions on applying preventive and corrective treatments based on proper assessment of the present status and accurate prediction of pavement future performance. Proper characterization of pavement structure (e.g., layer modulus, thickness) is required to effectively assess and predict pavement conditions (Chatti et al. 2017).

Nondestructive testing (NDT) is one of most well-recognized tools for evaluating the structural capacity and integrity of highway pavements. There are several NDT devices available such as Falling Weight Deflectometer (FWD), Dynamic Cone Penetrometer (DCP), Air-coupled Ground Penetrating Radar (GPR), Ground-coupled GPR, Seismic-based tools like Portable Seismic Pavement Analyzer (PSPA), Nuclear Density Gauge, Non-Nuclear Electrical Gauges, etc. (TxDOT 2021).

Currently FWD is the most popular device for project level NDT (Gedafa 2008). FWD is a device designed to simulate deflection of a pavement surface caused by a fast-moving truck and has been used by US state highway agencies since early 1980s (Choubane 2003; Scanalzer 2006). In 1993, the American Association of State Highway and Transportation Officials (AASHTO) incorporated the use of FWD testing in the pavement design guide for pavement design and rehabilitation, and since then 97 percent of the state highway agencies use FWD as their primary NDT and deflection testing device. FWD simulates the deflection caused by traffic on pavement structures (Choubane 2003). It is less invasive to pavements, quick and inexpensive, causes less interruption to traffic, and can cover more areas compared to the conventional and destructive methods.

Although FWD measures deflection with high accuracy, it requires lane closures causing traffic delays and posing safety concerns for operators and motorists. These drawbacks have limited the use of FWD to project level applications only and paved the way to the introduction of Traffic-Speed Deflection Devices (TSDDs) (Elseifi et al. 2018). Several TSDDs are introduced and used. These TSDDs include Portancemetre, measuring ball, moving FWD, Traffic Speed Deflectometer (TSD), Rolling Dynamic Deflectometer (RDD), Rolling Wheel Deflectometer (RWD), Airfield Rolling Weight Deflectometer (ARWD), Pavement Deflection Tester (RDT), and image-based deflection measuring devices (Flintsch et al. 2012). Meanwhile, Strategic Highway Research Program 2 (SHRP2) identified the TSD and RWD as the most promising candidates for continuous deflection measurement devices. Since the TSD can measure pavement deflection at traffic speeds, which enable large spatial coverage and can generate continuous deflection profiles rather than only measuring deflection at discrete points (Flintsch et al. 2012), it is considering as future of NDT and PMS.

1.1 Problem Statement

ITD uses non-destructive testing to assess pavement conditions in order to select and program pavement maintenance and rehabilitation. The Falling Weight Deflectometer (FWD) is a non-destructive tool used to evaluate the structural capacity and stiffness of pavements. It is less invasive to pavements, faster, and can cover more areas compared to the conventional and destructive methods. In addition, the department has recently used the Traffic Speed Deflectometer (TSD) to collect deflection data across the state as part of Transportation Pooled Fund study TPF-5(385) - Pavement Structural Evaluation with Traffic Speed Deflection Devices. Such data are used to monitor the structural performance of pavements at the network level. The deflection basins measured by both FWD and TSD are different due to the difference in the operating conditions of FWD and TSD. The FWD is a stationary device while the TSD measures the deflection under a continuously moving load. Due to the complexity of FWD analysis, the use of the FWD is currently limited to determining layer stiffness for overlay thickness design. In addition, various indices are proposed to analyze the TSD deflection basin. This study conducts a thorough analysis of the collected TSD and FWD deflection data and calculated various Deflection Basin Parameters (DBPs), Effective Structural Number (SN_{eff}) using three different methods (i.e., deflection value, Rohde's Equation, and iterative AASHTO method) and calculated the overlay requirements and remaining service life.

1.2 Project Objectives

Currently, ITD invests a lot of resources in FWD testing, yet the use of FWD data is limited to project-level analysis and often employed in overlay thickness design. In addition, ITD plans to continue its investment in collecting deflection data using TSD. There is a need to compare and assess the agreement between the FWD and TSD in assessing the conditions and structural capacity of flexible pavements.

The main objectives of this study are:

- Evaluate various techniques and models used to analyze the TSD and FWD data to evaluate the pavement conditions and assess the structural capacity and overlay requirements of flexible pavements.
- Provide recommendations on the use of TSD Data to collect deflection data at the network level and the agreement between FWD and TSD.
- Develop an Excel-based utility that can utilize the deflection data and other information (e.g., traffic, layer thickness) to calculate various Deflection Basin Parameters (DBPs) and assess the structural capacity and overlay requirements for flexible pavements.

1.3 Research Tasks

The goal of this project was achieved by executing several tasks. First, the research team conducted an extensive literature search to review the findings of previous studies conducted to analyze the FWD and TSD deflection data and techniques used to determine the structural capacity and remaining service life of flexible pavements. The researchers identified several test sections with different characteristics (i.e., different thicknesses, layer materials) and traffic levels. Third, the research team examined the collected FWD and TSD deflection data as well as pavement surface conditions. Fourth, the team calculated and evaluated various FWD and TSD deflection parameters used to evaluate the structural capacity of flexible pavements. Fifth, the researchers selected the proper techniques and methods to evaluate the structural capacity and determine the remaining service life of asphalt pavement. Sixth, the team examined the performance decay curves that describe the deterioration of asphalt pavements over time. Finally, the team developed an Excel-based utility to facilitate the analysis of FWD and TSD deflection data and evaluate the pavement conditions.

Task 1: Conduct literature review

Under this task, the research team conducted a thorough literature review to collect pertinent information to the following subjects:

- Principles, operations, and types of FWD and TSD,
- Advantages of FWD and TSD,
- Factors affecting the deflection measurements by FWD and TSD,
- Temperature correction of deflection measurements,
- FWD data collection and analysis procedure,
- TSD data collection and analysis procedure, and
- Use of FWD and TSD deflection data in the PMS.

The outcome of the literature review assisted the research team to evaluate the proper deflection parameters and techniques to analyze the FWD and TSD data and assess pavement conditions.

Task 2: Identify and select pavement sites for evaluation

Under this task, the research identified and selected candidate pavement sites across Idaho for comprehensive evaluation. The researchers compared the FWD deflection parameters to those of TSD under Task 4. Several criteria were considered when selecting the test sections. These criteria include:

- Structural design: pavements with different structure design (number of layers and thickness) were selected.
- Environmental conditions: the test sections were distributed across the state and sites from many districts were included in this study.
- Pavement conditions: pavements with and without surface distresses (e.g., cracking, rutting, etc.) were also included.
- Deflection values: test sections with low and high FWD and TSD deflections were also included.

Task 3: Examine the FWD/TSD deflection data and pavement conditions

The researchers collected and organized comprehensive information about the selected pavement projects (under Task 2) including:

- FWD and TSD deflection measurements,
- Pavement surface temperature, air temperature at the time of testing, previous day average temperature,
- Time and date of FWD and TSD deflection measurements,
- Location of the pavement sites,
- The number of pavement layers, layer thickness, and material properties as available,
- Pavement surface conditions (e.g., fatigue cracking, thermal cracking, rutting, roughness, texture, etc.), and
- Traffic level (i.e., ESALs).

Task 4: Calculate and evaluate various FWD and TSD deflection parameters

Under Task 4, the researchers conducted a theoretical parametric study to simulate the FWD and TSD loading using the 3D Move software. The theoretical parametric study included 243 different pavement structures with different layer thickness and modulus. The 3D-Move software was used to predict the pavement response including stresses, strains, and deflections. The team used the predicted pavement response to assess the relationship between various DBPs and mechanical response (e.g., horizontal tensile strain at bottom of asphalt layer and vertical compressive strain at top of subgrade) and layers' moduli. They also examined the correlation between TSD and FWD deflections, obtained using the 3D-Move. Furthermore, the researchers used the AASHTOWare Pavement ME software to predict the performance of all sections included in the parametric study. The AASHTOWare Pavement ME predicts and reports the performance of these test sections recorded every month over 20 years. The researchers

assessed the correlation between FWD and TSD DBPs and predicted stresses at the end of the design life for the examined test sections.

Under Task 4, the researchers also analyzed the deflection data collected using FWD and TSD for 24 field sections across Idaho. The FWD and TSD deflection data were corrected and normalized to account for the effect of pavement temperature using the same method. In addition, the team considered the deflection data without correction. The team calculated various DBPs and assessed the correlation with pavement layers' moduli and field performance. In addition, they used the deflection data and other information to calculate the Effective Structural Number (SN_{eff}) using three different methods (i.e., deflection value, Rohde's Equation, and iterative AASHTO method) and calculated the overlay requirements and remaining service life.

Task 5: Analyze the collected data

Under this task, the research team conducted the following subtasks:

- Compare the FWD and TSD deflection parameters to the mechanical response of pavements with different characteristics (e.g., tensile strain at the bottom of asphalt layer, compressive strain at the top of subgrade). The tensile strain at the bottom of asphalt layer controls the fatigue cracking in asphalt pavements, while the compressive strain controls rutting.
- Investigate the correlation between calculated FWD and TSD deflection parameters (calculated in Task 4) and observed field performance (e.g., cracking, rutting, and roughness).
- Compare the FWD and TSD deflection measurements, DBPs, SN_{eff}), and pavement structural conditions (e.g., remaining service life, overlay thickness). In this comparison, the research team considered both corrected and uncorrected FWD and TSD data.
- Provide recommendations on proper method(s) for determining the effective structural number.
- Provide recommendations on the use of TSD based on the results of Task 5.

Task 6: Study performance decay curves

The researchers expanded on the analysis conducted under Task 5 and explored the use of Artificial Intelligence (AI). They developed AI models using the FWD and TSD measurements to predict pavement performance over time as a function of deflection data and traffic level for the parametric study. Furthermore, the team developed preliminary models to estimate pavement layers' moduli as a function of layer thickness and FWD deflection data collected in the field. The data used in the AI models included theoretical as well as field data.

Task 7: Develop Excel-based utility

Based on the results of Task 5 and Task 6, the research team developed an Excel-based utility that uses the FWD and/or TSD deflection data, pavement structure information (number of layers, layer thickness, etc.), and traffic level to determine the structural capacity and overlay requirements of asphalt pavements. This spreadsheet can be used to facilitate the analysis of the FWD and TSD deflection data. In addition, the developed models can be incorporated in the TAMS to analyze the pavement conditions at the network level.

1.4 Report Organization

This report documents the research methodology, presents the results and analysis, summarizes the findings, and provides recommendations for future studies and implementation. The report has eight chapters. Chapter 1 provides background and problem statement, project goal and objectives, research tasks, and report organization. Chapter 2 presents the main findings of the literature review on the FWD and TSD current practice of deflection data collection and analysis. Chapter 3 presents the methodology and research plan, and data collection. Chapter 4 discusses the FWD data analysis and the correlation with field performance. Chapter 5 presents the results of TSD analysis and the correlation with the field performance. Chapter 6 provides comprehensive evaluation and comparison between FWD and TSD data. Chapter 7 summarizes the utilization of Artificial Intelligence (AI) to analyze the FWD and TSD data. Finally, Chapter 8 summarizes the main findings and conclusions of this study and provides recommendations for future research and implementation.

2. Review of Falling Weight Deflectometer and Traffic Speed Deflectometer

The FWD is a device used to measure the deflection of flexible and rigid pavements in response to a dynamic load. The dynamic load creates an impulse which is similar to a passing wheel load (Alvi et al. 2008). The FWD deflection and other data are used to evaluate the structural capacity of pavements which is used in research, design, maintenance, rehabilitation, and reconstruction of pavements at the project and network levels. FWD was developed in the 1970s and emerged as a worldwide standard for pavement deflection testing devices in the 1980s (Irwin et al. 2017). According to ASTM D-4694, deflection measurement by FWD is based on the principles of a plate-bearing test. The load is generated on the pavement surface in form a force pulse by a weight dropped on a buffer system and is transmitted through a plate resting on the pavement surface (ASTM 2015). The apparatus can be mounted in a vehicle or on a suitable trailer towed by a vehicle. The measured deflection at fixed distances from the loading plate is called deflection basin. Basic components of an FWD are shown in the Figure 2.1 and briefly described below (ASTM 2015):

- Force generating device which is the 'falling weight' with a guide system. It should be capable of being raised to one or several predetermined heights and then dropped. The resulting force pulse transmitted to the pavement should have the shape like a half-sine wave with a peak force of approximately 50 KN.

- Loading plate at the base capable of approximate uniform distribution of load on the pavement surface and constructed to facilitate deflection measurement at the center of the plate. Typical loading plates are 300 and 450 mm (12 and 18 in.) in diameter.

- Deflection sensors capable of measuring maximum vertical movement of the pavement. Linear variable displacement transducer (LVDT), geophones, and accelerometers are the sensors located at fixed distances from the loading plate to measure deflection (Chatti et al. 2017). The numbers and spacing of sensors depend on the purpose of the test and pavement surface characteristics. The Long-Term Pavement Performance (LTPP) FWD manual recommends a nine-sensor FWD with the sensor spacing at -12, 0, 8, 12, 18, 24, 36, 48, and 60 inches from the center of the baseplate (Lukanen et al. 2000).

- Load cell to measure the applied load after each impact. The system should display and store load measurements with a 45-lbf resolution.

- Data acquisition, processing and storage unit. All the recorded load and deflection data are stored on a personal computer located in the tow vehicle. Additional information such as air temperature, pavement surface temperature, distance measurement and site identification should be automatically or manually recorded. Usually, an infrared thermometer is installed on the FWD trailer to measure the pavement surface temperature during testing.

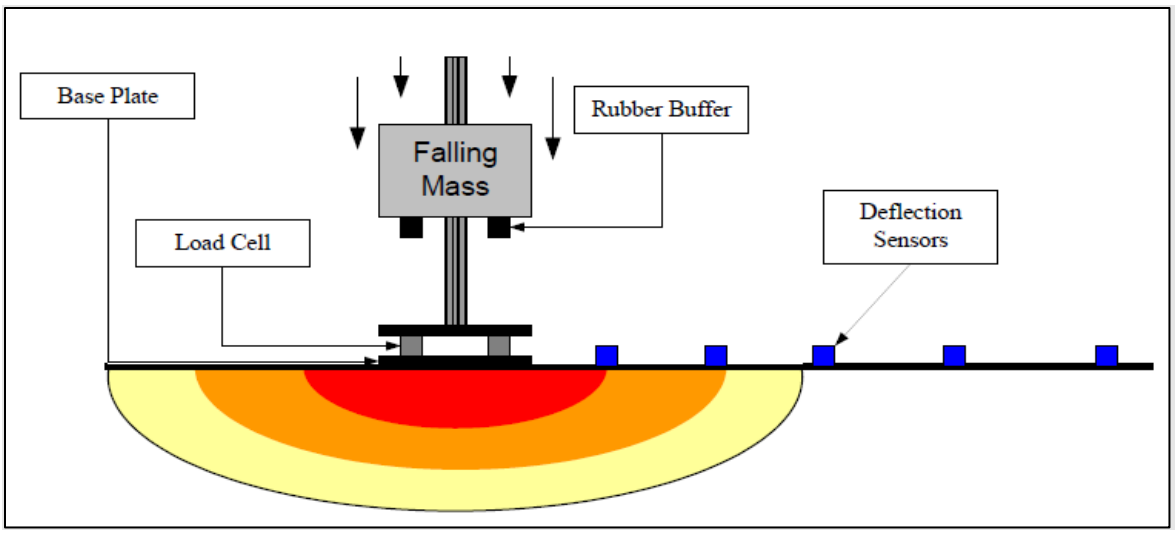

Figure 2.1 Schematic Diagram of Typical FWD Testing Setup (Chatty et al. 2017)

2.1 Types of FWD

According to a survey conducted by the National Cooperative Highway Research Program (NCHRP), 45 state highway agencies reported that they own 82 FWDs, most of them were manufactured by Dynatest. Some other manufacturers like Grontmij, JILS and KUAB were also mentioned (Alvi et al. 2008). Table 2.1 summarizes different FWDs based on their manufacturer and other device characteristics.

Table 2.1 Summary of Commonly Used FWD Devices

FWD Device	Manufacturer	Loading Range (lb)	Load Plate Type and Diameter	Load Actuator System	Number of Sensors	Cycle Duration (msec)
Dynatest® FWD 8000/8082	Dynatest	1,500-54,000	Circular Plate 11.8''/17.7'' Diameter	Dropping Mass	7-15	25-30
Carlo Bro FWD	Grontmij Pavement Consultants	1, 500-78,600	4-split circular load plate 12''/18'' Diameter	Dropping Mass	10-18	15-30
JILS™	Foundation Mechanics, Inc.	0- 67,000	Circular Plate 12'' Diameter	Dropping Mass	9	20-34
KUAB	Engineering and Research International, Inc.	3,000 - 66,000	Segmented or Solid Circular Plate 11.8''/17.7'' Diameter	Two dropping Masses	7	28

There are some other impulse deflectometers which are specially used in airfield pavements, known as Heavy Weight Deflectometer (HWD). Shell and WES are some HWDs (Bush et al. 1990).

Figure 2.2 Current FWD used by Idaho Transportation Department (ITD) with Truck and GPS horn (ITD 2017)

2.2 Advantages of FWD Against Other Nondestructive Testing Devices

FWD has certain advantages over other conventional nondestructive testing devices. Because of its reliability, simplicity and effectiveness, more than 45 state highway agencies extensively use FWD in their pavement management system (Alvi et al. 2008). Some other merits of FWD include:

- Multiple load magnitudes and load levels are possible. So, stress sensitivity of pavement can be easily understood (Eagleson et al. 1983).
- Less manpower and less lane closure time required.
- FWDs are not affected by shoulder movements.
- Dynamic FWD impulse loads provide a more realistic simulation of truck movements and digital signal analyzers can yield information for wave propagation analysis.
- Large existing empirical and historical database available (Eagleson et al. 1983).

2.3 FWD Testing Procedure

According to the Long-Term Pavement Performance (LTPP) manual for FWD measurements, before FWD testing, the operator must ensure that a traffic control plan is provided for FWD operations at the site. After arriving at the site, the operator should inspect for any evidence of recent maintenance activities and record such observations and notes. Pavement temperature should be measured by preparing the temperature gradient holes. Load level and drop heights must be adjusted and corrected using a standard buffer warm-up sequence (Schnalzer 2006). After recording air and pavement temperatures and lane specifications, the testing sequence should start. Sensor positions depend on the type of pavements and purpose of the test but according to the Strategic Highway Research Program (SHRP), the most efficient configuration of sensor positions for network level testing are 0, 8, 12, 18, 24, and 36 inches for the first six sensors. These six sensor positions cover both flexible pavement and rigid pavement tests taken at an interior position for jointed concrete pavements (Stubstad et al. 2012). The FWD field program software should be set up and prepared for data collection (Lukanen et al. 2000). There are four typical drop heights or load levels that are applied during testing. The acceptable load range for each drop height is between 90 percent and 110 percent of the targeted load value. At each drop height, four FWD deflection measurements should be recorded (i.e., four replicates). The four replicates associated to each drop height were averaged to represent a single deflection measurement reading at that specific location (Souliman et al. 2018). The operator or an associate can exit the vehicle during testing and examine the pavement surface in the vicinity of the FWD for signs of distresses and defects. If there is any distress present, it should be noted. When the test on the first section is completed and the load plate is up, the operator should proceed to the next test section. For every test section, a new data file should be used and if traffic control conditions permit, backup of the collected data and initial data processing can be performed before leaving the site (Schnalzer 2006).

2.4 Review of Traffic Speed Deflectometer Equipment

The Traffic Speed Deflectometer (TSD) is a continuous velocity-sensing laser-based deflection measuring device that loads the pavement while moving at the traffic speed and measure vertical deflection velocity using Doppler lasers at four or six points (Elseifi et al. 2018). This concept of measurement is built on the principal of Doppler sensors. These sensors are installed on a semi-trailer and attached to a beam that is kept parallel to the pavement surface as well as to the direction of travel. The rear axle of the semi-trailer is loaded with a static load, typically between 100 and 130 kN (22,000 to 30,000 lbs.) (Graczyk et al. 2014). TSDs can operate at a traffic speed . Figure 2.3 shows a TSD vehicle used by Louisiana Department of Transportation and Development (Elseifi et. al. 2018).

Figure 2.3 TSD used in an Experimental Program in Louisiana (Elseifi et. al. 2018)

The first two prototypes of the TSD were developed by a Danish company Greenwood Engineering A/S. Danish Pavement Institute (DRI) and Greenwood Engineering jointly developed the first model of TSD, initially called the high speed deflectograph (Flintsch et al. 2012). After the first TSD was delivered to Danish Pavement Directorate under the Ministry of Transport in 2004, since then it is still in regular use for bearing capacity measurements on state pavements in Denmark. The advancement of TSD has been continued since then and now more than a dozen of TSDs are used in different research projects and maintenance optimization tasks in USA, South Africa, Australia, China, England, Germany, Italy, Poland and Denmark (Greenwood Engineering 2018). Currently, TSDs can be custom equipped with Ground Penetration Radar (GPR), pavement surface profilers, ROW-camera, crack detection, line scanner etc. for collecting even more structural or functional data (Ferne et al. 2009). Figure 2.4 represents a detailed schematic of TSD.

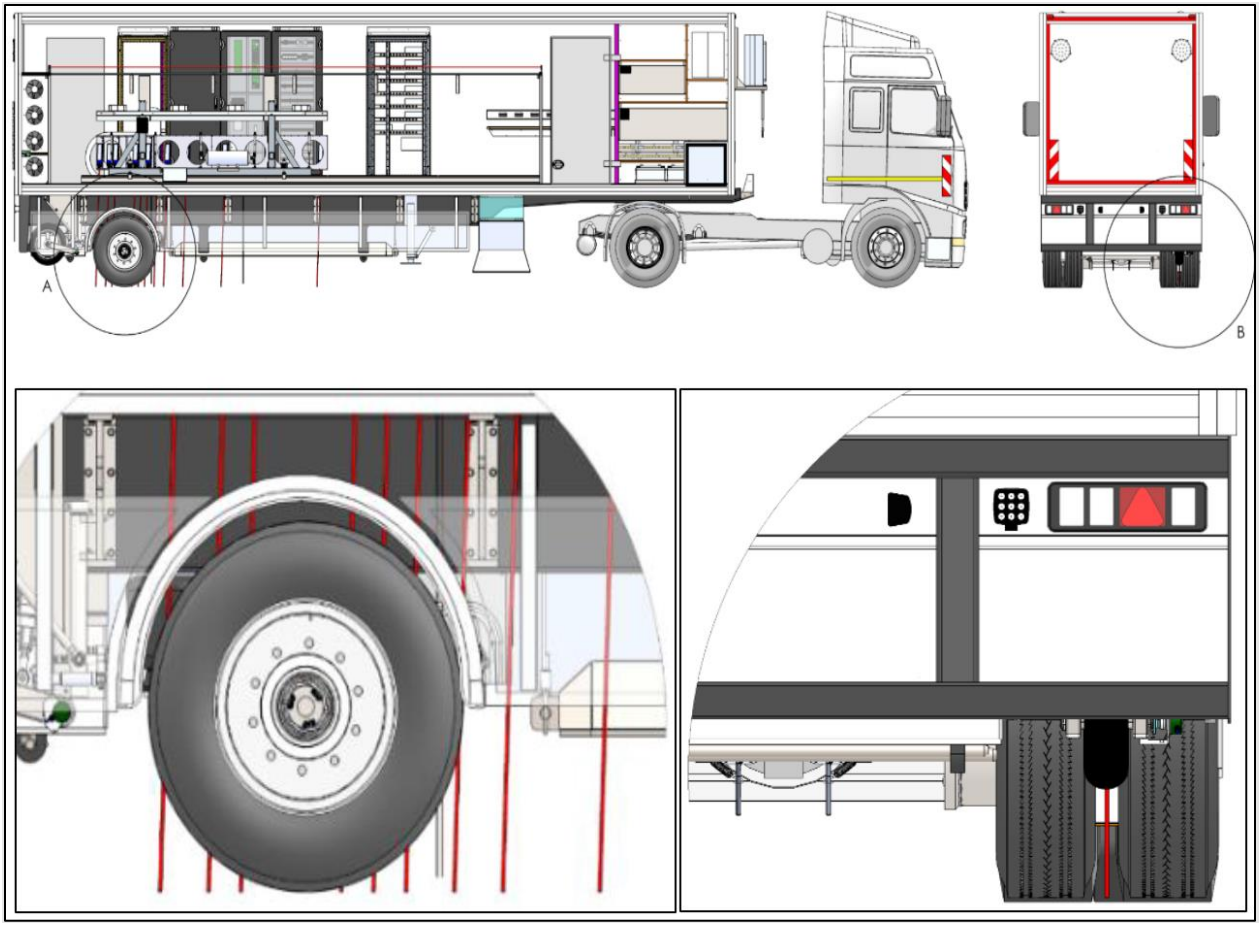

Figure 2.4 Schematic of a Greenwood TSD (Greenwood Engineering 2018)

2.5 TSD Operating Principal

The TSD consists of an articulated truck applying 22,000 lbs on the rear axle. The crew of the TSD system consists of a vehicle driver and an operator, who controls the measurement and recording of data during the measurements (Březina et al. 2017). There can be 10 or more Doppler lasers in the longitudinal centerline between the rear twin wheels with Doppler lasers behind and in front of the load axle. The pavement response to the load applied by the rear axle is measured as the vertical deflection velocity by the fixed Doppler lasers mounted on a servo-hydraulic beam. If four Doppler lasers are used, three are positioned in a way that they measure deflection velocity at a range of distances in front of the rear axle. The fourth sensor is positioned 3.6 m in front of the rear axle largely outside the deflection bowl, acting as a reference laser (Katicha et al. 2013). The servo-hydraulic beam can move with the movement of the trailer, which allows the Doppler lasers to maintain a fixed height from the surface of the pavement. To address thermal fluctuations during testing, a constant 68°F (20°C) temperature is maintained in the servo-hydraulic beam. The TSD can collect one measurement every 0.00001-mile (0.787 in.) of a pavement section at a rate of 1000 Hz while travelling at a traffic speed of up to 60 mph (Elseifi et al. 2018; Greenwood Engineering 2018).

2.6 Pros of TSD Over FWD and Other Conventional Deflection Measuring Devices

The most fundamental difference between FWD and TSD is the loading mechanism which could lead to some appreciable differences in the measured deflection values obtained from these two devices. Rolling Wheel Deflectometer (RWD) is another continuous deflection measuring device which is now considered promising and is used by many state DOTs on an experimental basis. Table 2.2 presents a detailed difference between TSD, FWD and RWD (Graczyk et al. 2014, Flintsch et al. 2012, Katicha et al. 2013, Rada et al. 2016 and Kannemeyer et al. 2014). From the comparison in Table 2.2, it is evident that TSD can be certainly more advantageous in the PMS as it has been emerging as a continuous pavement deflection-measuring device which operates at traffic speed and eliminates lane closure and user delays. TSD also ensures the safety of motorists as well as the crew. Another great advantage of TSD is the high measurement capacity. According to the Pavement and Bridge Research Institute of Poland, more than 500 miles (800 km) of pavement network can be measured with a TSD on a single day. One drawback of using TSD is that the measurements cannot be performed in rain or on wet pavements due to the use of laser sensors (Březina et al. 2017).

2.7 Data Collection and Analysis Procedure

2.8 Deflection Data from FWD

Data gathered from FWD testing should be preprocessed by the operator using FWDConvert and FWDScan (Schnalzer 2006). After receiving the electronic data files along with the required forms, office personnel should review FWDScan output and investigate warnings or errors present in the output file. LTPP manual recommended five specific error-checking methods on field data such as roll-off, nondecreasing deflections, overflow, load variation and deflection variation. The processed FWD data files should be uploaded to the Regional Information Management System (RIMS) of LTPP or Pavement Management System (PMS) of the respective state (Schnalzer 2006).

2.8.1 Factors Affecting FWD Measurements

There are several factors that can affect the deflection data obtained from the FWD. These factors need to be considered as they can be problematic in interpreting the deflection data. The factors can be categorized in to three major groups:

• Structural characteristics of pavement including pavement thickness and distresses,

• Loading on pavement including magnitude and type of loading (Irwin et al. 2017), and

• Climatic condition including air and pavement temperatures and seasonal effects, and subgrade moisture variation.

Table 2.2 TSD, FWD and RWD Comparison

Device Parameter	TSD	FWD	RWD
Applied load (kip)	11	approximately 11	18
Axle configuration	full-axle configurations	Half-axle configurations	full-axle configurations
Capability of computing surface curvature index (SCI)	Yes	Yes	No (Extra sensor needed)
Deflection accuracy (mil)	11	0.0254	2.5
Factors affect measurement accuracy	highly influenced by the irregularities in the surface	Influenced by discontinuities, and variability within the pavement structure	highly influenced by the irregularities in the surface
Loading mechanism	Moving load at traffic speeds	Stationary impulse load	Moving load at traffic speeds
Loading configuration	Dual tires	Single Plate	Dual tires
Measurement location of interest	Ahead the centerline of the load axle (three locations)	area measurable 1 to 2 meters away from the point of loading	Behind the centerline of load axle at 7.25 inches
Measurement Principle	Doppler laser	Falling mass on a load plate	Laser distance measurement system by lights and cameras
Measurement type (vertical)	Deflection velocity	Deflection	Deflection
Number of measurements	3	1-8 (Depending on sensors)	1
Operation speed (mi/h)	20-60	0-20	5–60
Sampling frequency (inches)	0.8	600	0.6
Traffic control	Not needed	Needed	Not needed

2.8.2 Temperature Correction of FWD data

It is well recognized that the temperature of Asphalt Concrete (AC) layer is the most critical factor that affects deflections in the flexible pavement (Park et al. 2002). Since FWD measurements are collected at different temperatures and different times of the day, temperature correction needs to be performed at the time of analysis. Researchers proposed several procedures to predict the temperature of asphalt layer and to adjust the deflection data to minimize the effect temperature.

The 1993 AASHTO pavement design guide (AASHTO 1993) proposed an empirical temperature correction procedure for FWD deflections based on American Association of State Highway Officials (AASHO) pavement test data. However, many researchers claimed that the AASHTO procedure is incorrect, especially at higher temperature (>38°C). A separate study attempted to improve the method described in the AASHTO guide based on prediction of composite modulus of the multilayered pavement. Although it provided more consistent results, a research study undertaken at the North Carolina State University

developed a more realistic temperature correction procedure for FWD deflections (Kim et al. 1995). The equation of correcting the FWD deflection at a reference temperature of 20°C (68°F) is presented in Equation 2.1.

$$D_{68} = 10^{\alpha(68-T)} \times D_T \quad \text{……Eqn. 2.1}$$

where,

D_{68} = Adjusted deflection to the reference temperature of 20°C (68°F)

$\alpha = 3.67 \times 10^{-4} \times t^{1.4635}$ for wheel path and $3.65 \times 10^{-4} \times t^{1.4241}$ for lane center

t = Thickness of the AC layer (in.)

T = The AC layer mid-depth temperature (°F) at the time of FWD testing

D_T = Deflection measured at temperature T (°F)

Kim et al. (1995) indicated that the mid-depth temperature of asphalt layer was predicted using a database approach which was an improvement over the AASHTO method and a separate temperature prediction model. The prediction model was verified using BELLS equation for temperature correction (MPC 2002). Another study in Texas (Chen et al. 1999) developed universal temperature correction equations for FWD deflection measurements for flexible pavements in Texas. Repeated falling weight deflectometer (FWD) tests have been done at three different sites. The tests were conducted at frequent intervals of 2 to 3 consecutive days for each location and during different periods to obtain a wide range of temperatures. The effect of cracks on temperature correction was also examined. Temperature correction equations for deflection and moduli were developed so that users can input their own reference temperatures. This study also found that the deflections at a radial distance of 0 and 203 mm, corresponding to the first two sensors of FWD, were significantly affected by the surface temperature.

Later, Lukanen et al (2000) developed two equations based on the BELLS model which are considered the primary models for estimating mid-depth pavement temperature. These equations are known as BELLS 2 and BELLS 3 model which are described in Equations 2.2 and 2.3, respectively.

$$T_d = 2.78 + 0.912\ IR + \{\log(d) - 1.25\}\{-0.428\ IR + 0.553\ T_{1\text{-}day} + 2.63 \sin(hr_{18} - 15.5)\} + 0.027\ IR \sin(hr_{18} - 13.5) \quad \text{……Eqn. 2.2}$$

$$T_d = 0.95 + 0.892\ IR + \{\log(d) - 1.25\}\{-0.448\ IR + 0.621\ T_{1\text{-}day} + 1.83 \sin(hr_{18} - 15.5)\} + 0.042\ IR \sin(hr_{18} - 13.5) \quad \text{…… Eqn. 2.3}$$

where,

T_d = Pavement temperature at depth d (°C)

IR = Pavement surface temperature measured using an infrared gauge (°C)

d = Depth at which the temperature is predicted (mm)

$T_{1\text{-}day}$ = Average air temperature of the previous day (average of high and low temperatures) (°C)

hr_{18} = Time of the day, in a 24-hr system but calculated using an 18-hr asphalt concrete temperature rise- and fall-time cycle

Equation 2.2 represents BELLS 2 model which was developed based on the FWD testing protocols followed in the LTPP program and Equation 2.3 represents BELLS 3 model that considers the shade effect to suit the routine FWD testing operations undertaken by various transportation agencies. Both temperature prediction models have the same mathematical expression except the regression coefficients are different (Kassem et al. 2020).

Researchers in New Mexico (Zhang et al. 2008) developed two temperature correction models to correct measured FWD deflections based on the climatic zone. LTPP database was used for collecting deflection, temperature, and other associated data. In the LTPP database, the temperature was measured at six different depths. The reference temperature at which the corrections were made was chosen 25°C as the temperature in New Mexico is higher than the other parts of US. The corrected deflection was obtained using Equation 2.4.

$$D_{25} = f.\ D_T \qquad \text{.....Eqn. 2.4}$$

where,

D_{25} = Reference deflection at 25°C

f = Temperature correction factor

D_T = Recorded deflection at temperature T(°C)

The temperature correction factor (f) for the northern and southern part of New Mexico was obtained from regression analysis and is given in Equations 2.5 and 2.6, respectively.

$$f_n = -0.8772 - 0.0986\,(T/25) + 0.3188 \log (t_{ac}) - 0.6456 \log (t_T) + 2.4369\,(L/280) \qquad \text{.....Eqn. 2.5}$$

$$f_s = 6.0808 - 0.2944\,(T/25) - 1.710 \log (t_{ac}) + 0.0721 \log (t_T) - 0.7976\,(L/280)$$ ……Eqn. 2.6

where,

f_n, f_s = Temperature correction factors for the northern and southern parts of New Mexico

T = Layer temperature 3 (°C)

t_{ac} = Thickness of the AC layer (mm)

t_T = Depth of layer temperature 3 (mm)

L = Drop load (KPa)

Results from this study also proved that temperature correction models for deflections should be region specific. Kassem et al. (2020) developed a temperature prediction model utilizing pavement temperature collected in Idaho. This is known as Idaho 7-Term Model and is proposed for the use in Idaho.

2.8.3 Data Elements needed for FWD Data Analysis

Besides the load and deflection data, some additional information is required for the FWD data analysis. Table 2.3 lists the data elements required for the FWD analysis (Stubstad et al. 2012).

Table 2.3 Data Elements Needed for FWD Data Analysis (Stubstad et al. 2012)

Type of Data	Data Element
General Information	• Objective/type of the test • Site reference and length • Lanes to be tested with direction • Testing interval • Pavement design life
Pavement Structure Information	• No. of layers • Layer thickness • Material and type of each layer
FWD Deflection Testing Data	• Peak load • Peak deflection values • Drop height • FWD sensor information
Pavement Performance Data	• Hot Mix Asphalt (HMA) surface distresses • Rutting • Fatigue cracking • Transverse cracking • Longitudinal cracking • Alligator cracking • PCC surface distresses • PCC faulting at joints • PCC faulting at cracks • Number of corner breaks • Durability cracking • International Roughness Index (IRI)
Traffic Data	• Average annual daily truck traffic (AADTT) • Average equivalent single axle load (ESAL) • Percent heavy commercial vehicle (HCV) • Growth rate • Vehicle classifications
Climatic Data	• Average air temperature • Pavement temperature • Average precipitation

2.8.4 FWD Data Analysis

After collecting the FWD field test data and all other pertinent information needed, analysis is performed according to the needs of the agency and purpose of the test. Researchers used the FWD data to estimate the subgrade modulus and calculated several deflection basin parameters (Mishra and Rabbi 2017).

2.8.5 Subgrade Modulus Analysis

Although different agencies have different approaches regarding the use of FWD data in their PMS; according to a survey conducted by NCHRP, 90 percent of the state highway agencies use FWD data for

the estimation of pavement layer modulus (Alvi et al. 2008). There are several established approaches for determining subgrade modulus using FWD data analysis and interpretation. These can be categorized into two groups: 1) forward calculation or forward analysis and 2) backcalculation.

Forward Calculation

This is a method where pavement responses such as stresses, strains, and deflections caused by surface loads are calculated at any point. The process is called forward as it is closed from. Forward calculation uses three methods for calculating pavement response: 1) closed-form solutions based on Boussinesq's original half-space solution, 2) layered elastic solutions based on Burmister's original two- and three-layer solutions, and 3) Finite Element Method (FEM) based solutions (Gedafa 2008). Computer programs such as BISAR, CHEVLAY2, CHEVRON, ELSYM5, KENPAVE, NELAPAV, PADAL, and VESYS are generally used for forward calculation (Chatti 2017; Gedafa 2008). For FEM based forward solutions three dimensional (3-D) general-purpose programs like SAP, ABAQUS, and ANSYS can be used (Chatti et al. 2017).

Backcalculation

This is a method of interpretation of pavement responses through iteration of forward calculation with numerical methods to assist with convergence (Alvi et al. 2008). Backcalculation method can be static or dynamic.

Static Backcalculation Methods

The load on the pavement surface is considered static under this method. Static backcalculation methods can be grouped into three major categories based on the technique used to achieve the solution. The first category is basically an iteration technique which repeatedly uses a forward analysis method to adjust the layer moduli until the calculated and measured deflection basins are matched with an acceptable tolerance. Microcomputer program EVERCALC© is the most widely used program for iterative backcalculation method (Lee et al. 1988). The second category is based on generating a database of deflection basins considering different combinations of layer moduli, specified layer thicknesses, material properties, pavement types, and loading conditions using a forward calculating scheme and finding a best possible solution for the observed deflection basin. MODULUS is the commonly used linear elastic model for this technique (Rohde et al. 1990). This model uses the database generated by the fully competent three-dimensional computer program WESLEA (Cauwelaert 1989). The third and final category incorporates sets of regression equations fitted to a database of deflection basins generated by a forward calculation scheme. This is a closed form technique which uses the Odemark-Boussinesq method of equivalent layer thickness concept and the radius of curvature method. ELMOD3 is a popular program for this third type of backcalculation technique (Chatti et al. 2017). Table 2.4 summarizes the commonly available backcalculation computer programs for flexible pavements (Alvi et al. 2008; Chatti et al. 2017).

Dynamic Backcalculation Methods

Most common dynamic backcalculation methods use dynamic, damped-elastic finite-layer or FEMs for their forward solution approach. This backcalculation method is either frequency or time domain solutions. In the frequency domain solution, the applied load and measured deflection time histories are transformed into a frequency domain by using the Fast Fourier Transform (FFT). On the other hand, in time-domain backcalculation, the measured deflection time histories are directly compared with the predicted results from the forward analysis and the comparison can be achieved for any time interval desired. A comparison was made between these two solution techniques, and it was concluded that time domain backcalculation should be preferred over frequency domain backcalculation (Uzan 1994).

2.8.6 Deflection Basin Parameters Analysis

When a pavement deflects due to the loading caused by FWD, the influence of the load can extend over an area measurable 1 to 2 meters away from the point of loading. This deflected area tends to form a circular deflected indentation called a deflection bowl or basin (Horak et al. 2006). Figure 2.5 shows schematic of a deflection basin during FWD testing.

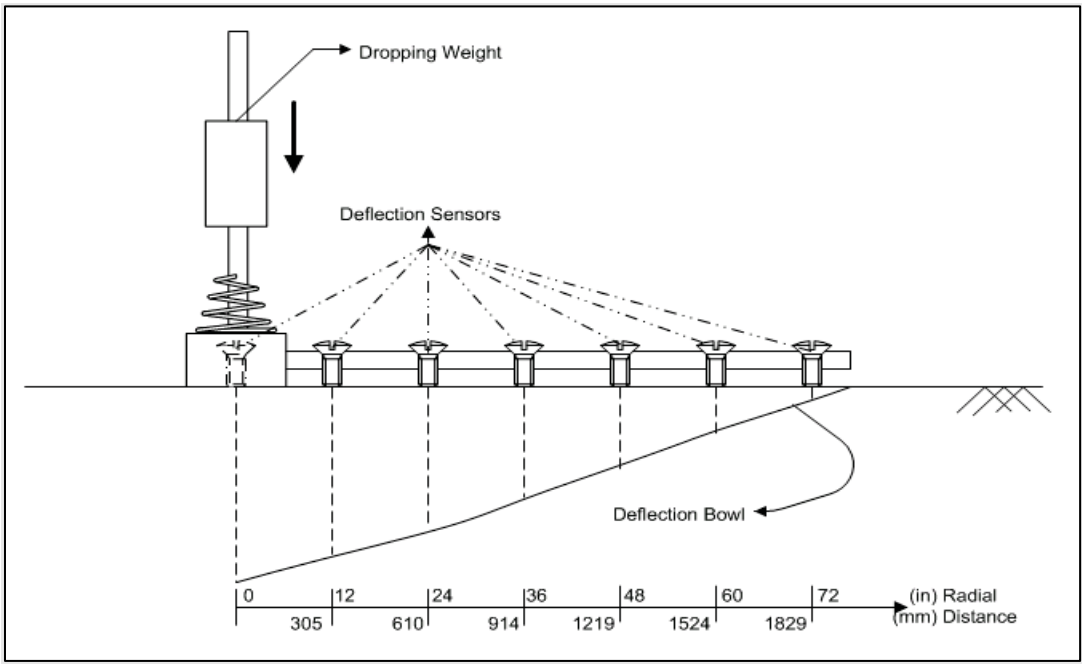

Figure 2.5 FWD Deflection Bowl (Horak et al. 2006)

During the FWD testing, the deflection measurements (deflection bowl) are recorded up to a distance of 1.8 m to 2 m away from the center of loading plate. This measurement of the whole deflection bowl led to the definition of various deflection bowl parameters (DBPS) from which various aspects of the measured deflection bowl can be measured (Horak et al. 2006). DBPs are commonly used to make inferences about the structural condition of individual pavement layers. Additionally, threshold values for

different DBPs demarcating the boundaries between different structural condition rankings differ from one agency to another. Different DBPs found in the literature are compiled and presented in Table 2.4. These DBPs are mostly used in US (Horak and Emery 2006, Hossain and Zaniewski 1991, Kim and Heemum 2002, Kim et al. 2000, Mishra and Rabbi 2019, and Talvik and Aavik 2009). Some common DBP of Australia and South Africa (Horak et al. 2006, Rabbi and Mishra 2019) are also listed in Table 2.5.

Program Name	Developer	Forward Calculation Method	Backcalculation Method	Maximum Number of Layers incorporated	Convergence Scheme
BISDEF	U.S. Army Corps of Engineers	Multilayer Elastic Theory	Iterative	Best for 3	Sum of squares of absolute error
BOUSDEF	Oregon State University	Method of Equivalent Thickness	Iterative	At least 4	Sum of percent errors
CalBack	Caltrans, University of California at Berkeley, and the University of California at Davis	Linear Elastic Theory	Linear Elastic Theory	5	-
CHEVDEF	U.S. Army Corps of Engineers	Multilayer Elastic Theory	Iterative	Best for 3	Sum of squares of absolute error
COMDEF	U.S. Army Corps of Engineers	Multilayer Elastic Theory	Database	3	Various
DBCONPAS	University of Florida	Finite Element Method	Database	-	-
ELMOD/ELCON	Dynatest®	Method of Equivalent	Iterative	4 exclusives of rigid layer	Relative error of 5 sensors
ELSDEF	Texas A&M, U.S. Army Corps of Engineers	Multilayer Elastic Theory	Iterative	Best for 3	Sum of squares of absolute error
EMOD	PCS/Law Engineering	Multilayer Elastic Theory	Iterative	3	Sum of relative squared error
ERIDA	Engineering and Research International, Inc.	Multilayer Elastic Theory	Iterative	4	Relative deflection error
EVERCALC	Washington State Department of Transportation	Multilayer Elastic Theory	Iterative	5	Sum of absolute error
FPEDD1	Texas State Department of Highways and Public	Multilayer Elastic Theory	Iterative	-	-
ISSEM4	Dynatest Consulting, Inc	Multilayer Elastic Theory	Iterative	4	Relative deflection error
MICHBACK	Michigan State University	Multilayer Elastic Theory	Newton method	Best for 3	Sum of relative squared error
MODCOMP5	Cornell University Local Pavements Program	Multilayer Elastic Theory	Iterative	2 to 15 layers; maximum of 5 unknown layers	Relative deflection error at sensors
ModTag	Virginia Department of Transportation	Multilayer Elastic Theory	Iterative	2 to 15 layers; maximum of 5 unknown layers	Relative deflection error at sensors
MODULUS	Texas Transportation Institute	Multilayer Elastic Theory	Database	4 unknown plus stiff layer	Sum of relative squared error
PADAL	University of Michigan, Ann Arbor	Multilayer Elastic Theory	Iterative	-	Sum of relative squared error
RPEDD1	Texas State Department of Highways and Public	Multilayer Elastic Theory	Iterative	-	-
WESDEF	U.S. Army Corps of Engineers	Multilayer Elastic Theory	Iterative	5	Sum of relative squared error
RoSy DESIGN	Grontmij Pavement Consultants	Linear Elastic Theory	Linear Elastic Theory	4	-
PRIMAXdesign	Grontmij Pavement Consultants	Linear Elastic Theory	Linear Elastic	4	-

Table 2.4 Commonly Available Backcalculation Computer Programs (Alvi et al. 2008; Chatti et al. 2017)

Table 2.5 Summary of Available Deflection Basin Parameters (Horak et al. 2006, Rabbi and Mishra 2019)

Deflection Basin Parameter (DBP)	Formula	Structural Indicator
Area	$A = 6\,(D_0 + 2D_{12} + 2D_{24} + D_{36})/D_0$	Overall pavement strength
Additional Areas	$A_2 = \frac{6(D_{12}+2D_{18}+D_{24})}{D_0}$	Base strength
Additional Areas	$A_3 = \frac{6(D_{24}+2D_{36}+D_{48})}{D_0}$	Lower layer strength
Area Indexes	$AI_1 = \frac{D_0+D_{12}}{2D_0}$	Area index for surface layer strength
Area Indexes	$AI_2 = \frac{D_{12}+D_{24}}{2D_0}$	Area index for base layer strength
Area Indexes	$AI_3 = \frac{D_{24}+D_{36}}{2D_0}$	Area index for lower layers strength
Area Indexes	$AI_4 = \frac{D_{36}+D_{48}}{D_0}$	Area index for lower layers strength
Area Under Pavement Profile	$AUPP = \frac{5D_0 - 2D_{12} - 2D_{24} - D_{36}}{2}$	Gives an indication of tensile strain at the bottom of the AC Layer. Characterizing condition of the pavement upper layers
Australian Curvature Function	$CF=D_0-D_{12}$	Gives an indication of the structural condition of the surfacing and base layers
Base Curvature Index	$BCI = D_{24} - D_{36}$	Gives an indication of the lower structural layers like the selected and the subgrade layers

Deflection Basin Parameter (DBP)	Formula	Structural Indicator
Base Damage Index	$BDI = D_{12} - D_{24}$	Gives an indication of tensile strain at the bottom of the AC Layer and compressive stress at the top of the subgrade
Base Layer Index	$BLI = D_0 - D_{12}$	Gives an indication of primarily the base layer structural condition
Basin Slope	$SLOP = D_0\text{-}D_{48}$	
Bending Index	$BI = D_0/a$	
Deflection Ratio	$DR = D_r/D_0$	Determination of condition of the layer at the equivalent depth
Difference of BCI	$DBCI = BCI_{15kips} - BCI_{9kips}$	Gives an indication of the lower structural layers like the selected and the subgrade layers
Difference of BDI	$DBDI = BDI_{15kips} - BDI_{9kips}$	Gives an indication of tensile strain at the bottom of the AC Layer and compressive stress at the top of the subgrade
Load Spreadability Index	$LSI = (D_{48}/D_{24})\chi F$	
Lower Layer Index	$LLI = D_{24} - D_{36}$	Gives an indication of the lower structural layers like the selected and the subgrade layers
Maximum Deflection	D_0	Gives an indication of all structural layers with about 70% contribution by the subgrade
Middle Layer Index	$MLI = D_{12} - D_{24}$	Gives an indication of the subbase and probably selected layer structural condition
Radius of Curvature	$R = \frac{r^2}{(2D_0(\frac{D_0}{D_r} - 1)}$	Structural Indicator of Surface and Base Layer

Deflection Basin Parameter (DBP)	Formula	Structural Indicator
Radius of Influence	$RI = \chi/D_0$	
Shape Factor 1	$F_1 = (D_0-D_{24})/D_{12}$	Structural Indicator of Surface and Base Layer.
Shape Factor 2	$F_2 = (D_{12}-D_{36})/D_{24}$	Determination of condition of the layer at the equivalent depth.
Additional Shape Factor	$F_3 = (D_{12}-D_{36})/D_{24}$	Lower layer strength
Slope Difference	$SD = (D_{36}-D_{60})_{15kips} - (D_{36}-D_{60})_{9kips}$	
Slope of Deflection	$SD = \tan^{-1}[(D_0- D_r)/r]$	
South African Radius of Curvature	$ROC = \frac{L^2}{2D_0(1-\frac{D_{200}}{D_0}}$	Gives an indication of the structural condition of the surfacing and base condition
Spreadability	$S= \frac{25(D_0+D_{12}+D_{24}+D_{36})}{D_0}$	Overall pavement strength
Structural Strength Index	$SSI = A_x / (X_{min} \times E_{min})$	Overall pavement strength
Structural Integrity Index	$SII = A_x (X_s \times E_m)$	Overall pavement strength
Surface Curvature Index	$SCI = D_0 - D_{12}$	Make inferences regarding the asphalt layer
Tangent Slope	$TS = (D_0- d_x) / x$	

Note:

D_r = Measured surface deflection

r = Distance/sensor position from load center (inch)

a= ¼ of the deflection basin length

χ = Distance from point of maximum deflection to tangent point

F= Minimum of D_{12}/D_0, D_{24}/D_{12} ,…., or $D_{72}/D6_0$

L = 200 mm for FWD

A_x = Area under the surface modulus profile to X_s

X_s = Radial distance from the test load

E_m = Estimated subgrade modulus

2.8.7 Determination of Structural Capacity of Pavement

Structural capacity of the pavement can be determined from the backcalculated layer moduli and deflection data from FWD testing.

Subgrade Modulus Backcalculation

The surface deflection measured at a sufficiently large distance from the center of FWD loading plate is affected by the subgrade strength and is independent of the size of the loading plate. The subgrade resilient modulus can be estimated using Equation 2.7 (AASHTO 1993).

$$M_{\mathrm{R}} = \frac{0.24\,P}{d_{\mathrm{r}} r} \quad \text{.....Eqn. 2.7}$$

where,

M_R = Backcalculated subgrade resilient modulus (psi)

P = Applied load (psi)

d_r = Deflection at a distance r (in.) from the center of the loading plate (in.)

To achieve a good estimate of the subgrade modulus, the deflection must be measured far enough away from the load independent of the effects of any layers above but also close enough so that it does not become too small to measure accurately. The AASHTO 1993 guide further suggested that the minimum sensor distance (r) should be greater than or at least equal to the radius of the stress bulb (a_e) at the subgrade-pavement interface (AASHTO 1993) as presented in Equation 2.8.

$$a_{\mathrm{e}} = \sqrt{a^2 + \{D\sqrt[3]{\frac{E_{\mathrm{P}}}{M_{\mathrm{R}}}}\}^2} \quad \text{.....Eqn. 2.8}$$

where,

a = Radius of load plate (in.)

D = Total thickness of the pavement layers above the subgrade (in.)

E_P = Effective modulus of all pavement layers above the subgrade (psi) (Eqn. 2.9)

M_R = Subgrade resilient modulus (psi)

Effective pavement modulus

Effective pavement modulus (E_P) is another structural capacity indicator that can be obtained from the FWD deflection data if subgrade resilient modulus and total thickness of all layers above the subgrade are known. Equation 2.9 can be used to compute the effective pavement modulus (AASHTO 1993).

$$\frac{M_R d_0}{qa} = 1.5 \left\{ \frac{1}{\sqrt{1+\left(\frac{D}{a} \times \sqrt[3]{\frac{E_P}{M_R}}\right)^2}} + \frac{\left[1 - \frac{1}{\sqrt{1+\left(\frac{D}{a}\right)^2}}\right]}{\left(\frac{E_P}{M_R}\right)} \right\} \quad \text{.....Eqn. 2.9}$$

where,

M_R = Subgrade resilient modulus (psi)

d_o = Deflection measured at the center of the load plate and adjusted to a standard temperature of 68° F (in.)

q = Load plate pressure (psi)

D= Total thickness of the pavement layers above the subgrade (in.)

a = Radius of load plate (in.)

E_P = Effective modulus of all pavement layers above the subgrade (psi)

Effective structural number

The Structural Number (SN) is considered the most powerful indicator of the structural condition of a pavement due to its versatile applicability and adaptability to various material types and environmental conditions. The SN can be an easy and reliable way of expressing performance of flexible pavements using FWD deflection data as it does not require the complex backcalculation process. The approach is based on several simplifying assumptions of soil support, traffic load, terminal serviceability, and environment. Because of the simplicity of this process, SN can be efficiently used as a network level pavement management tool (Gedafa 2008, Romanoschi and Metcalf. 1999).

Various studies established different approaches to estimate SN of an existing flexible pavement directly from the FWD deflection data. A mechanistic procedure to estimate SN from FWD deflections was first introduced by Jameson (Jameson 1993) as presented in Equation 2.10.

$$SN = 13.47 - 6.47 \log (DEF_0) + 3.697 \log (V_{900}) \quad \text{.....Eqn. 2.10}$$

where,

SN = Structural number of the pavement

DEF_0 = Temperature-corrected central deflection (microns)

V_{900} = Normalized deflection at 900-mm offset (microns)

AASHTO design guide for pavement structures (1993) suggested two approaches for estimating SN. The first one was calculating SN of existing flexible pavements based on the condition survey data. In this method, structural layer coefficients for the surface and base layers are assigned according to severity of distresses at the pavement surface. Equation 2.11 presents the first AASHTO method of calculating SN.

$$SN = \Sigma\, m_i \times a_i \times h_i \quad \text{.....Eqn. 2.11}$$

where,

m_i = Drainage coefficient of layer i, applied only to granular materials

a_i = Structural coefficient of layer i

h_i = Layer thickness of layer i (in)

The layer coefficients used in this procedure indicate the contribution of each layer to the overall performance of pavement structure and derived from stress-and-strain calculations in a multilayered pavement system. Typical values of structural-layer coefficients for different pavement materials are suggested in literature (Yoder and Witczak 1975, Paterson 1987).

To remove the complications of stress-strain calculations and uncertainties from using typical layer coefficients value, AASHTO (1993) prescribed another method of estimating SN directly from the FWD testing results. This method is known as the Effective structural number (SN_{eff}) as presented in Equation 2.12.

$$SN_{eff} = 0.0045D(Ep)^{1/3} \quad \text{.....Eqn. 2.12}$$

where,

D= Total thickness of the pavement layers (in.)

E_P = Effective modulus of all pavement layers above the subgrade (psi) (Eqn. 2.9)

2.9 TSD Data Collection and Analysis Procedure

2.9.1 Factors Affecting TSD Data

Data obtained from TSD measurements can be influenced by some factors such as:

- Effect of speed on TSD measurements: Findings from the literature demonstrated that TSD measured deflection can be sensitive to the operating speed of the truck. A study collected TSD measurements at two different speeds of 30 and 45 mph on low volume pavements (LVR) and at 45 and 60 mph on the mainline. The results showed that coefficient of variation (COV) in the deflection slope values was significant (25 to 40 %) when the operating speed was higher (45 mph on LVR and 60 mph on mainline) (Rada et al. 2016). However, another study conducted by South African National Pavements Agency (SANRAL) concluded that TSD can measure the pavement behavior at a range of operating speed between 10 to 50 mph and can be very repeatable even at lower speeds (<10 mph) (Kannemeyer et al. 2014).
- Effect of pavement structure on TSD measurements: The effect of pavement stiffness and surface roughness on TSD deflection slope measurements was investigated by Gonzalo et al. (2016). The results demonstrated that there were some variations in deflection slope due to change in pavement stiffness and surface roughness. Pavement stiffness was quantified in terms of FWD central deflection, and the researchers found that section with higher FWD central deflections (i.e., less stiff) showed less variation in terms of deflection slope than the stiffer pavement sections. Meanwhile, there was no strong correlation between surface roughness and the TSD deflection slope (Rada et al. 2016). Another study suggested that the effect of pavement structure on TSD slope measurements is not clearly evident since the axle load can be dynamically amplified due to not only surface stiffness but also due to vehicle suspension type, travelling speed, tire contact pressure, tire thread pattern, axle load and wheel configuration.

2.9.2 TSD Data Collection

The most ideal operation of the TSD requires constant velocity input. This is achieved by mounting the Doppler lasers at an angle of approximately 2° from the vertical to ensure providing a constant speed input as a component of the measured horizontal vehicle velocity. Also, to nullify the effect that comes from the highly variable vertical suspension movement of the trailer. The lasers can measure velocities from three sources (Ferne et al. 2009):

- Horizontal vehicle velocity,
- Vertical and horizontal vehicle suspension velocities, and
- Vertical pavement deflection velocity.

The reference laser is expected to measure very little vertical pavement deflection velocity because of its location, so the response from this laser can be used to remove unwanted signals from the other principal measurement lasers. Calibration is required for TSD to produce deflection velocity measurements that depend primarily on traffic speed (Katicha et al. 2013).

Transport Research Laboratory (TRL) of United Kingdom proposed a TSD calibration procedure to ensure an accurate and reliable calibration technique. Such procedure aimed to minimize the inevitable error due to lack of precise alignment of the measuring and reference lasers (Ferne et al. 2009). The procedure suggested by TRL includes running the TSD over a relatively shorter stretch of pavement with uniform deflection. The deflection velocity recorded from this short travel by each of the four lasers will be integrated to calculate a distance. The calculated distance then become dependent on the following three variables:

- The horizontal distance travelled by the TSD,
- The deflection velocity of the pavement under TSD loading, and
- The angle from the vertical at which the laser is mounted.

If the horizontal distance travelled by the TSD and the vertical deflection velocity are known, it is possible to calculate the correct angle from the vertical for all four lasers. The researchers of TRL also suggested that an accelerometer can be used to record the deflection velocity under TSD loading so that calibration process become smooth (Ferne et al. 2009).

2.9.3 Principle of TSD Deflection Measurement

The primary output of the TSD is the deflection slope, which is obtained from dividing the deflection velocity by the instantaneous survey speed of the truck (Figure 2.6).

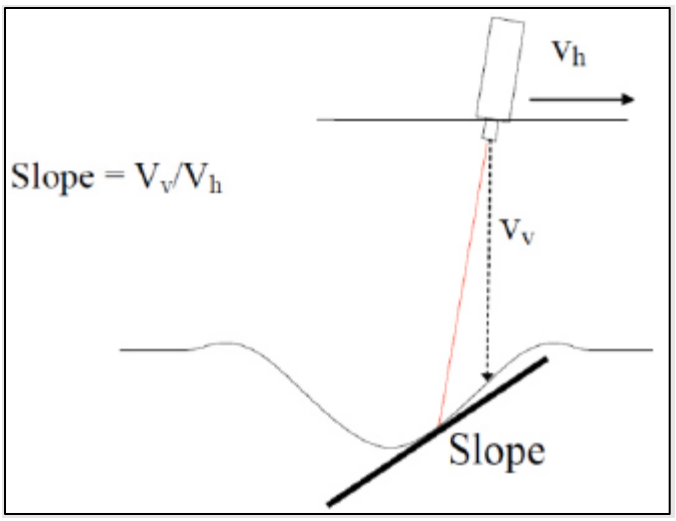

Figure 2.6 Calculation of Slope from TSD Deflection Bowl (Březina et al. 2017)

Deflection velocity is measured in mm/s, whereas the driving or survey speed is measured in m/s. Therefore, the deflection slope measurements are in units of mm/m (Katicha et al. 2013).

2.9.4 TSD Data Analysis

As discussed earlier, the main output from the TSD measurements is vertical velocity collected by the Doppler lasers and the deflection slope calculated from the velocity, determining deflection measurements from these data has always been a key issue (Muller and Roberts 2012). In this section some existing methodologies of analyzing TSD data and obtaining a deflection profile from it are outlined.

Researchers of Danish Pavement Institute (Taybji and Erland 2000) proposed a method of transformation of velocity data derived from TSD into absolute deflections by integration. Based on their earlier work at the Danish Pavement Institute in 1990, the researchers fitted a sixth-order polynomial curve fit to FWD deflection bowl measurements and determining the velocity profile from the first derivative of that curve fit, the approach of curve fitting multiple measured deflection velocities and integrating the fit to produce the absolute deflection profile was proposed. However, the idea is unclear in a sense that the TSD produces an instantaneous measurement of surface velocity, so there is no obvious time period over which surface velocities can be integrated to produce any deflection measurement (Muller and Roberts 2012).

Earlier work included a High Speed Deflectograph (HSD), which is a prototype of TSD, reported that the slope measurements are sensible to weather conditions like temperature, precipitation, and wind during the time of measurements. Simonin et al. (2005) found that HSD slope measurements are comparable with FWD and can detect clear differences in bearing capacity levels of pavements. However, HSD

measurements should not be converted into deflection measurements using the linear regression method (Simonin et al. 2005).

Later, European researchers and scientist demonstrated that the current TSD output with three deflection slopes can be used to derive a two-parameter model such as an elastic beam on a Winkler foundation of linear springs shown in Figure 2.7 (Krarup et al. 2006).

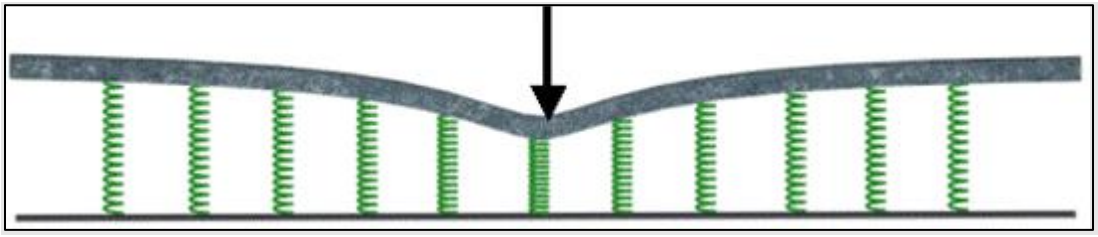

Figure 2.7 Deflection Basin from a point load on a Winkler foundation Model (Krarup et al. 2006)

Based on the proposed theory, a group of researchers and scientists and industry partners known as European Study Group with Industry (ESGI) developed equations to describe relevant deflection parameters and bearing capacity characteristics as summarized in Table 2.6 (Krarup et al. 2006).

Table 2.6 Family of Functions Proposed by ESGI (Krarup et al. 2006)

Deflection Parameter	Equation
Deflection	$d\,(x) \;=\; -\frac{A}{2B}\,(\cos(Bx) \;+\; \sin(Bx))e^{-Bx}$
Deflection Slope	$d'\,(x) \;=\; A\sin(Bx)\;e^{-Bx}$
Curvature	$d"\,(x) \;= AB\,(\cos(Bx) \;-\; \sin(Bx))\;e^{-Bx}$
Elasticity	$E \;=\; \frac{3\sqrt{2}}{4h^3}\,F\,.\frac{1}{AB^2}$
Stiffness	$k \;=\; \frac{\sqrt{2}}{AB}F$
Maximum Deflection	$d(0) \;=\; -\frac{A}{2B}$
Structural Curvature Index 300	SCI_{300} = d (0) – d (300)
Maximum Slope	$d'\,(\frac{\pi}{AB}) \;=\; \frac{e^{-\pi/4}}{\sqrt{2}}A$
Curvature Under the Wheel	d"(0) = AB

This modelling approach was redefined by Rasmussen et al. (2008) by theorizing that the TSD slope measurements is based on Euler-Bernoulli beam equation and the results can only be considered reliable in the vicinity of the measurement points near the wheel load. Promising results and repeatability were obtained in terms of Structural Curvature Index (SCI_{300}) and maximum deflection under the center of the load from this simple two-parameter model. The study recommended to get further reliable results from the load center, more sensors should be installed at positions further from the center of the load.

While the researchers of Denmark and Italy focused on SCI_{300} for TSD data interpretation, TRL from UK reported most data in terms of the slope of the velocity (Figure 2.8) data from a single laser measure (Lorenzetti, 2013). The principle aim of the UK researchers was to develop a simple relationship between slope measured by TSD to deflection as measured by the Deflectograph (Muller and Roberts 2012).

Muller et al. (2012) proposed a revised approach for analyzing TSD data based on the general approach of curve fitting described by his predecessors (Tayabji and Erland 2000, Krarup et al. 2006 and Rasmussen et al. 2008) that enable full deflection bowl prediction. The deflection profile presented in their study was built up by numerically integrating the plot working from a fixed point at or beyond the edge of the deflection bowl towards the wheel load. Although the direction of integration and use of numerical methods were simple, the deflection bowl was built up in a way that highlighted the contribution of velocity measurements further from the wheel to both the shape of the deflection bowl and accuracy of maximum deflection predictions. The researchers demonstrated that this approach also enabled the use of more flexible curves or the use of a combination of different curve segments to better fit the TSD measurements. A graphical representation of the proposed approach is shown in Figure 2.8. Based on the proposed approach, a fairly strong correlation was observed between the shape and magnitude of TSD deflection bowls and the corresponding FWD measurements. Although maximum deflection (d_0) and SCI_{300} obtained from this TSD deflection bowl showed slight overestimation than the corresponding FWD measurements, this variability is expected due to differences in the nature of pavement loading, use of averaging in the TSD measurements and other aspects such as too few measurement lasers on the TSD configuration used in the study.

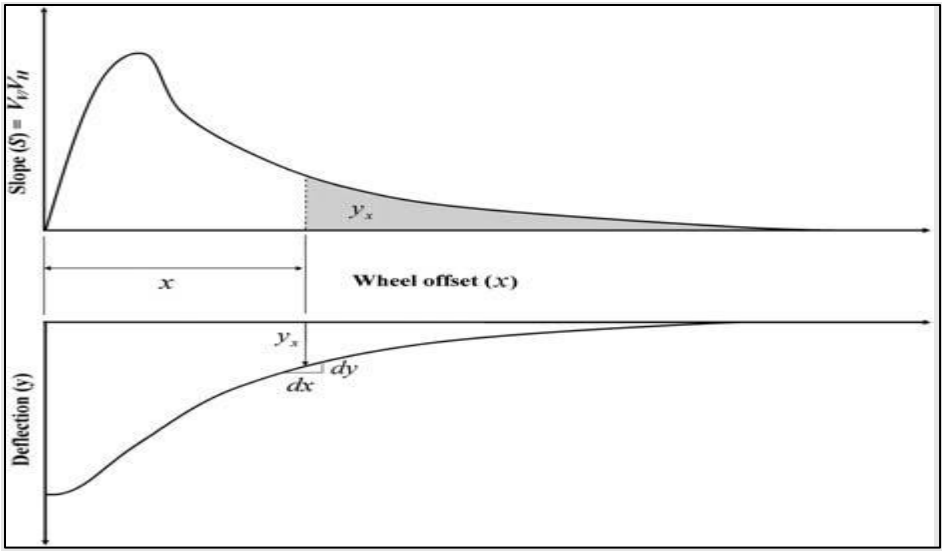

Figure 2.8 The deflected Pavement Profile (bottom) can be Determined as the Cumulative Area under the Plot of VV/VH vs. Wheel Offset (x) (top) (Muller and Roberts 2012)

After revisiting the existing models for estimating deflections under a moving wheel load, Pedersen (2013) proposed a visco-elastic deflection model framework by using Finite Element Modeling (FEM) combined with Laplace transformation (Pedersen 2013). Both simulated and real TSD data was used to measure the slope and fit this slope into a sum of two probability density functions to estimate deflection basin up to 60 inches (Rada et al. 2016). Pedersen (2013) recommended further calibration of the synthetic model for better understanding of pavement dynamics and fitting TSD data more effectively.

2.9.5 Use of FWD Data in the PMS in USA

Emergence of a PMS in the highway system of the US was first paved by a pioneer research work conducted through NCHRP research project 215 (NCHRP 1979). Pavement management includes all the activities involved in the planning, design, construction, maintenance, rehabilitation and reconstruction of the pavements that are part of a public works program. PMS consists of a set of tools and methodologies that can assist decision makers and engineers in finding optimum solutions and strategies for evaluating, providing, and maintaining pavements in a serviceable condition over a period (AASHTO 1990). Main purpose of a PMS is to ensure the best possible yield from the limited available funding by a systematic, efficient, and consistent method for selecting proper Maintenance and Rehabilitation (M&R) strategies to determine priorities and optimal time of repair by predicting future pavement conditions (NCHRP 1979, Shahin 2005).

FWDs have been in use since 1980s in the PMS in US. According to a survey conducted by NCHRP, 45 state highway agencies are using 82 FWDs in their PMS. Since most of the state highway agencies have created their own guidelines of using FWD rather than following the LTPP guideline and there is no particular

standard of data collection, analysis, maintenance and calibration. Therefore, project and network level FWD data collection and analysis vary from state to state (Alvi et al. 2008). In this section, current practices and proposed research outcomes from different states regarding FWD data collection and analysis are briefly summarized.

2.9.6 Modified Structural Index by Virginia Department of Transportation

Virginia Department of Transportation (VDOT) uses a Dynatest Model 8000 FWD to collect deflection data at the network level. Common practice of VDOT is to compute two different indices such as Load-related Distress Rating (LDR) and Non-load-related Distress Rating (NDR) from the data collected during the periodic distress survey. The minimum value between two indices is defined as the Critical Condition Index (CCI), which ranges from 1 to 100. Based on the obtained CCI, different M&R strategies are selected. In addition, a structural condition-based index was developed by utilizing the FWD deflection data collected during the period between 2005-2007 (Bryce et al. 2013). The index is known as the Modified Structural Index (MSI) and is presented in Equation 2.13.

$$MSI = \frac{0.4728*(D_0-D_{1.5HP})^{-0.481}*Hp^{0.7581}}{0.05716 * (\log(ESAL) - 2.32 * \log(Mr) 9.07605)^{2.36777}} \quad \text{..... Eqn. 2.13}$$

where,

D_0= FWD central deflection (thousandth of an inch [mils.])

$D_{1.5Hp}$= FWD deflection at a distance 1.5 x total pavement thickness from the center of the FWD loading plate (mils.)

H_p = Pavement thickness (in.)

ESAL = Equivalent single axle load

M_r = Subgrade resilient modulus (ksi)

Although there were no significant correlations between the MSI values and pavement surface distresses, MSI values showed a strong correlation with the rate of deterioration of pavements. Sections with lower MSI values deteriorated functionally a lot faster compared to the sections with higher MSI values. A numerical threshold between 0 and 1 was developed so that it could be readily available for implementation into the VDOT decision tree/matrix (Elbagalati et al. 2016).

2.9.7 Structural Strength Index by Indiana Department of Transportation

Indiana collects FWD deflection data both in network level (every three to five years) and project level (according to the specific needs of the project). Utilizing these large datasets, a structural condition-based index between zero to 100 was proposed for implementation by Indiana Department of Transportation (INDOT) (Flora et al. 2010). Necessary deflection and distress survey data for this study were collected from INDOT pavement management databases. Associated data such as traffic information, highway classification, weather conditions etc. were obtained from INDIPAVE (a database that includes data of over 10,000 one-mile pavement sections in Indiana). This data includes information on 12,250 pavement sections from 1999 to 2007. For the analysis, different types of pavements were grouped into six families based on the type of pavement (e.g., flexible or rigid) and the functional class (Interstate, National Highway System [NHS], and Non-NHS). The model presented in Equation 2.14 was developed to calculate the Structural Strength Index (SSI) for each of the six families knowing the FWD central deflection. Threshold and trigger values were proposed for SSI implementation in INDOT PMS decision matrices (Elbagalati et al. 2016).

$$SSI_{jk}=100\left\{1-\alpha e^{\frac{-\beta}{\sigma^{\gamma}}}\right\} \quad \text{……Eqn. 2.14}$$

where,

j,k = indices identifying the pavement family

α, β, γ = regression coefficients based on the pavement family

σ = center surface deflection (mils.)

2.9.8 Structural Health Index and Pavement Condition Index by Louisiana Department of Transportation

Common practice at Louisiana Department of Transportation and Development (LADOTD) is to calculate Pavement Condition Index (PCI) based on the collected distresses and performance data once every two years. The distresses and performance data are collected using the Automatic Pavement Analyzer (ARAN®) system which provides a continuous assessment of the pavement network. The PCI has an established scale from zero to 100 with threshold values that are used to trigger a specific course of M&R strategies. In addition, a research initiative was undertaken to develop a structure condition-based index for Louisiana which is known as Structural Health Index (SHI), which is on a scale of zero to 100. The SHI can predict the structural integrity of the pavement structure based on the backcalculated layer moduli of in-service pavements obtained from FWD testing. The approach of using backcalculated layer moduli

instead of deflection values was chosen to incorporate the structural contribution of each layer along with its impact on the pavement overall structural capacity (Elbagalati et al. 2016).

The first step of obtaining SHI is to conduct the backcalculation analysis using the deflection basin method of ELMOD 6 software. After getting the backcalculated layer moduli, changes in SN can be quantified as the difference between the pavement SN at the time of construction and at the time of FWD testing. Then, Equation 2.15 is used to calculate the SHI. The SHI can be defined based on the loss in SN such that it was scaled logistically from zero to 100. A sigmoidal function was selected with constant parameters to represent the correlation between loss in SN percent and the SHI such that sections with loss in SN ≥ 50 percent have SHI value near zero, and sections with minimal or no loss in SN have SHI value near 100 (Elbagalati et al. 2016). After the successful evaluation and validation of the SHI, a modified decision matrix was developed with established threshold values so that the SHI can be implemented in the LADOTD PMS.

$$SHI = \frac{100}{1+e^{0.15\,(SN\ loss\ \%-30)}} \qquad \text{.....Eqn. 2.15}$$

2.9.9 Structural Condition Index by Texas Department of Transportation

Texas Department of Transportation (TxDOT) periodically collects FWD data and stores the data in the Pavement Management Information System (PMIS). But due to the lack of proper thickness information of each layer in the PMIS, backcalculation of the layer moduli cannot be determined from the FWD data. To assess the structural condition of pavements using FWD deflection data without information about the thickness of each layer, TxDOT PMIS currently uses a structural screening index known as the Structural Strength Index (SSI). Later, studies found that the SSI is not sensitive enough to the real condition of the pavement. Therefore, researchers suggested a new approach for determining FWD-based structural condition, primarily based on the SN and Structural Condition Index (SCI) (Zhang et al. 2003).

The FWD deflection and other data used in the study was collected from TxDOT PMIS. The researchers found that the existing practice of determining SN can be a reasonable indicator of structural condition of a pavement. Rhode (1994) proposed Rhode's method for calculating SN based on an established "two-third" rule (Irwin 1983) that assumes that 95 percent of the deflections measured on the surface of a pavement originate below a line deviating 34 degrees from the horizontal (Figure 2.9).

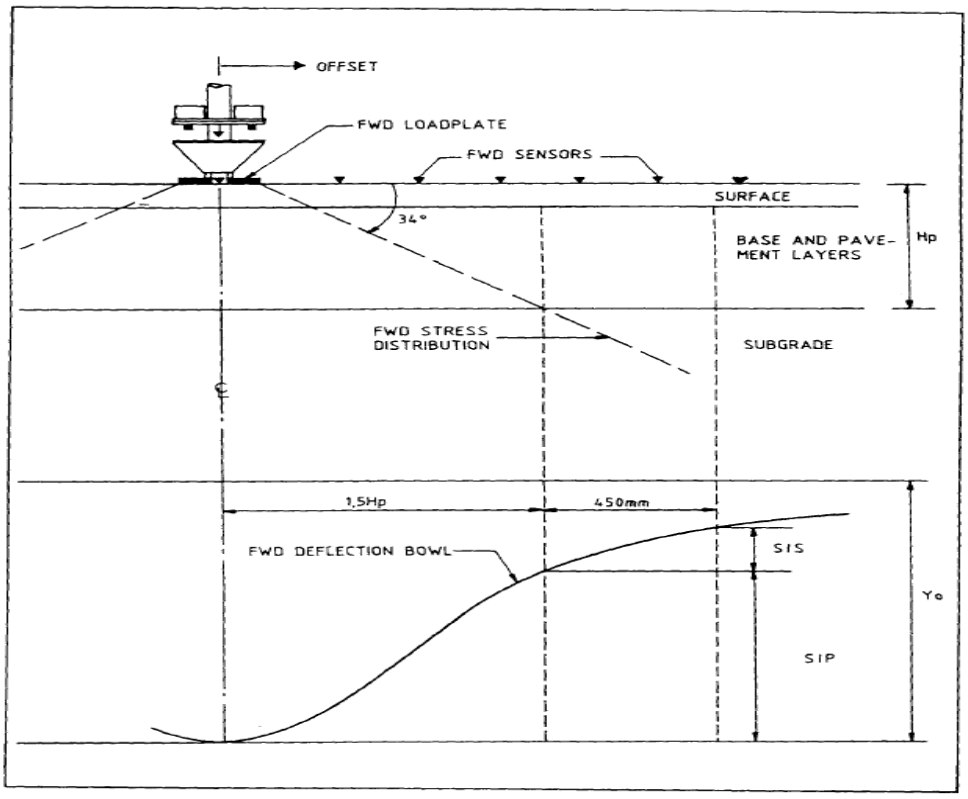

Figure 2.9 The Stress Distribution and Measured Deflection Bowl Beneath FWD Load (Rohde 1994)

Based on this simplification, Rhode concluded that the surface deflection measured at an offset of 1.5 times the pavement thickness originates entirely in the pavement subgrade. Comparing this deflection value with the peak deflection under the loading plate, the Structural Index of Pavement (SIP) could be determined. SIP can be defined as the amount of deflection that has occurred within the pavement structure (Equation 2.16).

$$SIP = D_0 - D_{1.5Hp} \quad \text{.....Eqn. 2.16}$$

where,

SIP = Structural index of pavement

D_0 = Peak deflection measured under a standard 9,000-lb FWD load

$D_{1.5Hp}$ = Surface deflection measured at offset of 1.5 times of Hp under a standard 9,000-lb FWD load

H_p = Total pavement thickness

Finally, the SN can be calculated with the known total thickness of pavement and the SIP value (Equation 2.17).

$$SN = k_1 SIP^{K2} H_p^{K3} \quad \text{.....Eqn. 2.17}$$

where,

SN = Pavement structural number (in.)

SIP = Structural Index of pavement (microns)

Hp = Total pavement thickness (mm)

K1, K2, K3 = Regression coefficients

This procedure of calculating the SN from the deflection data with the "two-third" rule is relatively simple, sensitive to pavement deterioration and the researchers indicated that it can be easily implemented in the TxDOT PMIS (Zhang et al. 2003).

If the existing and required SN values of a pavement is known, another structural condition estimator SCI can be obtained. SCI can be expressed by the ratio of the existing SN and the required SN as presented in Equation 2.18.

$$SCI = \frac{SN_{\text{eff}}}{SN_{\text{req}}} \quad \text{.....Eqn. 2.18}$$

where,

SCI = Structural Condition Index

SN_{eff} = Existing structural number

SN_{req} = Required structural number

The required SN is calculated based on the estimated ESALs for the next 20 years or whatever time frame the agency determines for estimating the accumulated ESALs. SCI value equal or greater than one would indicate that the pavement is in a sound structural condition, while SCI less than one implies that the pavement is no longer structurally adequate. Because of the simplicity of the SCI, interpretation and implementation of this index should be straightforward.

2.9.10 Pavement Structural Evaluation by Kansas Department of Transportation

The Kansas Department of Transportation (KDOT) used a subjective pavement rating known as Pavement Structural Evaluation (PSE). Researchers proposed an improved method for determining PSE based on the classical multiple regression analysis using deflection data and network level distress survey (Chowdhury et al. 1999). A parallel study used Bayesian regression methodology developed by Canadian strategic highway research program and the Bayesian regression models provided slightly better results for some pavements (Chowdhury 1998).

KDOT categorized flexible pavements as Full-Design Bituminous (FDBIT) and Partial-Design Bituminous (PDBIT) pavements and the researchers collected the following data for the abovementioned study:

- Pavement surface deflection from FWD data,
- Average annual ESALs,
- Age of pavement (years) since last rehabilitation action,
- Thickness of Asphalt Concrete (AC) and overlays, and
- Types and years corresponding to different rehabilitation actions.

Based on the observed distress level, three simple linear regression models were developed for FDBIT to predict PSE.

Distress Level 1:

$$PSE = 0.216* (AGE)^{1.5} - 20.82*\exp [SN] + 0.138*TH + 0.328* PSE + 17.65*DL1 \quad \text{……..Eqn. 2.19}$$

Distress Level 2:

$$PSE = 0.216* (AGE)^{1.5} - 20.82*\exp [SN] + 0.138*TH + 0.328* PSE + 18.06* DL2 \quad \text{……..Eqn. 2.20}$$

Distress Level 3:

$$PSE = 0.216* (AGE)^{1.5} - 20.82*\exp [SN] + 0.138*TH + 0.328* PSE + 18.38* DL3 \quad \text{……Eqn. 2.21}$$

where,

PSE = Predicted decrease in the PSE value

AGE = Age of pavement since the last rehabilitation action (in years)

SN = Decrease in structural number (SN obtained from the FWD first sensor deflection)

TH = AC layer thickness (inches)

PSE = PSE value assigned to the pavement section immediately after the last action

DL_i = Distress level due to transverse cracking (I =1, 2 and 3)

Three simple linear regression models were also developed for PDBIT pavements. The PSE values obtained from the proposed models were recommended to be used as "suggested PSE values" along with the current KDOT practice (Chowdhury et al. 1999).

2.9.11 Practice of Idaho Transportation Department

FWD is an integral part in the PMS of Idaho Transportation Department (ITD). ITD collects FWD data every year from April to October on sections of the state highways that are eligible for paving projects and uses the obtained data for pavement design and rehabilitation. Deflection data collected from the FWD test is used to backcalcuate the layer moduli and estimate resilient modulus properties. MODULUS 7.0 computer program developed by TxDOT and Texas Transportation Institute (TTI) is the primary deflection data analysis tool used by ITD. A limited amount of subsurface drilling and sampling program is also used to confirm the backcalculated resilient modulus values and correlation with other strength design parameters (ITD 2017, Flora et al. 2010).

2.9.12 Use of TSD Data in the PMS in USA

Some state highway agencies in US incorporated TSDs in their PMS lately. This section highlighted some of these efforts.

To incorporate moving pavement deflection measurement technology in the PMS of highway agencies, FHWA undertaken a project in 2012 (Rada et al. 2016). The main purposes of this study were to assess, evaluate, and validate the capability of TSDs for structural evaluation of pavements at the network level and develop robust analysis methodologies to pave its application. Data for this study was collected from field trial testing in MnRoad facility and adjacent test sections in Wright County of Minnesota. Geophones and accelerometers were installed as embedded sensors to measure deflection velocity and displacement parameters. Deflection velocity data was collected from TSD measurements and surface deflections were also estimated based on the two methodologies found in the literature (Krarup et al. 2006, Pedersen 2013). High precision and repeatability were achieved for data collected with the first three sensors of TSD. The 3D Move software was used to calibrate the data collected from both the TSD and from the installed sensors. Although some discrepancies were noticed between the vertical pressure data collected by MnRoad sensors and those computed by the 3D Move software, overall, it was concluded that the 3D

Move could predict field measured surface displacements histories and interior pavement responses like stresses and strains. Therefore, it was recommended by the authors that the 3D Move could be used to evaluate pavement response under TSD loading. A temperature correction procedure for TSD data was also proposed by the researchers. The authors also attempted to identify some effective deflection basin indices from the TSD measurements which can relate to critical pavement responses and thus structural adequacy of the pavement can be determined. Seventy-five individual indices were calculated and correlated with pavement structure related responses. Based on the goodness of the correlation between the indices and pavement responses, most appropriate indices for TSD were selected as radius of curvature (R1 and R2), SCI, Deflection Slope Index (DSI), Slope of Deflection (SD), Tangent Slope (TS), and Area Under Pavement Profile (AUPP). However, DSI and SCI300 were found to be the most effective indices that can predict pavement structural condition at the network level from TSD data. The study also recommended improvement in the number of sensors and their locations can augment the information that can be derived from a TSD.

Another study in Louisiana (Elseifi et al. 2018) aimed to assess the feasibility of using TSD measurement at the network level for structural condition evaluation of pavements and in backcalculation analysis. Data from both FWD and TSD measurements were collected from district five of Louisiana, MnPAVEMENT research test facility and some sections of Idaho. Collected raw measurements from the TSD were converted into deflection basin using the Area under the Curve (AUTC) methodology proposed by Muller (Muller and Roberts 2012). This study also utilized the Artificial Neural Network (ANN) methodology to backcalculate the layer moduli for flexible pavements using the TSD deflection values. In addition, this study demonstrated that there was a clear statistical difference between the FWD and TSD deflection data due to the fact that loading characteristics and load type are different for two devices, the ANN model converted the TSD deflection basin to a corresponding FWD deflection basin, which was referred as TSD*. The converted deflection values obtained from the ANN model (TSD*) were then used to conduct the backcalculation analysis using the ELMOD6 software. Both the FWD and TSD* deflection basin data were used to calculate the 3D Move generated critical pavement responses such as horizontal tensile strain at the bottom of the AC layer (ε_t) and the vertical compressive strain at the top of the subgrade (ε_v). A non-linear regression model was also proposed by the researchers to calculate the Structural Number (SN) of in-service pavements from the TSD data. The model is presented in Equation 2.22.

$$SN_{TSD} = 18.67\, e^{(-0.013D_0)} + 8.65\,(D_{48})^{0.11} + 0.18\,(T_{th}) + 0.31 \ln(ADT) - 24.28 \quad \text{……Eqn. 2.22}$$

where,

SN_{TSD} = SN based on TSD measurement

D_0 = Deflection of pavement under loaded tire or Center Deflection (mils)

D_{48} = Deflection at 48 in. distance from Center Deflection (mils)

T_{th} = Total layer thickness of pavement (in.)

ADT = Average Daily Traffic (veh/day)

The model was successfully validated with SN calculated based on TSD and FWD deflection data obtained from two contrasting data sets from Louisiana and Idaho.

In a separate study, Nasimifar et al. (2019) developed a practical approach of estimating SN from TSD data of in-service flexible pavements. The basic principle of determining SN was same as the study described above, SN_{eff} from the TSD data using the proposed method should be in good agreement with SN_{eff} from the FWD testing using the AASHTO method. A database of 426 pavement structures was generated and analyzed in the 3D Move software using both linear elastic and viscoelastic approach to generate FWD and TSD deflection bowls. The model presented in Equation 2.23 was proposed based on the analysis.

$$SN_{eff} = C1SIP^{C2}H_p{}^{C3} \quad \text{……Eqn. 2.23}$$

where,

SN_{eff} = Effective SN from TSD data

SIP = Structural Index of Pavement (μm) = $D_0 - D_{1.5H_P}$ (D_o and $D_{1.5HP}$ are corresponding to TSD data)

H_p = Total pavement thickness (mm)

C1, C2, and C3 = Calibration coefficients (C1 = 0.4369; C2 = -0.4768; C3 = 0.8182)

The proposed model was validated using field FWD and TSD data collected from the same pavement sections at the same time. A good correlation was observed between the calculated SN using the proposed model and the AASHTO NDT method.

Another study by Virginia Transportation Research Council (Katicha et al. 2020) attempted to incorporate pavement structural condition information obtained from TSD into the Virginia Department of Transportation (VDOT) pavement management system decision making process for bituminous pavement sections. TSD data were collected from 4,000 miles of pavements (interstate and primary pavements) in the VDOT network. Deflection values were transformed from deflection slope using mathematical integrations. Several deflection indices including SCI_{300}, D_0, and SN_{eff} from TSD data were calculated and compared with FWD-based indices and VDOT performance parameters such as rutting, cracking, Critical Condition Index (CCI), Load- related Distress Rating (LDR) and non- LDR (NDR). TSD-based SN_{eff} was found similar to the FWD-based SN_{eff} and the calculated consistency between the TSD-based SN_{eff} and FWD-

based SN_{eff} was higher than the consistency between the SN_{eff} from two repeated sets of FWD measurements. The lower limit of TSD-based SN_{eff} to identify structurally deficient sections was proposed as the 30th percentile value. The use of S_{Neff} calculated from TSD measurements would be easier as this index is currently used by VDOT with FWD data. However, the study also concluded that using SCI300 would be more advantageous as it does not require the pavement thickness information and this parameter is mechanistically related to the tensile strain at the bottom of the asphalt layer.

2.9.13 Remaining Service Life from FWD Data

Remaining Service Life (RSL) can be defined as the anticipated number of years that a pavement will be functionally and structurally serviceable with only routine maintenance operations (Gedafa et al. 2010). The primary advantage of RSL is that the whole condition of the network can be assessed using a single numeric (Elkins et al. 2013). Usually, pavement condition survey results are used to determine RSL, although different researchers have tried to estimate RSL from FWD surface deflection data (Gedafa et al. 2010).

Scullion (1988) used a mechanistic approach of determining RSL back in 1988. The main purpose of his study was to determine a procedure through which FWD data can be used at the network level to calculate a structural health index (i.e., remaining life index). FWD data was used to calculate the tensile strains at the bottom of asphalt layer (ε_t) and the compressive strains at the top of subgrade (ε_v) with the help of backcalcuated layer moduli. Using the monthly deflection values, strains within the pavement for each month were calculated. Then, the Shell rutting model and Finn cracking model were used to estimate pavement remaining life.

KDOT used Equation 2.24 to estimate the design life of a nonroutine maintenance action for flexible pavements.

$$DL\ flex = 15.4 + 0.873 \times FDBit + 1.05 \times eq\ thick - 3.27 \times \ln(TCR_{prior} + 1) - 1.78 \times \ln\left(\frac{D - ADL}{eq\ thick}\right) - 0.0662 \times d_6$$

….. ……..…Eqn. 2.24

where,

DL flex = Design life of a nonroutine maintenance action

FDBit = Full-design bituminous (FDBit) index (FDBit pavement=1; otherwise=0)

eq thick=Equivalent thickness (in.) of the action (For example, equivalent thicknesses for conventional seal (chip seal), 25-mm cold mill, and 38-mm overlay are 6.4, 12.7, and 38 mm, respectively)

TCR_{prior}=Equivalent transverse cracking before the action

D – ADL = Design lane ADL (number of 80-kN single axle/day) in the year of the action

d_6 = Average surface deflection (microns) obtained from the most distant sensor of FWD

Later, Gedafa et al. (2010) demonstrated that there is a sigmoidal relationship between RSL and center deflection of FWD. They developed a sigmoidal RSL model based on multiple linear submodels where RSL was used as a dependent variable and the center deflection (d_0) was an independent variable. The RSL model and the linear submodels are presented in Equations 2.25 through 2.29. The sigmoidal RSL models can be used to predict RSL at the network level based on the center (first sensor) deflection of FWD.

$$RSL = \delta + \frac{\alpha}{1+ e^{\beta-\gamma d_0}} \quad \text{.....Eqn. 2.25}$$

$$\delta = \delta_0 + \delta_1 D + \delta_2 EAL + \delta_3 ETCR + \delta_4 EFCR + \delta_5 RUT + \delta_6 SN_{eff} \quad \text{.....Eqn. 2.26}$$

$$\alpha = \alpha_0 + \alpha_1 D + \alpha_2 EAL + \alpha_3 ETCR + \alpha_4 EFCR + \alpha_5 RUT + \alpha_6 SN_{eff} \quad \text{.....Eqn. 2.27}$$

$$\beta = \beta_0 + \beta_1 D + \beta_2 EAL + \beta_3 ETCR + \beta_4 EFCR + \beta_5 RUT + \beta_6 SN_{eff} \quad \text{.....Eqn. 2.28}$$

$$\gamma = \gamma_0 + \gamma_1 D + \gamma_2 EAL + \gamma_3 ETCR + \gamma_4 EFCR + \gamma_5 RUT + \gamma_6 SN_{eff} \quad \text{.....Eqn. 2.29}$$

where,

RSL = Remaining service life (years)

d_0 = FWD center deflection (mils)

D = Total pavement thickness above subgrade (in.)

EAL = Equivalent axle load per day

ETCR = Equivalent transverse cracking

EFCR = Equivalent fatigue cracking

RUT = Rut Depth (in.)

SN_{eff} = Effective structural number

Another study conducted by FHWA attempted to reformulate (FHWA 2013), the RSL concept as the term 'life' can represent multiple points in the pavement construction history. They suggested a more consistent approach would be adopting terminology which would indicate the amount of time remaining until a defined construction treatment is required. The RSL was replaced by Remaining Service Interval (RSI) which has the ability to unify the outcome of different approaches to determine needs by focusing on when and what treatments are needed, and the service interruption created. Step by step guidelines of different stages for implementing RSI were also prescribed (FHWA 2013).

2.9.14 Limitation of FWD Data and Research Gaps

Although FWDs have been used in the PMS in US for more than four decades, this device can certainly mark with some disadvantages like high initial cost, need for traffic control measure and lane closure, and relatively complex electromechanical system (Irwin et al. 2017). Some researchers also mentioned that the FWD operation could be time consuming and hazardous to motorists (Souliman et al. 2018). Since the process is relatively slower, it is often not possible to perform deflection testing throughout the entire length of a pavement project. Therefore, there is a high risk of missing critical sections and doubts arise whether the test sections measured are representative of the whole pavement section. These shortcomings become more critical at network level which often require measuring thousands of pavement miles (Rada et al. 2016). The collected data needs to go through complex computations based backcalculation analysis using multilayer elastic analysis software. Due to the complexity in the analysis process, FWD data are now mostly used in determining layer stiffness for overlay design. More research should be undertaken on how structural indices can be effectively calculated from the FWD data.

2.9.15 Emerging Needs/ Research Gaps in the Field of TSD

There are a number of studies throughout the last decade that demonstrated that the TSD can be effectively used at network level for PMS application with adequate repeatability. However, there is room for improvement so that state highway agencies can gain more confidence and use this state-of-the art technology in their routine pavement management operations. Some areas related to TSD where more research work needs to be invested are discussed below.

- Another area of concern regarding TSD measurements is the conciliation between repeatability and loss of details with spatial averaging. Some threshold values for repeatability and spatial averaging should be determined for future practice (Rada et al. 2015).
- Setting up accuracy and precision levels for TSDs is a viable equipment related to research need. Load levels applied to the pavement should also be standardized (Rada et al. 2012).
- A systematic calibration method is also needed for TSD.

- Pavement parameters need to be established for a specific TSD application (Rada et al. 2012).
- Examine more indices that can effectively relate pavement deflection to pavement conditions.
- Additional research is needed to accurately account for the effect of temperature on TSD measurements (Shrestha et al. 2018).

3. Methodology and Data Collection

Chapter 3 discusses the research methodology, FWD and TSD deflection data collection, pavement performance data (e.g., roughness, cracking, rutting), and a parametric theoretical study conducted using the 3D-Move software.

3.1 Traffic Speed Deflectometer (TSD) Data Collection

The TSD is a rolling wheel deflectometer that measures the pavement response to applied load. The TSD provides continuous deflection and performance results at the project and network levels while at traffic speed up to 50 mph. In Idaho, TSD was first used in 2016 to collect pavement deflection and field. Meanwhile, since 2019, it is being regularly used to collect deflection data across the state. Each year about 3,500 miles of pavement are typically examined using an intelligent Pavement Assessment Vehicle (iPAVe) developed by Australian Pavement Research Board (ARRB). In addition, TSD data were collected as part of a pilot study across multiple states. Figures 3.1 and 3.2 depict the type of data collected using the iPAVe. The performance data include IRI, rutting, alligator cracking, longitudinal cracking, and transverse cracking. In addition, the deflection data are collected as discussed later in this chapter.

ROAD_N	BLOCK	SECTION_SUB_CHAINAGE_FROM (mi)	D0 (mils)	D36 (mils)	D72 (mils)	IRI_AVG (in/mi)	RUT_LANE (in)	PERCENT_ALLIG_CRACK (%)	PERCENT_LONG_CRACK (%)	PERCENT_TRANS_CRACK (%)
SH-50	1	0.000	-16.8	-7.0	-2.8	261	0.27	0.00	1.09	0.33
SH-50	1	0.010	-10.2	-3.5	-1.1	131	0.28	0.00	0.00	0.00
SH-50	1	0.020	-7.3	-1.5	-0.4	87	0.26	0.13	1.47	2.41
SH-50	1	0.030	-7.1	-1.4	-0.4	41	0.17	0.00	0.00	0.00
SH-50	1	0.040	-10.0	-3.8	-1.6	60	0.28	0.00	0.26	0.00
SH-50	1	0.050	-7.6	-2.5	-0.7	34	0.28	0.00	0.00	0.00
SH-50	1	0.060	-8.0	-2.6	-0.8	32	0.28	0.00	0.00	0.00

SECTION_SUB_CHAINAGE_FROM (mi)	SECTION_SUB_CHAINAGE_TO (mi)	SCI_8	SCI_12	SCI_SUBGRADE	D0 (mils)	D8 (mils)	D12 (mils)	D18 (mils)	D24 (mils)	D36 (mils)	D48 (mils)	D60 (mils)	D72 (mils)
0.000	0.010	0.8	1.2	-1.7	-8.2	-7.4	-6.9	-6.2	-5.3	-3.8	-2.9	-2.1	-1.5
0.010	0.020	0.8	1.2	-1.7	-8.8	-7.9	-7.6	-6.9	-6.0	-4.5	-3.6	-2.8	-2.0
0.020	0.030	1.1	1.8	-2.2	-10.4	-9.2	-8.5	-7.5	-6.3	-4.4	-3.2	-2.2	-1.5
0.030	0.040	0.9	1.5	-2.1	-9.8	-8.8	-8.2	-7.2	-6.2	-4.4	-3.2	-2.3	-1.5
0.040	0.050	1.2	2.0	-2.1	-11.9	-10.6	-9.8	-8.5	-7.2	-5.1	-4.0	-3.0	-2.2
0.050	0.060	1.3	2.0	-2.5	-11.8	-10.5	-9.7	-8.5	-7.2	-5.0	-3.6	-2.5	-1.7
0.060	0.070	1.1	1.8	-2.4	-11.9	-10.7	-10.0	-8.9	-7.7	-5.6	-4.3	-3.2	-2.3

Figure 3.1 TSD Collected Data

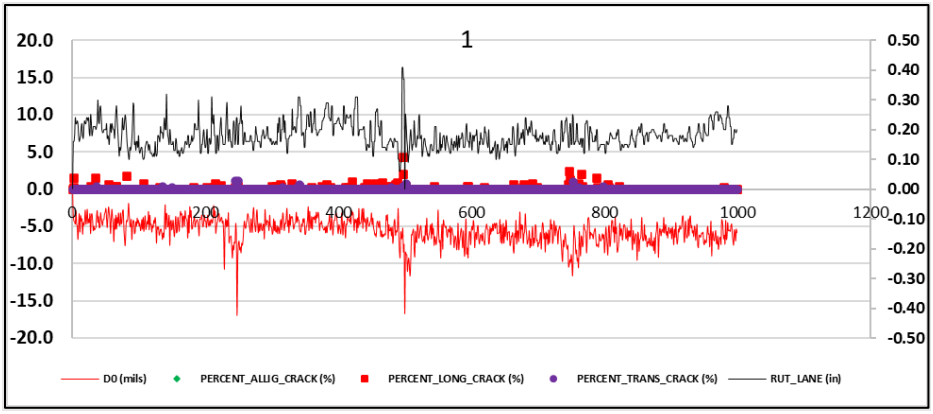

Figure 3.2 TSD Profile Data

The TSD measures the pavement deflection using a set of Doppler lasers mounted on a servo-hydraulic beam on the midline of the dual tires near the rear axle of a semitruck. The lasers are angled to measure the horizontal vehicle speed, vertical and horizontal vehicle suspension velocity, and vertical pavement deflection velocity (Ferne et al., 2009). The last sensor, positioned approximately 3.6 m in front of the rear axle, is located outside the deflection bowl and serves as a reference laser to eliminate unwanted measurements (Katicha et al., 2014) as shown in Figure 3.3.

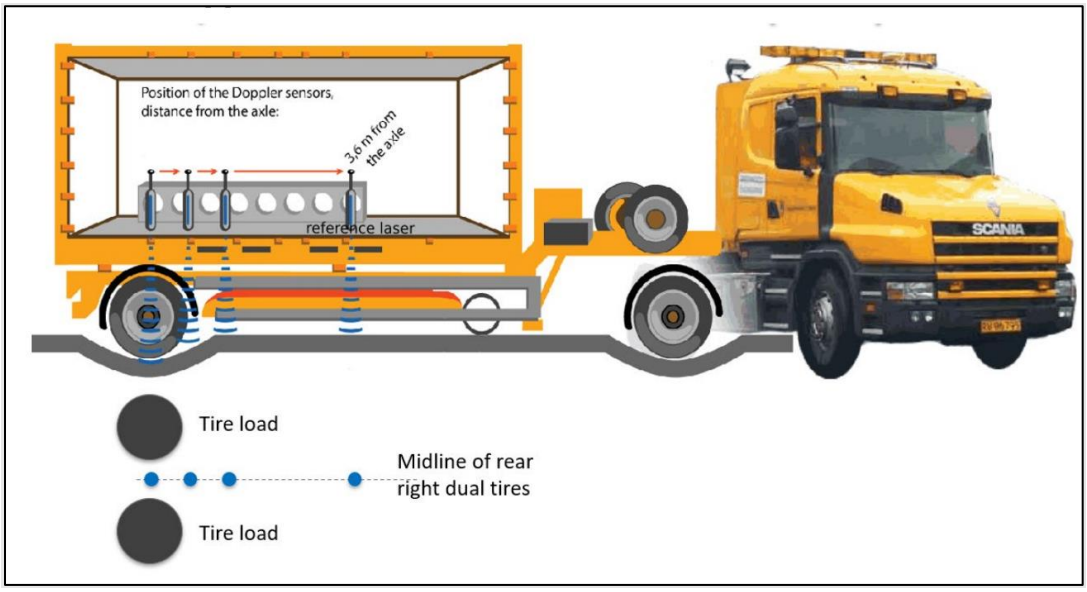

Figure 3.3 TSD truck and doppler lasers (Smith et al. 2017)

The TSD data are collected every 0.01 mile by a semitruck and aggregated into blocks of 5 miles, yielding 500 data points per block in each direction. Table 3.1 provides a summary of the pavement sections tested using the TSD and included in this study.

Table 3.1 Summary of Pavement Sections Tested using TSD

Section	Number of blocks
I-15	40
I-84	14
I-86	13
SH-25	12
SH-33	18
SH-39	11
SH-55	29
SH-75	9
US-20-D	10
US-20-E	28
US-26	21
US-30	27
US-91	18
US-93	48

3.2 Falling Weight Deflectometer (FWD) Data Collection

ITD collects FWD deflection data on eligible state highways annually for pavement design and rehabilitation purposes. The FWD equipment used by ITD consists of a trailer-mounted, non-destructive testing unit towed behind an F-250 pickup, as depicted in Figure 3.4 (ITD 2017).

Figure 3.4 ITD FWD Equipment (ITD 2017)

Modulus 6 software is often used to analyze the FWD deflection data and backcalculate the modulus values of different layers of examined pavement structure as shown in Figure 3.5. Modulus 6 is developed at the Texas A&M Transportation Institute for the Texas Department of Transportation (TxDOT). In this study, Modulus 6 was used by the researchers to process the FWD data.

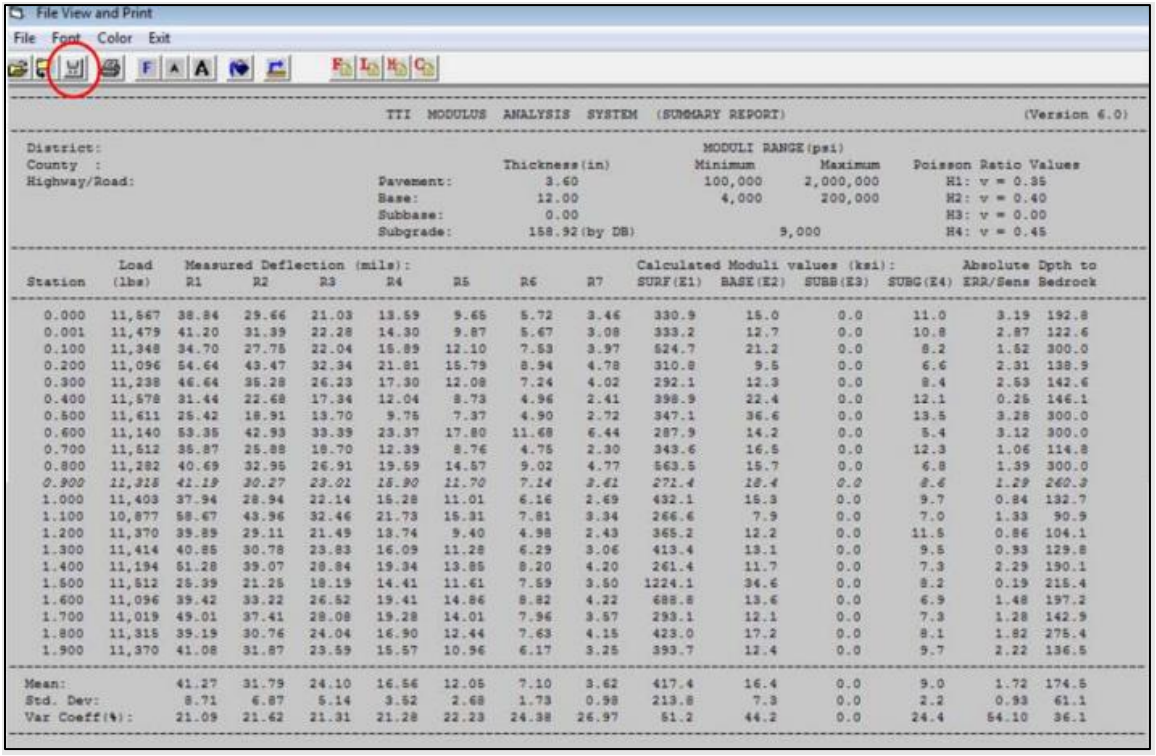

File View and Print

File Font Color Exit

TTI MODULUS ANALYSIS SYSTEM (SUMMARY REPORT) (Version 6.0)

District:
County :
Highway/Road:

	Thickness(in)	MODULI RANGE(psi) Minimum	Maximum	Poisson Ratio Values
Pavement:	3.60	100,000	2,000,000	H1: v = 0.35
Base:	12.00	4,000	200,000	H2: v = 0.40
Subbase:	0.00			H3: v = 0.00
Subgrade:	158.92(by DB)	9,000		H4: v = 0.45

Station	Load (lbs)	Measured Deflection (mils): R1	R2	R3	R4	R5	R6	R7	Calculated Moduli values (ksi): SURF(E1)	BASE(E2)	SUBB(E3)	SUBG(E4)	Absolute Dpth to ERR/Sens	Bedrock
0.000	11,567	38.84	29.66	21.03	13.59	9.65	5.72	3.46	330.9	15.0	0.0	11.0	3.19	192.8
0.001	11,479	41.20	31.39	22.28	14.30	9.87	5.67	3.08	333.2	12.7	0.0	10.8	2.87	122.6
0.100	11,348	34.70	27.75	22.04	15.89	12.10	7.53	3.97	524.7	21.2	0.0	8.2	1.62	300.0
0.200	11,096	54.64	43.47	32.34	21.81	15.79	8.94	4.78	310.8	9.5	0.0	6.6	2.31	138.9
0.300	11,238	46.64	35.28	26.23	17.30	12.08	7.24	4.02	292.1	12.3	0.0	8.4	2.53	142.6
0.400	11,578	31.44	22.68	17.34	12.04	8.73	4.96	2.41	398.9	22.4	0.0	12.1	0.25	146.1
0.500	11,611	25.42	18.91	13.70	9.75	7.37	4.90	2.72	347.1	36.6	0.0	13.5	3.28	300.0
0.600	11,140	53.35	42.93	33.39	23.37	17.80	11.68	6.44	287.9	14.2	0.0	5.4	3.12	300.0
0.700	11,512	35.87	25.88	18.70	12.39	8.76	4.75	2.30	343.6	16.5	0.0	12.3	1.06	114.8
0.800	11,282	40.69	32.95	26.91	19.59	14.57	9.02	4.77	563.5	15.7	0.0	6.8	1.39	300.0
0.900	*11,315*	*41.19*	*30.27*	*23.01*	*15.90*	*11.70*	*7.14*	*3.61*	*272.4*	*18.4*	*0.0*	*8.6*	*1.29*	*260.3*
1.000	11,403	37.94	28.94	22.14	15.28	11.01	6.16	2.69	432.1	15.3	0.0	9.7	0.84	132.7
1.100	10,877	58.67	43.96	32.46	21.73	15.31	7.81	3.34	266.6	7.9	0.0	7.0	1.33	90.9
1.200	11,370	39.89	29.11	21.49	13.74	9.40	4.98	2.43	365.2	12.2	0.0	11.5	0.86	104.1
1.300	11,414	40.85	30.78	23.83	16.09	11.28	6.29	3.06	413.4	13.1	0.0	9.5	0.93	129.8
1.400	11,194	51.28	39.07	28.84	19.34	13.85	8.20	4.20	261.4	11.7	0.0	7.3	2.29	190.1
1.500	11,512	26.39	21.25	18.19	14.41	11.61	7.59	3.50	1224.1	34.6	0.0	8.2	0.19	215.4
1.600	11,096	39.42	33.22	26.52	19.41	14.86	8.82	4.22	688.8	13.6	0.0	6.9	1.48	197.2
1.700	11,019	49.01	37.41	28.08	19.28	14.01	7.96	3.57	293.1	12.1	0.0	7.3	1.28	142.9
1.800	11,315	39.19	30.76	24.04	16.90	12.44	7.63	4.15	423.0	17.2	0.0	8.1	1.82	275.4
1.900	11,370	41.08	31.87	23.59	15.57	10.96	6.17	3.25	393.7	12.4	0.0	9.7	2.22	136.5
Mean:		41.27	31.79	24.10	16.56	12.05	7.10	3.62	417.4	16.4	0.0	9.0	1.72	174.5
Std. Dev:		8.71	6.87	5.14	3.52	2.68	1.73	0.98	213.8	7.3	0.0	2.2	0.93	61.1
Var Coeff(%):		21.09	21.62	21.31	21.28	22.23	24.38	26.97	51.2	44.2	0.0	24.4	54.10	36.1

Figure 3.5 Modulus 6 to Processing FWD Data

FWD data are used to determine the required overlay thickness by ITD. The modulus values calculated using Modulus 6 are used in Winflex software, which is developed at the University of Idaho, to calculate the overlay thickness. Winflex determines the tensile strain at the bottom asphalt layers and the compressive strain at the top of the subgrade and calculates the allowable fatigue life of each layer as a function of Equivalent Single Axle Loads (ESALs). Figures 3.6 and 3.7 show screenshots of the Winflex data entry and output, respectively (Bayomy and Abo Hashema 2000).

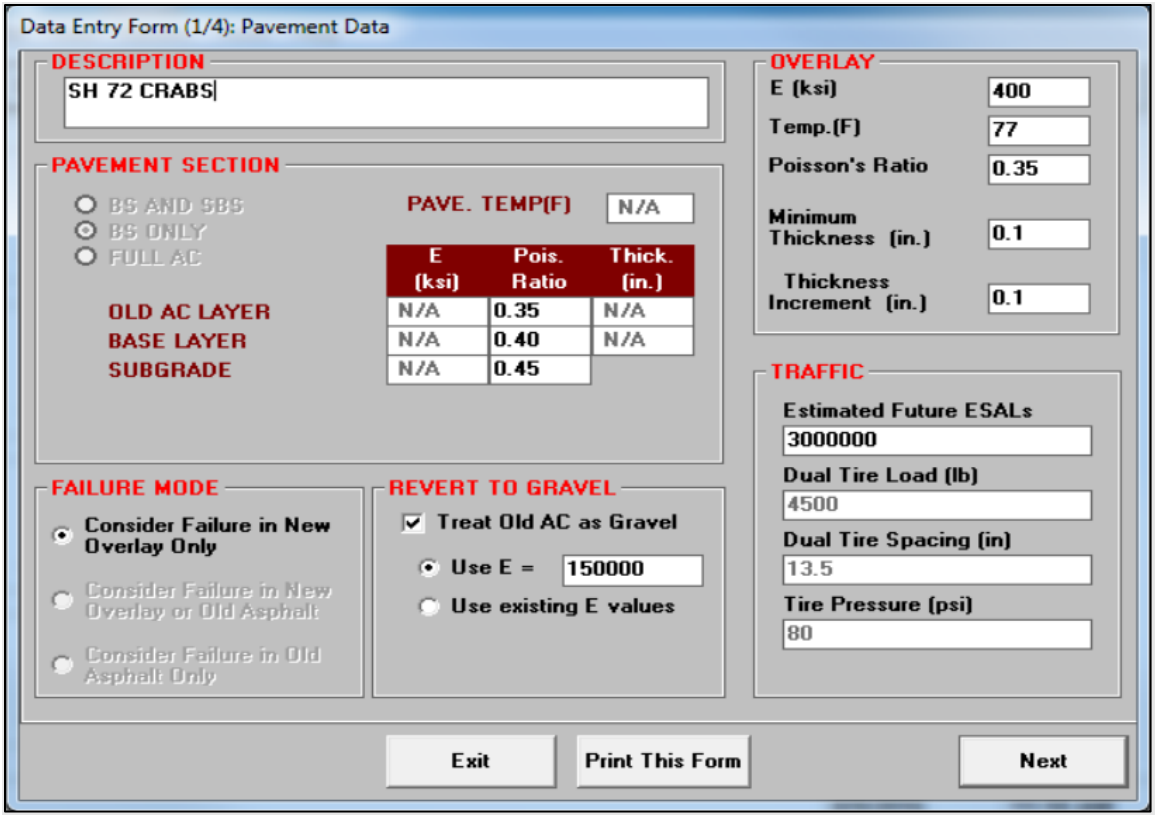

Figure 3.6 Winflex data Entry (Bayomy and Abo Hashema 2000)

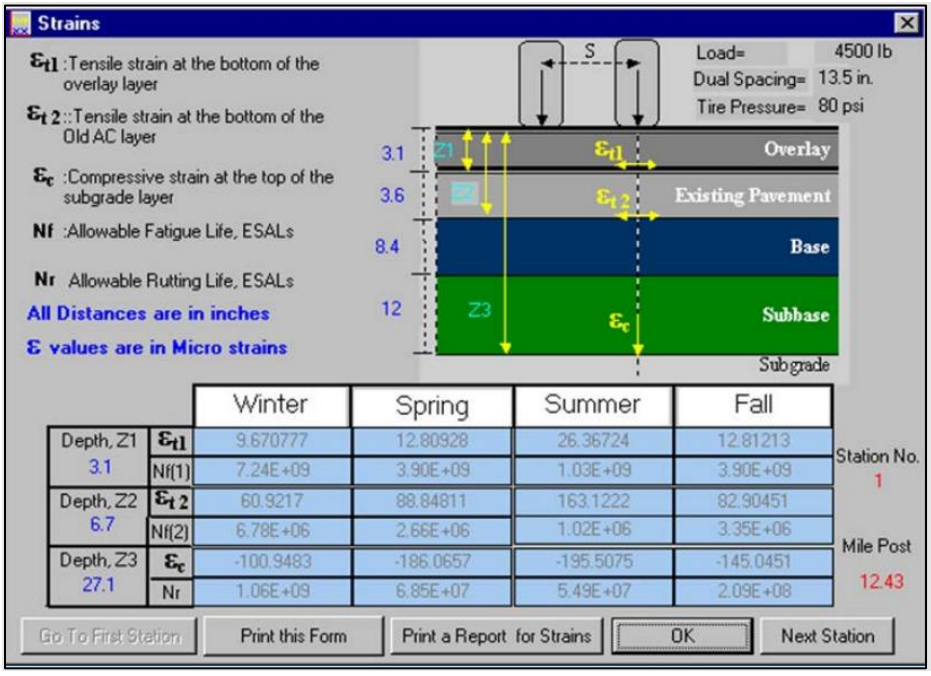

Figure 3.7 Winflex Strain Calculations (Bayomy and Abo Hashema 2000)

The research team examined the TSD and FWD data obtained from ITD to identify and select pavement sections that were examined using both FWD and TSD. Twenty pavement sections were selected. These sections included interstate and state highways. In addition, these sections had different pavement thicknesses. Tables 3.2 through 3.5 show the FWD and TSD deflection data for the selected pavement sections.

Table 3.2 Uncorrected FWD Deflection Data

FWD	D0	D8	D12	D18	D24	D36	D60
Project	W1 (mils)	W2 (mils)	W3 (mils)	W4 (mils)	W5 (mils)	W6 (mils)	W7 (mils)
Project I-15 40.70-43.80 2020	10.30	6.98	5.29	3.89	3.01	2.00	1.06
Project I-15 89.412-92.191 2020	10.30	4.82	2.56	1.55	1.20	0.93	0.68
Project I-15 99.00-104 2020	9.33	5.86	4.13	2.90	2.31	1.67	1.02
Project SH-39 44.50-49.80 2020	11.90	8.44	6.53	4.72	3.52	2.16	1.12
Project SH-27 19.445-22.0 2020	13.84	11.72	10.05	7.92	6.34	4.28	2.41
Project US-93 203-208.0 2020	14.16	11.23	9.05	6.89	5.40	3.60	2.00
Project US-93 211.3-216.20 2020	20.10	15.23	11.90	8.57	6.38	3.86	1.86
Project US-93 216.30-221.20 2020	13.80	9.75	7.53	5.41	3.96	2.27	0.95
Project US-30 249-253.10 2020	11.84	9.44	7.80	5.82	4.32	2.49	1.21
Project SH-55 101.50-105.20 2020	16.05	12.17	10.56	8.66	7.17	4.92	2.34
Project SH-55 110.30-114 2020	10.08	7.46	6.17	4.85	3.87	2.62	1.49
Project SH-52 19.00-22.00 2019	21.98	16.83	13.57	10.24	7.95	5.19	2.57
Project US 95 MP 0.00-4.800 2019	11.17	8.13	6.77	5.53	4.56	3.22	1.80
Project US 95 MP 5.0-16.5 2019	15.16	10.25	7.74	5.63	4.20	2.53	1.21
Project US 95 MP 16.6-23.9 2019	18.54	12.96	10.27	7.28	5.28	3.18	1.75
Project US 95 MP 24.0-28.70 2019	13.61	9.80	8.46	6.84	5.47	3.63	1.91
Poject US 95 MP 28.80-35.60 2019	16.00	11.74	10.09	8.23	6.64	4.39	2.12
Project US 95 MP 35.8-42.4 2019	11.21	8.61	7.03	5.43	4.26	2.77	1.38
Project US 95 MP 42.6-46.60 2019	7.27	6.00	5.32	4.52	3.82	2.78	1.53
Project US 95 MP 65.00-70.3 2019	15.39	11.49	9.14	6.65	5.05	3.18	1.66

Table 3.3 Corrected FWD Deflection Data

FWD	D0	D8	D12	D18	D24	D36	D60
Project	W1 (mils)	W2 (mils)	W3 (mils)	W4 (mils)	W5 (mils)	W6 (mils)	W7 (mils)
Project I-15 40.70-43.80 2020	7.35	4.98	3.78	2.77	2.15	1.42	0.76
Project I-15 89.412-92.191 2020	4.84	2.26	1.20	0.73	0.56	0.44	0.32
Project I-15 99.00-104 2020	4.93	3.09	2.18	1.53	1.22	0.88	0.54
Project SH-39 44.50-49.80 2020	10.05	7.12	5.51	3.98	2.98	1.82	0.94
Project SH-27 19.445-22.0 2020	12.82	10.85	9.30	7.33	5.87	3.96	2.23
Project US-93 203-208.0 2020	13.81	10.95	8.83	6.72	5.26	3.51	1.96
Project US-93 211.3-216.20 2020	14.99	11.36	8.87	6.39	4.76	2.88	1.39
Project US-93 216.30-221.20 2020	9.28	6.55	5.06	3.64	2.66	1.53	0.64
Project US-30 249-253.10 2020	13.46	10.73	8.86	6.61	4.91	2.83	1.37
Project SH-55 101.50-105.20 2020	14.58	11.05	9.59	7.87	6.51	4.46	2.12
Project SH-55 110.30-114 2020	7.03	5.20	4.30	3.38	2.70	1.82	1.04
Project SH-52 19.00-22.00 2019	16.96	12.99	10.47	7.90	6.13	4.00	1.98
Project US 95 MP 0.00-4.800 2019	7.57	5.51	4.59	3.74	3.09	2.18	1.22
Project US 95 MP 5.0-16.5 2019	9.49	6.42	4.85	3.53	2.63	1.58	0.76
Project US 95 MP 16.6-23.9 2019	12.24	8.55	6.78	4.81	3.48	2.10	1.15
Project US 95 MP 24.0-28.70 2019	9.90	7.13	6.16	4.98	3.98	2.64	1.39
Poject US 95 MP 28.80-35.60 2019	11.37	8.34	7.17	5.85	4.72	3.12	1.51
Project US 95 MP 35.8-42.4 2019	8.88	6.82	5.57	4.30	3.38	2.19	1.09
Project US 95 MP 42.6-46.60 2019	4.69	3.87	3.43	2.91	2.46	1.79	0.99
Project US 95 MP 65.00-70.3 2019	12.35	9.22	7.33	5.34	4.05	2.55	1.33

Table 3.4 Uncorrected TSD Deflection Data

TSD	D0	D8	D12	D18	D24	D36	D48	D60	D72
Project	W1 (mils)	W2 (mils)	W3 (mils)	W4 (mils)	W5 (mils)	W6 (mils)	W7 (mils)	W8 (mils)	W9 (mils)
Project I-15 40.70-43.80 2020	9.82	8.11	7.15	5.84	4.65	3.03	2.21	1.60	1.11
Project I-15 89.412-92.191 2020	9.77	7.52	6.35	4.88	3.83	2.55	1.84	1.31	0.91
Project I-15 99.00-104 2020	9.63	7.62	6.63	5.33	4.33	2.96	2.12	1.48	1.00
Project SH-39 44.50-49.80 2020	15.12	12.19	10.57	8.52	6.72	4.47	3.41	2.53	1.81
Project SH-27 19.445-22.0 2020	23.07	17.81	14.92	11.41	8.64	5.12	3.33	2.18	1.38
Project US-93 203-208.0 2020	17.65	13.09	10.81	8.26	6.41	4.24	3.10	2.23	1.55
Project US-93 211.3-216.20 2020	19.39	14.10	11.53	8.65	6.57	4.09	2.80	1.91	1.27
Project US-93 216.30-221.20 2020	11.50	8.67	7.20	5.46	3.99	2.25	1.52	1.02	0.67
Project US-30 249-253.10 2020	17.21	13.74	11.77	9.32	7.29	4.93	3.83	2.87	2.08
Project SH-55 101.50-105.20 2020	18.83	15.43	13.62	11.32	9.30	6.23	4.36	2.97	1.93
Project SH-55 110.30-114 2020	12.10	10.21	9.20	7.80	6.51	4.50	3.22	2.23	1.47
Project SH-52 19.00-22.00 2019	25.96	18.50	14.92	11.00	8.08	4.27	2.40	1.46	0.89
Project US 95 MP 0.00-4.800 2019	11.36	8.98	8.15	7.20	6.27	4.52	3.26	2.40	1.74
Project US 95 MP 5.0-16.5 2019	15.60	10.99	9.37	7.58	6.25	4.13	2.75	1.83	1.19
Project US 95 MP 16.6-23.9 2019	14.52	10.63	8.78	6.69	5.29	3.25	2.02	1.26	0.76
Project US 95 MP 24.0-28.70 2019	15.50	12.76	11.25	9.21	7.44	4.48	2.69	1.72	1.09
Poject US 95 MP 28.80-35.60 2019	13.00	9.82	8.36	6.67	5.37	3.32	2.07	1.33	0.84
Project US 95 MP 35.8-42.4 2019	8.83	6.96	6.00	4.89	3.93	2.49	1.62	1.04	0.64
Project US 95 MP 42.6-46.60 2019	11.79	8.72	7.28	5.65	4.43	2.71	1.70	1.08	0.67
Project US 95 MP 65.00-70.3 2019	16.91	12.25	10.12	7.78	5.95	3.32	1.88	1.14	0.69

Table 3.5 Corrected TSD Deflection Data

TSD	D0	D8	D12	D18	D24	D36	D48	D60	D72
Project	W1 (mils)	W2 (mils)	W3 (mils)	W4 (mils)	W5 (mils)	W6 (mils)	W7 (mils)	W8 (mils)	W9 (mils)
Project I-15 40.70-43.80 2020	11.16	9.22	8.13	6.64	5.28	3.45	2.52	1.81	1.26
Project I-15 89.412-92.191 2020	10.52	8.10	6.84	5.26	4.12	2.74	1.99	1.42	0.98
Project I-15 99.00-104 2020	17.21	13.61	11.85	9.53	7.74	5.30	3.79	2.64	1.78
Project SH-39 44.50-49.80 2020	13.82	11.14	9.66	7.79	6.14	4.09	3.11	2.31	1.65
Project SH-27 19.445-22.0 2020	19.34	14.93	12.51	9.57	7.24	4.29	2.80	1.83	1.16
Project US-93 203-208.0 2020	17.95	13.32	11.00	8.40	6.51	4.31	3.16	2.27	1.57
Project US-93 211.3-216.20 2020	19.72	14.33	11.72	8.79	6.69	4.16	2.85	1.95	1.29
Project US-93 216.30-221.20 2020	11.90	8.97	7.45	5.65	4.13	2.32	1.57	1.06	0.70
Project US-30 249-253.10 2020	18.03	14.39	12.33	9.76	7.64	5.16	4.01	3.01	2.18
Project SH-55 101.50-105.20 2020	19.36	15.87	14.01	11.64	9.56	6.41	4.49	3.05	1.99
Project SH-55 110.30-114 2020	13.13	11.08	9.98	8.46	7.07	4.88	3.49	2.41	1.60
Project SH-52 19.00-22.00 2019	27.84	19.84	16.00	11.79	8.66	4.58	2.57	1.56	0.95
Project US 95 MP 0.00-4.800 2019	8.10	6.40	5.81	5.13	4.47	3.22	2.33	1.71	1.24
Project US 95 MP 5.0-16.5 2019	9.36	6.60	5.62	4.55	3.75	2.48	1.65	1.10	0.71
Project US 95 MP 16.6-23.9 2019	8.94	6.55	5.40	4.12	3.26	2.00	1.24	0.78	0.47
Project US 95 MP 24.0-28.70 2019	11.18	9.20	8.12	6.65	5.37	3.23	1.94	1.24	0.78
Poject US 95 MP 28.80-35.60 2019	9.77	7.38	6.28	5.01	4.03	2.49	1.55	1.00	0.63
Project US 95 MP 35.8-42.4 2019	7.26	5.72	4.93	4.02	3.23	2.04	1.33	0.85	0.53
Project US 95 MP 42.6-46.60 2019	7.81	5.78	4.82	3.74	2.93	1.80	1.13	0.71	0.44
Project US 95 MP 65.00-70.3 2019	14.42	10.45	8.63	6.63	5.08	2.84	1.60	0.97	0.59

3.3 3D-Move and Structural Data

The researchers used the 3D-Move software to simulate both FWD and TSD testing and predict pavement surface deflections. The predicted deflection values obtained by 3D-Move were compared to field measurements. A theoretical parametric study included 243 different pavement structures was performed using the 3D-Move software as discussed in detail in Chapter 4. These pavement structures had different layer thickness and modulus. The 3D-Move software was used to predict the pavement response including stresses, strains, and deflections. The predicted pavement response was used to assess the relationship between various DBPs and pavement conditions (e.g., layer modulus). The correlation between TSD and FWD deflections, obtained using 3D Move, was also investigated. The 3D-Move software is a powerful analytical tool that can accurately simulate pavement responses under complex loading conditions, such as non-uniform tire-pavement contact stress distributions and moving loads. It was developed by the University of Nevada, Reno in 2010. It utilizes a continuum-based finite-layer approach and the Fourier transform technique to accurately model pavement layers as continua. This approach has been recognized as more efficient than traditional finite-element methods and has been

validated using field measured responses in previous studies include Penn State University test track and MnRoad and UNR Off-road Vehicle study (UNR 2010).

3D-Move Inputs

The 3D-Move software was used to simulate the loading configurations of the FWD and TSD, separately to predict the theoretical FWD and TSD deflection basins as well as pavement responses (e.g., stresses and strains). The loading characteristics of TSD and FWD, material properties of different pavement layers, and other essential parameters are defined in the 3D-Move. Some primary inputs of 3D-Move software are discussed in this section.

Type of Load Response

The user needs to specify the type of analysis whether it is static or dynamic. Static analysis is specified for FWD whereas dynamic analysis is specified for TSD. The operating speed of the TSD truck is also required. The speed of TSD trailer is recorded and reported during TSD field operations.

FWD Loading

The stationary impulse loading applied by FWD was defined in 3D-Move by a circular area with a radius of 5.9 inches and a load of 9,000 lb. Such loading generates a uniform pressure of 82.2 psi on the pavement surface. This configuration simulates the FWD equipment used by ITD as the loading plate has a radius of 5.9 inches and the applied load is often normalized to 9000 lb. during data analysis and processing.

TSD Loading

TSD applies loading on pavements using its rear axle tires while travelling at traffic speed. Deflection velocities are measured along the midline between these dual tires by articulated Doppler lasers which are mounted over the right wheel of the rear axles, as shown in Figure 3.8.

The dynamic tire-pavement load variations are considered in the 3D-Move using the Dynamic Load Coefficient (DLC). The DLC implies the variation of tire loads in the form of coefficient of variation which takes into account surface roughness, speed of the vehicle and the suspension system of the truck. The DLC is only applicable to dynamic analysis and in this study DLC was defined as a function of vehicle suspension system and average surface roughness using an analytical model, which also takes vehicle speed into consideration (Zihan et al. 2020).

The contact tire pressure of the ARRB TSD was reported as 115 psi under static condition. It was also noted that the TSD used in the field was intentionally slightly biased to the right dual tire with a greater magnitude of load to increase the deflection as it measures the deflection along the midline between the

right dual tires (Zihan et al. 2020). According to ARRB, a set of TSD wheels apply approximately 11,240 lb. loading on the pavement surface.

Material Characteristics of Different Pavement Layers

The pavement structure was divided into three layers such as Asphalt Concrete (AC), base and subgrade layers and each layer was defined in the 3D-Move. The thickness of these layers was obtained from a historical database of pavements in Idaho established in a previous study (Bayomy et al. 2018). Constant values of Poisson's ratio were assumed for each layer (i.e., 0.35, 0.40, and 0.45 for the AC, base, and subgrade layers, respectively).

AC Layer

Since the FWD load nature is impulse static, elastic material properties were assumed for the AC layer in the static 3D-Move analysis for FWD. For the simplicity of analysis, AC dynamic modulus values at 70 °F and 1 Hz were used as a single input for the modulus value of AC layer in the dynamic 3D-Move analysis for TSD.

Base and Subgrade Layers

The base and subgrade layers for both TSD and FWD were characterized by defining the elastic moduli of these layers in the 3D-Move software. Backcalculated moduli for the base and subgrade layers from FWD were considered as the seed moduli and the final moduli were obtained by trial and error to achieve acceptable fitting between the field measured and calculated deflections. A constant Poisson's ratio and damping ratio (for TSD) were specified for these layers.

Locations of Deflection Measurements

The user specifies the locations where pavement responses to be calculated for the static and dynamic analysis. For FWD analysis, all the required number of response points needed to be defined as shown in Figure 3.8b. The maximum deflection occurs at the center of the loading plate which is denoted as D_0. On the other hand, 3D-Move produces a time-deflection history as an output during dynamic analysis. So, defining only one response point is sufficient to obtain deflection measurements at different points from the applied load. The time can be multiplied by the speed of the vehicle to calculate the distance and thus their corresponding deflection can be obtained from the defined response point. TSD measures deflections at the midline between the tires and D_0 is the deflection caused by tire loading at mid-point between the loaded dual tires; and D_8, D_{12}, D_{18}, D_{24}, D_{36}, D_{48}, D_{60}, and D_{72} indicate deflections at a distance of 8, 12, 18, 24, 36, 48, 60, and 72 in. respectively from D_0 (Figure 3.8a).

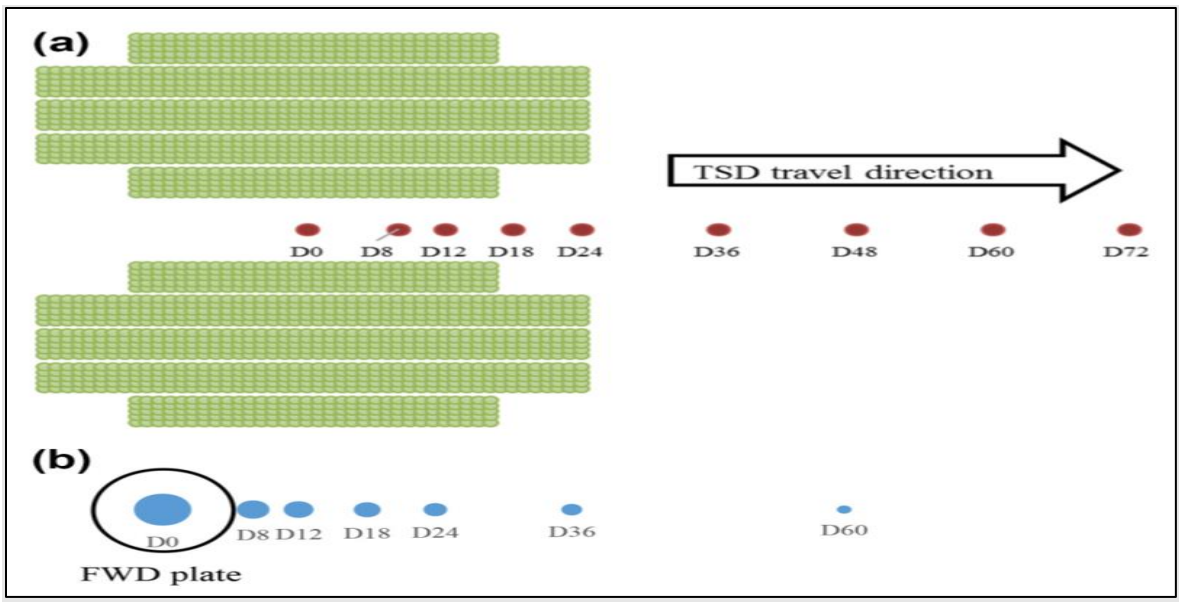

Figure 3.8 Illustration of response points in 3D-Move: (a) response points specified for TSD and (b) response points specified for FWD (Zihan et al. 2020)

3.4 Pavement Performance Data Collection

The researchers collected performance data for the examined test sections. The collected data can be divided into two main categories, design information (e.g., traffic, pavement structure, layer properties) and performance data (e.g., rutting, load-related cracking [alligator and longitudinal], thermal cracking [transverse cracking], reflective cracking in AC overlays, and International Roughness Index [IRI]). ITD houses a comprehensive Transportation Asset Management database referred to as TAMS. Historical data of performance and traffic information about state network is registered in TAMS. Table 3.4 Shows an example of TAMS data.

Table 3.6 Distress Information Registered in ITD-TAMS

Distress Type	ITD-TAMS
Permanent deformation - total pavement	Total rut depth (inch)
Permanent deformation - AC only	Not reported
Permanent deformation – Unbound Layers	Not reported
Bottom-up fatigue (alligator) cracking	Light/moderate/heavy extent Slight/moderate/heavy severity
Thermal (transverse) cracking	Light/moderate/heavy extent Slight/moderate/heavy severity
Top-down fatigue (longitudinal) cracking	Light/moderate/heavy extent Slight/moderate/heavy severity

ITD uses a profiler minivan that is equipped with high resolution cameras and sensors to create video log files for the entire pavement surface. Using the PathView software provided to ITD, the amount of alligator, longitudinal, and thermal cracking can be accurately measured. The data is collected every 0.1 mile. Figures 3.9 and 3.10 show examples of the TAMS collected data.

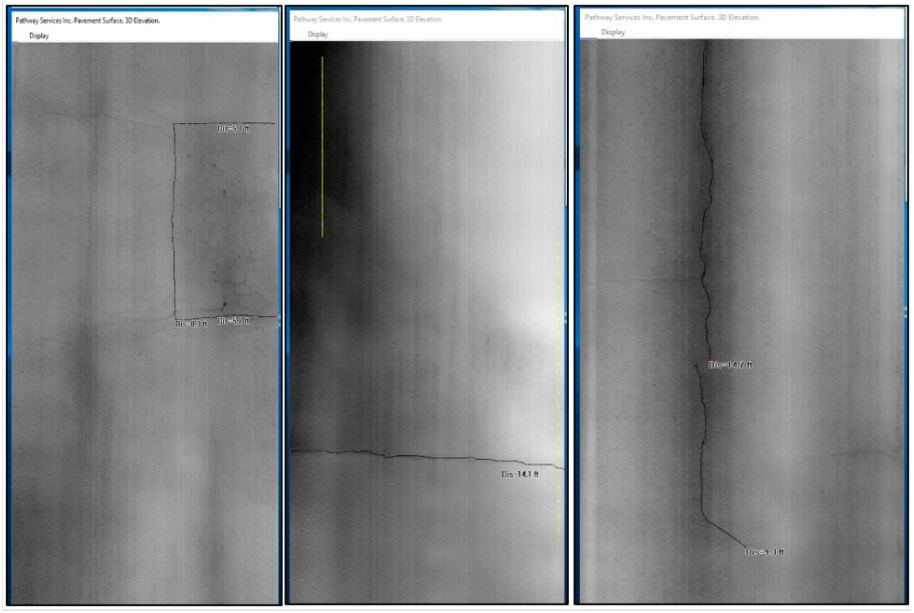

Alligator Cracking (ft^2) **Trans. Cracking (ft/mile)** **Long. Cracking (ft/mile)**

Figure 3.9 PathView Images for the TAMS Performance Data

Route	SH-27	Year	2017						
BMP	EMP	Direction	Condition State (OCI, IRI, Rutting)	IRI Average (inch/mile)	Rut Weighted Avg (in)	Rutting - Max. (in.)	Fatigue Cracking Index	Transverse Cracking Index	Overall Condition Index (OCI)
0.1	0.2	Asc.	Fair	109	0.14	0.4	100	92.7414	92.7414
0.2	0.3	Asc.	Good	79	0.15	0.4	99.9555	95.6647	95.52
0.3	0.399	Asc.	Fair	113	0.12	0.39	99.9482	92.0044	91.9319
0.399	0.499	Asc.	Good	87	0.12	0.46	100	92.4494	92.4312
0.499	0.599	Asc.	Good	91	0.13	0.37	99.9384	88.9818	88.9411
0.599	0.699	Asc.	Fair	98	0.18	0.42	99.773	91.2032	91.1843
0.699	0.799	Asc.	Fair	103	0.16	0.41	99.7594	89.6181	89.182
0.799	0.899	Asc.	Fair	105	0.12	0.39	98.8662	91.8894	91.5514
0.899	0.999	Asc.	Fair	101	0.14	0.44	99.8509	89.9072	89.6889
0.999	1.098	Asc.	Good	89	0.1	0.38	99.7909	84.5371	84.5197
1.098	1.198	Asc.	Good	81	0.13	0.37	100	92.1229	92.0033
1.198	1.298	Asc.	Good	78	0.11	0.35	99.8151	89.5236	89.4796
1.298	1.398	Asc.	Good	74	0.12	0.39	99.9651	93.9589	93.9449
1.398	1.498	Asc.	Good	81	0.11	0.39	99.8765	90.8053	90.7838
1.498	1.598	Asc.	Fair	98	0.1	0.33	98.8162	88.8638	88.7567
1.598	1.698	Asc.	Good	92	0.11	0.39	97.888	86.49	86.314
1.698	1.797	Asc.	Good	82	0.08	0.29	99.7049	87.7399	87.6666
1.797	1.897	Asc.	Good	92	0.12	0.42	99.8229	91.8894	91.8518
1.897	1.997	Asc.	Good	90	0.13	0.43	99.4294	89.7162	89.6465
1.997	2.097	Asc.	Fair	95	0.12	0.35	99.4123	83.0103	82.9331
2.097	2.197	Asc.	Fair	108	0.12	0.37	99.9279	85.8812	85.8752
2.197	2.297	Asc.	Fair	107	0.17	0.53	99.6592	87.1166	86.663
2.297	2.397	Asc.	Fair	96	0.18	0.44	99.4256	86.9399	86.892

Figure 3.10 Tabulated TAMs Performance Data

4. FWD Results and Analysis

Chapter 4 presents the results of FWD deflection measurements in the field and discusses the results of the FWD theoretical parametric study. The researchers simulated the FWD deflection basin using the 3D-Move software, calculated of deflection basin parameters from the FWD data collected in the field, correlated the parameters to the pavement conditions, and calculated pavement overlay thicknesses based on the deflection data, traffic level, and pavement conditions.

4.1 FWD Simulation Using 3D-Move Software

The researchers simulated the FWD deflection basin using the 3D-Move software. They compared the theoretical deflection basins to the measured ones before conducting the theoretical parametric study to ensure the accuracy of 3D-Move in simulating the FWD testing and pavement response. Figures 4.1 to 4.4 show the FWD data collected from field sections; three in District 3 and one in District 2 in Idaho. The results demonstrated good correlations between predicted deflection basins (using 3D-Move) and the measured ones. The 3D-Move software was able to reasonably model the pavement response to FWD loading upon selecting the proper layers' moduli.

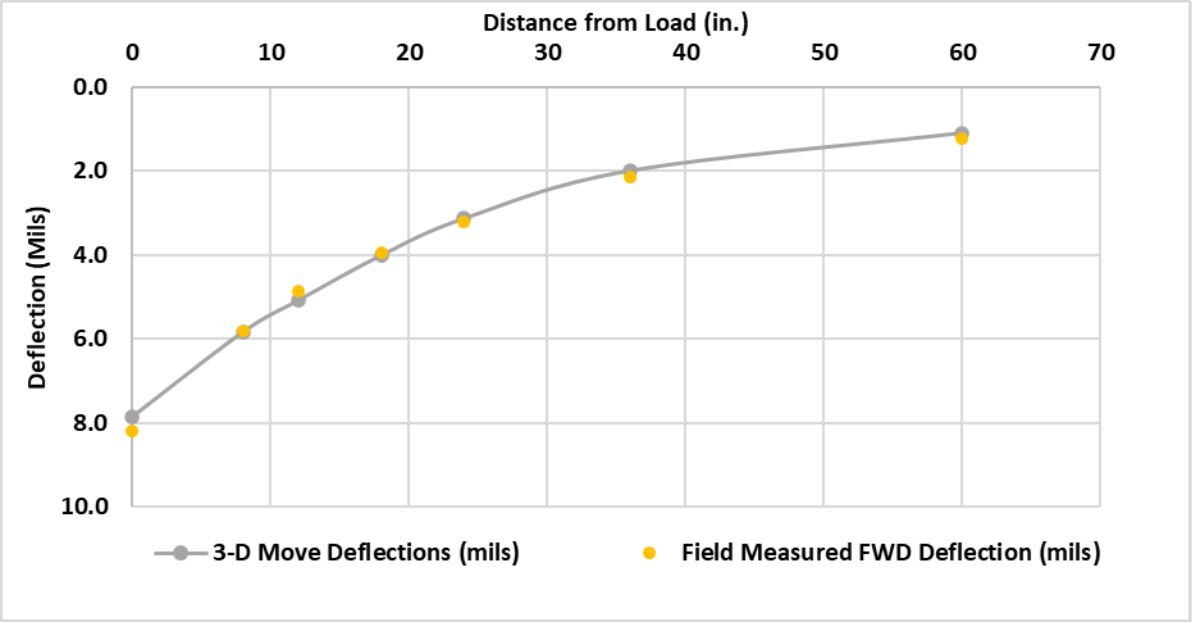

Figure 4.1 Comparison between Predicted and Measured Deflection Basin: Section D-3 SH-55 2020

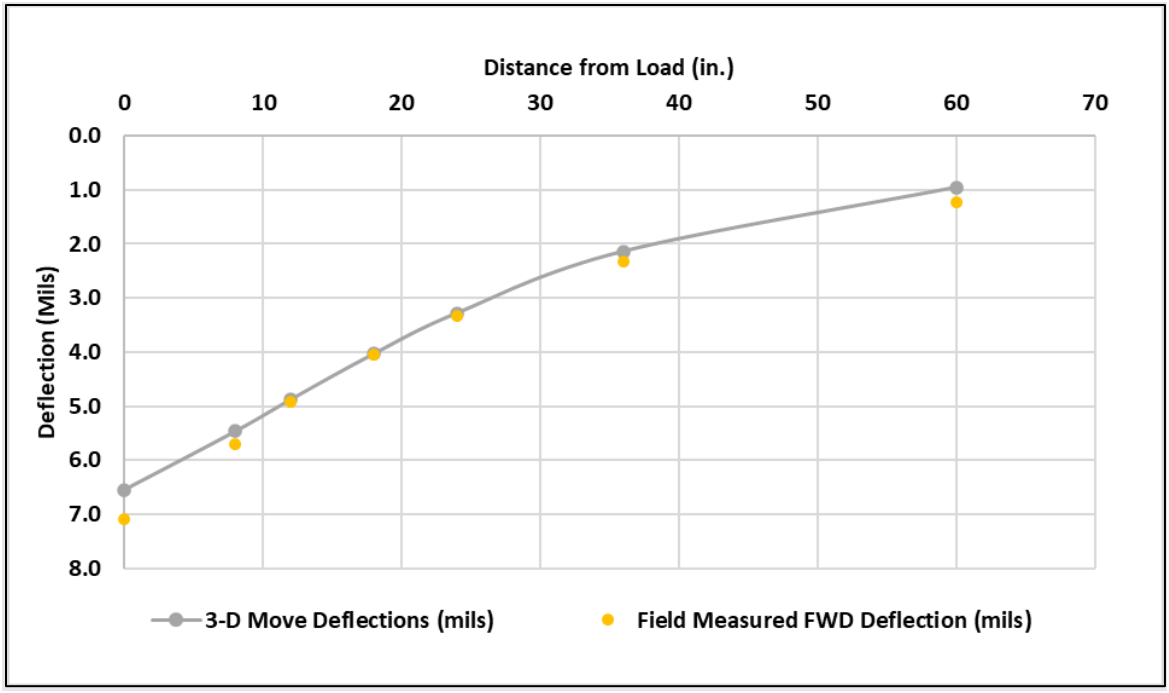

Figure 4.2 Comparison between Predicted and Measured Deflection Basin: Section D-3 US-95 2019 Wilder SCL to Parma SCL

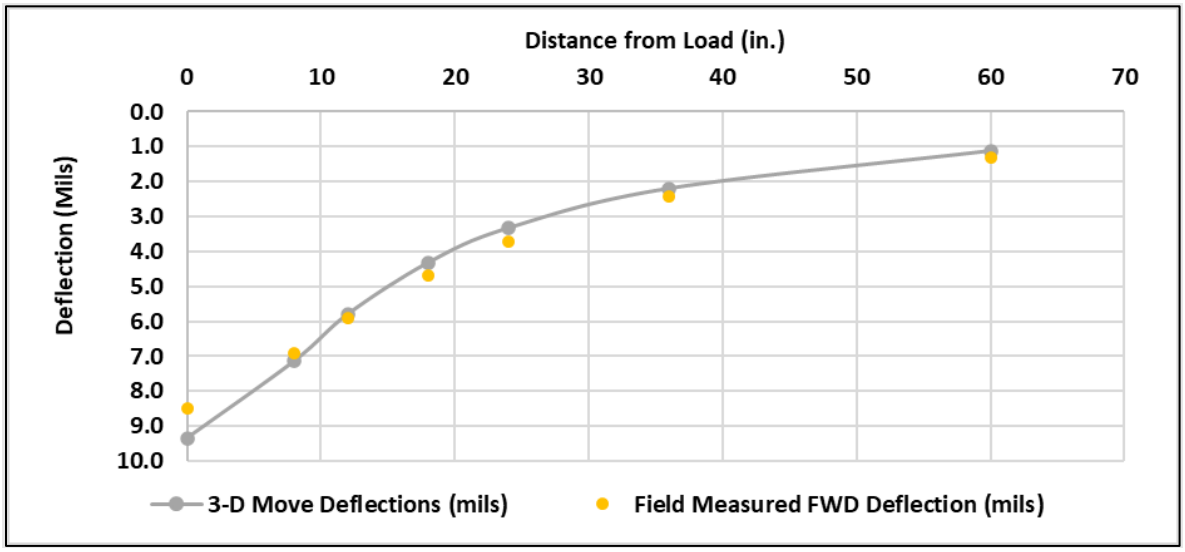

Figure 4.3 Comparison between Predicted and Measured Deflection Basin: Section D-2 SH-3 2019

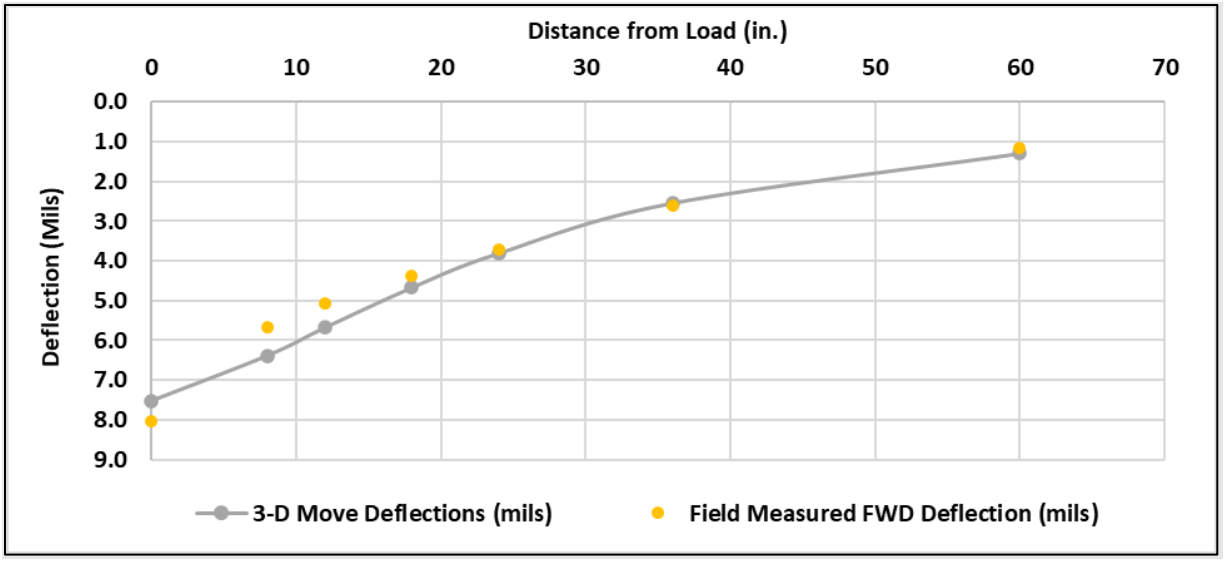

Figure 4.4 Comparison between Predicted and Measured Deflection Basin: Section D-3 US-95 2019 OSL to MP 6.81

4.2 FWD Parametric Study

After the successful validation of the 3D-Move models for FWD through field measurements, an extensive full-factorial parametric study was conducted. This study included 243 different pavement designs that varied in terms of asphalt and base layer thicknesses and moduli covering typical pavement structures and properties in the state (Bayomy et al. 2018). The design parameters for the parametric study are shown in Table 4.1. Each parameter was varied across three different levels.

Table 4.1 Full-Factorial FWD Parametric Study

Thickness of asphalt layer (in)	Thickness of base layer (in)	Modulus of asphalt layer (ksi)	Modulus of base layer (ksi)	Modulus of subgrade (ksi)
2.5	8	200	15	7
7	14	500	50	20
10	25	1000	200	35

4.2.1 Deflection Basin Parameters vs. Layers' Moduli

After conducting an extensive literature review, the researchers selected 39 deflection basin parameters for preliminary investigation. These parameters are often proposed to assess the pavement condition and layers' properties as discussed in detail in Chapter 2. From these 39 deflection basin parameters, the seven most established Deflection Basin Parameters (DBPs) were chosen for the final analysis as listed in Table 4.2.

Table 4.2 FWD Deflection Basin Parameters Used in the Evaluation

No.	DBP	Structural Indicator
1	Surface Curvature Index/Base Layer Index, SCI/BLI	Gives an indication of primarily the base layer structural condition
2	Base Curvature Index/Lower Layer Index, BCI/LLI	Gives an indication of the lower structural layers like the subgrade layers
3	Base Damage Index/Middle Layer Index, BDI/MLI	Gives an indication of tensile strain at the bottom of the AC Layer and compressive stress at the top of the
4	Maximum Deflection, D_0	Gives an indication of all structural layers with about 70% contribution by the subgrade
5	Deflection from Last Sensor, W_7	Subgrade strength
6	Normalized Comprehensive Area Ratio, CAr'	Overall Pavement strength
7	Radius of Curvature (RoC)	Gives an indication of the structural condition of the surfacing and base condition

The DBPs listed in Table 4.2 were calculated for the theoretical deflection basin of the parametric study (243 pavement structures) and correlated with the modulus values of different layers (e.g., asphalt layer modulus, base layer, subgrade). Some correlations and relationships are discussed in this section. Figure 4.5 shows the maximum deflection at the center of the loading plate (D0) versus the asphalt layer modulus. It should be noted that the asphalt layers had different thickness. There was no relationship between asphalt layer modulus and maximum deflection. Meanwhile, there was a trend between Radius of Curvature (RoC) asphalt layer modulus. The modulus increased with the increase of RoC (Figure 4.6). Also, there was no strong correlation between maximum deflection (D0) and the moduli of base layers (Figure 4.7). However, there was a strong correlation between the deflection of the last sensor (W_7) and subgrade modulus which is consistent with the literature (R^2 of 0.94). Subgrade with higher modulus resulted in low deflection for the last geophone as shown in Figure 4.8. Next, the researchers examined the relationship between the DBPs and the mechanistic response such as horizontal tensile strain on bottom of the asphalt layer and vertical compressive strain at the top of subgrade.

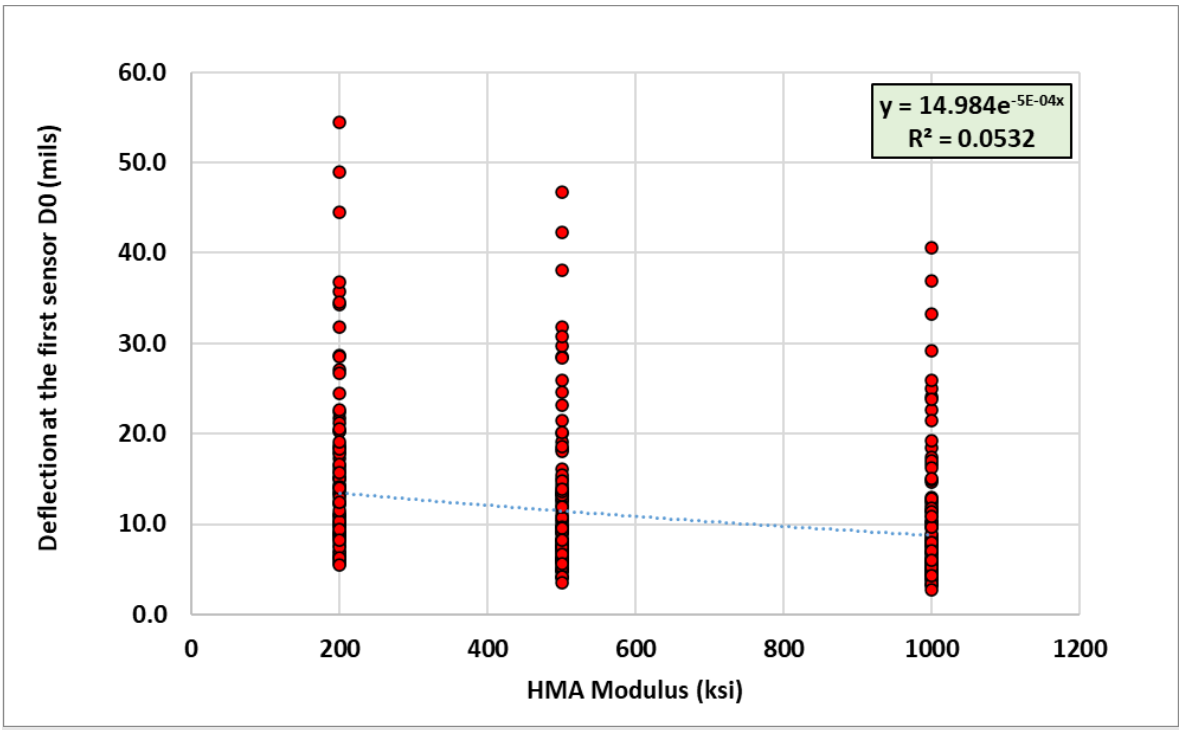

Figure 4.5 Maximum Deflection (D_0) vs. Asphalt Layer Modulus for FWD Parametric Study

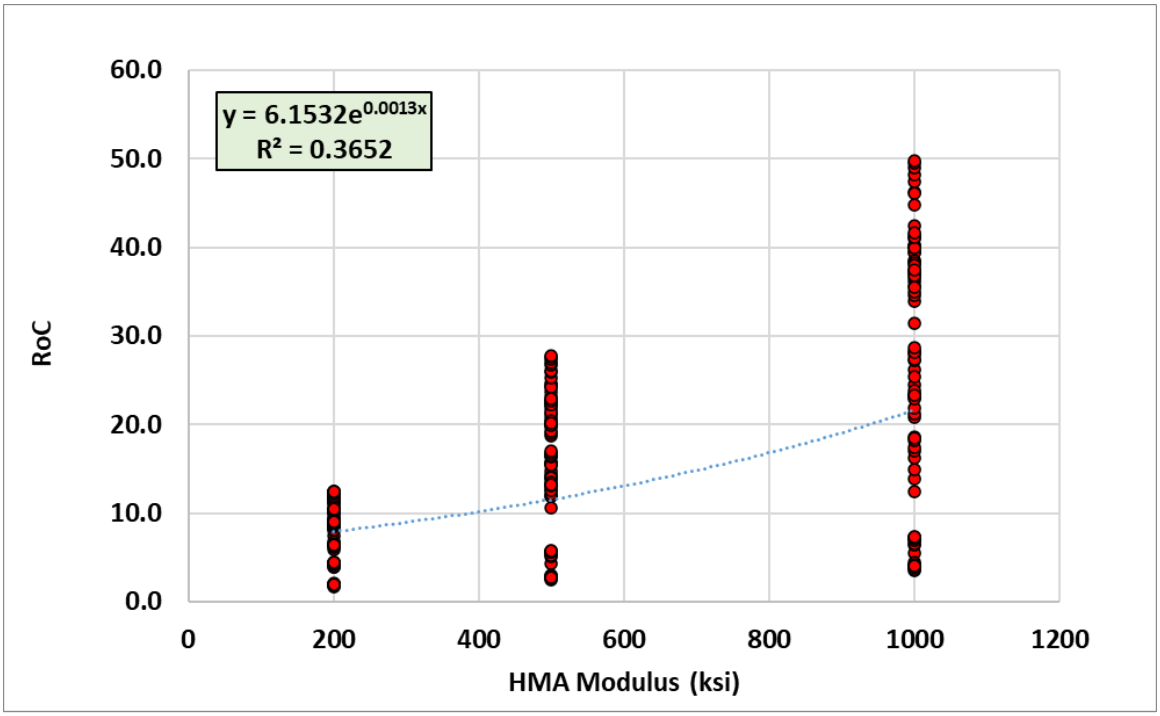

Figure 4.6 Radius of Curvature (RoC) vs. Asphalt Layer Modulus for FWD Parametric Study

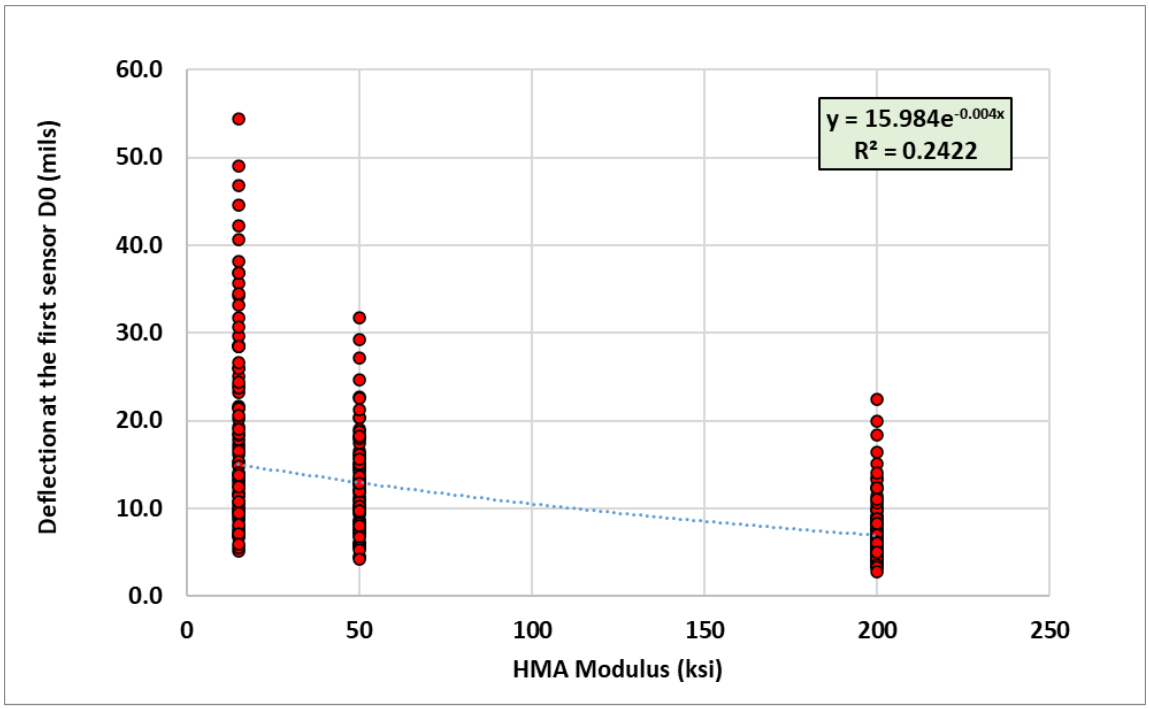

Figure 4.7 Maximum Deflection (D_0) vs. Base Layer Modulus for FWD Parametric Study

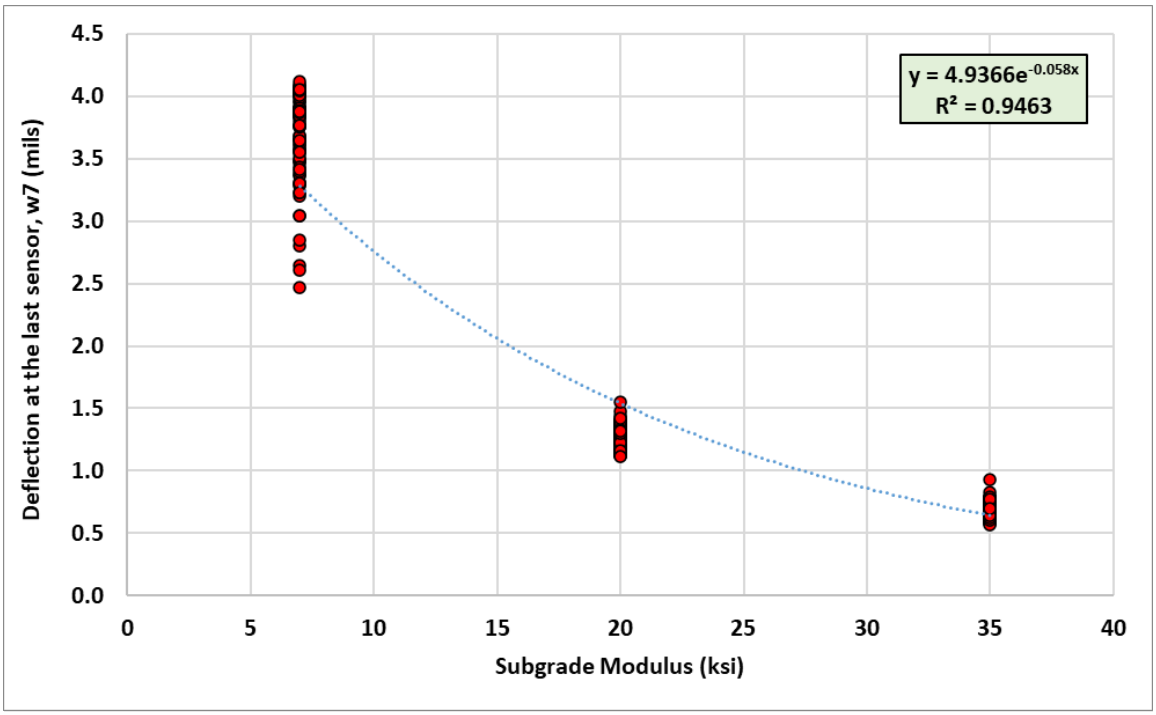

Figure 4.8 W_7 vs. Subgrade Layer Modulus for FWD Parametric Study

4.2.2 Deflection Basin Parameters and Mechanistic Response

The researchers further utilized the 3D Move to calculate critical pavement responses (e.g., horizontal tensile strain on bottom of the asphalt layer and vertical compressive strain at top of subgrade). These critical responses are then compared with various DBPs obtained from the theoretical deflection basin of the parametric study as discussed in this section.

4.3.2.1 Vertical Compressive Strain on top of Subgrade

Effective structural number (SN_{eff}) using the AASHTO equation presented in Equation 4.1 was computed for all sections included in the parametric study. The researchers assessed the correlation between the SN_{eff} and various DBPs listed in Table 4.2.

$$SN_{eff} = 0.0045*D*E_p^{0.333} \quad \text{.....Eqn. 4.1}$$

where,

D = total thickness of the pavement layers.

Ep = existing pavement modulus of all layers above the subgrade and can be calculated using Equation 4.2 below.

$$E_p/E_{subgrade} = 5.16.94*(W_7/W_1)^{5/2} - 214.46*(W_7/W_1)^2 + 159.56*(W_7/W_1)^{3/2} - 6.143*(W_7/W_1) + 1.0826*(W_7/W_1)^{1/2}$$

……Eqn. 4.2

where,

$(E_p/E_{subgrade})$ = pavement to subgrade modulus ratio.

W_1 = deflection at sensor 1.

W_7 = deflection at sensor 2.

Figure 4.9 shows that there is a good correlation (R^2 = 0.72) between the vertical compressive strain (ε_v) at top of subgrade and $SN_{eff.}$ The vertical compressive strain (ε_v) at the top of subgrade is a parameter that is used to predict the rutting life of flexible pavements. The SN_{eff} is computed based on the total thickness of pavements section and FWD deflection measurements. Such relationship can be used as a simple approach to estimate the vertical compressive strain (ε_v) at the top of subgrade without the need for complicated analysis methods.

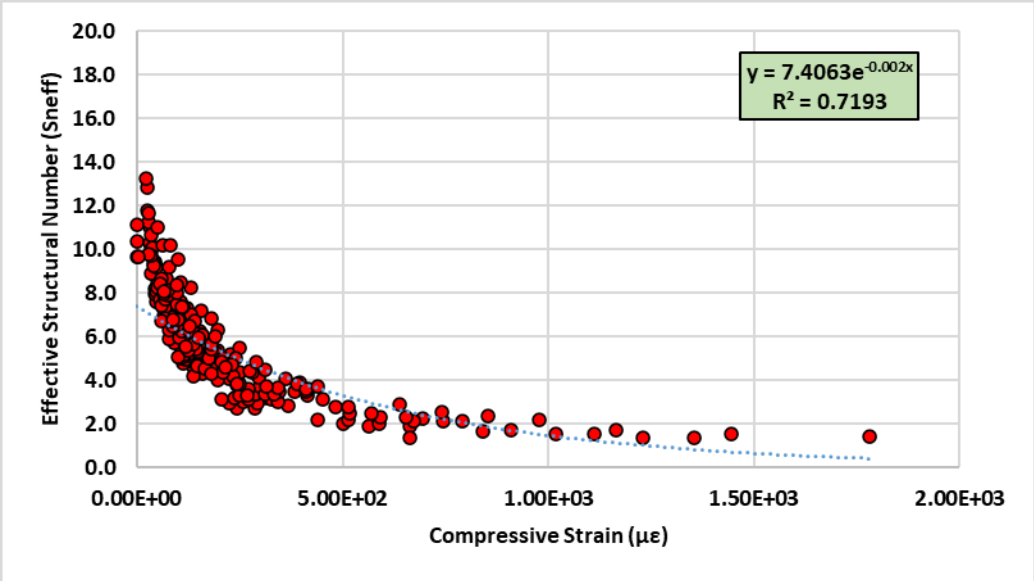

Figure 4.9 Correlation between FWD SNeff and Vertical Compressive Strain on top of Subgrade

4.3.2.2 Horizontal Tensile Strain on bottom of Asphalt Layer

Similarly, the effective structural numbers were compared to the horizontal tensile strain at the bottom of asphalt layer as shown in Figure 4.10. Also, all the DBPs selected were compared with the horizontal tensile strain at the bottom of the asphalt layer. Both SCI and AUPP were found to be highly correlated with the tensile strain as shown in Figures 4.11 and 4.12, respectively.

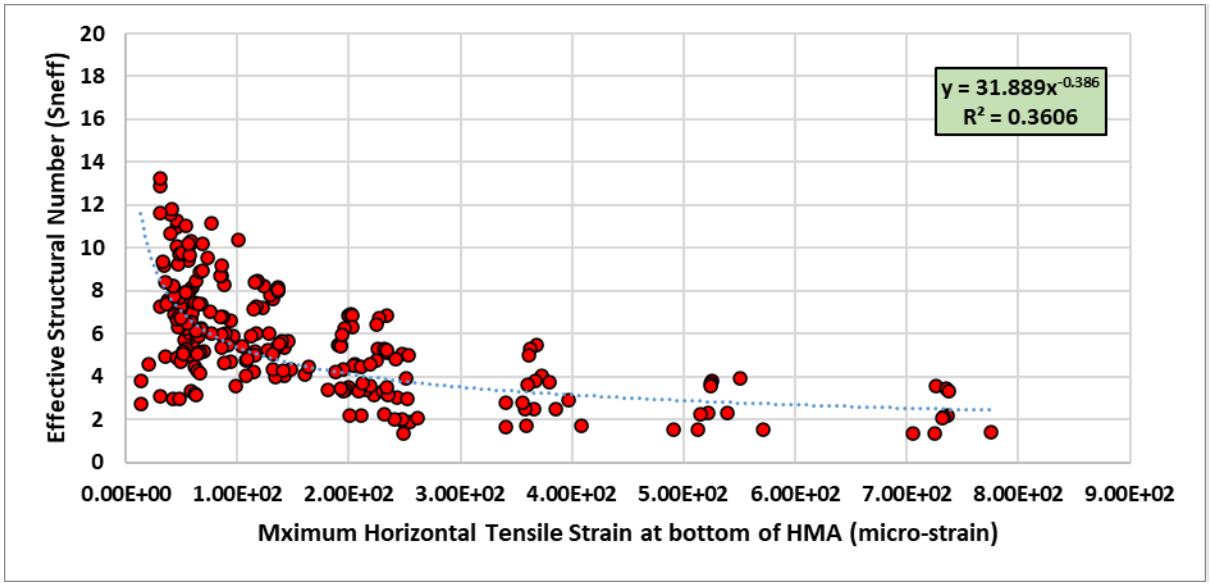

Figure 4.10 Effective Structural Number (SNeff) vs. Horizontal Tensile Strain on bottom of Asphalt Layer

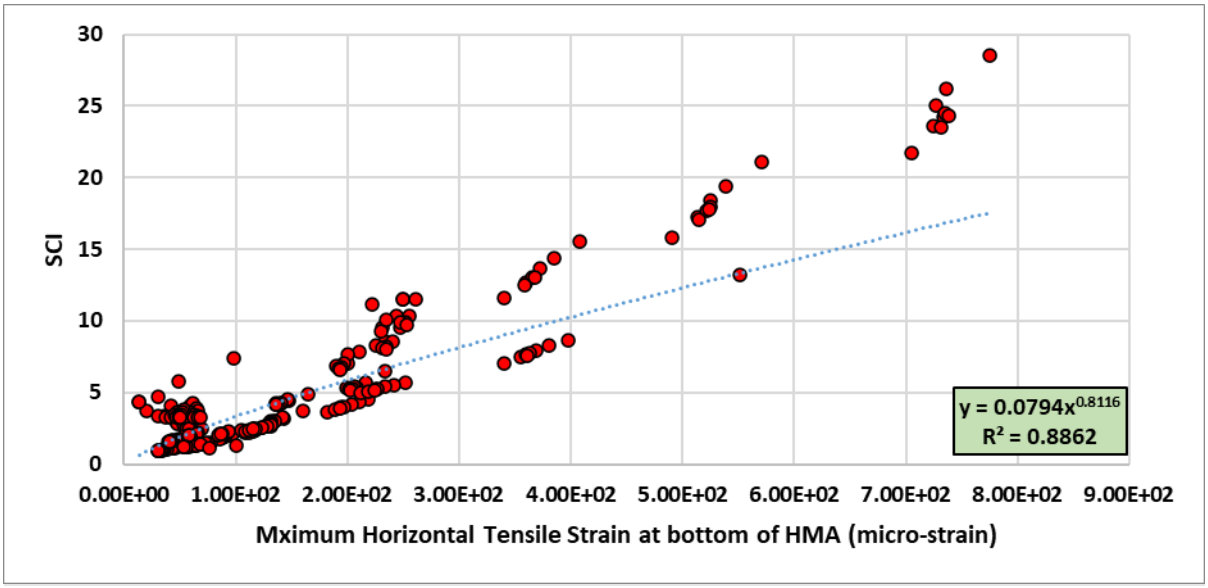

Figure 4.11 Correlation between FWD SCI and horizontal tensile strain on bottom of asphalt layer

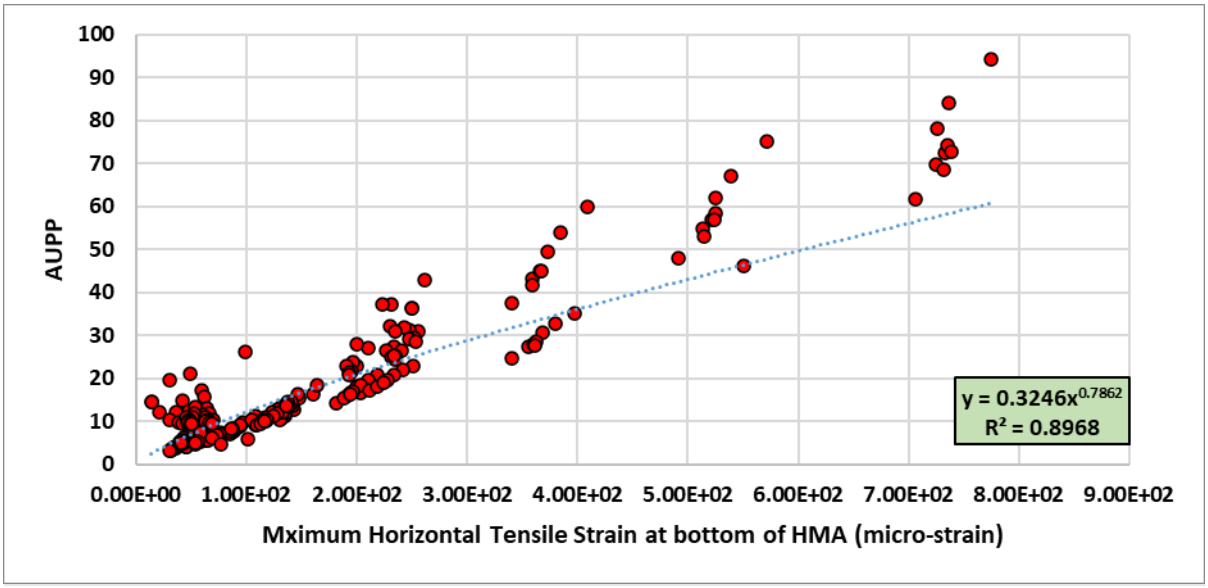

Figure 4.12 Correlation between FWD AUPP and horizontal tensile strain on bottom of asphalt layer

4.2.3 Deflection Basin Parameters vs. PMED Performance

The researchers used the AASHTOWare Pavement ME software to predict the performance of all sections included in the parametric study. This software uses a mechanistic-empirical approach to design and analyze the performance of pavements (ME Design Guide, 2008). The parametric study included 243 pavement designs with different layer thickness and modulus as presented in Table 4.1. The AASHTOWare Pavement ME predicts and reports the performance of these test sections recorded every month over 20 years. The researchers assessed the correlation between FWD DBPs and predicted stresses at the end of the design life for the examined test sections (243 sections). The results demonstrated that there is a good correlation (R^2 = 0.77) between the Structural Condition Index (SCI) and the terminal International Roughness Index (IRI) as shown in Figure 4.13. In addition, the maximum deflection (D_0) also had a good correlation (R^2 = 0.75) with IRI as shown in Figure 4.14. Similarly, there was a fair correlation between maximum deflection (D_0) and rutting (R^2 = 0.69) and between SCI and rutting (R^2 = 0.65) as shown in Figures 15 and 16, respectively. Furthermore, there was a trend between bottom-up cracking and both SCI and D_0 (Figures 4.17 and 4.18). However, there was no correlation with these indices (i.e., SCI and D_0) and top-down cracking as shown in Figures 4.19 and 4.20. The researchers further investigated the correlations between FWD and TSD deflection-based parameters and pavement distresses using the Artificial Intelligence (AI) techniques as discussed in detail in Chapter 7. The AI models demonstrated great potential for the AI applications in predicting pavement conditions using parameters that include FWD and TSD deflection measurements as traffic level (i.e., ESALs) as discussed in Chapter 7.

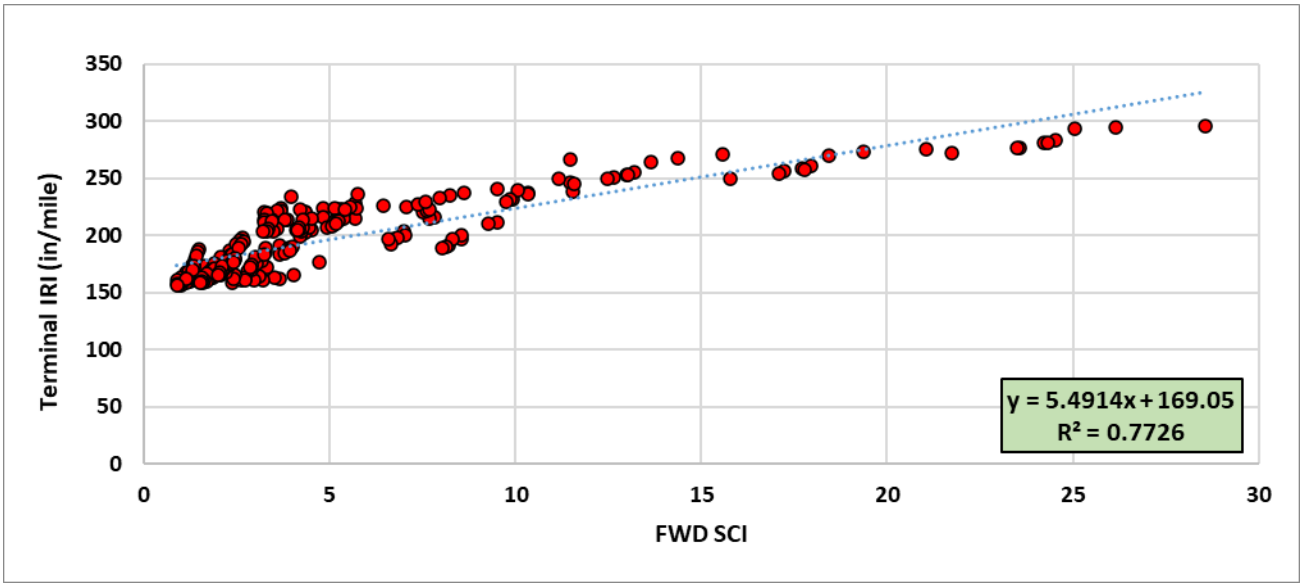

Figure 4.13 FWD SCI vs. Terminal IRI

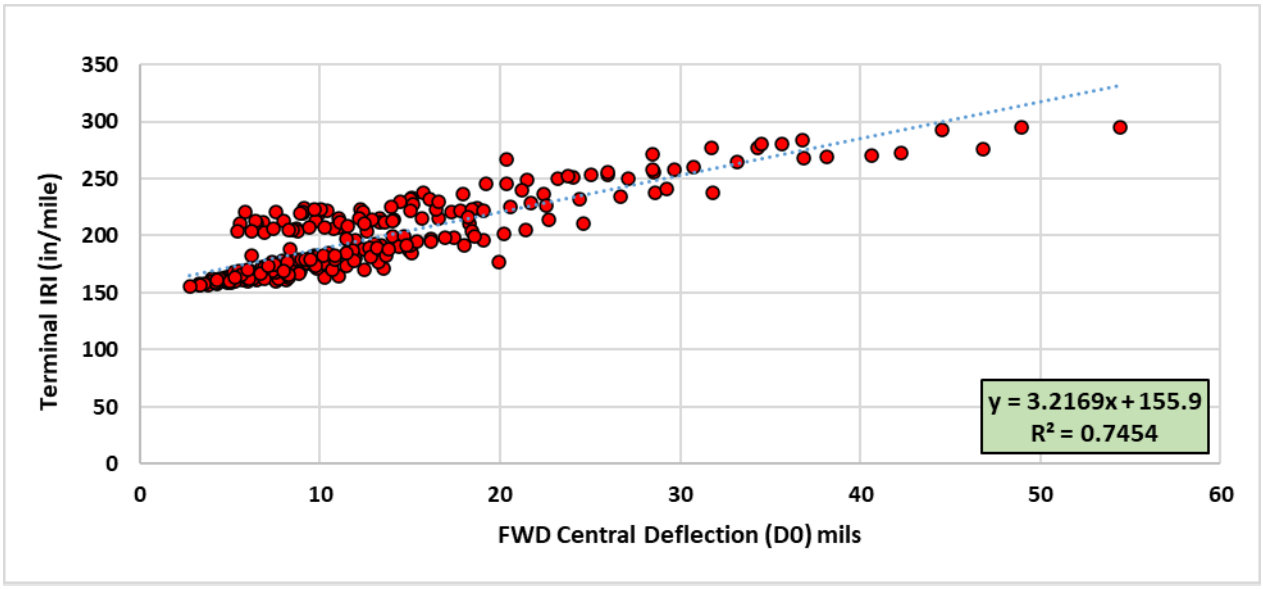

Figure 4.14 FWD Theoretical Maximum Deflection (D0) vs. Terminal IRI

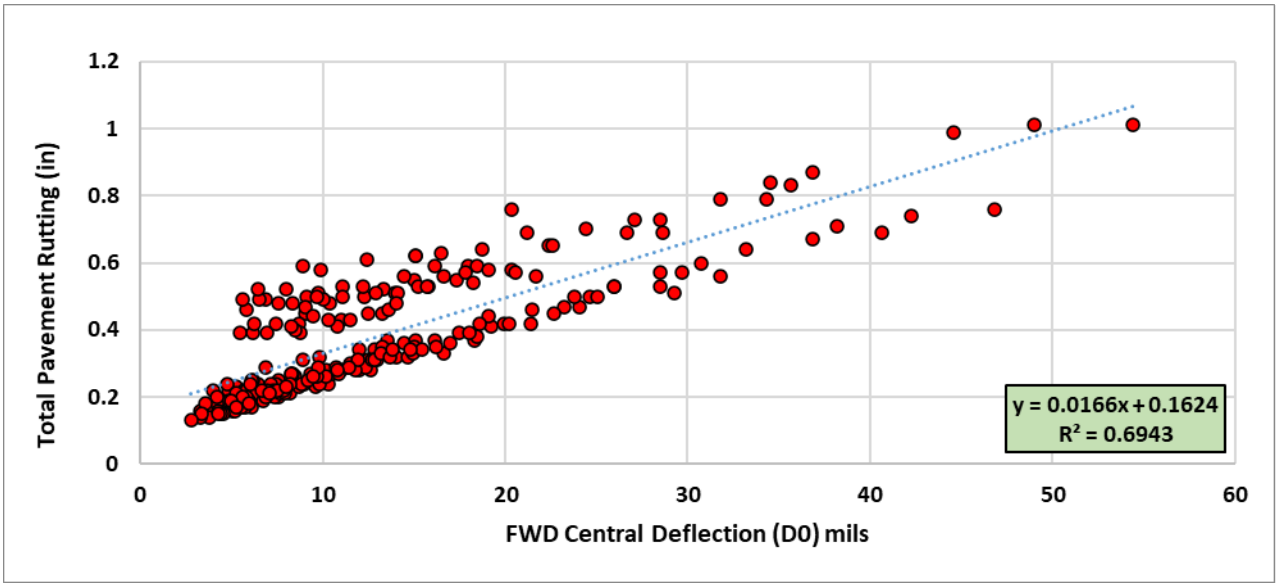

Figure 4.15 FWD Theoretical Maximum Deflection (D0) vs. Rutting (in)

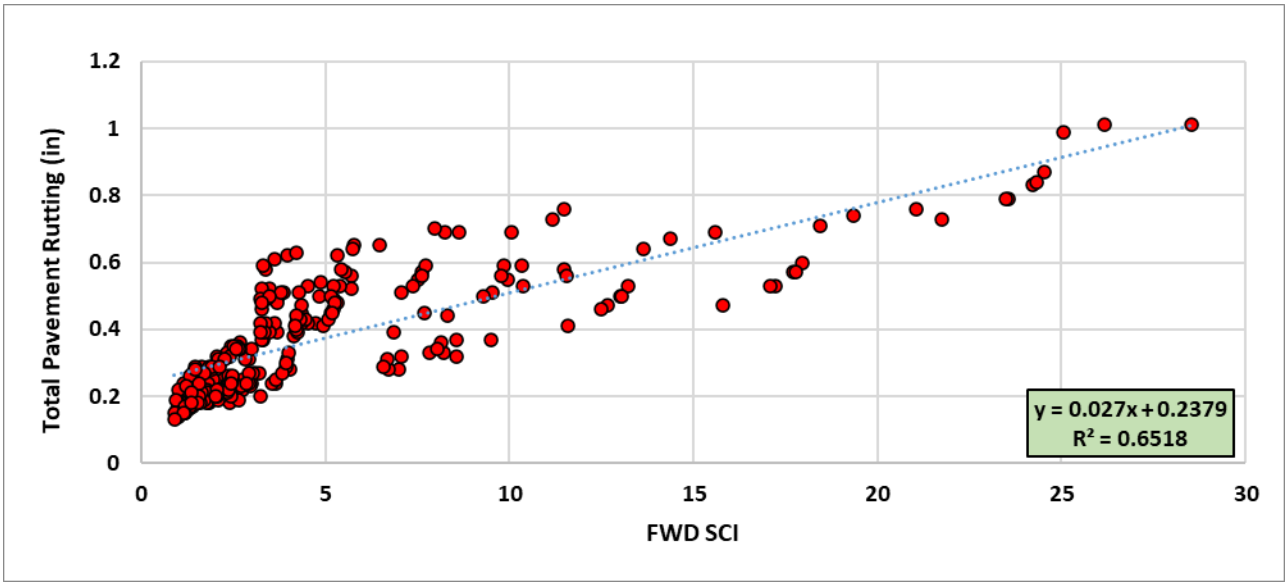

Figure 4.16 FWD SCI vs. Rutting (in)

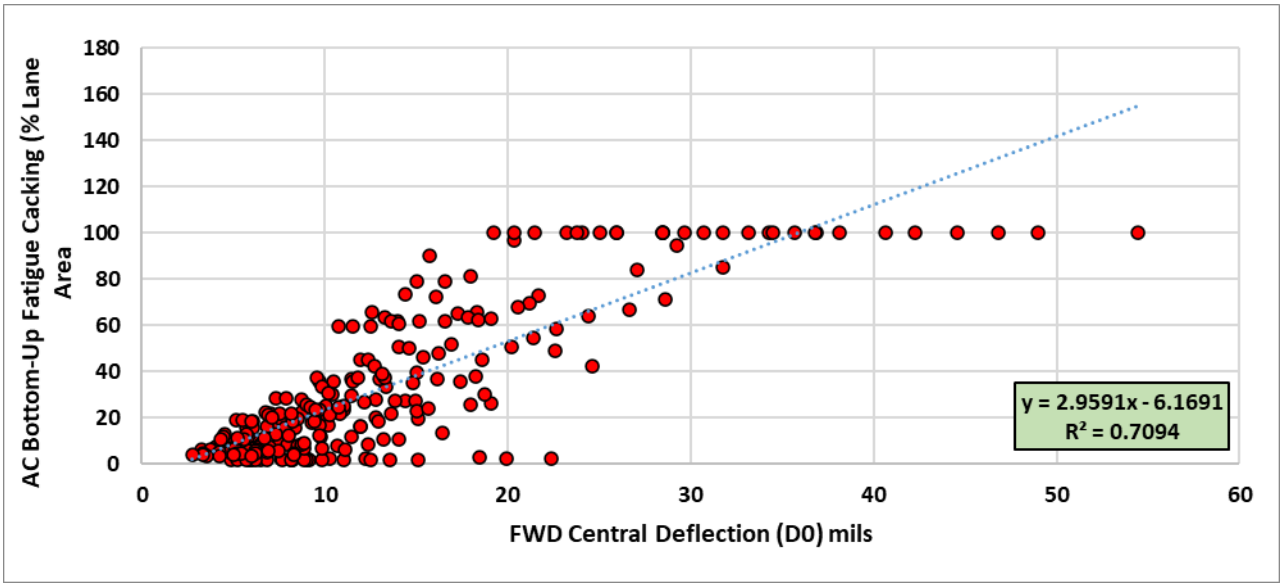

Figure 4.17 FWD Theoretical Maximum Deflection (D0) vs. Bottom-Up Cracking

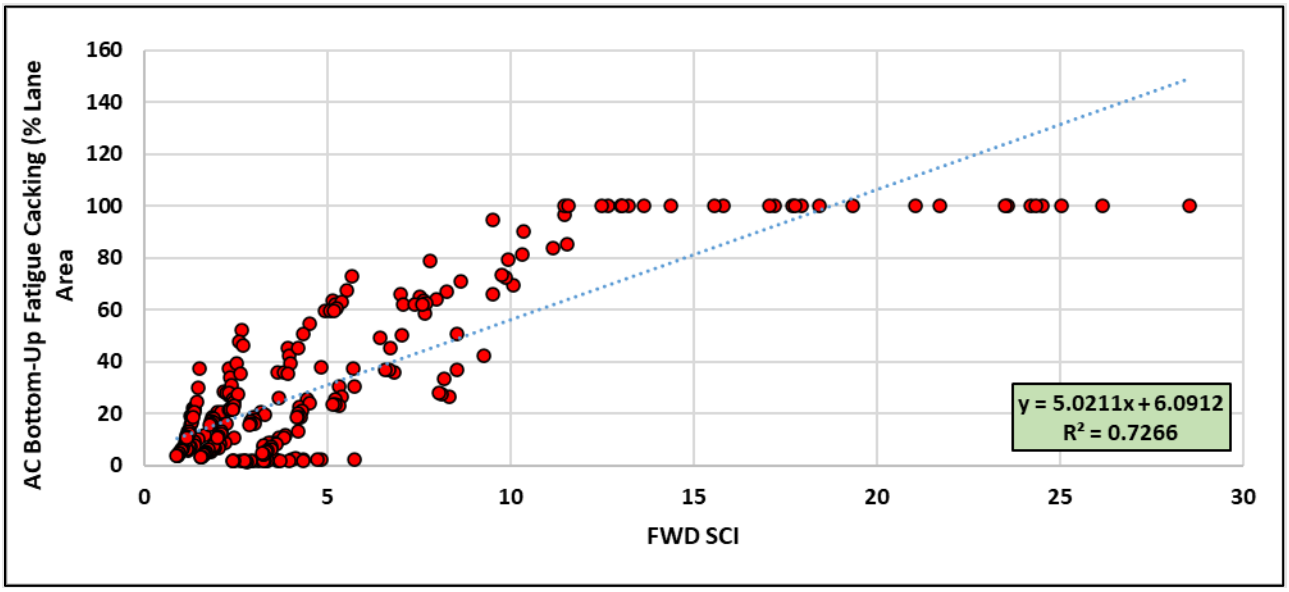

Figure 4.18 FWD SCI vs. Bottom-Up Cracking

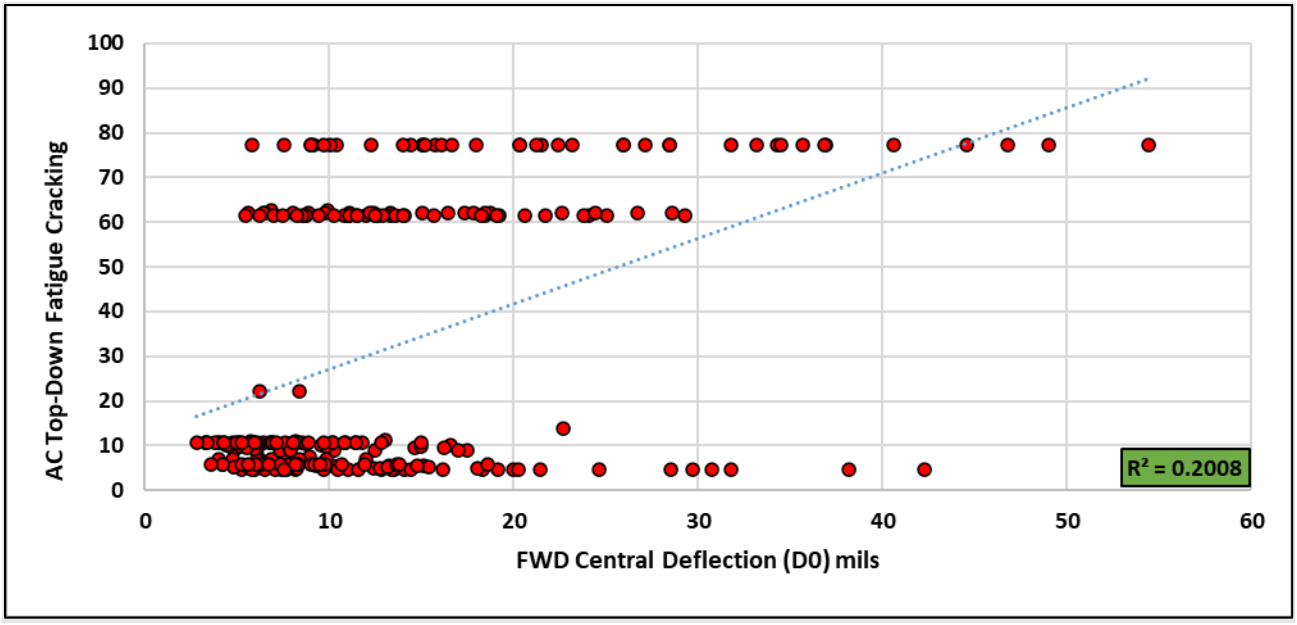

Figure 4.19 FWD Theoretical Maximum Deflection (D0) vs. Top-Down Cracking

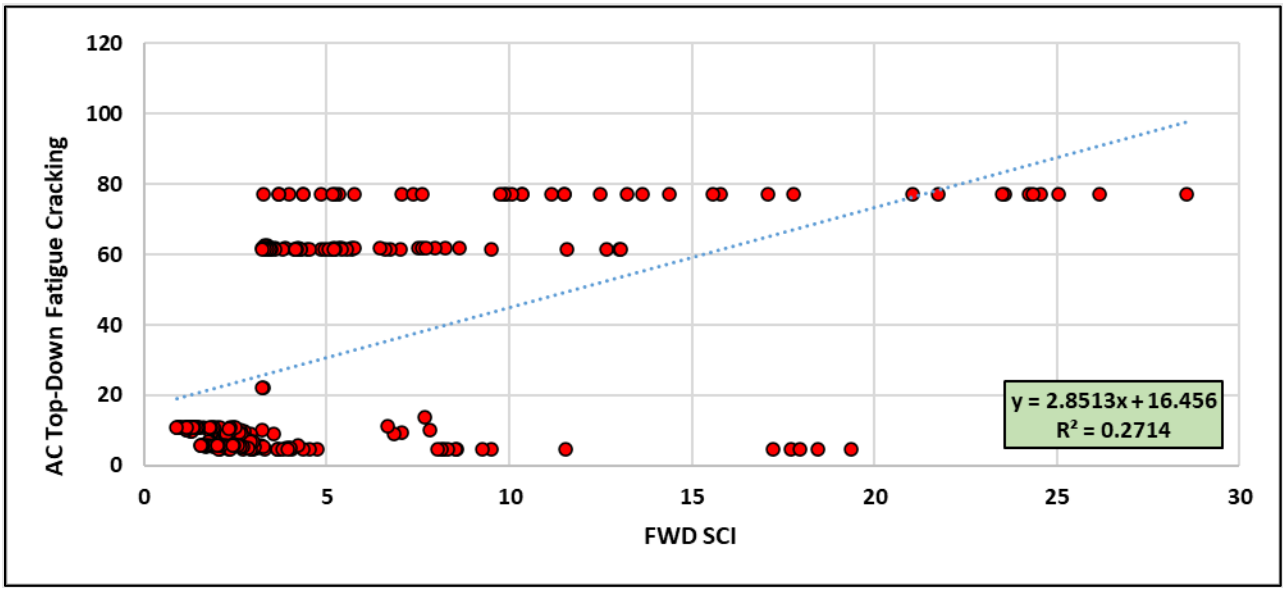

Figure 4.20 FWD SCI vs. Top-Down Cracking

4.3 FWD Field Deflection Data Analysis

4.3.1 Load Normalization of the Field Deflection Data

The FWD deflection data collected in the field were normalized to reference load and mid-depth pavement temperature. The target FWD applied load is 9,000 lb. The raw FWD deflection data showed that the applied load has a slight deviation, which is normal, from the target value. Thus, the FWD deflections were normalized using Equation 4.3.

$$d_{0n} = (L_{norm}/L_{applied}) * d_0 \quad \text{.....Eqn. 4.3}$$

where

d_{0n} = Normalized deflection

L_{norm} = Normalized load

$L_{applied}$ = Applied load

d_0 = Measured deflection at selected sensor location

4.3.2 Temperature Normalization of the Field Deflection Data

In addition to the applied load, the pavement temperature also has a significant impact on the deflection results obtained from FWD. The pavement temperature affects the moduli and deflection values of flexible pavements; therefore, the deflection data should be normalized for the account for the effect of pavement temperature at the time of testing. Kassem et al. (2020) developed a procedure to predict the mid-depth pavement temperature in Idaho. The model uses several parameters including pavement surface temperature, previous day's average air temperature, depth, and time of testing. Figure 4.21 shows a screen shot from the software developed by Kassem et al. (2020). This model used in this study, to predict the mid-depth pavement temperature. The reader is referred to Kassem et al. (2020) for more information about various models developed and selected to suit Idaho's conditions.

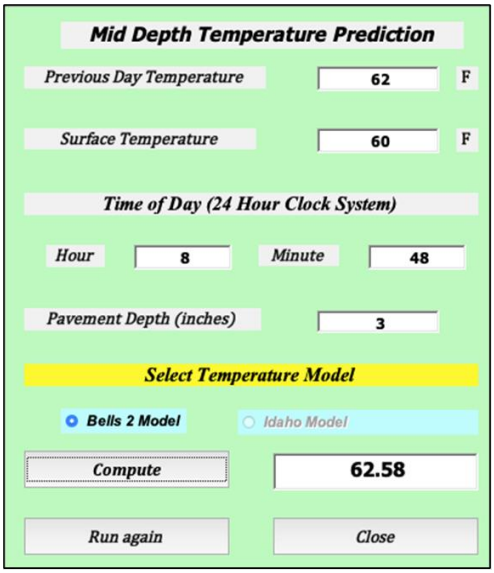

Figure 4.21 Mid-Depth Pavement Temperature Prediction Software

The research team utilized Equation 4.4 to normalize the deflection data to a refence temperature in accordance with the procedure that was developed for Idaho roads (Kassem et al. 2020). This step in important to factor out the effect of temperature on FWD and TSD deflection measurements.

$$D_{68} = D_T * [10^{\alpha(68-T)}] \quad \text{.....Eqn. 4.4}$$

where

D_{68} = adjusted deflection to the reference temperature of 68°F (in.)

D_T = deflection measured at temperature T (°F)(in.),

$\alpha = 3.67*10^{-4}*t^{1.4635}$ for wheel paths, and $3.65*10^{-4}*t^{1.4241}$ for lane centers,

t = thickness of the AC layer (in.), and

T = the AC layer mid depth temperature (°F) at the time of FWD testing.

4.3.3 Deflection Basin Parameters vs. Field Layers' Moduli

The researchers assessed the correlation between various DBPs and the pavement layer moduli (calculated using Modulus 7 software) as shown in Figure 4.22 through Figure 4.26. The results demonstrated that that there is a fair correlation between the deflection of the last sensor (D_{60} or W_7) and subgrade modulus (R^2 = 0.54). Also, there was a trend between SCI and the modulus of asphalt layer

(R^2 = 0.39). The modulus of asphalt layer increased with the decrease of SCI. Other DBPs didn't provide strong correlations with the pavement layer moduli. The correlations between additional DBPs and the pavement layer moduli didn't provide clear trends.

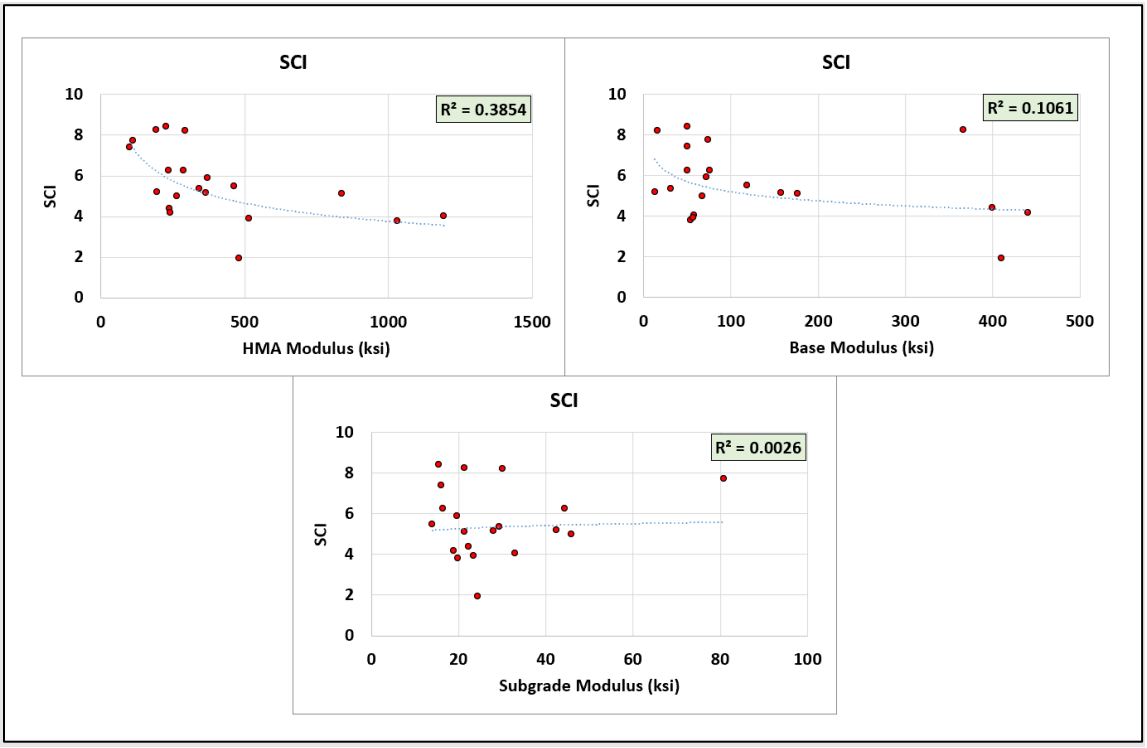

Figure 4.22 SCI vs. Pavement Layers' Moduli

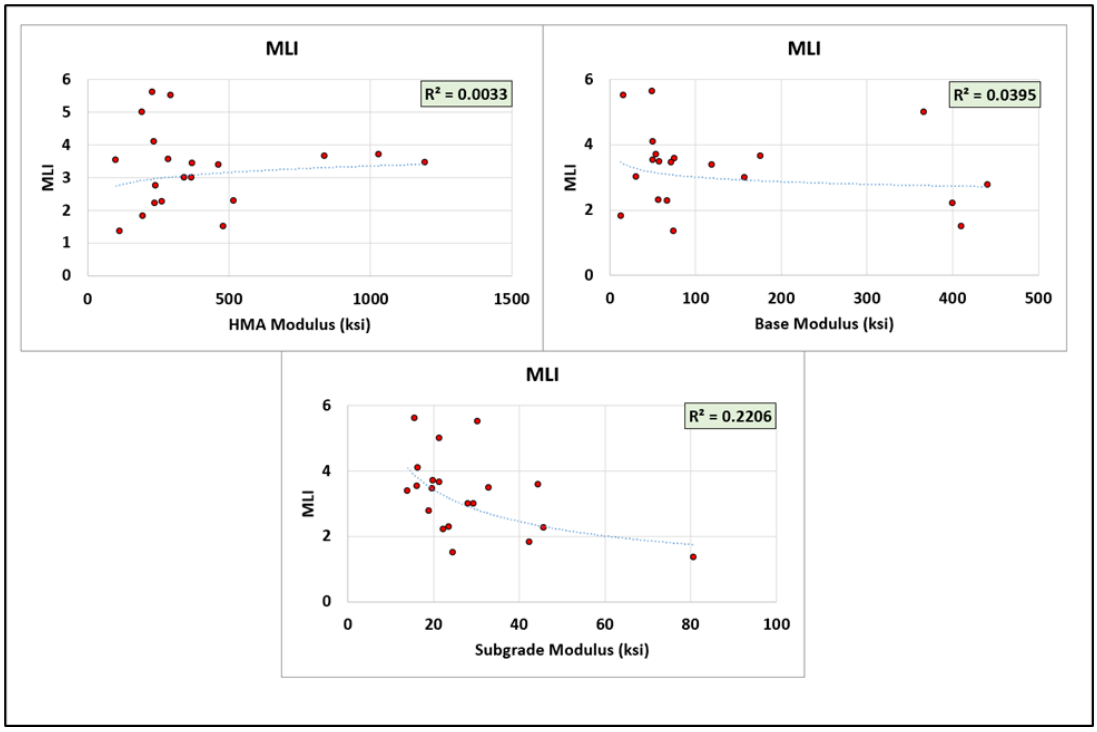

Figure 4.23 MLI vs. Pavement Layers' Moduli

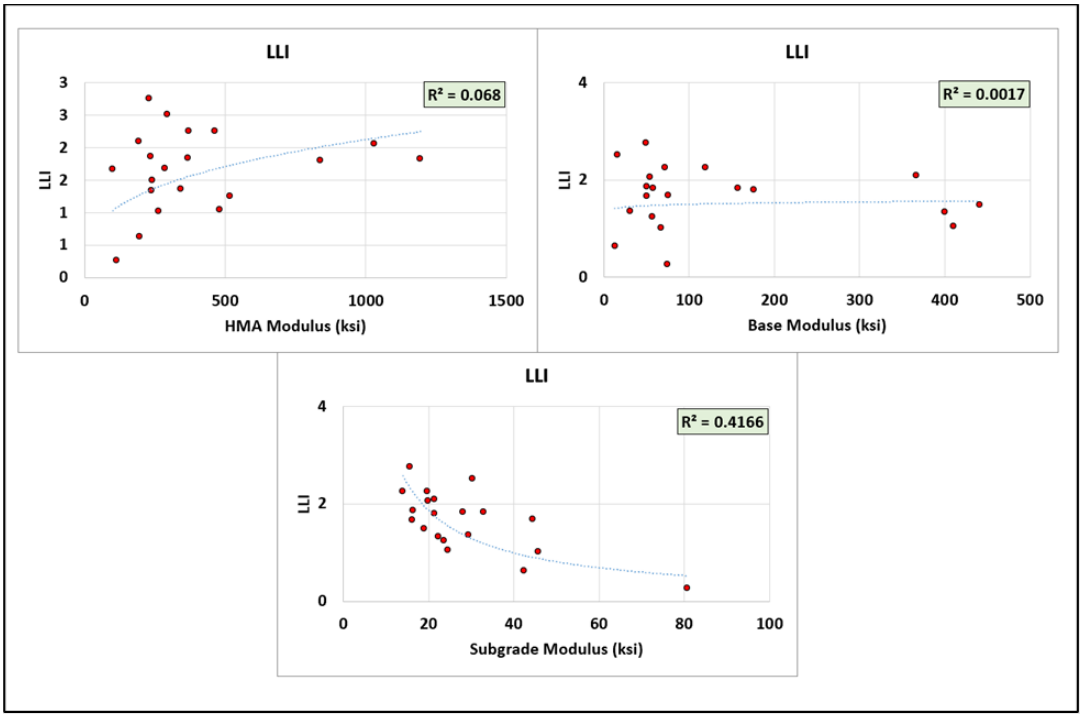

Figure 4.24 LLI vs. Pavement Layers' Moduli

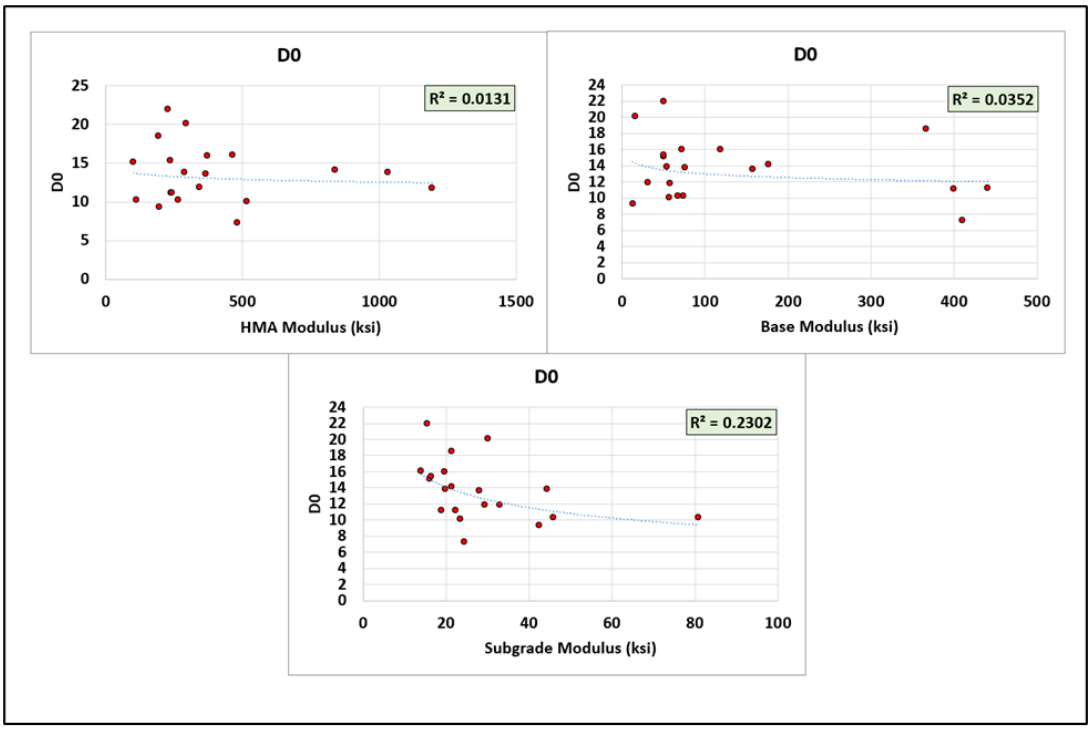

Figure 4.25 D_0 vs. Pavement Layers' Moduli

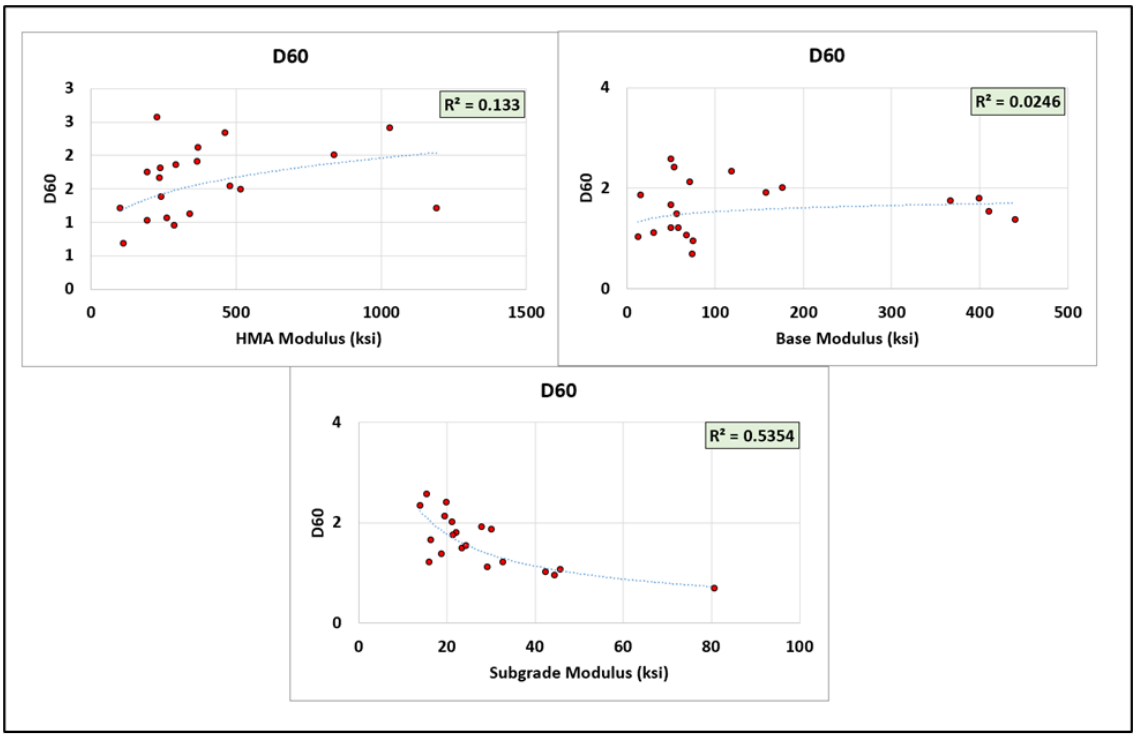

Figure 4.26 D_{60} vs. Pavement Layers' Moduli

4.3.4 Deflection Basin Parameters vs. Field Performance Data

The research team investigated the correlation between the field performance indicators such as rutting, IRI, and cracking with the FWD DBPs. The pavement performance data were collected from the Idaho Transportation Asset Management System (TAMS). The performance data are collected by ITD personnel and used to prioritize the maintenance and rehabilitation treatments based on the pavement conditions. The comparison between the deflection values and pavement performance indicators revealed a weak correlation between FWD deflections and rutting, as demonstrated in Tables 4.3 and 4.4. For example, some pavement sections with lower deflection values showed higher rutting measurements, while others showed lower rutting measurements. A similar trend was observed for the Overall Condition Index (OCI). However, a better correlation was observed between the deflection values and IRI performance where higher deflection values were associated with poor IRI performance. Furthermore, the researchers assessed the conditions of various layers (i.e., asphalt layer, base, subgrade) based on the DBPs thresholds proposed in previous studies and compared to the pavement performance thresholds for rutting, IRI, and OCI. The green color indicates good conditions, yellow color indicates fair conditions, while red indicates poor conditions in Tables 4.3 though Table 4.7. Tables 4.5 to 4.7 show the correlation between the pavement performance indicators and deflection basin parameters of BLI, MLI, and LLI, respectively. It should be noted that while some sections with higher IRI (poor performance) had relatively higher deflection parameters (e.g., D_0, BLI, MLI), there was no consistent trend to make definitive conclusions.

Table 4.3 D_0 versus Pavement Performance

Pavement Site	D_0 (mils)	OCI	IRI (inch/mile)	Rutting (in.)	Base Layer Condition	OCI Condition	IRI Condition	Rutting Condition
1	7.35	97.3	37	0.13	Sound	Good	Good	Good
2	4.84	94.82	62	0.3	Sound	Good	Good	Fair
3	4.93	89.28	56	0.29	Sound	Good	Good	Fair
4	10.05	89.52	73	0.19	Sound	Good	Good	Good
5	16.43	87.13	113	0.16	Sound	Good	Fair	Good
6	15.8	89.94	101	0.19	Sound	Good	Fair	Good
7	12.82	89.82	95	0.20	Sound	Good	Good	Good
8	13.46	82.88	84	0.25	Sound	Good	Good	Fair
9	13.81	100	193	0.27	Sound	Good	Poor	Fair
10	13.89	100	193	0.27	Sound	Good	Poor	Fair
11	14.99	100	201	0.25	Sound	Good	Poor	Fair
12	9.28	100	151	0.24	Sound	Good	Fair	Fair
13	14.58	97.63	74	0.3	Sound	Good	Good	Fair
14	10.5	93.19	80	0.18	Sound	Good	Good	Good
15	7.03	98.51	56	0.17	Sound	Good	Good	Good
16	7.57	99.47	76	0.24	Sound	Good	Good	Fair
17	9.49	96.63	70	0.24	Sound	Good	Good	Fair
18	12.24	98.69	65	0.27	Sound	Good	Good	Fair
19	9.9	99.59	59	0.39	Sound	Good	Good	Fair
20	11.37	98.56	77	0.27	Sound	Good	Good	Fair
21	8.88	90.44	78	0.14	Sound	Good	Good	Good
22	4.69	95.96	66	0.18	Sound	Good	Good	Good
23	12.35	75.9	72	0.2	Sound	Fair	Good	Fair

Table 4.4 W_7 versus Pavement Performance

Pavement Site	W7 (mils)	OCI	IRI (inch/mile)	Rutting (in.)	Subgrade Layer Condition	OCI Condition	IRI Condition	Rutting Condition
1	0.76	97.3	37	0.13	Good	Good	Good	Good
2	0.32	94.82	62	0.3	Very Good	Good	Good	Fair
3	0.54	89.28	56	0.29	Very Good	Good	Good	Fair
4	0.94	89.52	73	0.19	Good	Good	Good	Good
5	2.7	87.13	113	0.16	Very Poor	Good	Fair	Good
6	2.87	89.94	101	0.19	Very Poor	Good	Fair	Good
7	2.23	89.82	95	0.2	Poor	Good	Good	Good
8	1.37	82.88	84	0.25	Good	Good	Good	Fair
9	1.96	100	193	0.27	Poor	Good	Poor	Fair
10	1.28	100	193	0.27	Good	Good	Poor	Fair
11	1.39	100	201	0.25	Fair	Good	Poor	Fair
12	0.64	100	151	0.24	Very Good	Good	Fair	Fair
13	2.12	97.63	74	0.3	Very Poor	Good	Good	Fair
14	1.69	93.19	80	0.18	Poor	Good	Good	Good
15	1.04	98.51	56	0.17	Fair	Good	Good	Good
16	1.22	99.47	76	0.24	Good	Good	Good	Fair
17	0.76	96.63	70	0.24	Very Good	Good	Good	Fair
18	1.15	98.69	65	0.27	Good	Good	Good	Fair
19	1.39	99.59	59	0.39	Good	Good	Good	Fair
20	1.51	98.56	77	0.27	Fair	Good	Good	Fair
21	1.09	90.44	78	0.14	Good	Good	Good	Good
22	0.99	95.96	66	0.18	Very Good	Good	Good	Good
23	1.33	75.9	72	0.2	Good	Fair	Good	Fair

Table 4.5 BLI versus Pavement Performance

Pavement Site	BLI (mils)	OCI	IRI (inch/mile)	Rutting (in.)	Asphalt Layer Condition	OCI Condition	IRI Condition	Rutting Condition
1	3.57	97.3	37	0.13	Good	Good	Good	Good
2	3.63	94.82	62	0.3	Fair	Good	Good	Fair
3	2.75	89.28	56	0.29	Good	Good	Good	Fair
4	4.53	89.52	73	0.19	Good	Good	Good	Good
5	4.24	87.13	113	0.16	Very Good	Good	Fair	Good
6	3.87	89.94	101	0.19	Very Good	Good	Fair	Good
7	3.51	89.82	95	0.2	Very Good	Good	Good	Good
8	4.6	82.88	84	0.25	Very Good	Good	Good	Fair
9	4.98	100	193	0.27	Good	Good	Poor	Fair
10	5.46	100	193	0.27	Good	Good	Poor	Fair
11	6.12	100	201	0.25	Fair	Good	Poor	Fair
12	4.22	100	151	0.24	Good	Good	Fair	Fair
13	4.99	97.63	74	0.3	Good	Good	Good	Fair
14	3.2	93.19	80	0.18	Very Good	Good	Good	Good
15	2.73	98.51	56	0.17	Very Good	Good	Good	Good
16	2.98	99.47	76	0.24	Very Good	Good	Good	Fair
17	4.64	96.63	70	0.24	Good	Good	Good	Fair
18	5.46	98.69	65	0.27	Good	Good	Good	Fair
19	3.75	99.59	59	0.39	Very Good	Good	Good	Fair
20	4.2	98.56	77	0.27	Good	Good	Good	Fair
21	3.31	90.44	78	0.14	Good	Good	Good	Good
22	1.26	95.96	66	0.18	Very Good	Good	Good	Good
23	5.01	75.9	72	0.2	Good	Fair	Good	Fair

Table 4.6 MLI versus Pavement Performance

Pavement Site	MLI (mils)	OCI	IRI (inch/mile)	Rutting (in.)	Base Layer Condition	OCI Condition	IRI Condition	Rutting Condition
1	1.62	97.3	37	0.13	Good	Good	Good	Good
2	0.64	94.82	62	0.3	Very Good	Good	Good	Fair
3	0.96	89.28	56	0.29	Very Good	Good	Good	Fair
4	2.54	89.52	73	0.19	Good	Good	Good	Good
5	4.36	87.13	113	0.16	Poor	Good	Fair	Good
6	3.88	89.94	101	0.19	Fair	Good	Fair	Good
7	3.44	89.82	95	0.2	Fair	Good	Good	Good
8	3.95	82.88	84	0.25	Fair	Good	Good	Fair
9	3.56	100	193	0.27	Fair	Good	Poor	Fair
10	3.91	100	193	0.27	Poor	Good	Poor	Fair
11	4.11	100	201	0.25	Poor	Good	Poor	Fair
12	2.4	100	151	0.24	Fair	Good	Fair	Fair
13	3.07	97.63	74	0.3	Fair	Good	Good	Fair
14	2.41	93.19	80	0.18	Good	Good	Good	Good
15	1.6	98.51	56	0.17	Good	Good	Good	Good
16	1.5	99.47	76	0.24	Very Good	Good	Good	Fair
17	2.22	96.63	70	0.24	Good	Good	Good	Fair
18	3.3	98.69	65	0.27	Fair	Good	Good	Fair
19	2.18	99.59	59	0.39	Good	Good	Good	Fair
20	2.45	98.56	77	0.27	Good	Good	Good	Fair
21	2.19	90.44	78	0.14	Good	Good	Good	Good
22	0.97	95.96	66	0.18	Very Good	Good	Good	Good
23	3.28	75.9	72	0.2	Fair	Fair	Good	Fair

Table 4.7 LLI versus Pavement Performance

Pavement Site	LLI (mils)	OCI	IRI (inch/mile)	Rutting (in.)	Base/Lower Layer Condition	OCI Condition	IRI Condition	Rutting Condition
1	0.73	97.3	37	0.13	Sound	Good	Good	Good
2	0.13	94.82	62	0.3	Sound	Good	Good	Fair
3	0.34	89.28	56	0.29	Sound	Good	Good	Fair
4	1.15	89.52	73	0.19	Sound	Good	Good	Good
5	2.6	87.13	113	0.16	Sound	Good	Fair	Good
6	2.56	89.94	101	0.19	Sound	Good	Fair	Good
7	1.91	89.82	95	0.2	Sound	Good	Good	Good
8	2.08	82.88	84	0.25	Sound	Good	Good	Fair
9	1.76	100	193	0.27	Sound	Good	Poor	Fair
10	1.79	100	193	0.27	Sound	Good	Poor	Fair
11	1.88	100	201	0.25	Sound	Good	Poor	Fair
12	1.13	100	151	0.24	Sound	Good	Fair	Fair
13	2.05	97.63	74	0.3	Sound	Good	Good	Fair
14	1.52	93.19	80	0.18	Sound	Good	Good	Good
15	0.87	98.51	56	0.17	Sound	Good	Good	Good
16	0.91	99.47	76	0.24	Sound	Good	Good	Fair
17	1.04	96.63	70	0.24	Sound	Good	Good	Fair
18	1.38	98.69	65	0.27	Sound	Good	Good	Fair
19	1.34	99.59	59	0.39	Sound	Good	Good	Fair
20	1.6	98.56	77	0.27	Sound	Good	Good	Fair
21	1.18	90.44	78	0.14	Sound	Good	Good	Good
22	0.67	95.96	66	0.18	Sound	Good	Good	Good
23	1.5	75.9	72	0.2	Sound	Fair	Good	Fair

4.4 Effective Structural Number Calculation

Structural Number (SN) is a concept that quantifies the pavement structural requirements needed to support traffic loads. It considers factors such as traffic level (expressed in ESALs), soil support (modulus of subgrade), terminal serviceability, and environmental conditions to determine the required pavement thickness. The research team utilized the effective structural number to determine the required overlay thickness for the examined pavement sections using FWD deflection data. The team used three methods to calculate the effective structural number. Those three methods and the calculations of the effective structural number are discussed in the following section.

4.4.1 Deflection Value

The first method used to determine the effective structural number (SN_{eff}) is the deflection method (deflection value). The SN_{eff} is calculated using Equation 4.5. This method utilizes the existing pavement modulus of all layers above the subgrade calculated using 4.6. The existing pavement modulus is a function of the FWD deflection measurements for Sensor No. 1 (W_1) and Sensor No. 7 (W_7). The subgrade modulus is calculated using Equation 4.7 as function of loading pressure and the deflection measurement at W7. Table 4.8 summarizes the SN_{eff} calculations for the test sections. The researchers considered the corrected deflection measurements to account for the effect of temperature as discussed earlier. In addition, they used the deflection data without temperature correction and calculated the SN_{eff} for the test sections as summarized in Table 4.9. The reason for this is that FWD deflection measurements were found to have better correlations with TSD without temperature correction for both FWD and TSD. Therefore, the researchers examined the correlation between SN_{eff} calculated using corrected and uncorrected FWD as well as corrected and uncorrected TSD as discussed in detail in Chapter 6.

$$SN_{eff} = 0.0045*D*E_p^{0.333} \quad \text{.....Eqn. 4.5}$$

where,

D = total thickness of the pavement layers

Ep = existing pavement modulus of all layers above the subgrade calculated using Equation 4.6.

$$E_p/E_{subgrade} = 5.16.94*(W_7/W_1)^{5/2} - 214.46*(W_7/W_1)^2 + 159.56*(W_7/W_1)^{3/2} - 6.143*(W_7/W_1) + 1.0826*(W_7/W_1)^{1/2} \quad \text{.....Eqn. 4.6}$$

where,

($E_{subgrade}$) = subgrade modulus and it is calculated using Equation 4.7.

W_1 = deflection at Sensor 1

W_7 = deflection at Sensor 2

$$E_{Subgrade} = \frac{0.24 * P}{d_r * r}$$

……Eqn. 4.7

Table 4.8 SN_{eff} Results using Deflection Value Method (Corrected Deflections)

Pavement Site	D0	D60	Subgrade Moduli (psi)	AC Thickness	Base Thickness	Total Pavement Thickness (D) (in.)	Selected $E_{pavement}$ (psi)	Effective Structural Number (Sn_{eff})
1	7.35	0.76	41860	6	27.6	33.6	199787	8.80
2	4.84	0.32	112500	7.08	8.86	15.94	168387	3.95
3	4.93	0.54	66667	18	18	36	343295	11.30
4	10.05	0.94	30151	5.4	11.4	16.8	168387	4.16
5	12.82	2.23	15152	3.6	18	21.6	174721	5.41
6	13.81	1.96	17094	4.8	12	16.8	189623	4.33
7	13.89	1.39	18779	4.8	7.8	12.6	141513	2.94
8	9.28	0.64	32967	5.9	14.76	20.66	106268	4.39
9	13.46	1.37	18154	6	18.6	24.6	88633	4.92
10	14.58	2.12	13453	2.9	11.8	14.7	200560	3.86
11	7.03	1.04	32967	6	18	24	295433	7.16
12	16.96	1.98	18182	5.4	4.8	10.2	258265	2.91
13	7.57	1.22	27523	4.83	7.38	12.21	498489	4.34
14	9.49	0.76	33994	6.87	6.98	13.85	173683	3.46
15	12.24	1.15	24948	6.76	6.5	13.26	168178	3.28
16	9.90	1.39	22613	4.79	7.45	12.24	315736	3.73
17	11.37	1.51	19068	4.23	7.93	12.16	240059	3.39
18	8.88	1.09	26627	3.21	8.83	12.04	289970	3.57
19	4.69	0.99	33520	6.72	8.44	15.16	755285	6.18
20	12.35	1.33	22222	6.24	6.21	12.45	190894	3.21

Table 4.9 SN_{eff} Results using Deflection Value Method (Uncorrected Deflections)

Pavement Site	D0	D60	Subgrade Moduli (psi)	AC Thickness	Base Thickness	Total Pavement Thickness (D) (in.)	Selected $E_{pavement}$ (psi)	Effective Structural Number (Sn_{eff})
1	10.30	1.06	29854	6	27.6	33.6	141617.57	7.85
2	10.30	0.68	52639	7.08	8.86	15.94	143024.65	3.74
3	9.33	1.02	35175	18	18	36	181377.95	9.13
4	11.90	1.12	25419	5.4	11.4	16.8	143024.65	3.94
5	13.84	2.41	14025	3.6	18	21.6	161753.94	5.27
6	14.16	2.00	16679	4.8	12	16.8	184264.98	4.28
7	20.10	1.86	14008	4.8	7.8	12.6	91983.95	2.55
8	13.80	0.95	22166	5.9	14.76	20.66	71506.63	3.84
9	11.84	1.21	20632	6	18.6	24.6	100947.43	5.13
10	16.05	2.34	12204	2.9	11.8	14.7	182137.74	3.73
11	10.08	1.49	22941	6	18	24	205752.03	6.35
12	21.98	2.57	11320	5.4	4.8	10.2	161515.11	2.49
13	11.17	1.80	18626	4.83	7.38	12.21	337938.49	3.81
14	15.16	1.21	21296	6.87	6.98	13.85	107854.88	2.96
15	18.54	1.75	16480	6.76	6.5	13.26	111981.45	2.86
16	13.61	1.91	16452	4.79	7.45	12.24	228879.77	3.36
17	16.00	2.12	13556	4.23	7.93	12.16	169779.77	3.02
18	11.21	1.38	21123	3.21	8.83	12.04	229949.86	3.31
19	7.27	1.53	21620	6.72	8.44	15.16	486472.74	5.34
20	15.39	1.66	17827	6.24	6.21	12.45	153283.96	2.99

4.4.2 Rohde's Equation

The researchers used Rohde's equation (Equation 4.8) to determine the pavement structural number. The structural number is a function of the total pavement thickness, structural index of the pavement, and regression coefficients (Equation 4.8). The structural index is calculated using Equation 4.9. Table 4.10 and 4.11 summarize the SN_{eff} calculations for the test sections using correction and uncorrected FWD deflection data, respectively using the Rohde's equation.

$$SN_{eff} = k_1 SIP^{K2} H_p^{K3} \quad \text{.....Eqn. 4.8}$$

where,

SN = Pavement structural number (in.)

SIP = Structural Index of pavement (microns)

Hp = Total pavement thickness (mm)

K1, K2, K3 = Regression coefficients (0.4728, -0.4810, and 0.7581, respectively).

$$SIP = D_0 - D_{1.5Hp}$$

……Eqn. 4.9

where,

SIP = Structural index of pavement

D_0 = Peak deflection

$D_{1.5Hp}$ = Surface deflection measured at offset of 1.5 times of Hp

H_p = Total pavement thickness

Table 4.10 S_{Neff} Results Using Rohde's Equation (Corrected Deflections)

Pavement Site	W_1 (mils)	D_0 (μm)	Total Pavement Thickness (H_p) (in.)	Total Pavement Thickness (H_p) (mm)	$D_{1.5Hp}$ (mils)	$D_{1.5Hp}$ (μm)	SIP (μm)	Effective Structural Number (Sn_{eff})
1	7.350	186.69	33.6	853.44	0.93	23.55	163.14	6.80
2	4.840	122.94	15.9	404.88	0.91	23.07	99.87	4.89
3	4.930	125.22	36.0	914.40	0.53	13.40	111.82	8.59
4	10.050	255.27	16.8	426.72	3.25	82.54	172.73	3.91
5	12.820	325.63	21.6	548.64	4.83	122.57	203.06	4.38
6	13.810	350.77	16.8	426.72	5.61	142.58	208.20	3.58
7	13.890	352.81	12.6	320.04	6.47	164.45	188.36	3.02
8	9.280	235.71	20.7	524.76	2.14	54.24	181.47	4.47
9	13.460	341.88	24.6	624.84	3.14	79.66	262.22	4.27
10	14.580	370.33	14.7	373.38	7.02	178.34	192.00	3.36
11	7.030	178.56	24.0	609.60	2.01	51.11	127.45	5.93
12	16.960	430.78	10.2	259.08	4.26	108.17	322.62	1.98
13	7.570	192.28	12.2	310.13	3.93	99.74	92.54	4.15
14	9.490	241.05	13.9	351.79	3.43	87.17	153.88	3.57
15	12.240	310.90	13.3	336.80	4.83	122.62	188.27	3.14
16	9.900	251.46	12.2	310.90	5.04	128.06	123.40	3.62
17	11.370	288.80	12.2	308.86	5.89	149.48	139.32	3.40
18	8.880	225.55	12.0	305.82	4.47	113.66	111.89	3.74
19	4.690	119.13	15.2	385.06	2.58	65.59	53.53	6.36
20	12.350	313.69	12.5	316.23	5.60	142.21	171.48	3.13

Table 4.11 S_{Neff} Results using Rohde's Equation (Uncorrected Deflections)

Pavement Site	W_1 (mils)	D_0 (μm)	Total Pavement Thickness (H_p) (in.)	Total Pavement Thickness (H_p) (mm)	$D_{1.5Hp}$ (mils)	$D_{1.5Hp}$ (μm)	SIP (μm)	Effective Structural Number (Sn_{eff})
1	10.297	261.54	33.6	853.44	1.30	32.95	228.59	5.78
2	10.301	261.64	15.9	404.88	1.93	49.10	212.54	3.40
3	9.334	237.09	36.0	914.40	1.00	25.39	211.69	6.32
4	11.901	302.29	16.8	426.72	3.85	97.88	204.42	3.61
5	13.844	351.64	21.6	548.64	5.21	132.38	219.26	4.22
6	14.160	359.67	16.8	426.72	5.75	146.12	213.56	3.53
7	20.104	510.63	12.6	320.04	8.80	223.43	287.20	2.46
8	13.800	350.52	20.7	524.76	3.18	80.68	269.84	3.69
9	11.839	300.71	24.6	624.84	2.76	70.12	230.59	4.55
10	16.054	407.78	14.7	373.38	7.73	196.41	211.37	3.21
11	10.083	256.10	24.0	609.60	2.89	73.35	182.75	4.99
12	21.984	558.39	10.2	259.08	11.95	303.45	254.94	2.22
13	11.172	283.77	12.2	310.13	5.80	147.25	136.52	3.44
14	15.158	385.01	13.9	351.79	5.48	139.16	245.85	2.85
15	18.540	470.93	13.3	336.80	7.32	185.84	285.08	2.57
16	13.611	345.71	12.2	310.90	6.93	175.97	169.74	3.10
17	15.997	406.33	12.2	308.86	8.28	210.25	196.08	2.88
18	11.214	284.83	12.0	305.82	5.65	143.48	141.34	3.35
19	7.270	184.67	15.2	385.06	4.01	101.73	82.94	5.15
20	15.388	390.87	12.5	316.23	6.98	177.24	213.62	2.81

4.4.3 Iterative AASHTO Equation

The researchers used the iterative AASHTO method to calculate the SNeff using Equation 4.10. This method uses the same concept as the deflection method; however, the existing pavement modulus of all layers above the subgrade in Equation 4.10 was calculated using an iterative method using Equation 4.11. This equation has different variables including the maximum deflection under the plate (D_0), resilient modulus of subgrade, and loading plate radius. Table 4.12 and 4.13 summarize the SN_{eff} calculations for the test sections using correction and uncorrected FWD deflection data, respectively using the iterative AASHTO method.

$$SN_{eff} = 0.0045 * D * E_p^{0.333} \quad \text{.....Eqn. 4.10}$$

where,

D = total thickness of the pavement layers.

Ep = existing pavement modulus of all layers above the subgrade and it is calculated using an iterative equation (Equation 4.11).

$$d_0 = 1.5 * P * a * \left[\frac{1}{M_R \sqrt{1 + \left(\frac{D}{a} * \sqrt[3]{\frac{E_P}{M_R}} \right)^2}} + \frac{\left[1 - \frac{1}{\sqrt{1 + \left(\frac{D}{a} \right)^2}} \right]}{E_P} \right]$$

……..…Eqn. 4.11

where,

P = Pressure of the loading plate

D = total thickness of the pavement layers.

EP= existing pavement modulus of all layers above the subgrade.

M_R = Subgrade modulus calculated using Equation 4.12

$$M_R = \frac{0.24 * P}{d_r * r}$$

……. ……Eqn. 4.12

where,

r = the distance from the center of the plate to sensor which used for deflection measurement, (W7)

d_r = The deflection measurement at used (W7)

Table 4.12 SN_{eff} Results using AASHTO Iterative Equation (Corrected Deflections)

Pavement Site	W_1 (mils)	d_0 (inches)	Total Pavement Thickness (D) (in.)	M_R (psi)	$E_{pavement}$ (psi)	Least Sequre Error	d_0 (inches) from Iterative Equation	Effective Structural Number (Sn_{eff})
1	7.350	0.00735	33.6	41860	115814	7.18184E-24	0.00735	7.34
2	4.840	0.00484	15.94	112500	166908	1.67585E-22	0.00484	3.93
3	4.930	0.00493	36	66667	168130	1.526E-21	0.00493	8.91
4	10.050	0.01005	16.8	30151	105477	2.62793E-25	0.01005	3.56
5	12.820	0.01282	21.6	15152	93318	8.51652E-26	0.01282	4.39
6	13.810	0.01381	16.8	17094	90207	1.48114E-18	0.01381	3.38
7	13.890	0.01389	12.6	18779	104801	7.42554E-19	0.01389	2.66
8	9.280	0.00928	20.66	32967	104176	1.96048E-19	0.00928	4.36
9	13.460	0.01346	24.6	18154	74211	1.03626E-26	0.01346	4.63
10	14.580	0.01458	14.7	13453	112102	4.01938E-24	0.01458	3.18
11	7.030	0.00703	24	32967	146909	1.08634E-19	0.00703	5.68
12	16.960	0.01696	10.2	18182	89330	5.66601E-23	0.01696	2.04
13	7.570	0.00757	12.21	27523	252953	1.14218E-24	0.00757	3.46
14	9.490	0.00949	13.85	33994	119192	1.96381E-26	0.00949	3.06
15	12.240	0.01224	13.26	24948	99181	7.98072E-19	0.01224	2.75
16	9.900	0.0099	12.24	22613	177741	3.17453E-25	0.00990	3.08
17	11.370	0.01137	12.16	19068	161750	2.00563E-25	0.01137	2.97
18	8.880	0.00888	12.04	26627	190317	1.82337E-21	0.00888	3.10
19	4.690	0.00469	15.16	33520	420559	4.21579E-19	0.00469	5.09
20	12.350	0.01235	12.45	22222	113566	2.1472E-27	0.01235	2.70

Table 4.13 SN_{eff} Results using AASHTO Iterative Equation (Uncorrected Deflections)

Pavement Site	W_1 (mils)	d_0 (inches)	Total Pavement Thickness (D) (in.)	M_R (psi)	$E_{pavement}$ (psi)	Least Sequre Error	d_0 (inches) from Iterative Equation	Effective Structural Number (Sn_{eff})
1	10.297	0.010296715	33.6	29854	82689	7.09023E-26	0.01030	6.56
2	10.301	0.010300686	15.94	52639	78559	2.85323E-18	0.01030	3.06
3	9.334	0.009334164	36	35175	88821	1.9922E-21	0.00933	7.20
4	11.901	0.011901341	16.8	25419	89155	1.62718E-26	0.01190	3.36
5	13.844	0.013844096	21.6	14025	86434	2.47568E-26	0.01384	4.28
6	14.160	0.014160402	16.8	16679	87944	3.39112E-18	0.01416	3.35
7	20.104	0.020103717	12.6	14008	67386	2.13801E-24	0.02010	2.30
8	13.800	0.013799969	20.66	22166	70058	3.48039E-18	0.01380	3.82
9	11.839	0.011839055	24.6	20632	84386	1.79243E-21	0.01184	4.84
10	16.054	0.016054287	14.7	12204	101917	6.23828E-26	0.01605	3.08
11	10.083	0.010082625	24	22941	102522	2.46762E-25	0.01008	5.04
12	21.984	0.02198399	10.2	11320	89548	4.54069E-25	0.02198	2.05
13	11.172	0.011172097	12.21	18626	171642	1.13374E-27	0.01117	3.04
14	15.158	0.015157916	13.85	21296	74590	1.14403E-19	0.01516	2.61
15	18.540	0.018540444	13.26	16480	65444	1.09827E-27	0.01854	2.40
16	13.611	0.01361068	12.24	16452	129246	3.24258E-22	0.01361	2.77
17	15.997	0.015997154	12.16	13556	114929	2.49275E-18	0.01600	2.65
18	11.214	0.011213643	12.04	21123	150421	2.26053E-19	0.01121	2.87
19	7.270	0.007270491	15.16	21620	271321	8.41725E-19	0.00727	4.40
20	15.388	0.015388429	12.45	17827	91178	2.742E-26	0.01539	2.51

Table 4.14 summarizes the SN_{eff} calculated using the three methods (i.e., deflection value, Rohde's equation, and iterative AASHTO method) used in this study. The three methods provided comparable SN_{eff}; however, the results demonstrated that the iterative AASHTO method is the most conservative and resulted in lower SN_{eff} compared to other methods for most sections. While the deflection value method was the least conservative and provided higher SN_{eff} compared to iterative AASHTO method and Rohde's Equation for most of the section. Therefore, the researchers used the iterative AASHTO method (the most conservative method) to determine the required overlay thickness for the examined test sections as discussed in the following section.

Table 4.14 Summary of SN_{eff} using Different Methods

Pavement Site	Effective Structural Number (Sn_{eff}) Deflection Equation	Effective Structural Number (Sn_{eff}) Rhode Equation	Effective Structural Number (Sn_{eff}) AASHTO Iterative
1	7.85	5.78	6.56
2	3.74	3.4	3.06
3	9.13	6.32	7.2
4	3.94	3.61	3.36
5	5.27	4.22	4.28
6	4.28	3.53	3.35
7	2.55	2.46	2.3
8	3.84	3.69	3.82
9	5.13	4.55	4.84
10	3.73	3.21	3.08
11	6.35	4.99	5.04
12	2.49	2.22	2.05
13	3.81	3.44	3.04
14	2.96	2.85	2.61
15	2.86	2.57	2.4
16	3.36	3.1	2.77
17	3.02	2.88	2.65
18	3.31	3.35	2.87
19	5.34	5.15	4.4
20	2.99	2.81	2.51

4.5 Structural and Required Overlay Thickness

The SN_{eff} can be used to determine the required overlay thickness for flexible pavements. In this study, the SN_{eff} calculated using the iterative AASHTO method was used to determine the required overlay thickness for the examined pavement sections to serve the traffic for 20 years. The overlay thickness is calculated as a function of SN_{eff} and required structural number (SN_{req}) as presented in Equation 4.13. The SN_{req} is calculated using Equation 4.14. Table 4.15 summarizes the SN_{req} calculations for the examined test sections.

$$OT = (SN_{eff} - SN_{req}) \times a$$

……Eqn. 4.13

where

OT = overlay thickness

SN_{eff} = effective structural number

SN_{req} = required structural number calculated using Equation 4.14

a = Layer coefficient (taken 0.44)

$$log_{10}(W_{18}) = Z_R * S_0 + 9.36 * log_{10}(SN + 1) - 0.20 + \frac{log_{10}(\frac{\Delta PSI}{4.2 - 1.5})}{0.40 + \frac{1094}{(SN + 1)^{5.19}}} + 2.32 * log_{10}(M_R) - 0.87$$

……Eqn. 4.13

where

S_0 = Overall standard deviation (taken 0.45)

Z_R = Standard normal deviate (taken 1.645)

ΔPSI = serviceability loss (taken 1.7)

M_R = Subgrade resilient modulus

SN = Required structure number

W_{18} = Number of ESALs

Table 4-15 Required Structural Number Results using Iterative AASHTO Method

Pavement Site	Total Accumulated ESALs	MR (psi)	Least Squares Error	Calculated ESALs	SNReq
1	37178979	29854	37.864930	37178972.5	3.945
2	53385200	52639	0.000005	53385200.2	3.380
3	52961508	35175	0.031235	52961507.9	3.928
4	10592302	25419	0.001222	10592301.6	3.420
5	5719843	14025	0.000001	5719842.9	3.870
6	1105836	16679	0.771127	1105835.4	2.766
7	1408776	14008	0.000435	1408776.1	3.080
8	1408776	22166	0.009130	1408776.0	2.581
9	7266319	20632	0.000016	7266318.9	3.481
10	6482489	12204	0.000547	6482488.6	4.153
11	4152182	22941	0.000145	4152182.2	3.048
12	3442498	11320	0.000040	3442498.0	3.864
13	10009725	18626	0.055424	10009724.8	3.810
14	10009725	21296	0.000938	10009725.0	3.624
15	10009725	16480	0.949173	10009724.1	3.986
16	5147859	16452	1.432354	5147857.4	3.585
17	6355381	13556	0.640029	6355380.2	3.985
18	7785342	21123	0.002775	7785341.6	3.489
19	11270209	21620	5.477939	11270206.6	3.673
20	6461304	17827	0.006635	6461303.9	3.609

Table 4.16 summarizes the required overlay thickness. The results demonstrated that some sections showed that the current pavement structure is sufficient and no overly is needed. However, other sections showed that an overly is required. The required overly thicknesses varied from 0.30 to 3.6 inches depending on the traffic level, and current conditions (SN_{eff}) of the pavement structure. These overlay thickness results are compared to those calculated from the TSD as discussed in detail in Chapter 6. Also, Table 4.16 shows the current pavement conditions; however, there was no direct correlations between the current conditions of pavement sections and the required overlay thickness. In order to facilitate the calculations of SN_{req}, SN_{eff}, and overlay thickness, the research team developed an Excel spreadsheet that can be used for this purpose as discussed in Chapter 7.

Table 4-16 Results of Structural Condition and Overlay Thickness

Pavement Site	Structural Condition/Overlay thickness (in)	OCI Condition	IRI Condition	Rutting Condition
Project I-15 40-45 2020	Sufficient	Good	Good	Good
Project I-15 90-95 2020	1.68	Good	Good	Fair
Project I-15 100-105 2020	Sufficient	Good	Good	Fair
Project SH-39 46.80-51.80 2020	1.80	Good	Good	Good
Project SH-27 15-20 2020	1.51	Good	Good	Good
Project US-93 201.85-206.20 2020	Sufficient	Good	Poor	Fair
Project US-93 211.20-216.20 2020	1.66	Good	Poor	Fair
Project US-93 216.20-221.20 2020	Sufficient	Good	Fair	Fair
Project US-30 250.90-255.90 2020	Sufficient	Good	Good	Fair
Project SH-55 100.20-105.20 2020	3.68	Good	Good	Fair
Project SH-55 110.20-115.20 2020	Sufficient	Good	Good	Good
Project SH-52 19.00-22.20 2019	4.86			
Project US 95 MP 0.00-4.826 2019	1.92	Good	Good	Fair
Project US 95 MP 4.836-16.581 2019	3.02	Good	Good	Fair
Project US 95 MP 16.591-23.957 2019	2.65	Good	Good	Fair
Project US 95 MP 23.967-28.710 2019	2.71	Good	Good	Fair
Poject US 95 MP 28.720-35.614 2019	1.92	Good	Good	Fair
Project US 95 MP 35.714-41.418 2019	0.18	Good	Good	Good
Project US 95 MP 42.518-50.742 2019	0.78	Good	Good	Good
Project US 95 MP 61.023-69.219 2019	2.47	Fair	Good	Fair

5. TSD Results and Analysis

The researchers repeated the analysis conducted for FWD data (Chapter 4) using the TSD data. Chapter 5 focuses on the results of the analysis conducted using the TSD data. In order to avoid repetition, the reader is referred to Chapter 4 for methodology and equations used in the analysis of TSD data presented in this chapter. Chapter 5 discusses the results of TSD deflection measurements in the field and the TSD theoretical parametric study. The researchers simulated the TSD deflection basin using the 3D-Move software, calculated of deflection basin parameters from the TSD data collected in the field, correlated the parameters to the pavement conditions, and calculated pavement overlay thicknesses based on the deflection data, traffic level, and pavement conditions.

5.1 TSD Simulation using 3D-Move Software

Figure 5.1 through Figure 5.4 shows the TSD deflection basin predicted using the 3D-Move software and field measurements for four test sections, three in District 3 and one in District 2 in Idaho. Similar to the FWD results, the 3D-Move software was able to simulate the deflection basin in the field upon selecting proper layer moduli for the examined pavement structure. These results demonstrated that the 3D-Move software can be used to examine the effect of various parameters including layer thickness and modulus of pavements on the TSD deflection basin. Similar to FWD, the researchers conducted a theoretical parametric study to examine the correlation between pavement response and TSD deflection parameters as discussed in the next section.

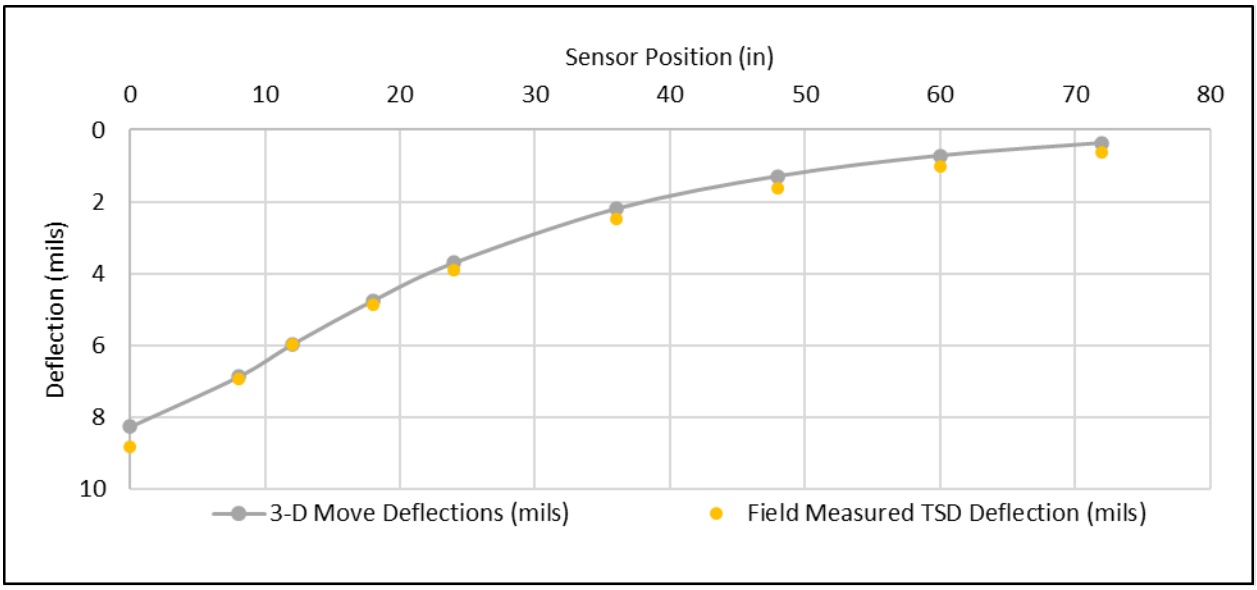

Figure 5.1 Comparison between Predicted and Measured TSD Deflection Basin: Section D-3 SH-55 2020

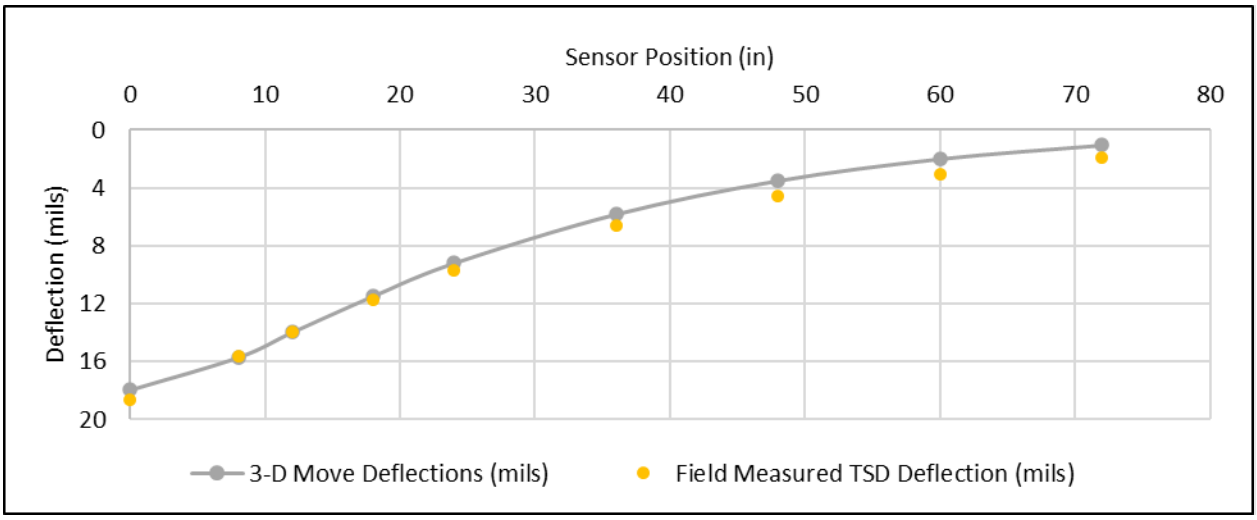

Figure 5.2 Comparison between Predicted and Measured TSD Deflection Basin: Section D-3 US-95 2019 Wilder SCL to Parma SCL

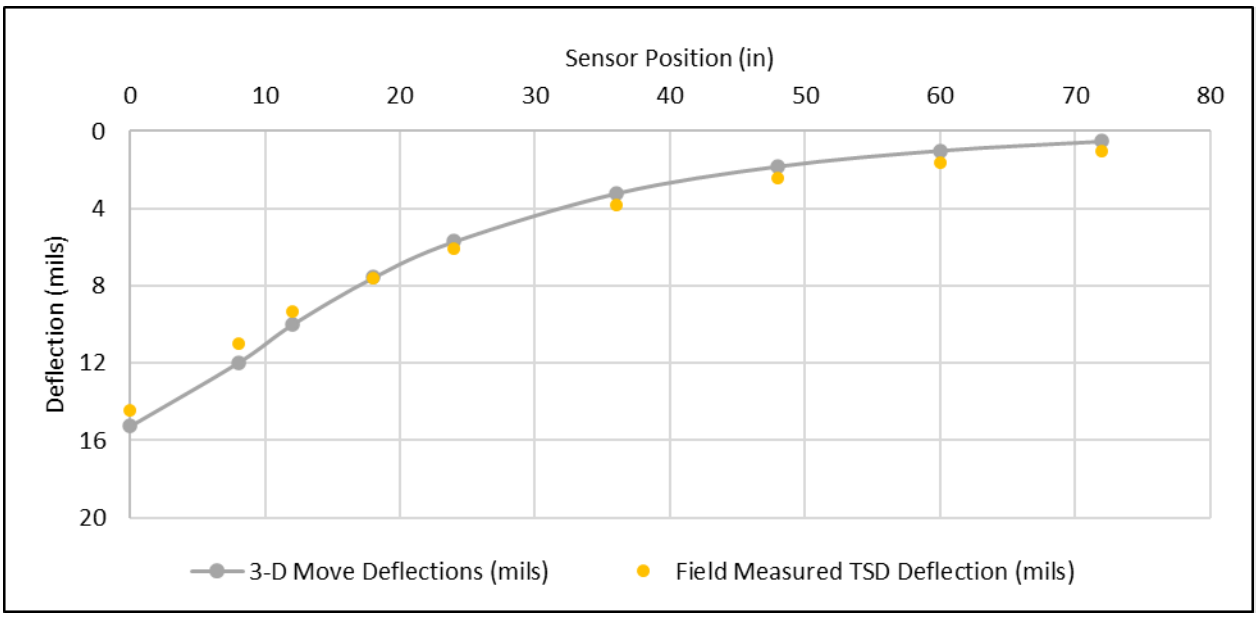

Figure 5.3 Comparison between Predicted and Measured TSD Deflection Basin: Section D-2 SH-3 2019

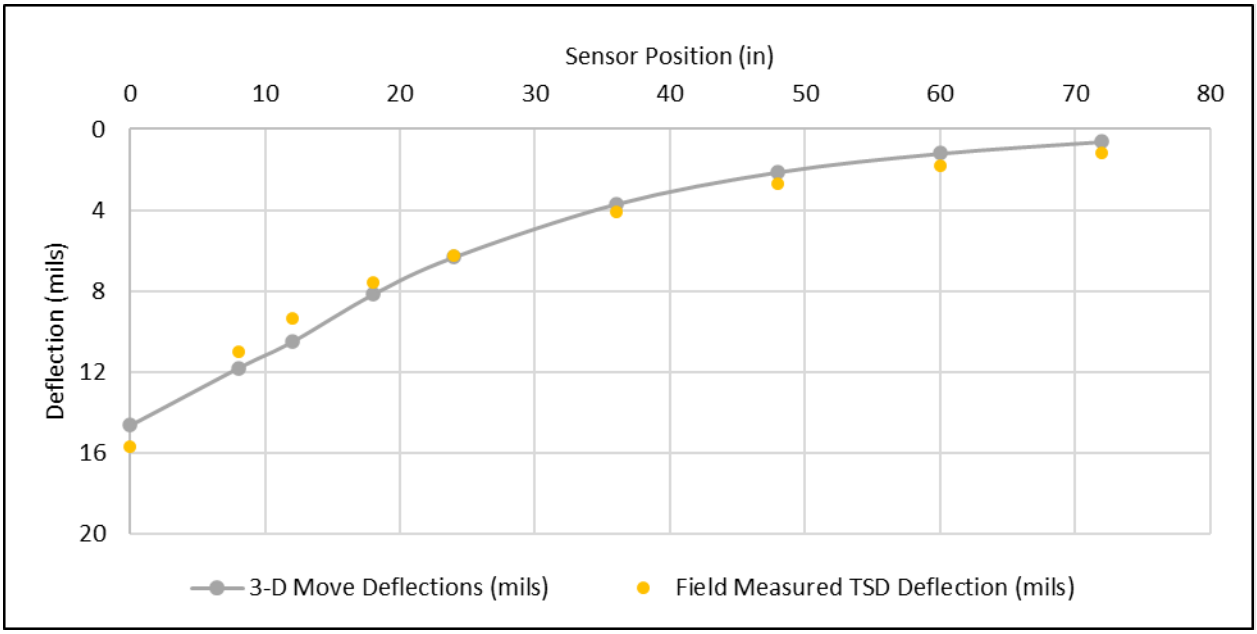

Figure 5.4 Comparison between Predicted and Measured TSD Deflection Basin: Section D-3 US-95 2019 OSL to MP 6.81

5.2 TSD Parametric Study

The research team conducted an extensive full-factorial parametric study, previously discussed in Chapter 4. The study included 243 different pavement designs that varied in terms of asphalt and base layer thicknesses and moduli covering typical pavement structures and properties in the state. The 3D Move was used to predict the TSD deflection basins as well as the pavement response.

5.2.1 Deflection Basin Parameters vs. Layers' Moduli

The deflection basin parameters (DBPs) discussed in Chapter 4, were evaluated for the TSD measurements. The researchers evaluated the correlation between various DBPs including Base Damage Index (BDI) or Middle Layer Index (MLI), Base layer index (BLI) or Surface Curvature Index (SCI), Base Curvature Index (BCI) or Lower Layer Index (LLI), and deflection at the last sensor (W_7). The results demonstrated that the higher the DBPs values, the lower the modulus as shown in Figures 5.5 to 5.13. However, the researchers studied only three modulus values for each layer. The results may not be conclusive, but in agreement with the FWD parametric study and field data.

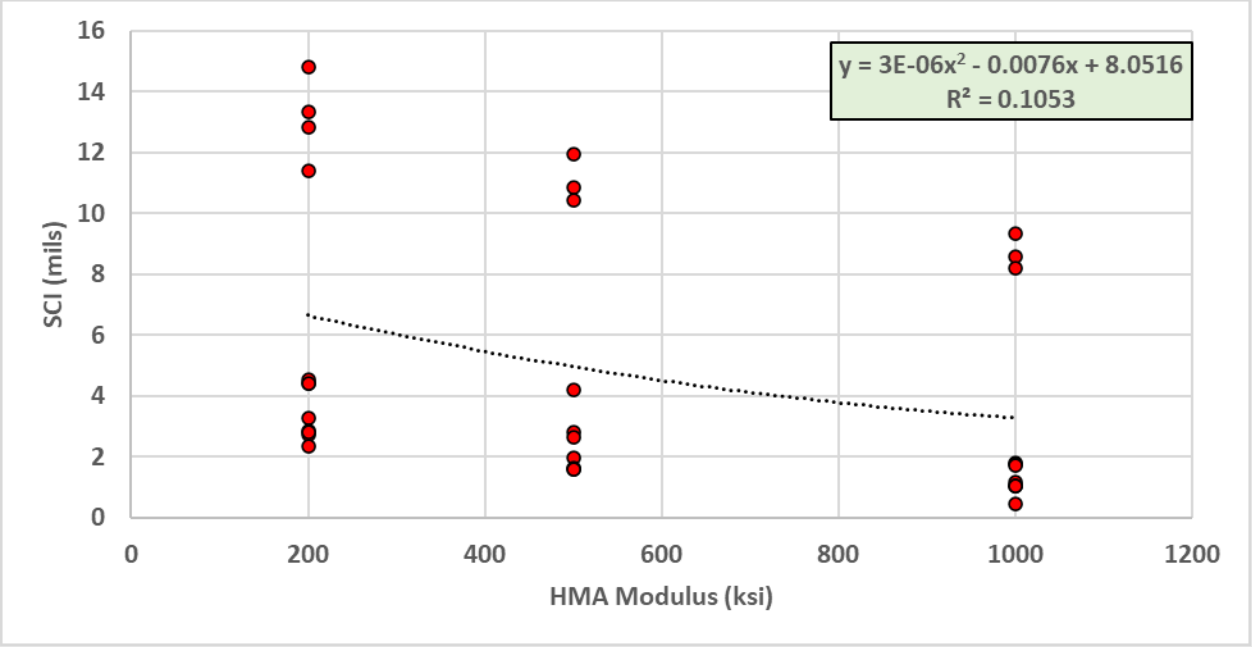

Figure 5.5 SCI vs. Asphalt Layer Modulus for TSD Parametric Study

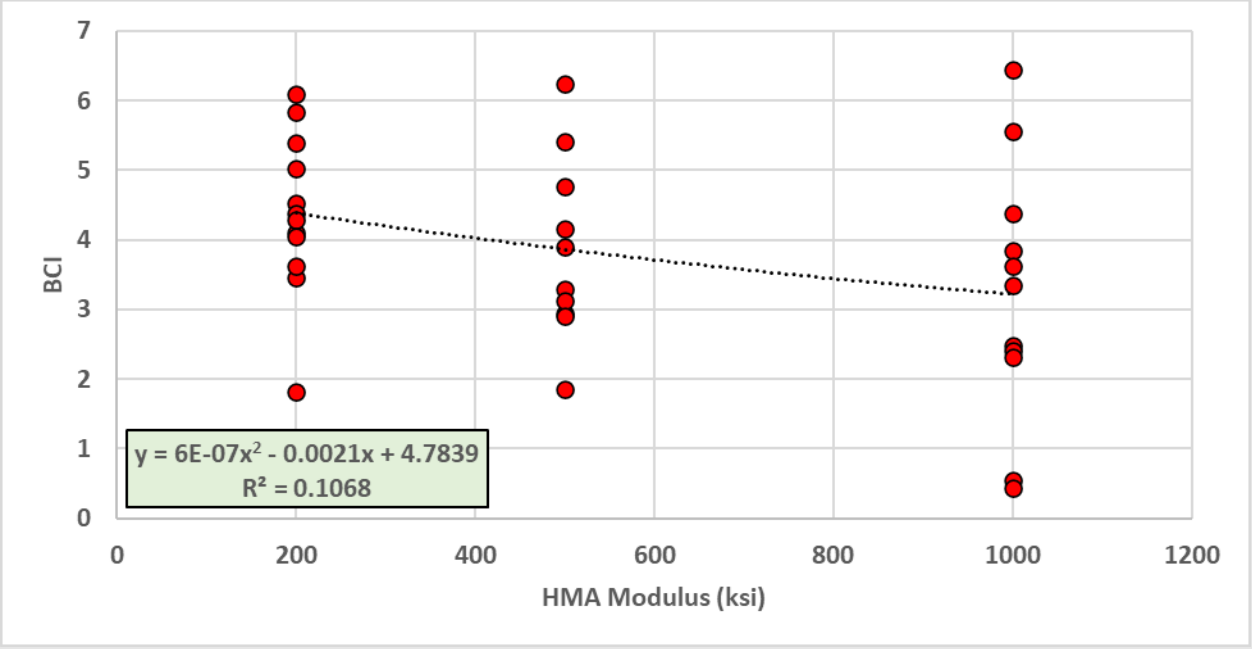

Figure 5.6 BCI vs. Asphalt Layer Modulus for TSD Parametric Study

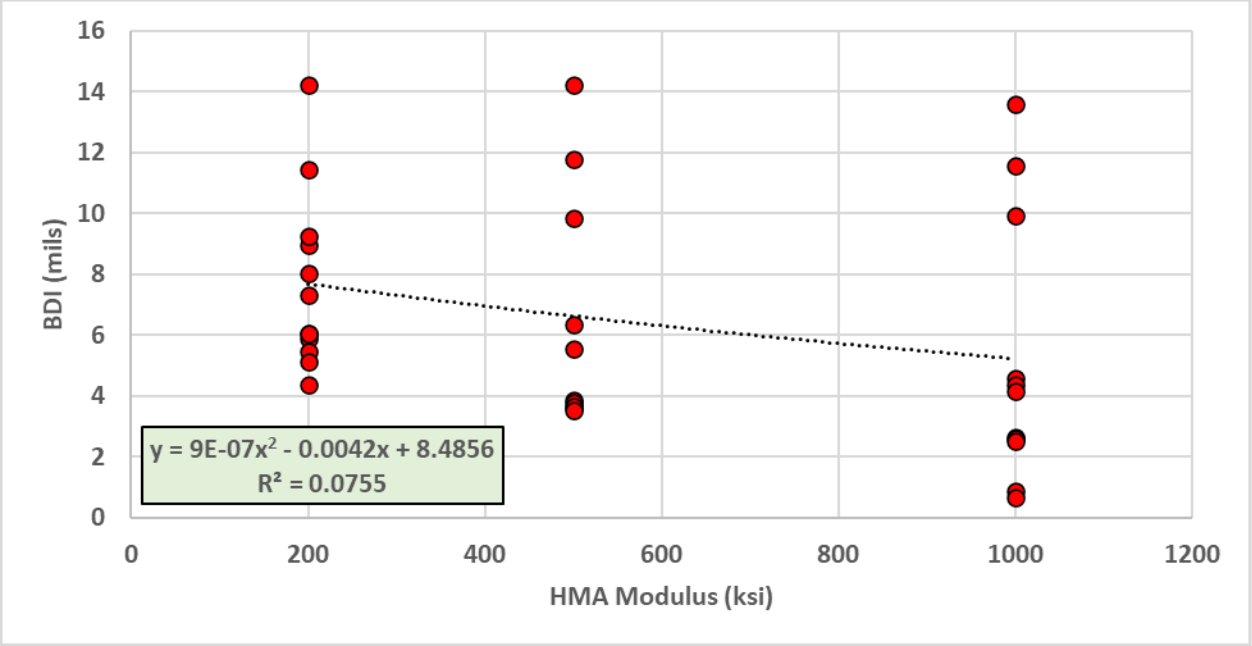

Figure 5.7 BDI vs. Asphalt Layer Modulus for TSD Parametric Study

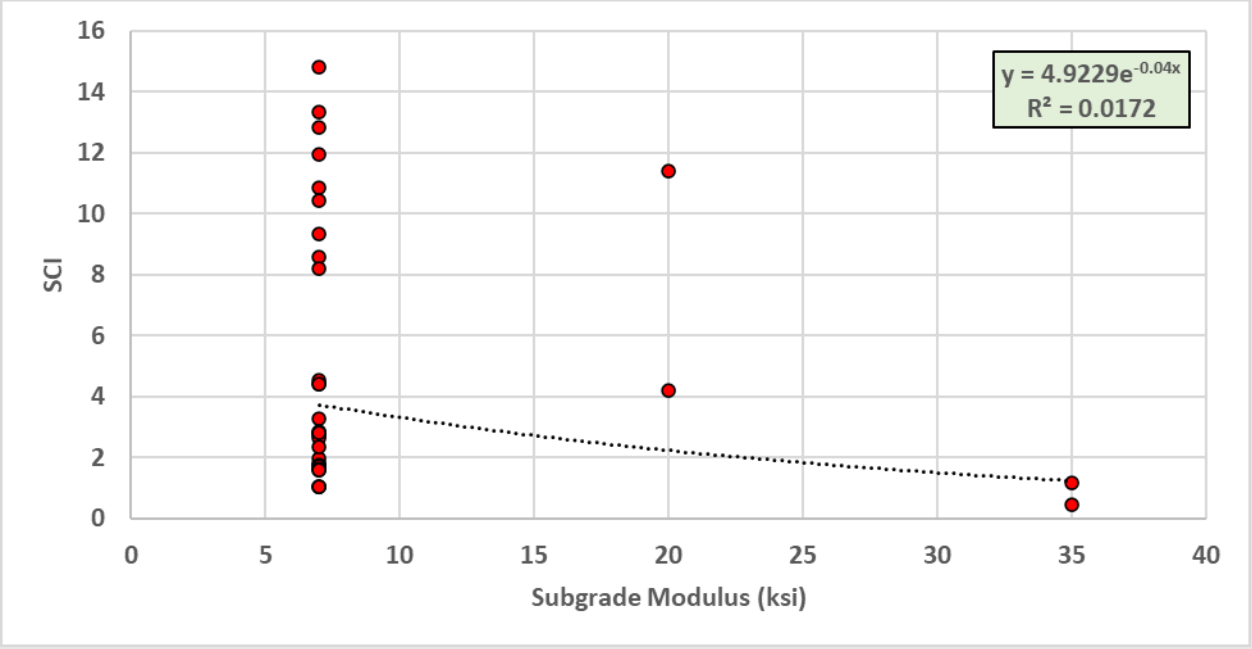

Figure 5.8 SCI vs. Subgrade Modulus for TSD Parametric Study

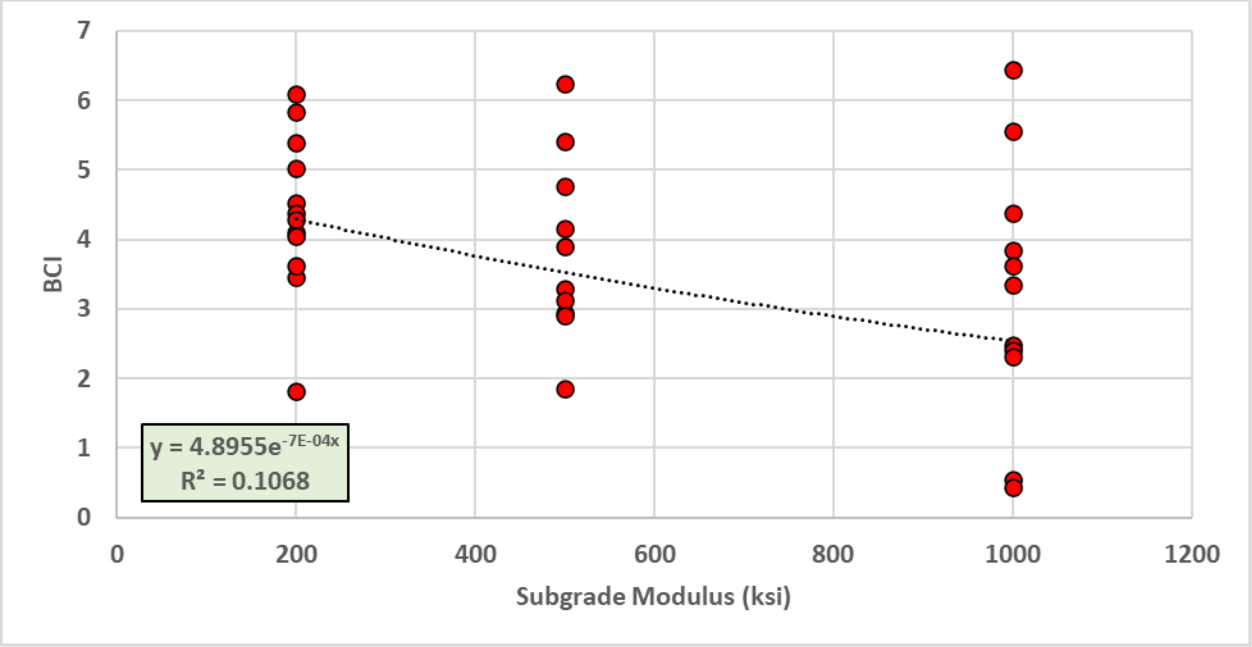

Figure 5.9 BCI vs. Subgrade Modulus for TSD Parametric Study

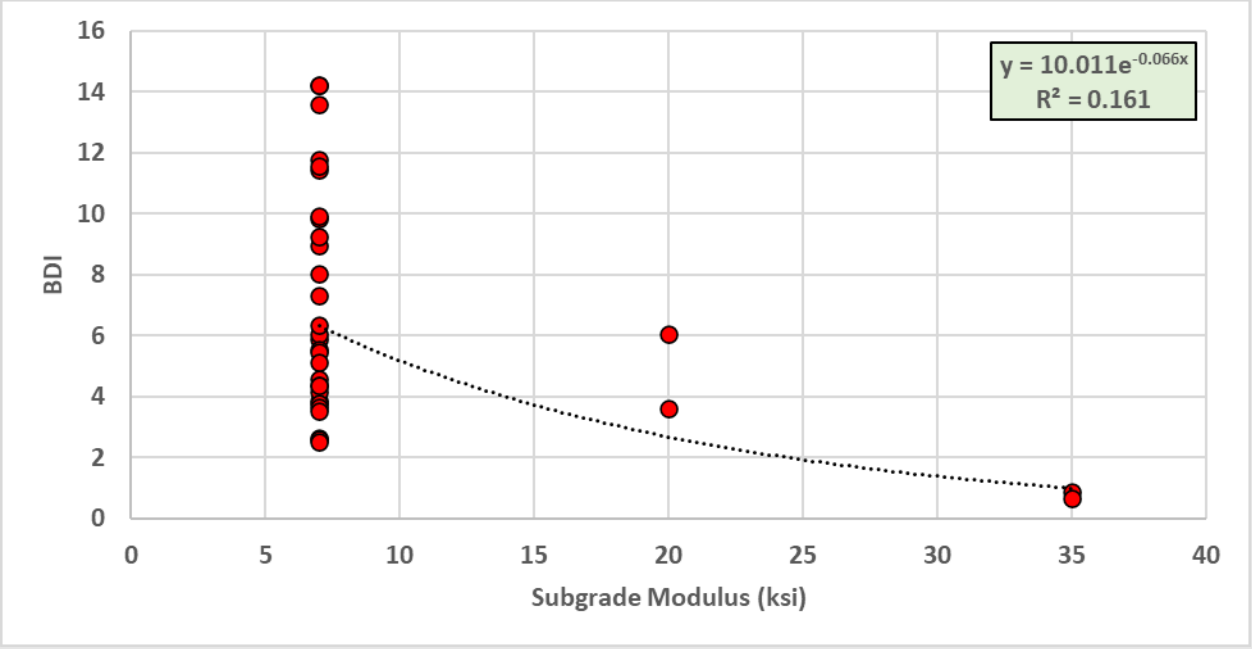

Figure 5.10 BDI vs. Subgrade Modulus for TSD Parametric Study

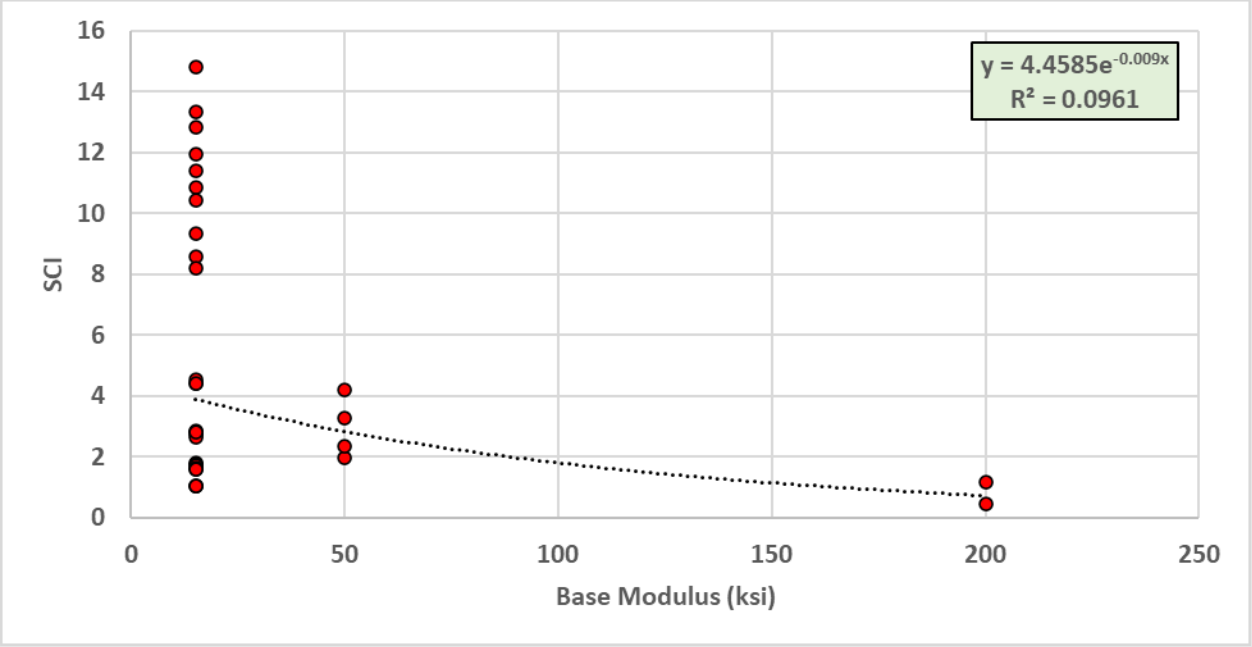

Figure 5.11 SCI vs. Base Modulus for TSD Parametric Study

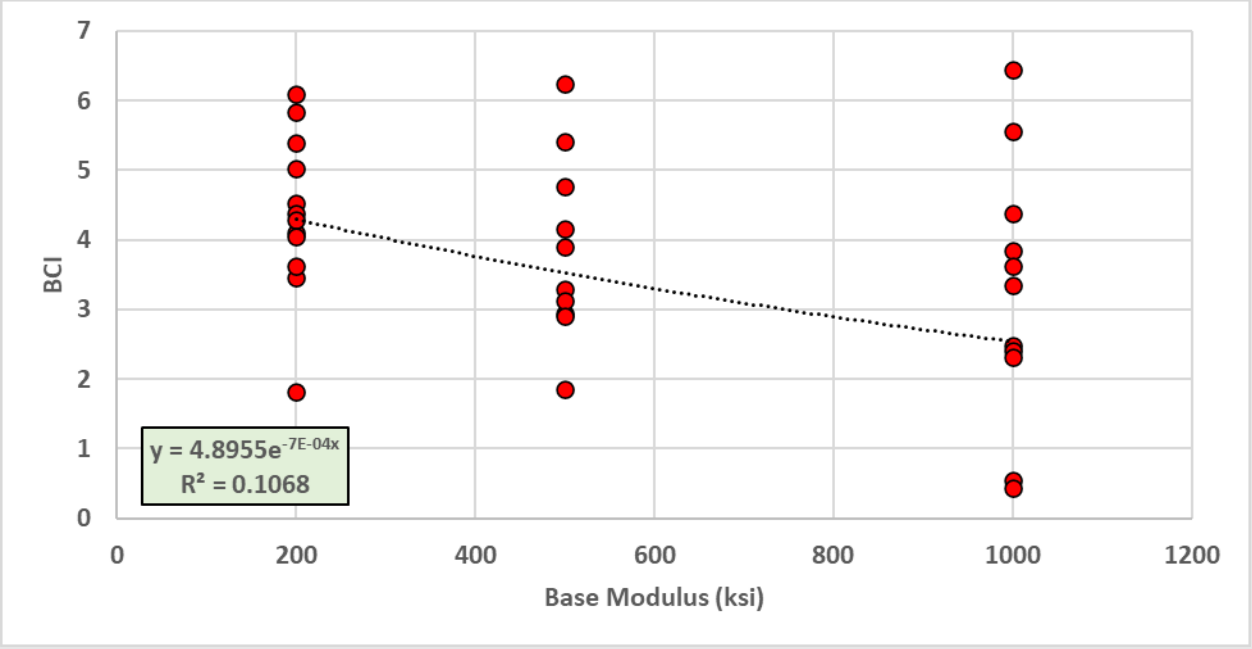

Figure 5.12 BCI vs. Base Modulus for TSD Parametric Study

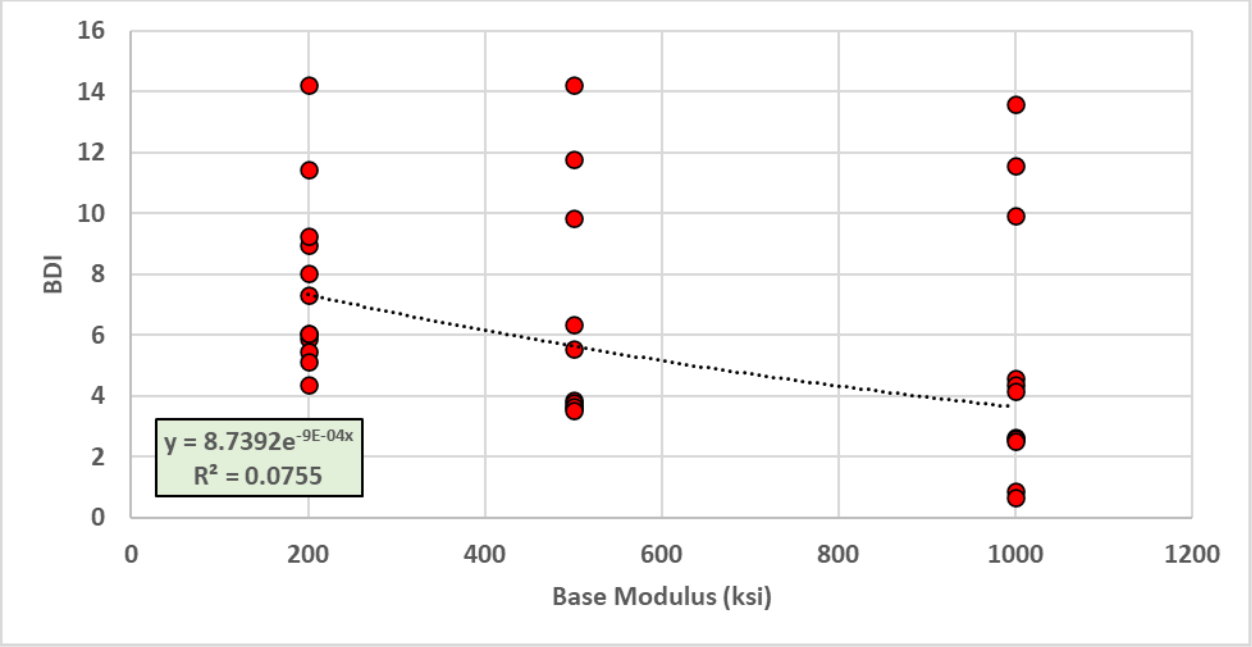

Figure 5.13 BDI vs. Base Modulus for TSD Parametric Study

5.2.2 Deflection Basin Parameters and Mechanistic Responses

The researchers further utilized the 3D Move to calculate critical pavement responses focusing on the horizontal tensile strain at the bottom of the asphalt layer and vertical compressive strain at top of subgrade were computed using the 3D-Move software. These critical responses are then compared with various TSD DBPs obtained from the theoretical deflection basin of the parametric study as discussed in this section.

5.3.2.1 Horizontal Tensile Strain on bottom of Asphalt Layer

For the TSD parametric study, SCI_8 defined as D_0–D_8 (the deflection at 0 in. minus the deflection at 8 in.), and SCI_{12} defined as D_0–D_{12} (the deflection at 0 in. minus the deflection at 12 in.), both have good correlation with the tensile strain (ε_t) at the bottom of the asphalt layer as presented in Figure 5.14 and 5.15, respectively. These correlations and relationships can be used as a simple approach to estimate the tensile strain (ε_t) at the bottom of the asphalt layer without the need for complicated analysis methods. These parameters (i.e., SCI_8 and SCI_{12}) are calculated from the TSD deflection measurements. The tensile strain (ε_t) is used to determine the allowable number of load repetitions before cracking in flexible pavement design.

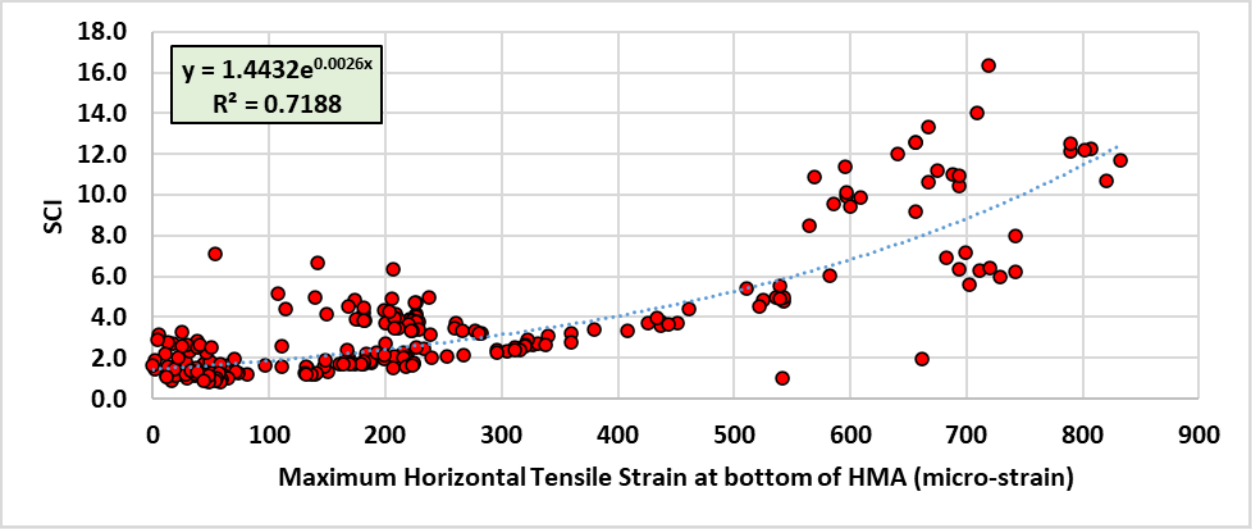

Figure 5.14 Correlation between SCI_8 and Horizontal Tensile Strain at the bottom of Asphalt Layer

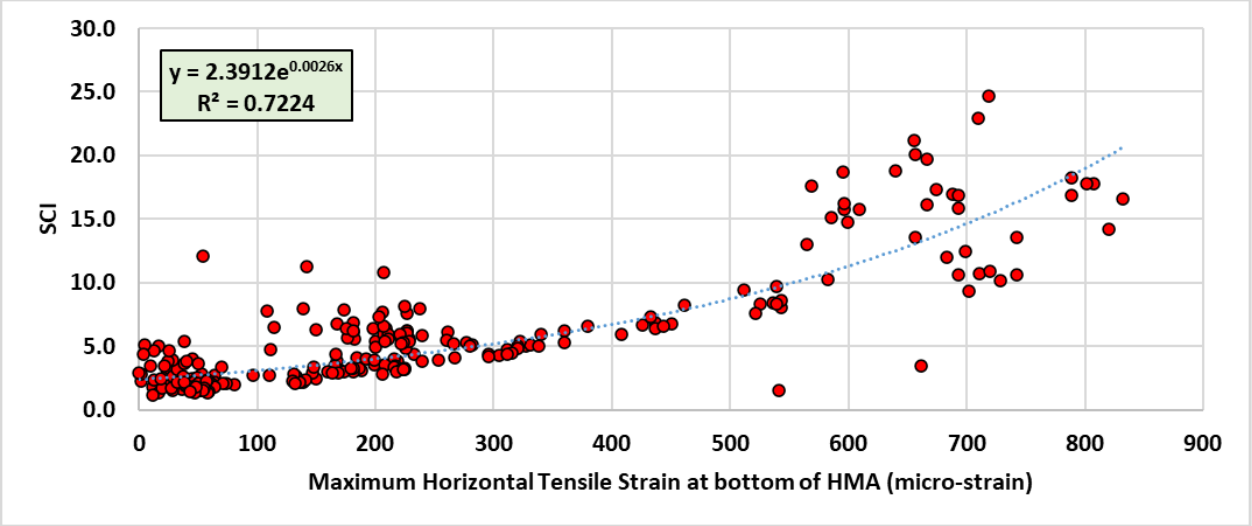

Figure 5.15 Correlation between SCI_{12} and Horizontal Tensile Strain at the bottom of Asphalt Layer

5.3.2.2 Vertical Compressive Strain on Top of Subgrade

Figures 5.16 and 5.17 show that higher vertical compressive strain (ε_v) at top of subgrade was associated with lower SN_{eff} and normalized comprehensive area ratio (CAr'), respectively. The correlation between ε_v and SN_{eff} had an R^2 of 0.83, while the correlation between ε_v and CAr' had an R^2 of 0.80. Pavements with higher SN_{eff} are expected to experience lower vertical compressive strain (ε_v) at top of subgrade compared to pavements with lower SN_{eff}. Furthermore, the compressive strain (ε_v) increased with the increase of the Area Under Pavement Profile (AUPP) (R^2 = 0.76) as shown in Figure 5.18. Such correlations are useful to predict the vertical compressive strain (ε_v) at top of subgrade which is used to estimate the allowable number of load repetitions before rutting in flexible pavement design. The use of the deflection-based parameters is an alternative approach and simpler than the complicated analysis methods used to calculated compressive strain (ε_v).

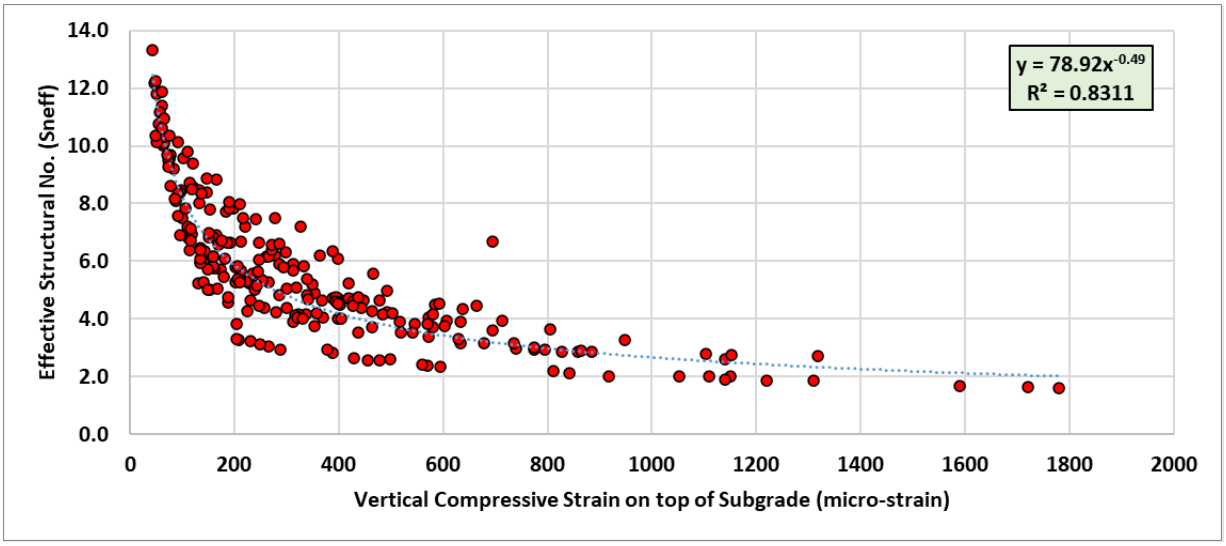

Figure 5.16 Correlation between TSD SNeff and Vertical Compressive Strain on top of Subgrade

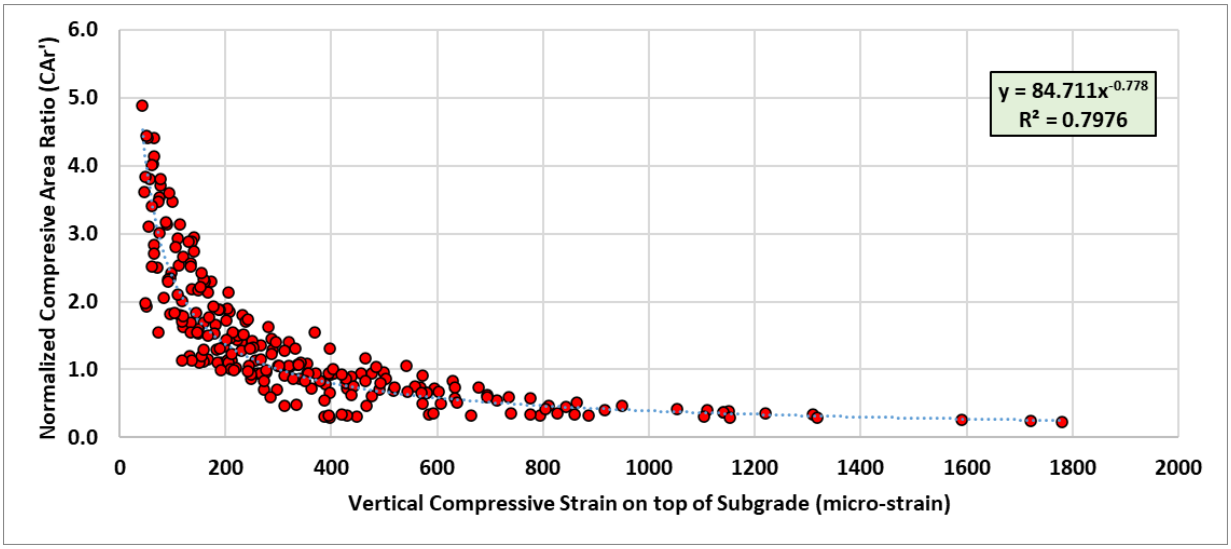

Figure 5.17 Correlation between TSD CAr' and Vertical Compressive Strain on top of Subgrade

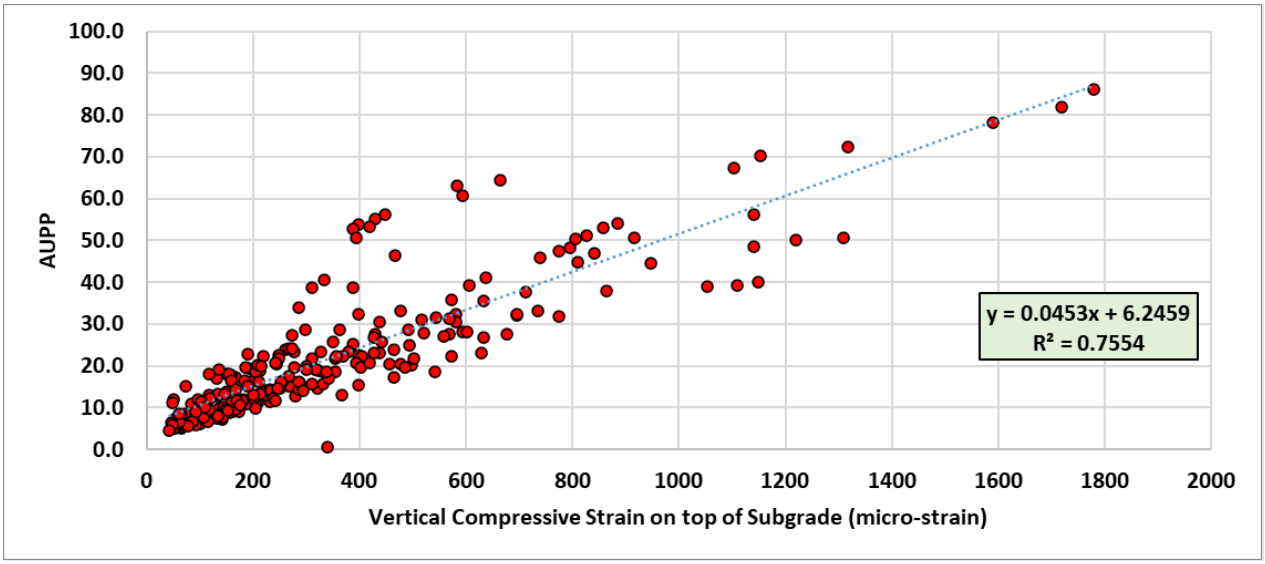

Figure 5.18 Correlation between TSD AUPP and Vertical Compressive Strain on top of Subgrade

5.2.3 Deflection Basin Parameters vs. PMED Performance

Similar to the FWD analysis, the researchers assessed the correlation between TSD DBPs and predicted distresses at the end of the design life for the examined test sections (243 sections of the parametric study). The results demonstrated that there is a good correlation (R^2 = 0.77) between the Structural Condition Index (SCI) and the terminal International Roughness Index (IRI) as shown in Figure 5.19. In addition, the maximum deflection (D_0) also had a fair correlation (R^2 = 0.50) with IRI as shown in Figure 5.20. Similarly, there was a fair correlation between SCI and rutting (R^2 = 0.60) and between maximum deflection (D_0) and rutting (R^2 = 0.50) as shown in Figures 5.21 and 5.22, respectively. In addition, there was a trend between bottom-up cracking and both SCI and D_0 (Figures 5.23 and 5.24). However, and similar to FWD, there was no correlation with these indices (i.e., SCI and D_0) and top-down cracking as shown in Figures 5.25 and 5.26. Also as mentioned in Chapter 4, the researchers further investigated the correlations between FWD and TSD deflection-based parameters and pavement distresses using the Artificial Intelligence (AI) techniques as discussed in detail in Chapter 7. The AI models demonstrated great potential for the AI applications in predicting pavement conditions using parameters that include FWD and TSD deflection measurements as traffic level (i.e., ESALs) as discussed in Chapter 7.

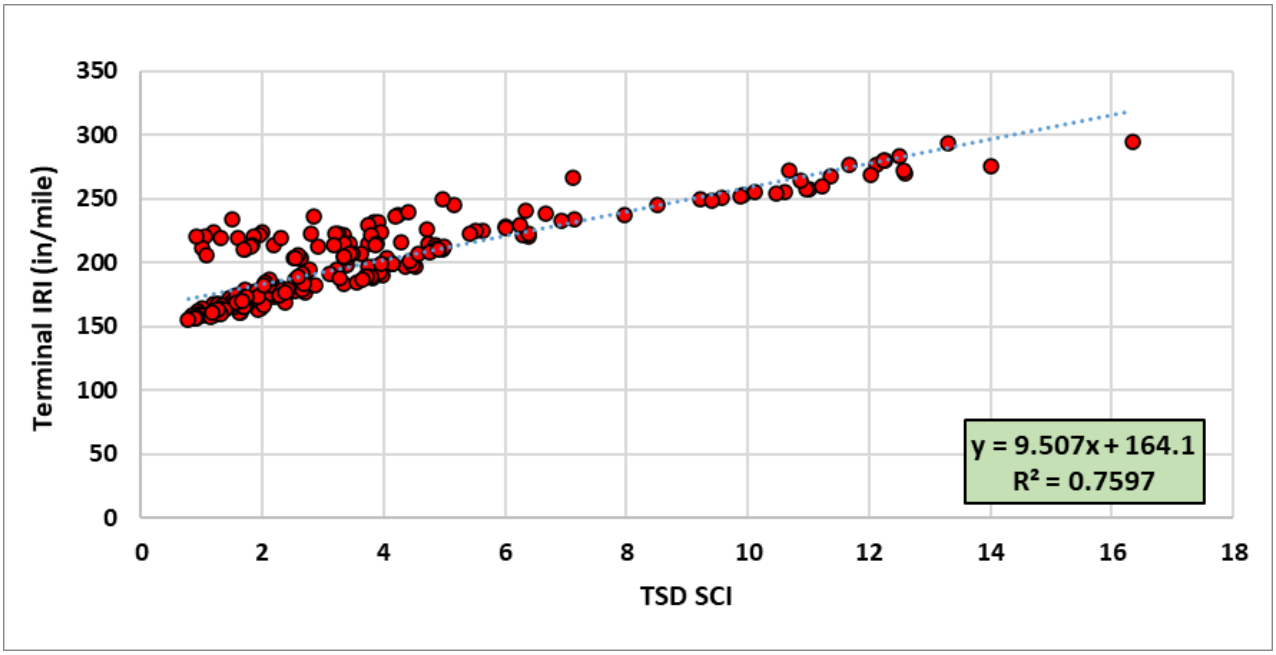

Figure 5.19 SCI vs. Terminal IRI

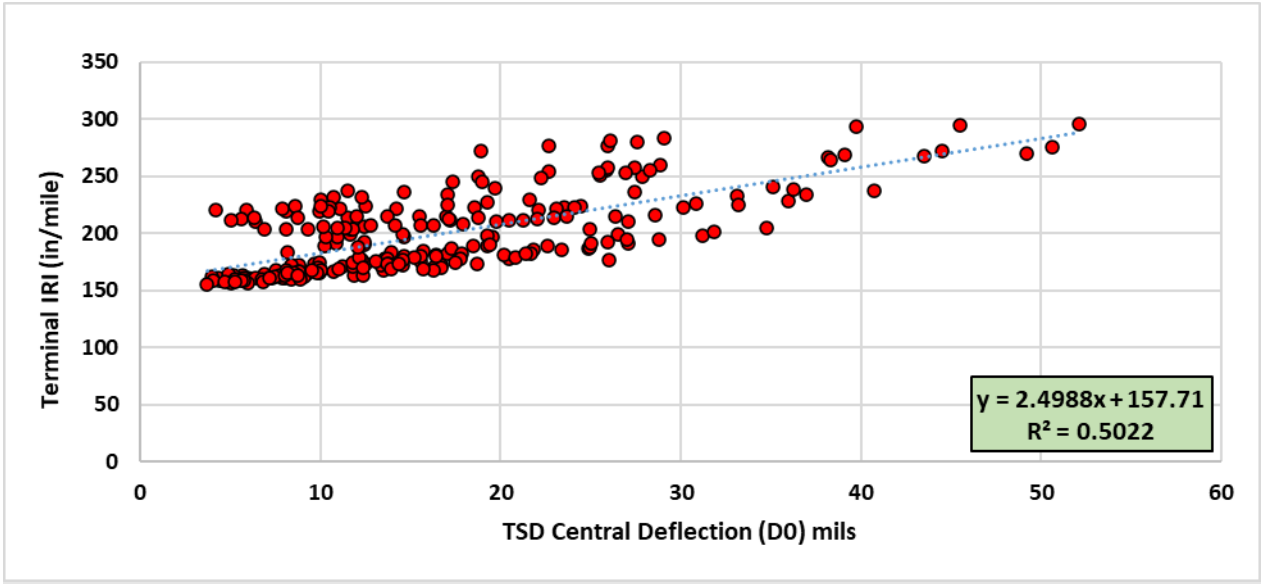

Figure 5.20 TSD Theoretical Maximum Deflection (D0) vs. Terminal IRI

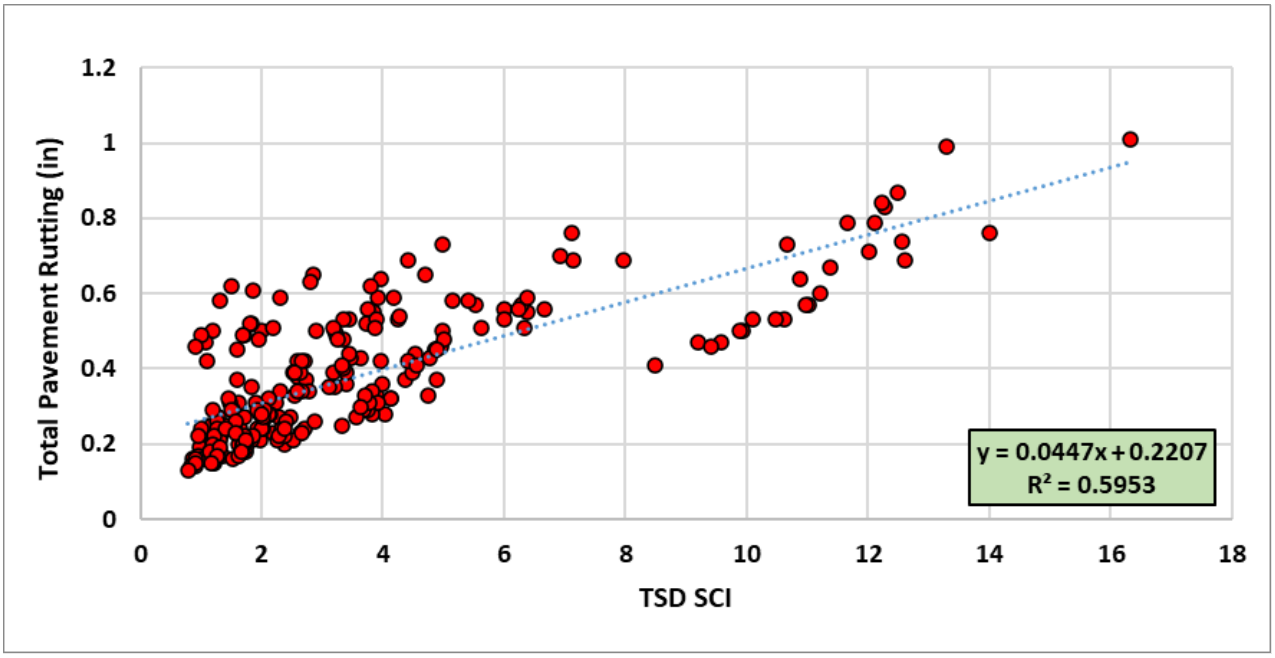

Figure 5.21 SCI vs. Rutting (in)

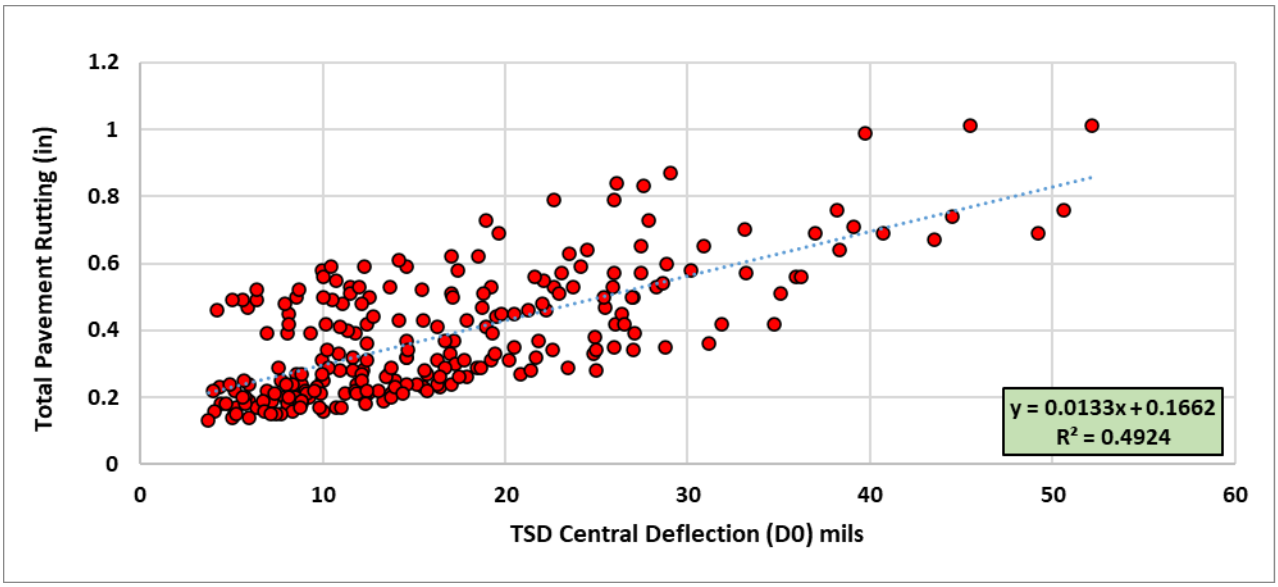

Figure 5.22 Theoretical Maximum Deflection (D0) vs. Rutting (in)

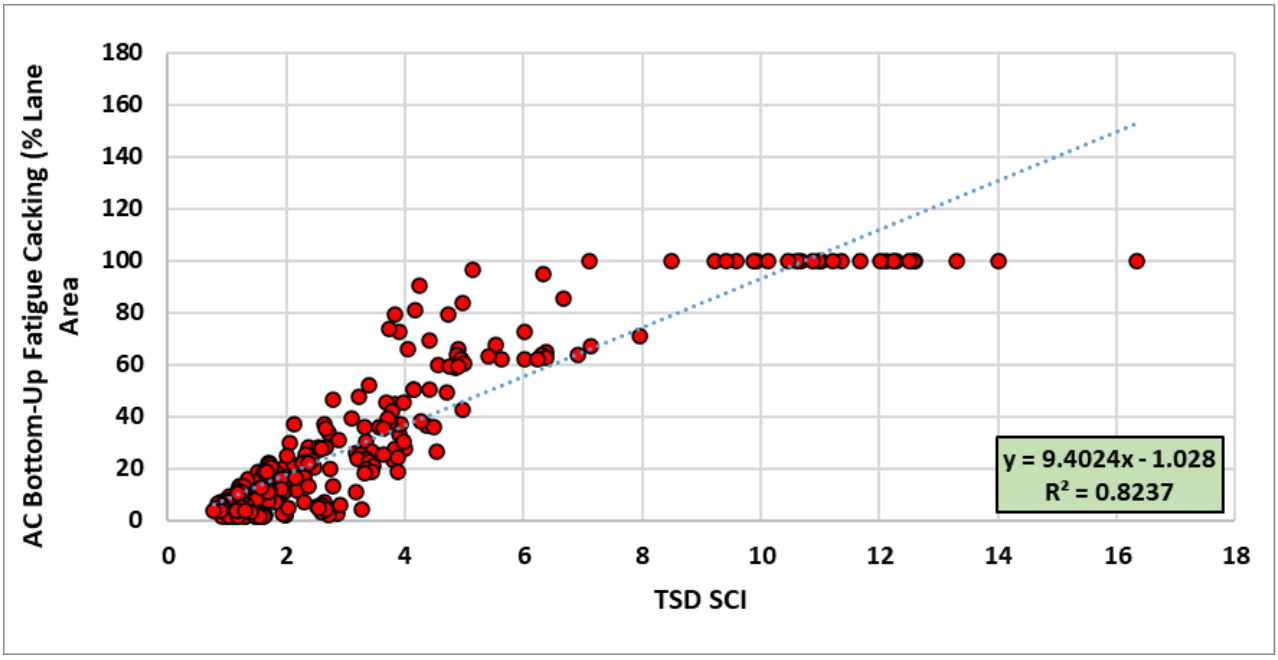

Figure 5.23 SCI vs. Bottom-Up Cracking

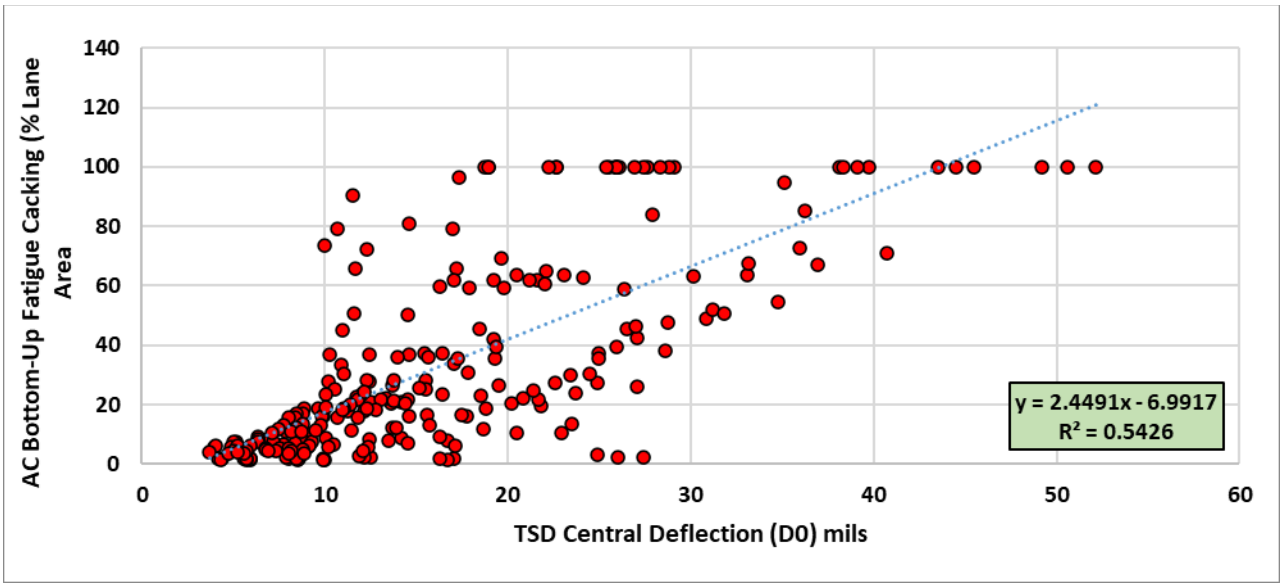

Figure 5.24 Theoretical Maximum Deflection (D0) vs. Bottom-Up Cracking

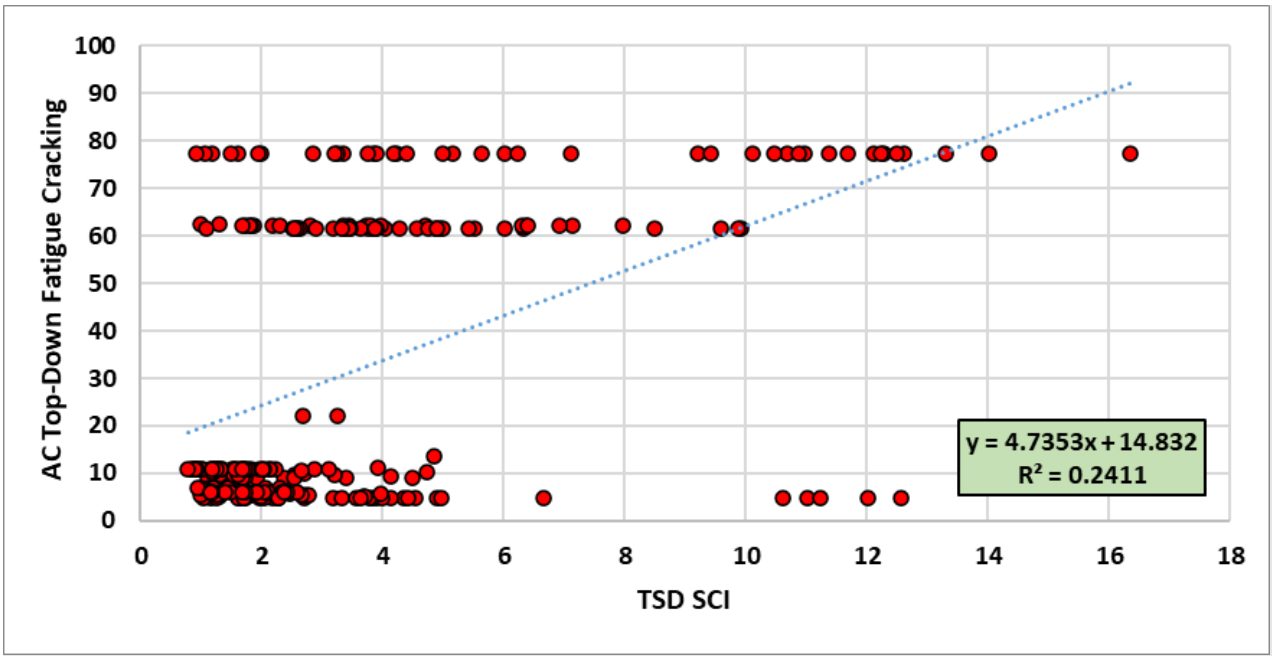

Figure 5.25 SCI vs. Top-Down Cracking

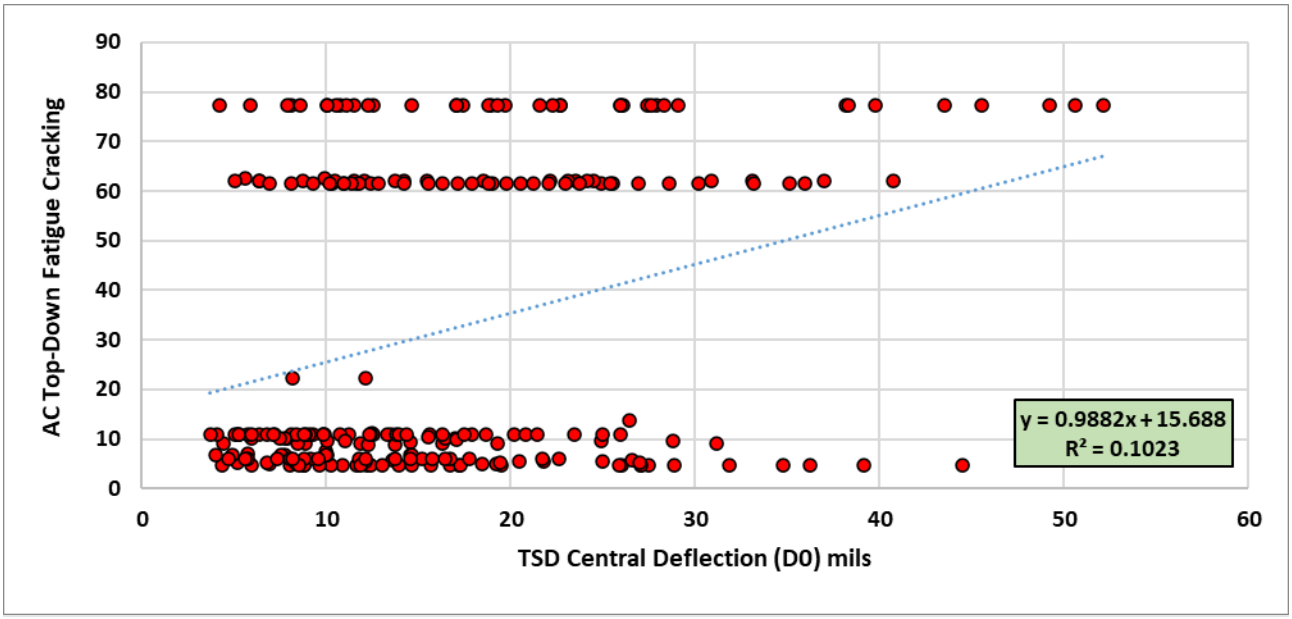

Figure 5.26 Theoretical Maximum Deflection (D0) vs. Top-Down Cracking

5.4 Field Deflection Data Analysis

The researchers assessed the correlation between TSD DBPs and field performance (rutting, cracking, IRI, OCI, etc.), calculated the SNeff and overlay thickness for the examined pavement sections. The TSD DBPs were compared to those of FWD in Chapter 6. Detailed methodologies were discussed in Chapter 4 and this section focuses on the results to avoid repetitions.

5.4.1 TSD Deflection Basin Parameters and Field Performance Data

The TSD trailer is equipped with the capability of measuring pavement surface conditions including cracking (e.g., alligator, longitudinal, transverse) and rutting. Figure 5.22 shows an example of the collected performance data along with the TSD maximum deflection (D_o). The results of Figure 5.22 demonstrated that the measured distresses (e.g., cracking and rutting) correlated well with the TSD maximum deflection (D_o) measurements. Figures 5.27 and 5.28 show the rutting measurements and percent alligator cracking and maximum deflection (D_o) along the test section, respectively. Sections with noticeable surface distresses experienced higher D_o as shown in Figures 5.28 and 5.29. However, there are some inconsistencies between the TSD maximum deflection (D_o) measurements and pavement distresses in other sections as shown in Figure 5.25. Figure 5.30 shows that this section had comparable maximum deflection (D_o) measurements along the test section; however, half of this section had a higher percentage of cracking that didn't result in increased deflection. Appendix A provides more plots for additional sections.

Furthermore, the researchers examined the correlation between TSD DBPs and field performance from TAMS. A comparison between the TSD DBPs and the TAMS pavement performance indicated some sections with higher IRI had higher maximum deflection (D_o); however, no trend was observed for TAMS rutting and cracking. Appendix A provides the correlation between TSD DBPs and the TAMS performance.

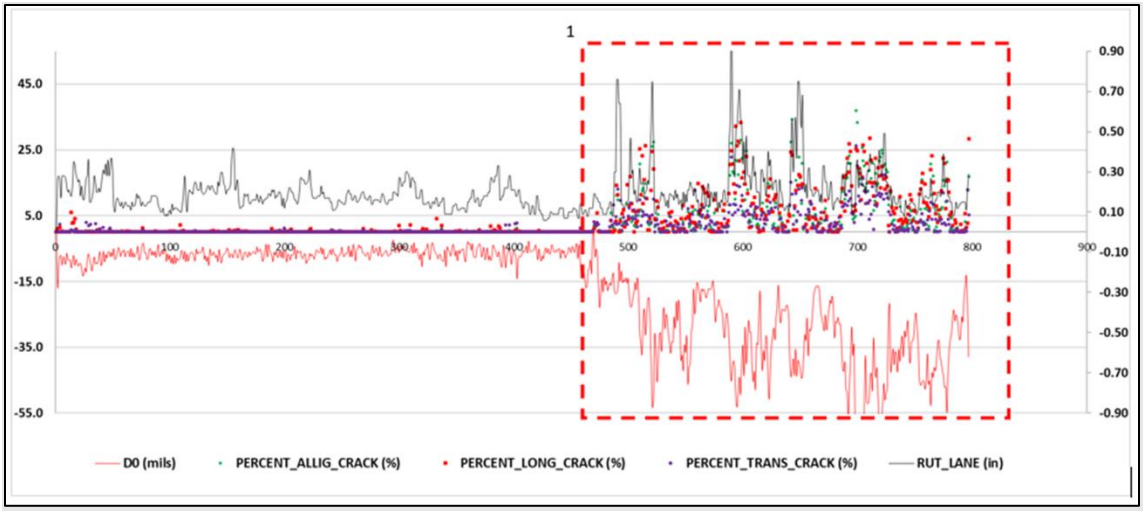

Figure 5.27 TSD Maximum Deflections (D0) vs. Pavement Distresses (SH-50)

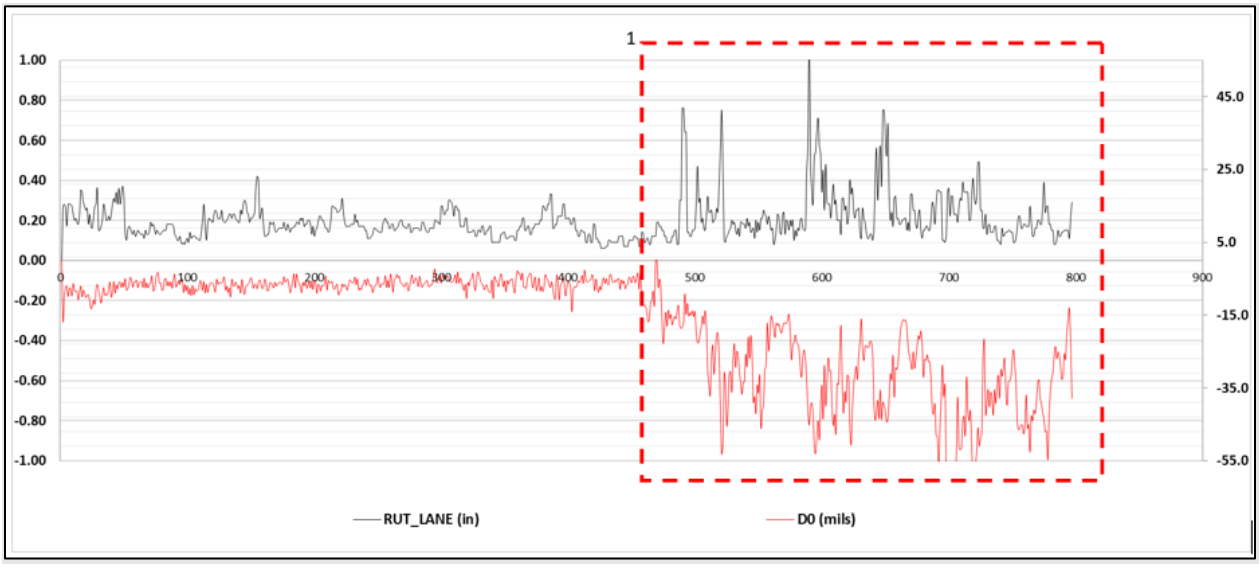

Figure 5.28 TSD Maximum Deflections (D0) vs. Rutting (SH-50)

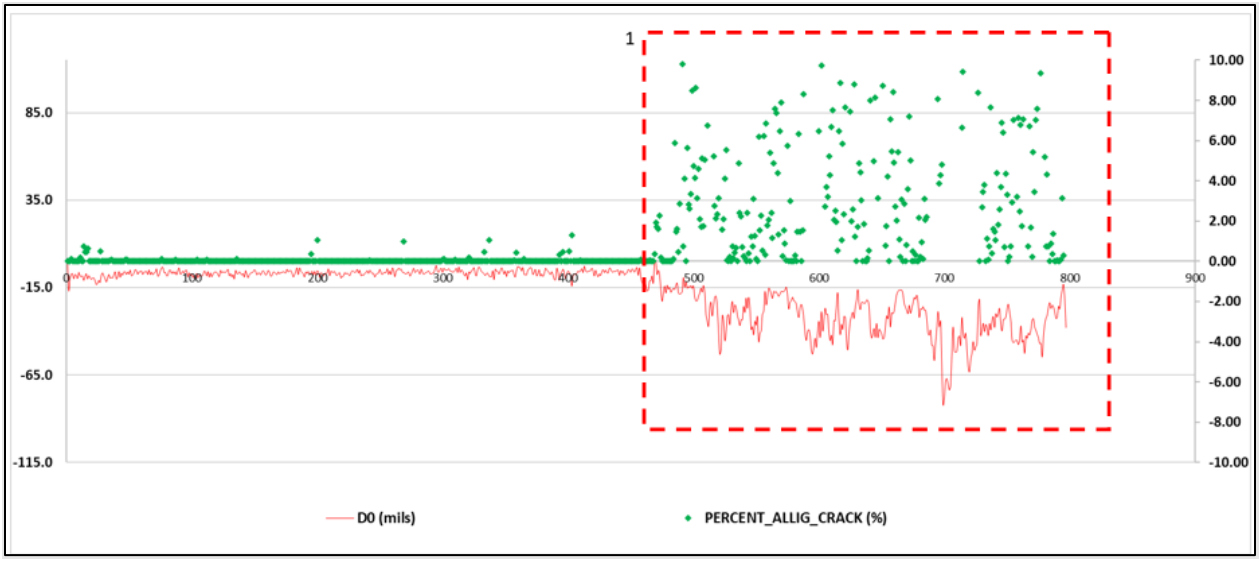

Figure 5.29 TSD Maximum Deflections (D0) vs. Percent Cracking (SH-50)

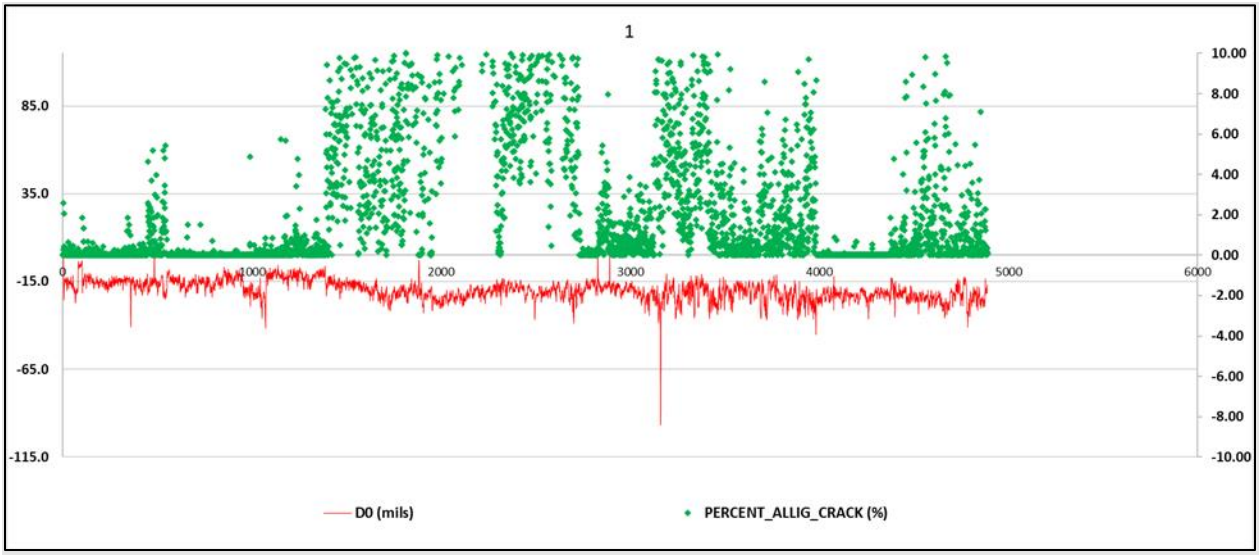

Figure 5.30 TSD Maximum Deflections (D0) vs. Percent Cracking (SH-25)

5.5 SN_{eff} Calculation

Similar to FWD analysis, the research team calculated the SN_{eff} using the TSD deflection data. Three methods were used to calculate SN_{eff} including the deflection value, Rohde's equation, and iterative AASHTO method. These methods were discussed in detail in Chapter 4. The SN_{eff} was calculated for the test sections using both the corrected and uncorrected TSD deflection data. Corrected TSD deflection data account for the effect of pavement temperature on measured TSD deflection data. The research team followed the same procedure used to correct the FWD deflection data (Equation 4.4) to correct the TSD data. Currently, there is no specific procedure to correct the TSD deflection data to account for the pavement temperature. However, and as mentioned in Chapter 4, the FWD deflection measurements were found to have better correlations with TSD without temperature correction. Therefore, the researchers examined the correlation between SN_{eff} calculated using corrected and uncorrected TSD as well as corrected and uncorrected FWD as discussed in detail in Chapter 6.

Tables 5.1, 5.2, and 5.3 summarize the SN_{eff} using the deflection value, Rohde's equation, and iterative AASHTO method, respectively. While Tables 5.4 summarizes the SN_{eff} using the iterative AASHTO method. Table 5.7 summarizes the SN_{eff} calculated using the three methods (i.e., deflection value, Rohde's equation, and iterative AASHTO method) used in this study. The three methods provided comparable SN_{eff}; however, and similar to the FWD SN_{eff} analysis, the results demonstrated that the iterative AASHTO method is the most conservative and resulted in lower SN_{eff} compared to other methods for most sections. While the deflection value method was the least conservative and provided higher SN_{eff} compared to iterative AASHTO method and Rohde's equation for most of the sections. Therefore, the researchers used the iterative AASHTO method (the most conservative method) to determine the required overlay thickness for the examined test sections as discussed in the following section.

Table 5.1 SNeff Results Using Deflection Value Equation

Pavement Site	D0	D60	Subgrade Moduli (psi)	AC Thickness	Base Thickness	Total Pavement Thickness (D) (in.)	Selected $E_{pavement}$ (psi)	Effective Structural Number (Sn_{eff})
1	9.82	1.60	19358	6	27.6	33.6	171907.89	8.37
2	9.77	1.31	23523	7.08	8.86	15.94	194630.33	4.14
3	9.63	1.48	20249	18	18	36	165818.22	8.86
4	15.12	2.53	13210	5.4	11.4	16.8	194630.33	4.36
5	23.07	2.18	10416	3.6	18	21.6	48773.49	3.54
6	17.65	2.23	14049	4.8	12	16.8	128014.74	3.80
7	19.39	1.91	13689	4.8	7.8	12.6	100694.54	2.63
8	11.50	1.02	21984	5.9	14.76	20.66	101763.11	4.32
9	17.21	2.87	11761	6	18.6	24.6	116204.31	5.38
10	18.83	2.97	9629	2.9	11.8	14.7	167170.67	3.63
11	12.10	2.23	13344	6	18	24	168216.13	5.94
12	25.96	1.46	10911	5.4	4.8	10.2	35855.79	1.51
13	11.36	2.40	13289	4.83	7.38	12.21	406894.06	4.05
14	15.60	1.83	14399	6.87	6.98	13.85	143887.38	3.25
15	14.52	1.26	17019	6.76	6.5	13.26	99662.41	2.76
16	15.50	1.72	12096	4.79	7.45	12.24	109233.37	2.62
17	13.00	1.33	16769	4.23	7.93	12.16	131418.33	2.77
18	8.83	1.04	22896	3.21	8.83	12.04	229436.35	3.30
19	11.79	1.08	20322	6.72	8.44	15.16	109210.46	3.25
20	16.91	1.14	15116	6.24	6.21	12.45	57841.84	2.16

Table 5.2 SNeff Results Using Rohde's Equation

Pavement Site	W_1 (mils)	D_0 (µm)	Total Pavement Thickness (H_p) (in.)	Total Pavement Thickness (H_p) (mm)	$D_{1.5Hp}$ (mils)	$D_{1.5Hp}$ (µm)	SIP (µm)	Effective Structural Number (Sn_{eff})
1	9.821	249.45	33.6	853.4	2.10	53.39	196.06	6.23
2	9.768	248.11	15.94	404.9	4.18	106.17	141.93	4.13
3	9.628	244.55	36	914.4	1.75	44.33	200.21	6.49
4	15.118	384.00	16.8	426.7	6.91	175.42	208.59	3.57
5	23.069	585.94	21.6	548.6	6.40	162.66	423.28	3.08
6	17.655	448.43	16.8	426.7	6.86	174.12	274.31	3.13
7	19.391	492.53	12.6	320.0	8.73	221.84	270.69	2.53
8	11.502	292.14	20.66	524.8	3.20	81.35	210.79	4.16
9	17.207	437.05	24.6	624.8	5.46	138.68	298.37	4.02
10	18.826	478.17	14.7	373.4	9.77	248.27	229.90	3.08
11	12.102	307.39	24	609.6	4.46	113.40	193.99	4.85
12	25.961	659.40	10.2	259.1	12.42	315.59	343.81	1.92
13	11.364	288.63	12.21	310.1	7.05	179.12	109.51	3.82
14	15.604	396.34	13.85	351.8	7.09	180.12	216.22	3.03
15	14.522	368.87	13.26	336.8	6.36	161.63	207.23	3.00
16	15.497	393.63	12.24	310.9	8.59	218.15	175.48	3.05
17	13.005	330.32	12.16	308.9	6.58	167.03	163.29	3.15
18	8.825	224.16	12.04	305.8	4.78	121.40	102.76	3.90
19	11.788	299.42	15.16	385.1	4.72	119.91	179.51	3.55
20	16.906	429.41	12.45	316.2	7.42	188.58	240.82	2.66

Table 5.3 SNeff Results Using AASHTO Iterative Equation

Pavement Site	W_1 (mils)	d_0 (inches)	Total Pavement Thickness (D) (in.)	M_R (psi)	$E_{pavement}$ (psi)	Objective	d_0 (inches) from Iterative Equation	Effective Structural Number (Sn_{eff})
1	9.821	0.009820833	33.6	19358	101750	1.7493E-08	0.009688571	7.03
2	9.768	0.009768037	15.94	23523	150483.4	3.153E-07	0.009206046	3.80
3	9.628	0.009627912	36	20249	96994.4	1.809E-08	0.009762429	7.41
4	15.118	0.015118233	16.8	13210	104443.4	8.0206E-07	0.014222654	3.55
5	23.069	0.023068511	21.6	10416	50430.3	1.716E-06	0.021758431	3.58
6	17.655	0.0176548	16.8	14049	70756.1	1.4746E-07	0.017270783	3.12
7	19.391	0.019391097	12.6	13689	73883.0	6.0526E-11	0.019383317	2.37
8	11.502	0.011501629	20.66	21984	92140.4	8.2485E-12	0.011498757	4.18
9	17.207	0.017206569	24.6	11761	62688.6	1.1266E-08	0.017312712	4.38
10	18.826	0.018825676	14.7	9629	81411.7	1.9444E-06	0.020220097	2.86
11	12.102	0.012101892	24	13344	94975.0	4.1274E-07	0.012744347	4.91
12	25.961	0.025960667	10.2	10911	61611.8	2.9492E-07	0.02650374	1.81
13	11.364	0.011363542	12.21	13289	254519.8	1.2380E-10	0.011352415	3.47
14	15.604	0.015604	13.85	14399	96944.7	6.9595E-09	0.015687424	2.85
15	14.522	0.014522345	13.26	17019	101128.0	2.6060E-09	0.014471295	2.77
16	15.497	0.015497234	12.24	12096	137407.3	1.3655E-08	0.01561409	2.83
17	13.005	0.013004559	12.16	16769	141215.3	9.9007E-10	0.012973093	2.84
18	8.825	0.008825303	12.04	22896	227971.1	5.2815E-10	0.008848285	3.30
19	11.788	0.011788	15.16	20322	117863.8	7.4457E-08	0.011515131	3.33
20	16.906	0.016905849	12.45	15116	108621.8	2.5348E-06	0.015313716	2.66

Table 5.4 Summary of SNeff using Different Methods

Pavement Site	Effective Structural Number (Sn_{eff}) Deflection Equation	Effective Structural Number (Sn_{eff}) Rhode Equation	Effective Structural Number (Sn_{eff}) AASHTO Iterative
1	8.37	6.23	7.03
2	4.14	4.13	3.80
3	8.86	6.49	7.41
4	4.36	3.57	3.55
5	3.54	3.08	3.58
6	3.80	3.13	3.12
7	2.63	2.53	2.37
8	4.32	4.16	4.18
9	5.38	4.02	4.38
10	3.63	3.08	2.86
11	5.94	4.85	4.91
12	1.51	1.92	1.81
13	4.05	3.82	3.47
14	3.25	3.03	2.85
15	2.76	3.00	2.77
16	2.62	3.05	2.83
17	2.77	3.15	2.84
18	3.30	3.90	3.30
19	3.25	3.55	3.33
20	2.16	2.66	2.66
	Least Conservative		**Most Conservative**

5.5.5 Structural and Required Overlay Thickness

The SN_{eff} calculated using the iterative AASHTO method was used to determine the required overlay thickness for the examined pavement sections to serve the traffic for 20 years. The same approach discussed in Chapter 4 (Equations 4.13 and 4.14) was used to determine the required overlay thickness using the TSD deflection data. Table 5.8 summarizes the SN_{req} calculations for the examined test sections.

Table 5.9 summarizes the required overlay thickness. The results demonstrated that some sections showed that the current pavement structure is sufficient and no overly is needed. However, other sections showed that an overly is required. The range of the overly thicknesses varied from 0.18 to 4.86 inches depending on the traffic level, and current conditions (SN_{eff}) of the pavement structure. These overlay thickness results are compared to those calculated from the FWD as discussed in detail in Chapter 6. Also, Table 5.9 shows the current pavement conditions; however, there was no direct correlations between the current conditions of pavement sections and the required overlay thickness. In order to facilitate the calculations of SN_{req}, SN_{eff}, and overlay thickness, the research team developed an Excel spreadsheet that can be used for this purpose as discussed in Chapter 7.

Table 5.5 Required Structural Number Results using Iterative AASHTO Method

Pavement Site	Total Accumulated ESALs	MR (psi)	Least Squares Error	Calculated ESALs	SNReq
1	37178978.7	19358	37.8649	36584342.5	3.945
2	53385200.18	23523	0.0000	53332137.7	3.380
3	52961508.12	20249	0.0312	60828089.7	3.928
4	10592301.62	13210	0.0012	10374688.5	3.420
5	5719842.877	10416	0.0000	5137000.0	3.870
6	1105836.289	14049	0.7711	996575.3	2.766
7	1408776.116	13689	0.0004	1389044.0	3.080
8	1408776.116	21984	0.0091	1407304.9	2.581
9	7266318.914	11761	0.0000	5568470.2	3.481
10	6482488.594	9629	0.0005	6079165.2	4.153
11	4152182.236	13344	0.0001	4619457.1	3.048
12	3442498.028	10911	0.0000	3598708.2	3.864
13	10009725.03	13289	0.0554	10063635.1	3.810
14	10009725.03	14399	0.0009	9921124.8	3.624
15	10009725.03	17019	0.9492	9934959.8	3.986
16	5147858.59	12096	1.4324	5194368.6	3.585
17	6355380.97	16769	0.6400	6354429.1	3.985
18	7785341.69	22896	0.0028	7681517.2	3.489
19	11270208.93	20322	5.4779	9780763.3	3.673
20	6461303.99	15116	0.0066	5570830.1	3.609

Table 5.6 Results of Structural Condition and Overlay Thickness

Project	Structural Condition/Overlay thickness (in)	OCI Condition	IRI Condition	Rutting Condition
Project I-15 40-45 2020	Sufficient	Good	Good	Good
Project I-15 90-95 2020	1.68	Good	Good	Fair
Project I-15 100-105 2020	Sufficient	Good	Good	Fair
Project SH-39 46.80-51.80 2020	1.80	Good	Good	Good
Project SH-27 15-20 2020	1.51	Good	Good	Good
Project US-93 201.85-206.20 2020	Sufficient	Good	Poor	Fair
Project US-93 211.20-216.20 2020	1.66	Good	Poor	Fair
Project US-93 216.20-221.20 2020	Sufficient	Good	Fair	Fair
Project US-30 250.90-255.90 2020	Sufficient	Good	Good	Fair
Project SH-55 100.20-105.20 2020	3.68	Good	Good	Fair
Project SH-55 110.20-115.20 2020	Sufficient	Good	Good	Good
Project SH-52 19.00-22.20 2019	4.86			
Project US 95 MP 0.00-4.826 2019	1.92	Good	Good	Fair
Project US 95 MP 4.836-16.581 2019	3.02	Good	Good	Fair
Project US 95 MP 16.591-23.957 2019	2.65	Good	Good	Fair
Project US 95 MP 23.967-28.710 2019	2.71	Good	Good	Fair
Project US 95 MP 28.720-35.614 2019	1.92	Good	Good	Fair
Project US 95 MP 35.714-41.418 2019	0.18	Good	Good	Good
Project US 95 MP 42.518-50.742 2019	0.78	Good	Good	Good
Project US 95 MP 61.023-69.219 2019	2.47	Fair	Good	Fair

6. Comparison Between FWD and TSD

Chapter 6 presents a comparison between the FWD and TSD results presented separately in Chapters 4, and 5, respectively. The comparison includes deflection measurements, deflection basin parameters, and pavement structural conditions (e.g., overlay thickness and remaining service life). In this comparison, the research team considered both corrected and uncorrected FWD and TSD data.

6.1 Parametric Study

6.1.1 FWD vs. TSD Deflection Data

The deflection basins measured by both FWD and TSD are different due to the difference in the operating conditions of FWD and TSD. The FWD is a stationary device while the TSD measures the deflection under a continuously moving load. The FWD device applies a stationary impact load to the pavement surface while the TSD applies a moving load at a traffic speed of up to 60 mph through its rear axle. Despite the difference in loading, recent studies in the United States and Australia demonstrated a strong correlation between FWD and TSD deflection measurements (Roberts et al. 2014, Katicha et al. 2017). The correlation between the theoretical deflection derived from the FWD and TSD deflection basins was evaluated as presented in Figure 6.1. The results showed a strong correlation between the FWD and TSD values, with an R^2 of 0.88. However, the TSD deflection values appeared to be slightly higher than those of FWD.

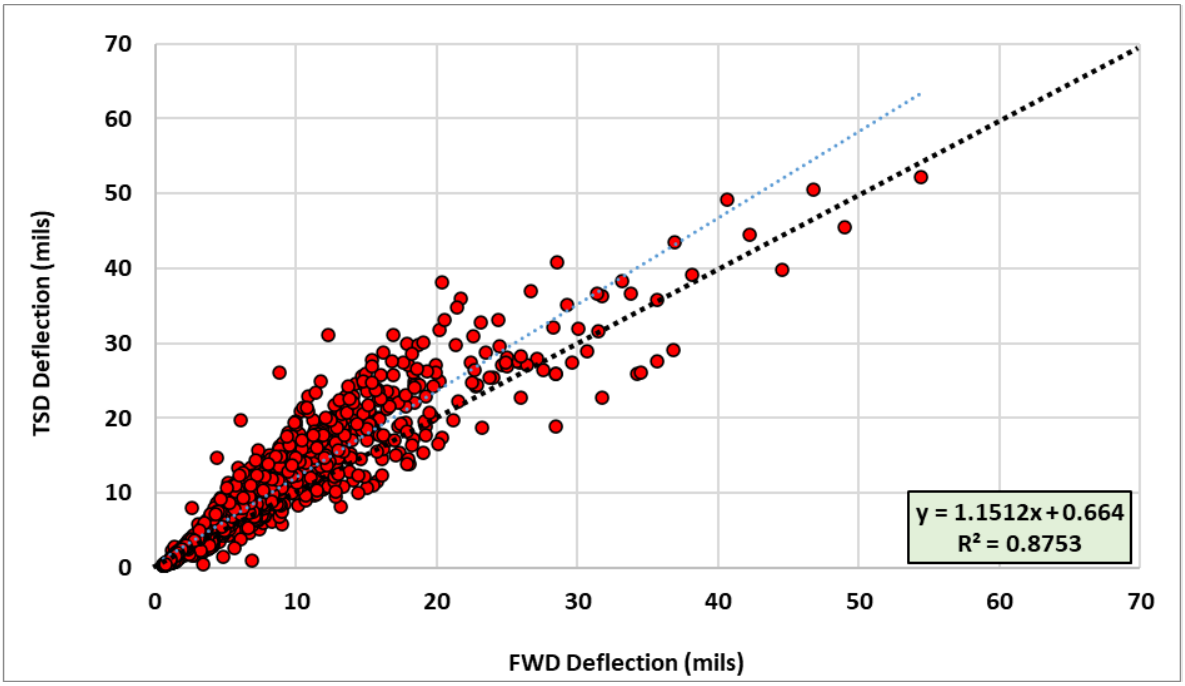

Figure 6.1 Correlation between FWD and TSD Deflection Measurements from the Parametric Study

The correlation between the maximum deflection (D_o) of FWD and TSD was also evaluated as presented in Figure 6.2. The maximum deflection (D_o) is the deflection at the center of the loading plate for FWD and the deflection of the first sensor for TSD. The results of the parametric study indicated a strong correlation between the maximum deflection (D_o) of FWD and TSD, with an R^2 of 0.80. Figure 6.3 shows the minimum deflection (D_{60}) from both FWD and TSD which indicated a strong correlation too.

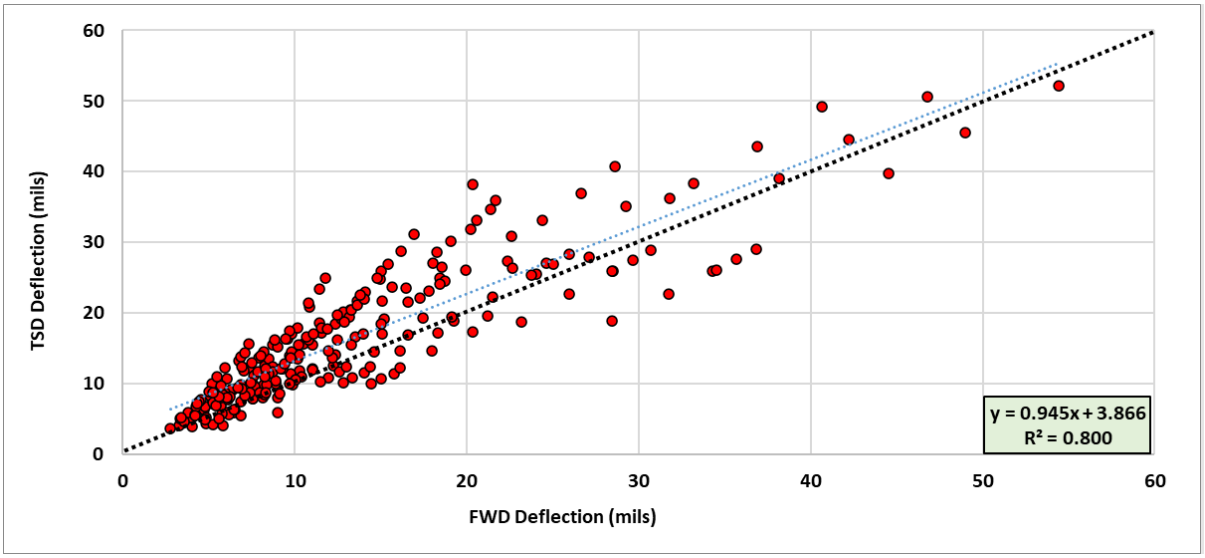

Figure 6.2 Theoretical Maximum Deflection (D0) form the Parametric Study

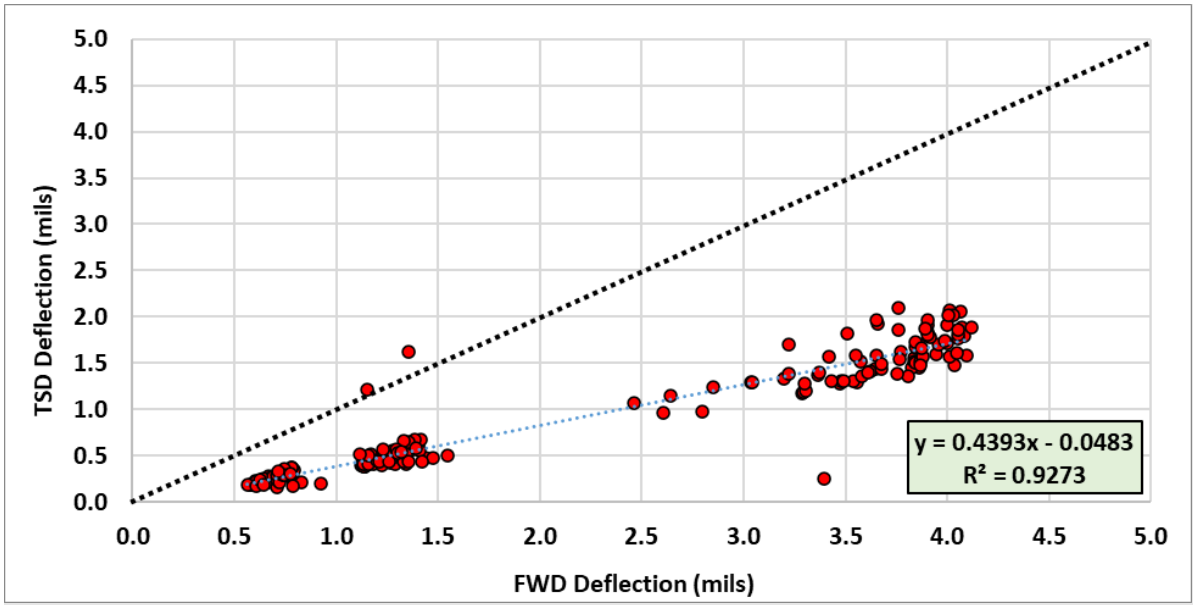

Figure 6.3 Theoretical Minimum Deflection (D_{60}) form the Parametric Study

6.2.1 FWD vs. TSD Deflection Basin Parameters (DBPs)

Surface Curvature Index (SCI) represents the condition of upper layers of pavements. The SCI values calculated based on the FWD data had a strong correlation with the ones calculated using the TSD data as shown in Figure 6.4. Similarly, the FWD Middle Layer Index (MLI), which represents the structural condition of the middle layer like base and subbase and correlated with the tensile strain at the bottom of the AC Layer and compressive stress at the top of the subgrade, had a fair correlation (R^2 = 0.70) with that of the TSD as shown in Figure 6.5. Furthermore, the Lower Layer Index (LLI), which indicates the strength of the lower pavement layers (e.g., subbase or subgrade), showed a good correlation (R^2 = 0.79) between the FWD and TSD data as shown in Figure 6.6. The results of these comparisons demonstrated that the TSD can provide a similar assessment to that of the FWD. The researchers assessed the correlations using the deflection data collected in the field as discussed next.

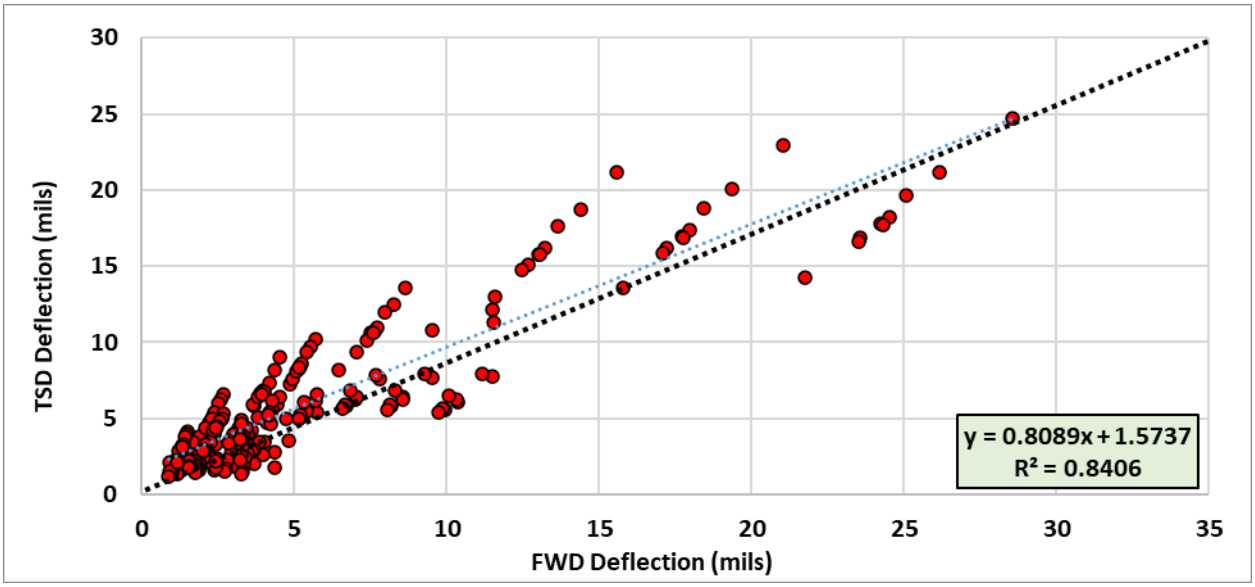

Figure 6.4 SCI form the Parametric Study

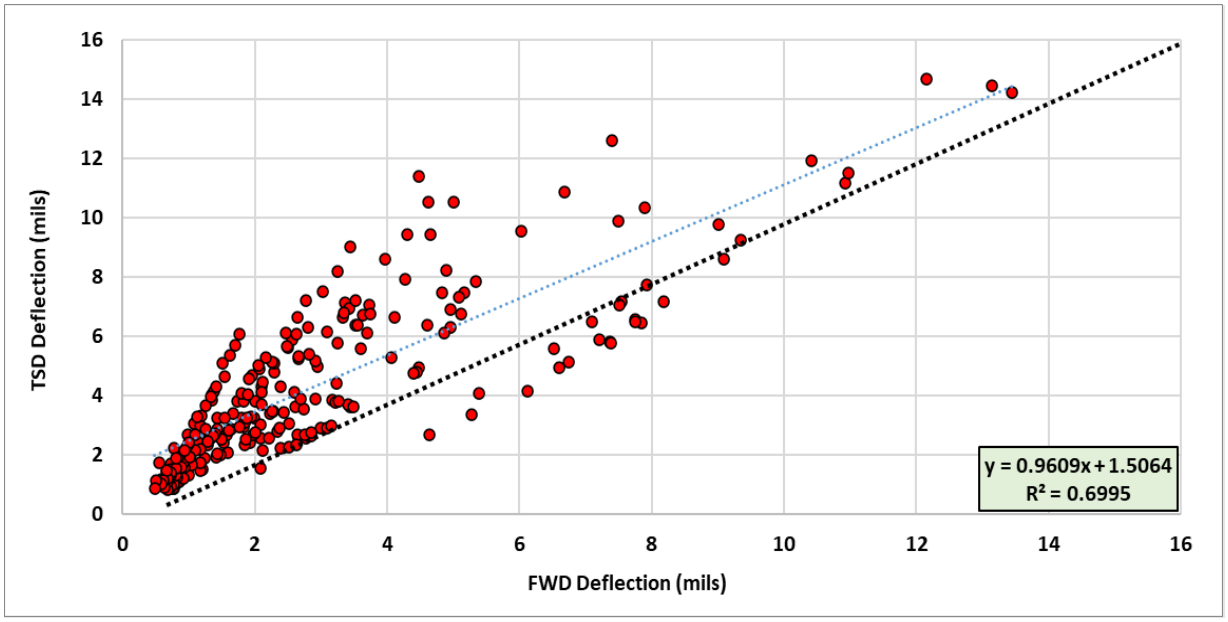

Figure 6.5 MLI form the Parametric Study

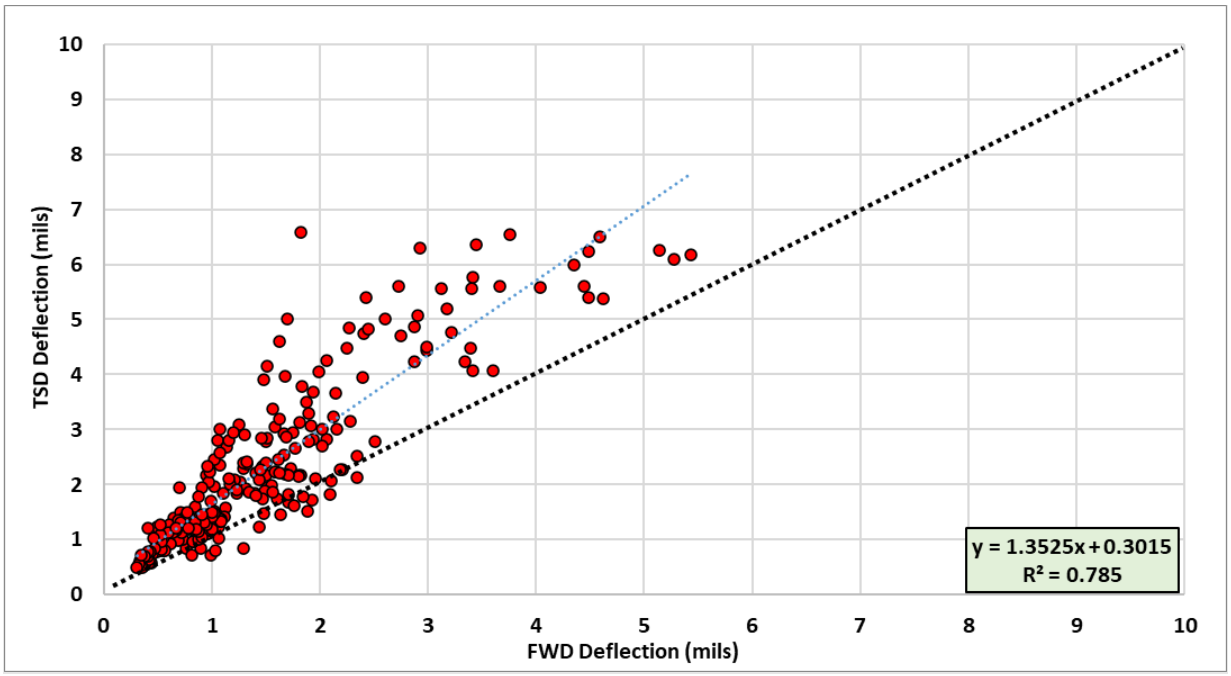

Figure 6.6 LLI form the Field Measured Value

6.2 Field Deflection Data Analysis

6.2.1 FWD vs. TSD Deflection Data

The researchers compared the FWD and TSD deflection data before and after correction. The researchers corrected both the FWD and TSD data for temperature; however, after analyzing the results, they noticed that the temperature correction tended to increase the deflection in the TSD data, while it tended to decrease the deflections in the FWD data. This difference in correction reduced the correlations between the two sets of data. In fact, the FWD deflection measurements were found to have better correlations with TSD without temperature correction for both FWD and TSD. As mentioned earlier, the research team followed the same procedure used to correct the FWD deflection data (Equation 4.4) to correct the TSD data.

Figure 6.7 compares the overall deflections from FWD and TSD, and the results demonstrated that there a strong correlation between the two sets with an R^2 of 0.86. Meanwhile, the TSD deflections appear to be slightly higher than the FWD. However, an analysis of variance (ANOVA) shows that the difference between the TSD and FWD deflections is statistically not significant, with a *p-value* of 0.056. Figure 6.8 shows the correlation between FWD and TSD deflection values after correction. FWD deflection measurements had better correlation with that of the TSD without correction compared to the corrected values. Figures 6.8 and 6.9 show the comparison between the Maximum Deflection (D_0) obtained from FWD and TSD for uncorrected and corrected deflection values, respectively. The values were close to the equality line for the uncorrected measurements. Figures 10 and 11 demonstrate that there was no good correlation for the Minimum Deflection (D_{60}) for both uncorrected and corrected deflection data sets, respectively.

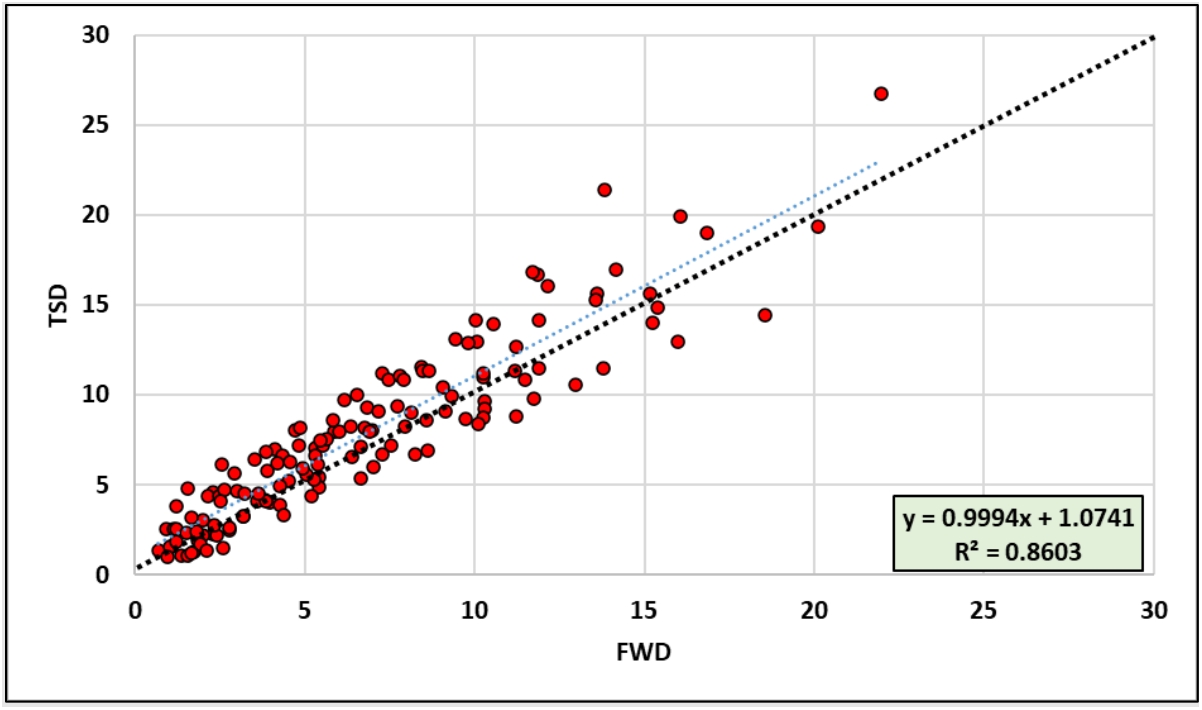

Figure 6.7 Correlation between Uncorrected FWD and TSD Deflections from Field Data

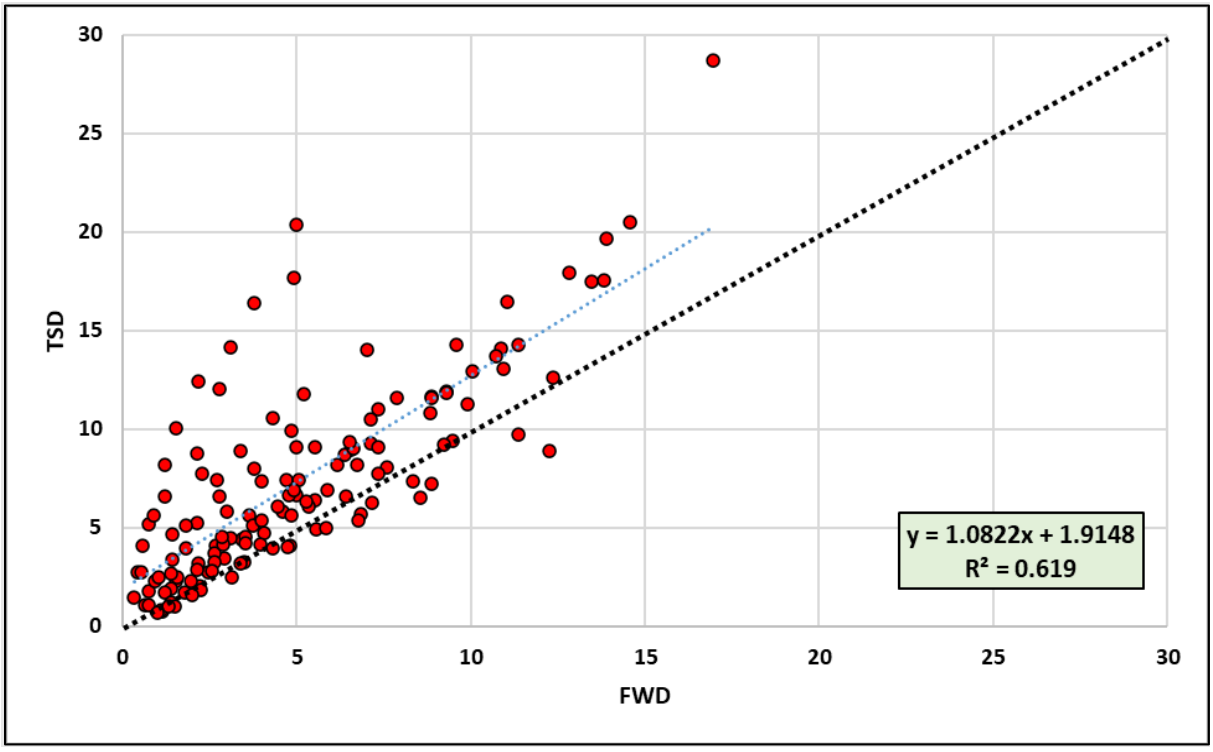

Figure 6.8 Correlation between Corrected FWD and TSD Deflections from Field Data

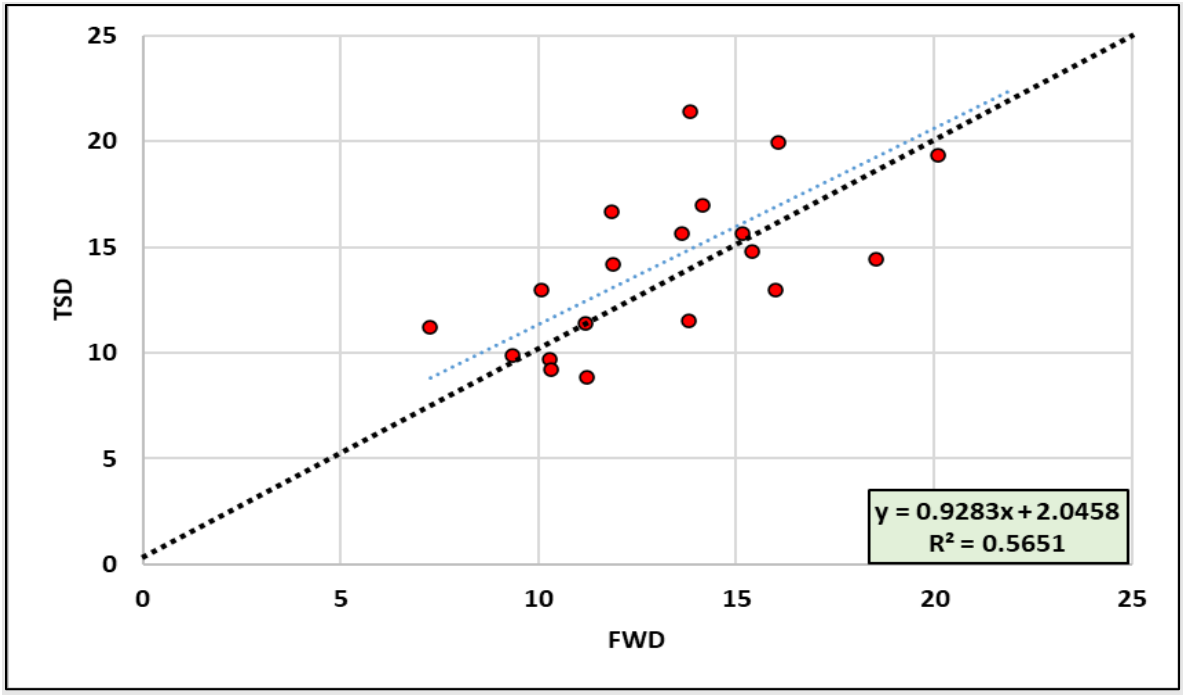

Figure 6.9 Theoretical Maximum Deflection (D_0) form Uncorrected Field Data

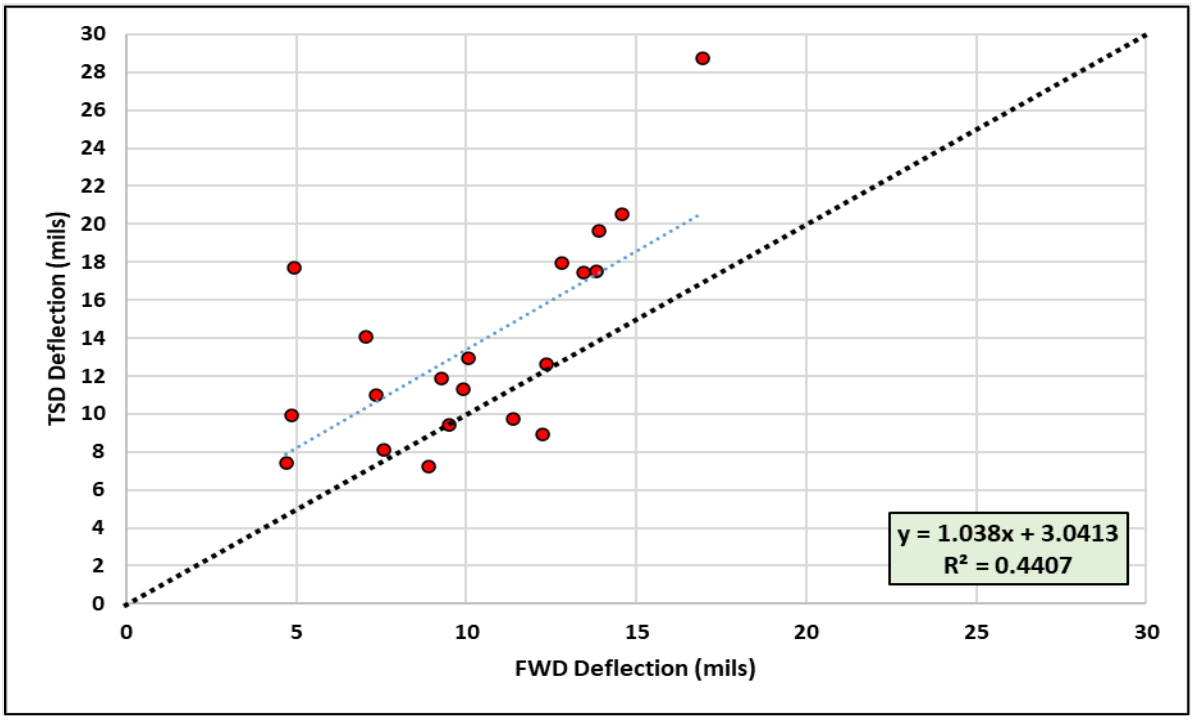

Figure 6.10 Theoretical Maximum Deflection (D_0) form Corrected Field Data

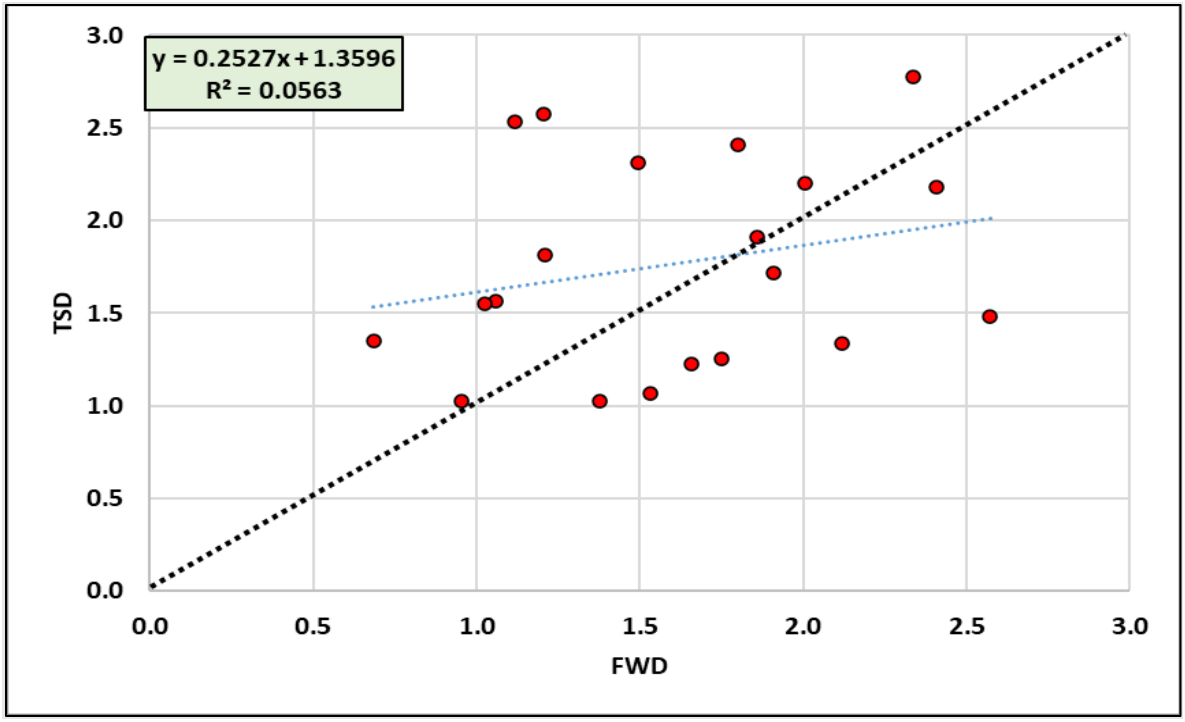

Figure 6.11 Theoretical Minimum Deflection (D_{60}) form Uncorrected Field Data

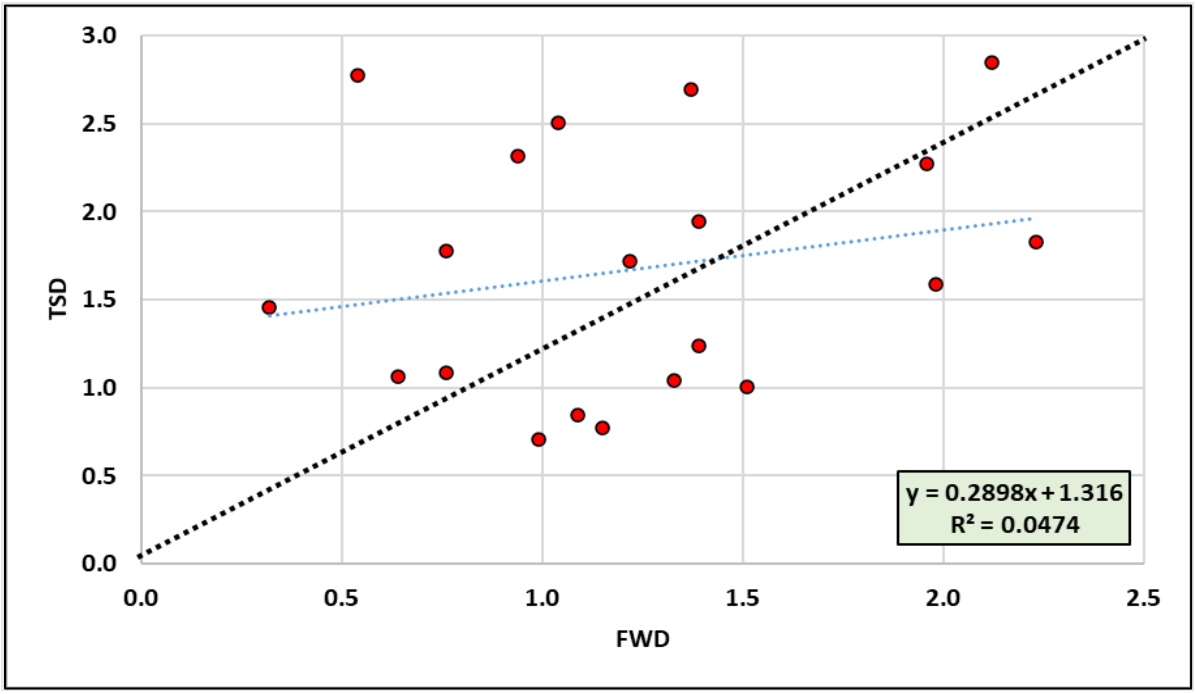

Figure 6.12 Theoretical Minimum Deflection (D_{60}) form Corrected Field Data

6.2.2 FWD vs. TSD Deflection Basin Parameters (DBPs)

The results of the comparison between the FWD and TSD deflection basin parameters (DBPs) are presented in Figures 6.13 through 6.16 based on uncorrected deflection measurements. These figures show the Surface Curvature Index (SCI), Lower Layer Index (LLI), Middle Layer Index (MLI), and Area Under Pavement Profile (AUPP) parameters respectively. Similar correlations were examined for the corrected deflection data. The results demonstrated that there was a fair correlation for LLI and MLI (R^2 of 0.60 and 0.55, respectively) for the FWD and TSD data. Also, there was a trend for SCI and AUPP, but such correlation was not strong (R^2 of 0.21 and 0.37, respectively) between the two sets of FWD and TSD data. Despite the strong correlation found between the two overall deflection measurements, the results demonstrated that the DBPs do not provide the same strong correlation between the FWD and TSD.

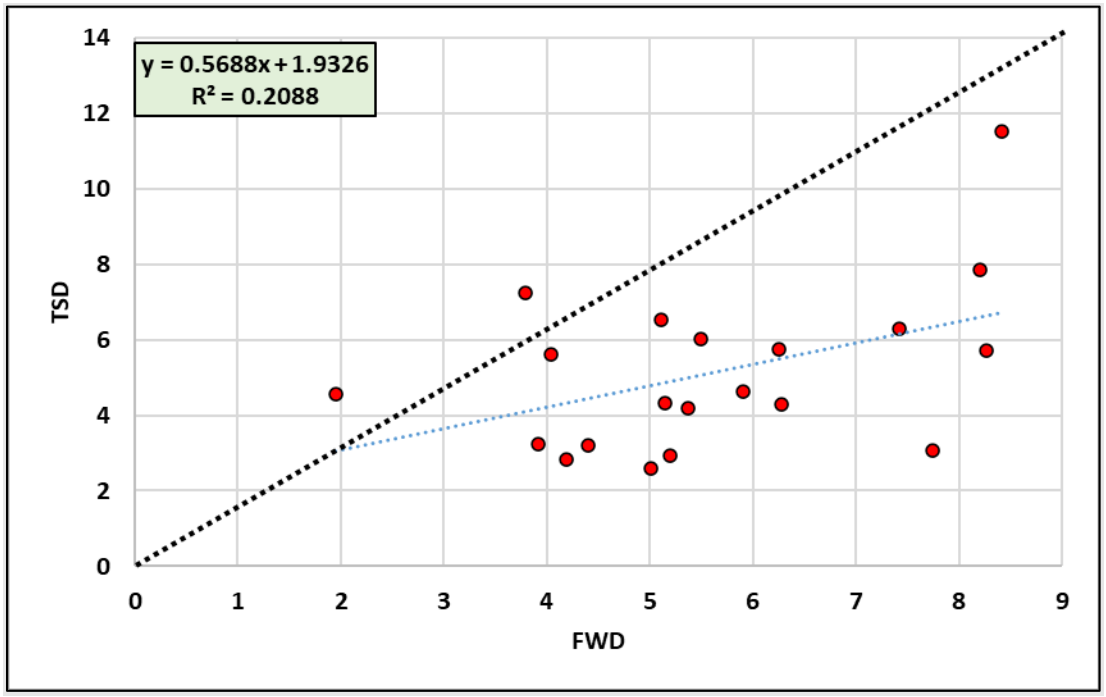

Figure 6.13 SCI for FWD and TSD Field Data

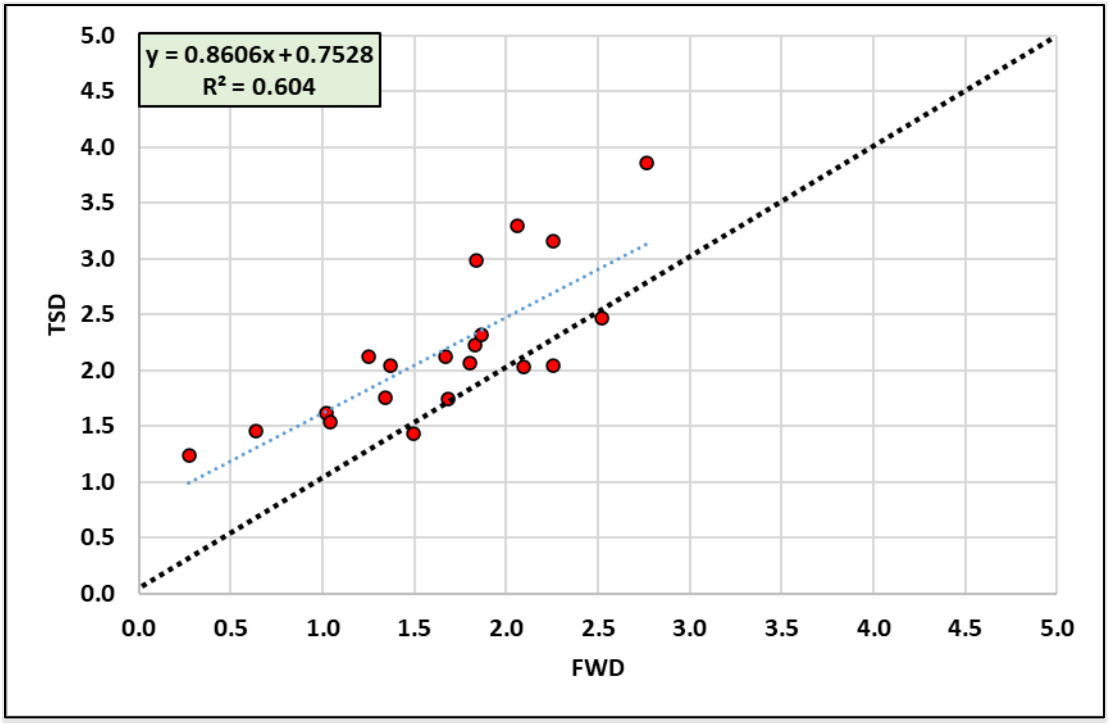

Figure 6.14 LLI for FWD and TSD Field Data

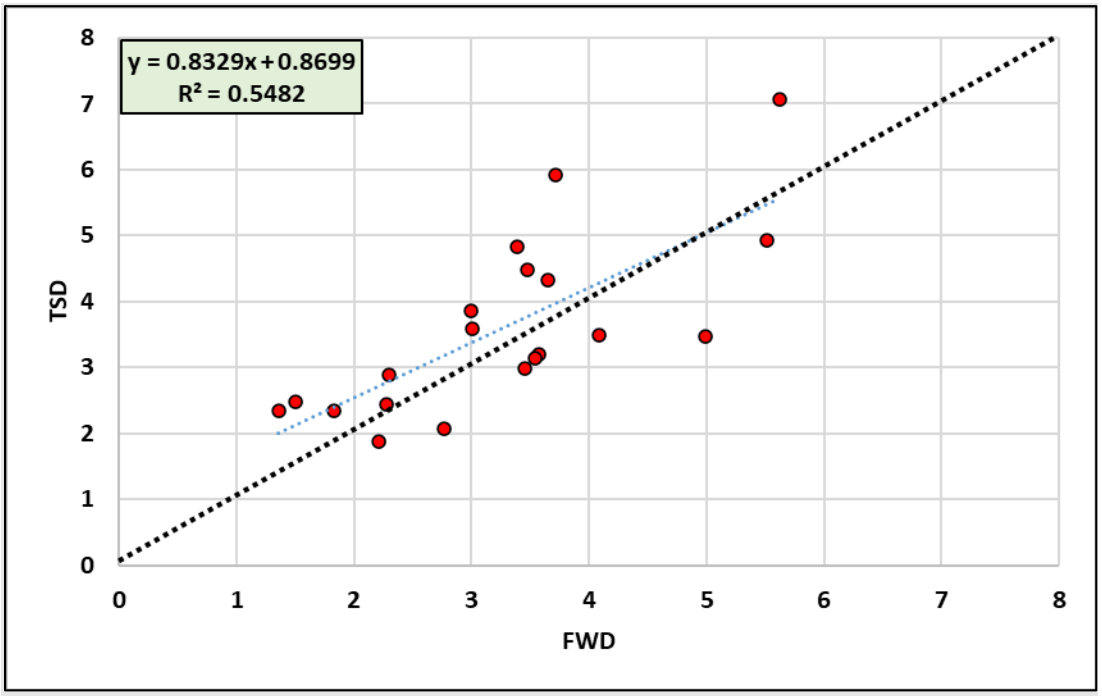

Figure 6.15 MLI for FWD and TSD Field Data

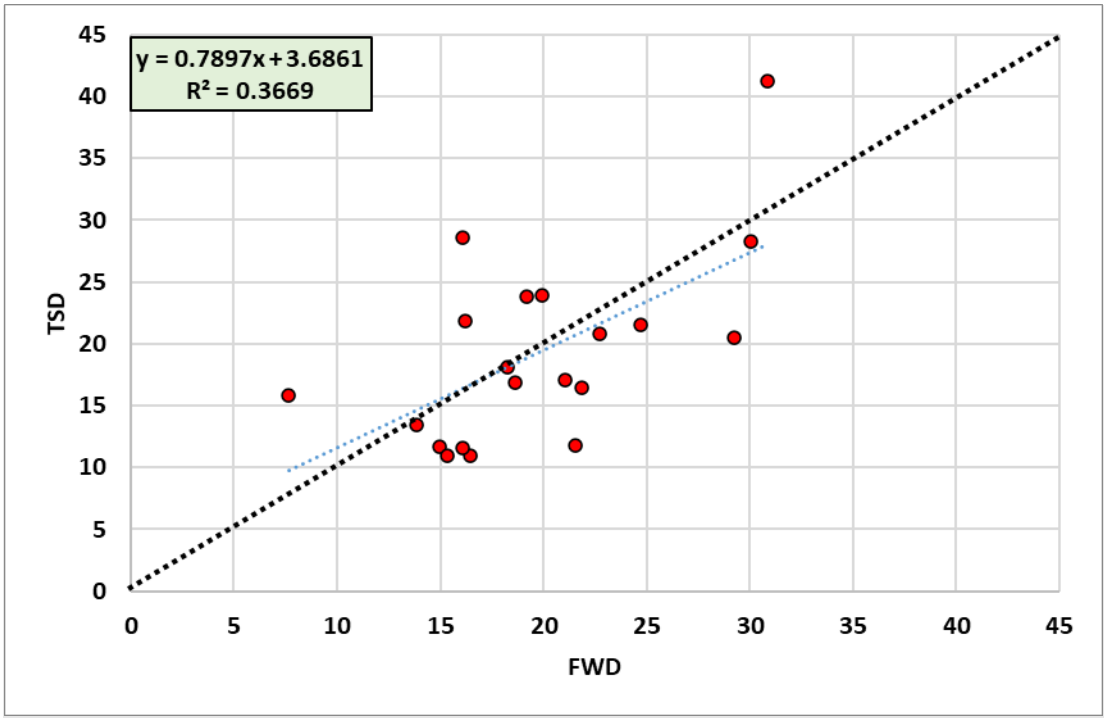

Figure 6.16 AUPP for FWD and TSD Field Data

6.3 Comparison between FWD and TSD SNeff and Overlay Thickness

The researchers compared SN_{eff} calculated using the FWD and TSD. Figures 6.17 and 6.18 show the SN_{eff} calculated using the iterative AASHTO equation for the uncorrected and corrected deflection data, respectively. The results demonstrated that there is a strong correlation between FWD SN_{eff} and TSD SN_{eff} with R^2 of 0.91 for the uncorrected deflection data and R^2 of 0.87 for the corrected deflection data. The SN_{eff} values were close to the quality line with higher R^2 using the uncorrected deflection data. Similarly, Figures 6.19 and 6.20 show the SN_{req} calculated using the AASHTO equation (Equation 4.13) and structural condition index or structural number ratio, respectively for both FWD and TSD. The results clearly demonstrate that the TSD can be used to assess the condition of existing pavement and assessment was close that that of the FWD. These results suggested that the TSD can be used effectively at the network level to identify the sections with potential structural deficiency for further FWD analysis at the project level. This can optimize the time and resources of employing the FWD crew and reduce traffic interruption and improve the safety of FWD crew and motorists.

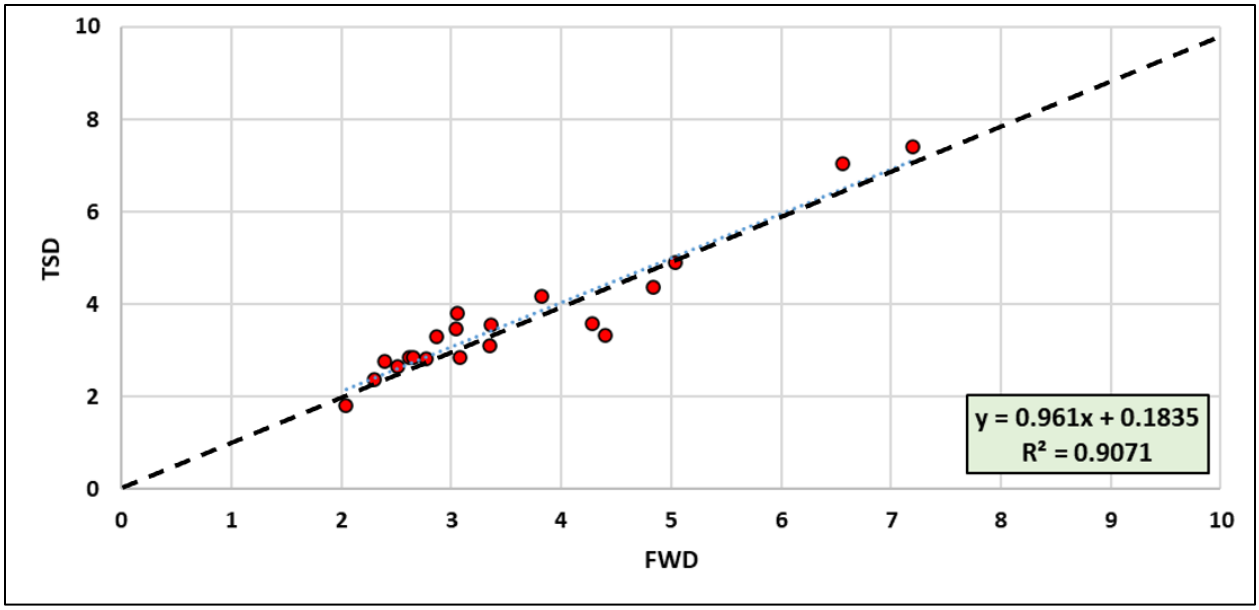

Figure 6.17 AASHTO SN_{eff} using FWD and TSD Uncorrected Deflection Data

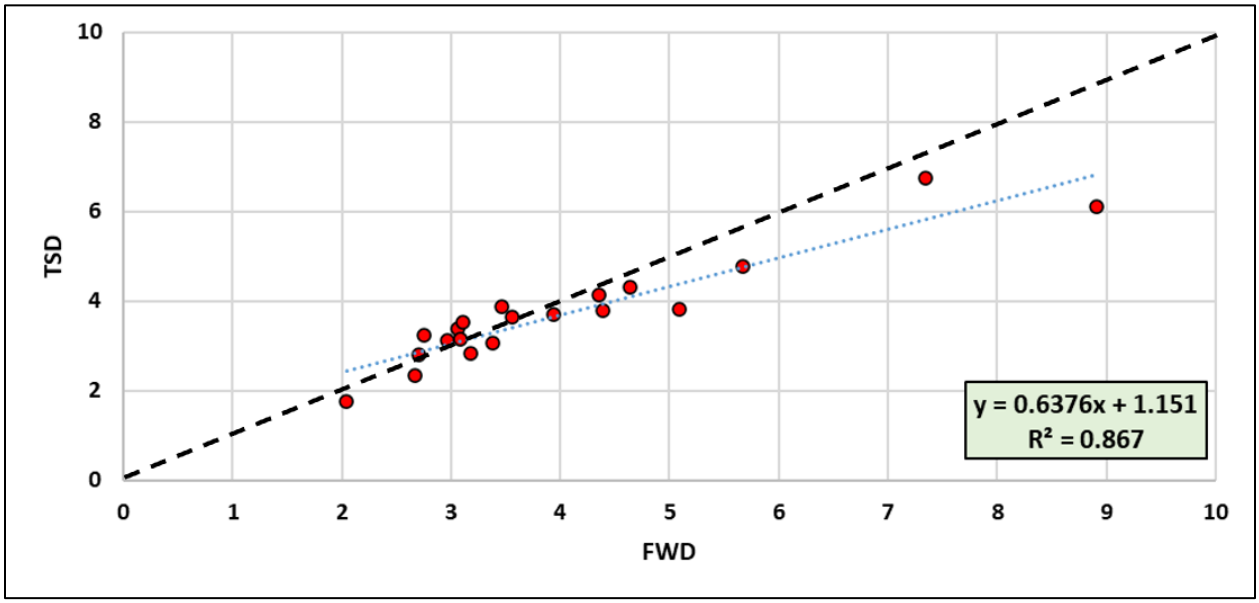

Figure 6.18 AASHTO SN_{eff} using FWD and TSD Corrected Deflection Data

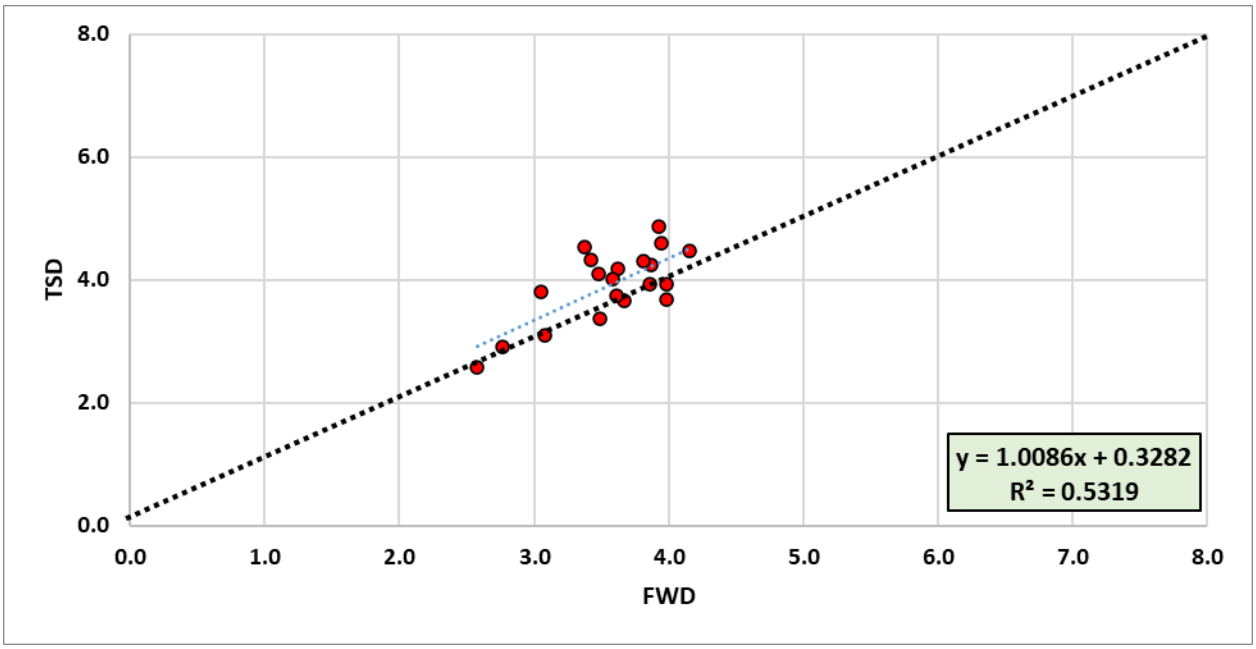

Figure 6.19 AASHTO SN_{req} using FWD and TSD Uncorrected Deflection Data

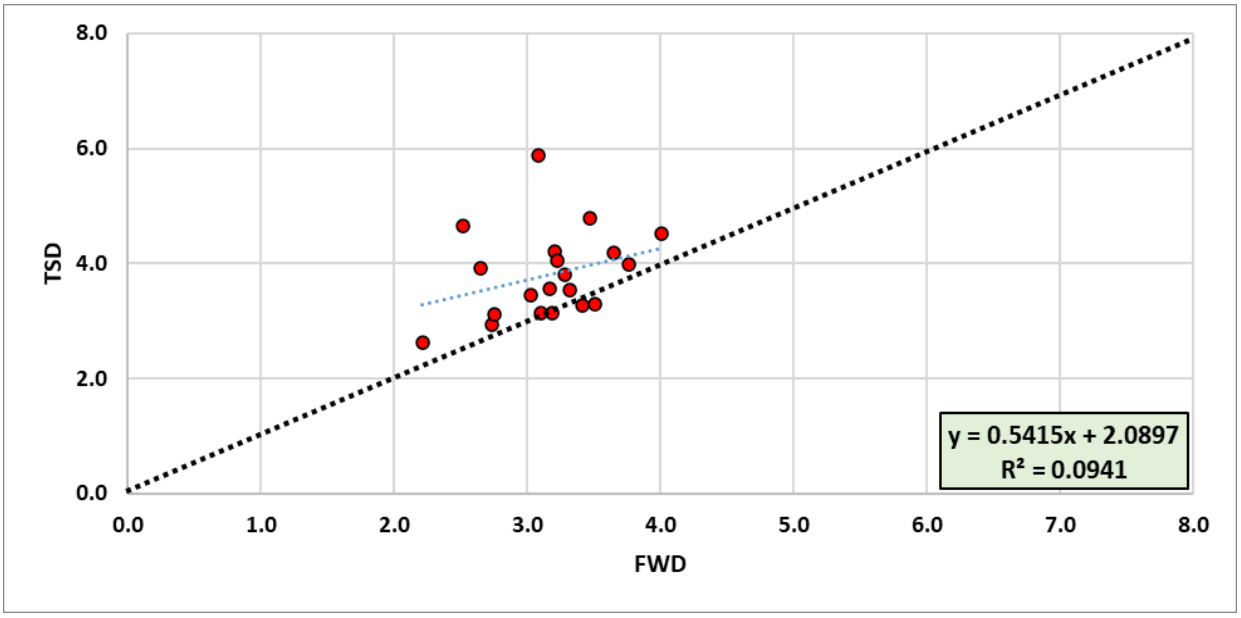

Figure 6.20 AASHTO SN_{req} using FWD and TSD Corrected Deflection Data

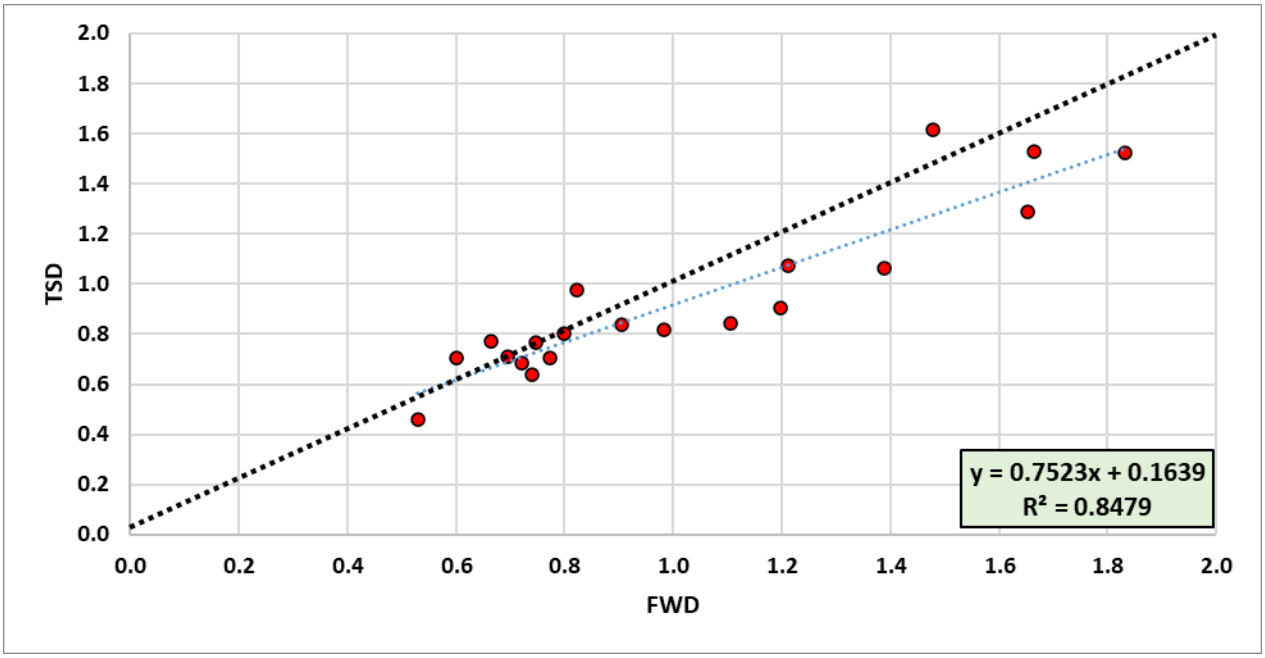

Figure 6.21 Structural Condition Index or Structural Number Ratio for Uncorrected FWD and TSD

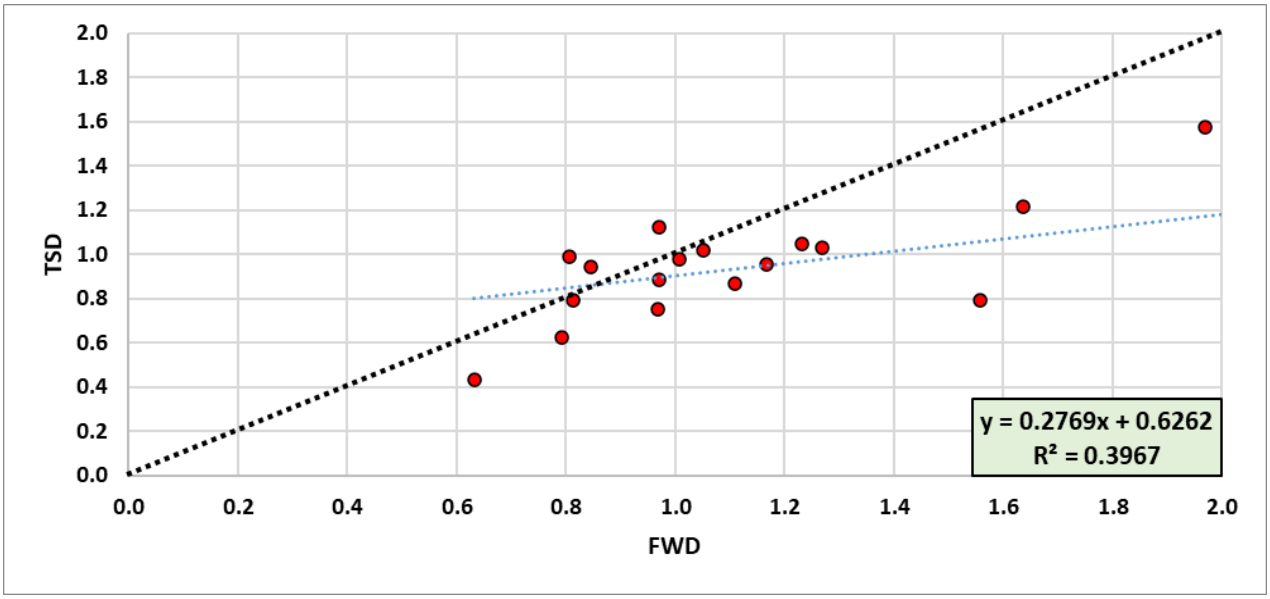

Figure 6.22 Structural Condition Index or Structural Number Ratio for Corrected FWD and TSD

Figure 6.21 further compares the remaining service life of the examined sections. Overall, there was a good agreement between both methods (i.e., FWD and TSD); however, there are two sections where there were conflicting calculations in assessing the remaining service life. Table 6.1 summarizes the required overlay thickness using the FWD and TSD deflection data. Overall, there was good agreement

between the two data sets (i.e., FWD and TSD); however, the FWD demonstrated that eight sections don't need an overlay while the TSD demonstrated that only six of those eight sections would need an overlay. Again, these results suggested that the two methods (FWD and TSD) provide comparable assessment of existing pavement structures based on the measured deflection basin.

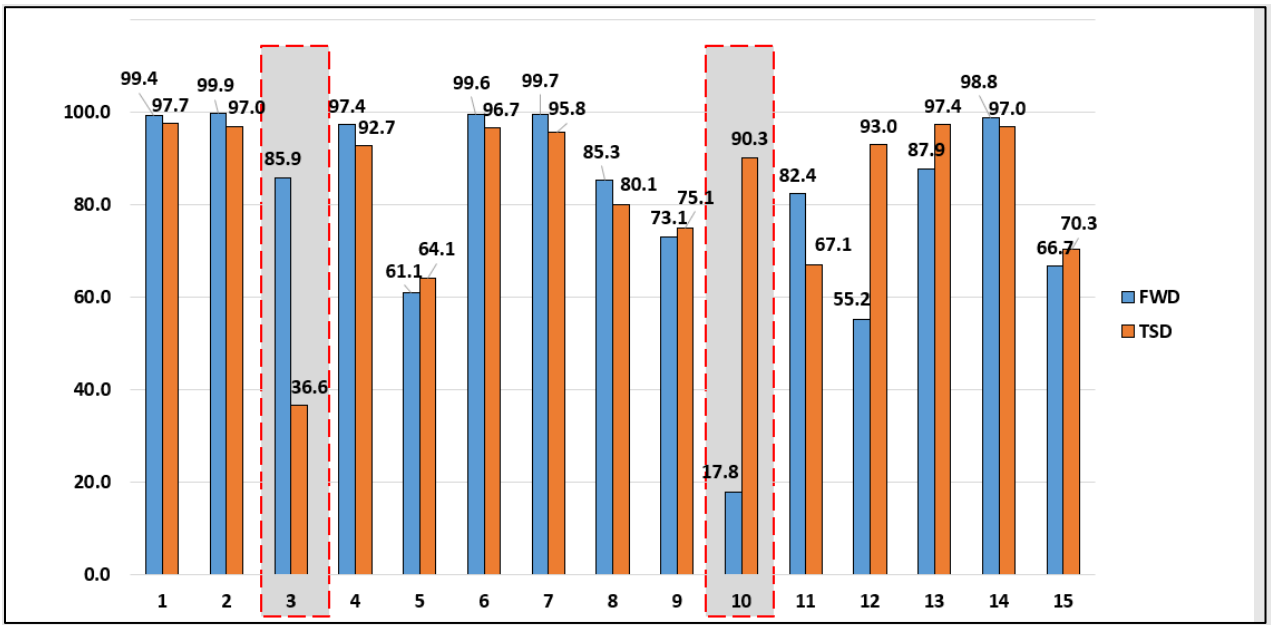

Figure 6.23 Remaining Service Life

Table 6.1 Structural Condition and Required Overlay Thickness

Project	FWD Structural Condition & Required Overly Thickness (in.)	TSD Structural Condition & Required Overly Thickness (in.)
I-15 40-45 2020	Sufficient	Sufficient
I-15 90-95 2020	0.73	1.68
I-15 100-105 2020	Sufficient	Sufficient
SH-39 46.80-51.80 2020	0.13	1.80
SH-27 15-20 2020	Sufficient	1.51
US-93 201.85-206.20 2020	Sufficient	Sufficient
US-93 211.20-216.20 2020	1.78	1.66
US-93 216.20-221.20 2020	Sufficient	Sufficient
US-30 250.90-255.90 2020	Sufficient	Sufficient
SH-55 100.20-105.20 2020	2.44	3.68
SH-55 110.20-115.20 2020	Sufficient	Sufficient
SH-52 19.00-22.20 2019	4.13	4.86
US 95 MP 0.00-4.826 2019	1.75	1.92
US 95 MP 4.836-16.581 2019	2.30	3.02
US 95 MP 16.591-23.957 2019	3.61	2.65
US 95 MP 23.967-28.710 2019	1.84	2.71
US 95 MP 28.720-35.614 2019	3.03	1.92
US 95 MP 35.714-41.418 2019	1.41	0.18
US 95 MP 42.518-50.742 2019	Sufficient	0.78
US 95 MP 61.023-69.219 2019	2.49	2.47

6.4 Developing Excel based Utility

To simplify the calculations of FWD and TSD deflection data, the researchers developed an Excel spreadsheet that automates the data processing procedure. Once the FWD and TSD data is imported into the spreadsheet, the relevant calculations are automatically performed, and all calculations are generated, and tables and figures are produced. The spreadsheet includes calculations for DBPs, effective and required structural numbers, and overlay thickness. Additionally, a representative graph of the overlay thickness results is produced for each milepost. The Excel spreadsheet is capable of processing 500 data points in a single run, which represents a single block of pavement test section, with TSD data being measured every 0.01 miles. Thus, each run covers up to five miles of a pavement section.

The following steps summarize the FWD and TSD deflection data calculations in the developed Excel spreadsheet tabs (Figure 6.23).

- Figure 6.24 presents the main interface of the Excel spreadsheet, which features two input icons for importing the FWD and TSD deflection data. The user is also required to complete the remaining inputs related to pavement structure information, such as layer thickness, traffic volume, number of lanes, and growth rate. After the inputs are completed and the deflection data are imported, as shown in Figure 6.25, the output data will automatically be generated and populated within the spreadsheet.

- The output data includes the Deflection Basin Parameters (DBPs). The researchers chose eight DBPs that are commonly used, based on a review of the literature and data analysis. Figure 6.26 displays the calculated average values for the imported deflection data.

- On the lower right portion of the main screen's outputs, the average effective and required structural numbers for the entire section can be viewed, along with the calculated required overlay thickness. Three methods for calculating overlay thickness are provided: deflection value, Rohde's equation, and iterative AASHTO method. The research team recommends using the AASHTO iterative method, as it has been proven to be the most conservative. However, the results of the other two methods are also reported for comparison and further analysis if necessary. Figure 6.27 displays the calculations of the effective structural number using the deflection method.

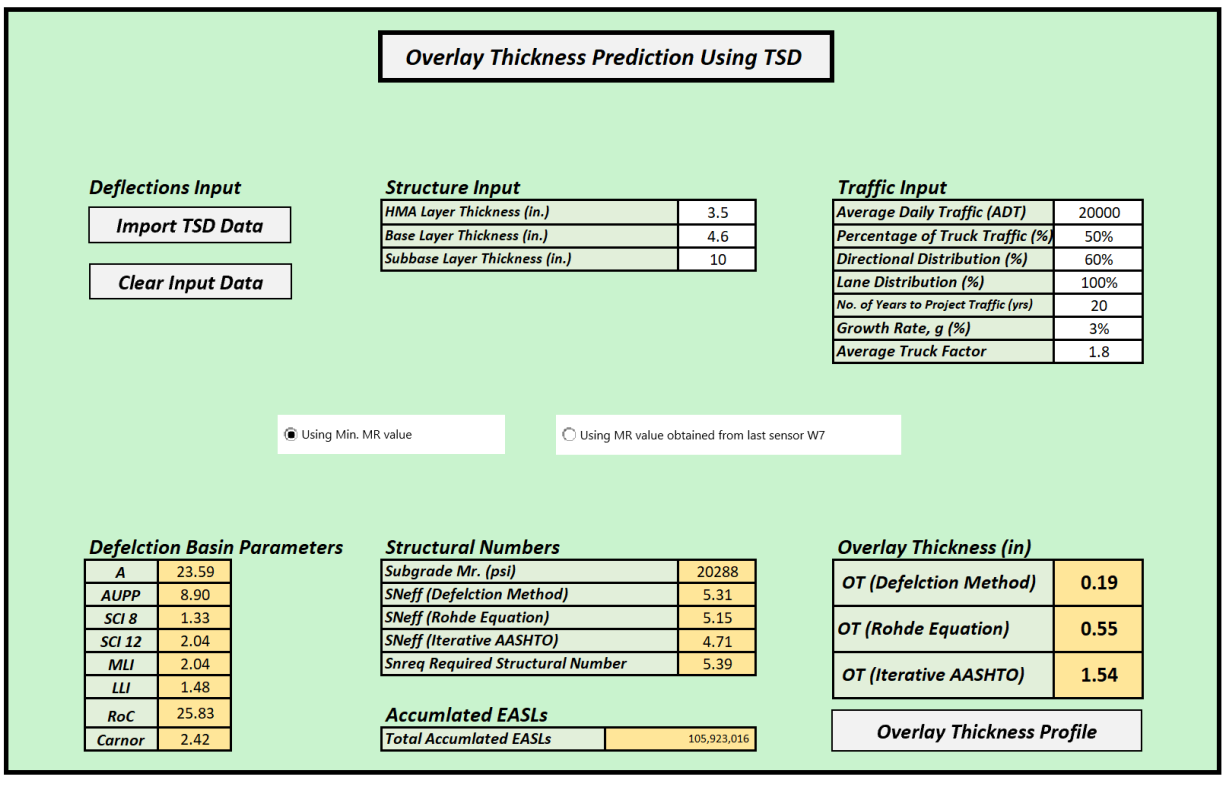

Figure 6.24 The Developed Excel Utility's Main Screen

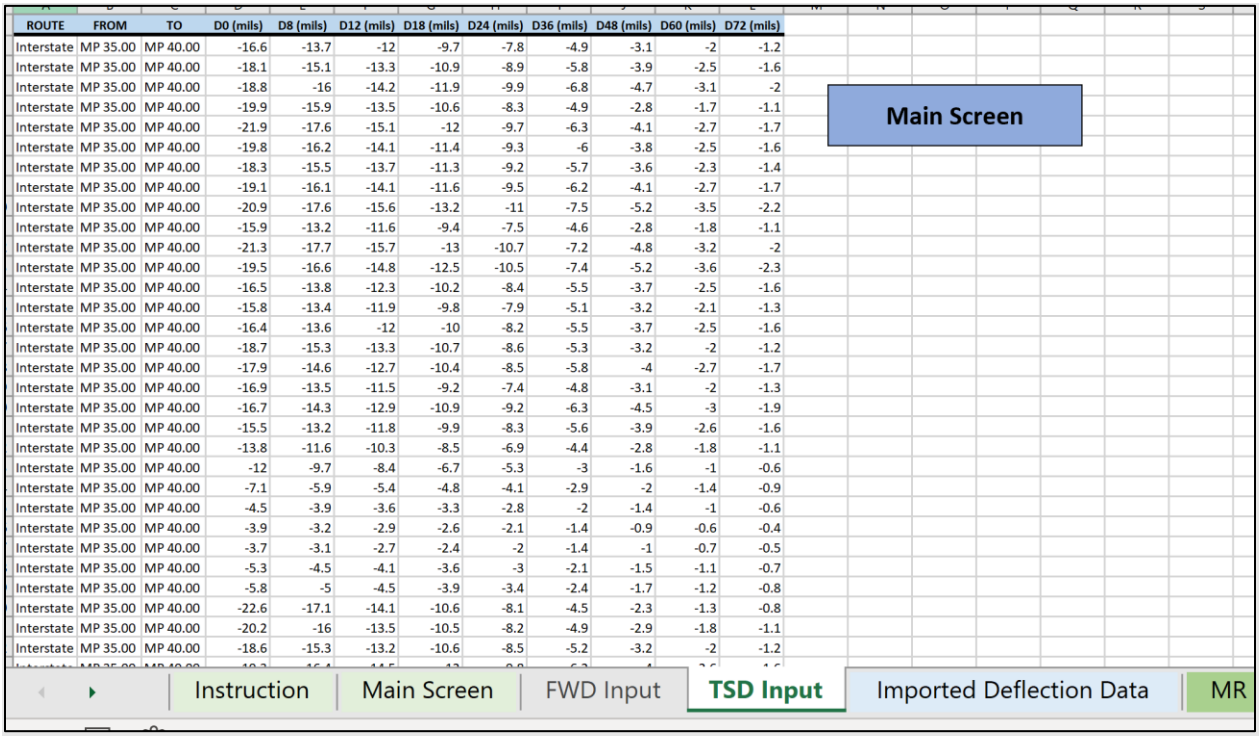

ROUTE	FROM	TO	D0 (mils)	D8 (mils)	D12 (mils)	D18 (mils)	D24 (mils)	D36 (mils)	D48 (mils)	D60 (mils)	D72 (mils)
Interstate	MP 35.00	MP 40.00	-16.6	-13.7	-12	-9.7	-7.8	-4.9	-3.1	-2	-1.2
Interstate	MP 35.00	MP 40.00	-18.1	-15.1	-13.3	-10.9	-8.9	-5.8	-3.9	-2.5	-1.6
Interstate	MP 35.00	MP 40.00	-18.8	-16	-14.2	-11.9	-9.9	-6.8	-4.7	-3.1	-2
Interstate	MP 35.00	MP 40.00	-19.9	-15.9	-13.5	-10.6	-8.3	-4.9	-2.8	-1.7	-1.1
Interstate	MP 35.00	MP 40.00	-21.9	-17.6	-15.1	-12	-9.7	-6.3	-4.1	-2.7	-1.7
Interstate	MP 35.00	MP 40.00	-19.8	-16.2	-14.1	-11.4	-9.3	-6	-3.8	-2.5	-1.6
Interstate	MP 35.00	MP 40.00	-18.3	-15.5	-13.7	-11.3	-9.2	-5.7	-3.6	-2.3	-1.4
Interstate	MP 35.00	MP 40.00	-19.1	-16.1	-14.1	-11.6	-9.5	-6.2	-4.1	-2.7	-1.7
Interstate	MP 35.00	MP 40.00	-20.9	-17.6	-15.6	-13.2	-11	-7.5	-4.6	-2.8	-1.1
Interstate	MP 35.00	MP 40.00	-15.9	-13.2	-11.6	-9.4	-7.5	-4.6	-2.8	-1.8	-1.1
Interstate	MP 35.00	MP 40.00	-21.3	-17.7	-15.7	-13	-10.7	-7.2	-4.8	-3.2	-2
Interstate	MP 35.00	MP 40.00	-19.5	-16.6	-14.8	-12.5	-10.5	-7.4	-5.2	-3.6	-2.3
Interstate	MP 35.00	MP 40.00	-16.5	-13.8	-12.3	-10.2	-8.4	-5.5	-3.7	-2.5	-1.6
Interstate	MP 35.00	MP 40.00	-15.8	-13.4	-11.9	-9.8	-7.9	-5.1	-3.2	-2.1	-1.3
Interstate	MP 35.00	MP 40.00	-16.4	-13.6	-12	-10	-8.2	-5.5	-3.7	-2.5	-1.6
Interstate	MP 35.00	MP 40.00	-18.7	-15.3	-13.3	-10.7	-8.6	-5.3	-3.2	-2	-1.2
Interstate	MP 35.00	MP 40.00	-17.9	-14.6	-12.7	-10.4	-8.5	-5.8	-4	-2.7	-1.7
Interstate	MP 35.00	MP 40.00	-16.9	-13.5	-11.5	-9.2	-7.4	-4.8	-3.1	-2	-1.3
Interstate	MP 35.00	MP 40.00	-16.7	-14.3	-12.9	-10.9	-9.2	-6.3	-4.5	-3	-1.9
Interstate	MP 35.00	MP 40.00	-15.5	-13.2	-11.8	-9.9	-8.3	-5.6	-3.9	-2.6	-1.6
Interstate	MP 35.00	MP 40.00	-13.8	-11.6	-10.3	-8.5	-6.9	-4.4	-2.8	-1.8	-1.1
Interstate	MP 35.00	MP 40.00	-12.0	-9.7	-8.4	-6.7	-5.3	-3	-1.6	-1	-0.6
Interstate	MP 35.00	MP 40.00	-7.1	-5.9	-5.4	-4.8	-4.1	-2.9	-2	-1.4	-0.9
Interstate	MP 35.00	MP 40.00	-4.5	-3.9	-3.6	-3.3	-2.8	-2	-1.4	-1	-0.6
Interstate	MP 35.00	MP 40.00	-3.9	-3.2	-2.9	-2.6	-2.1	-1.4	-0.9	-0.6	-0.4
Interstate	MP 35.00	MP 40.00	-3.7	-3.1	-2.7	-2.4	-2	-1.4	-1	-0.7	-0.5
Interstate	MP 35.00	MP 40.00	-5.3	-4.5	-4.1	-3.6	-3	-2.1	-1.5	-1.1	-0.7
Interstate	MP 35.00	MP 40.00	-5.8	-5	-4.5	-3.9	-3.4	-2.4	-1.7	-1.2	-0.8
Interstate	MP 35.00	MP 40.00	-22.6	-17.1	-14.1	-10.6	-8.1	-4.5	-2.3	-1.3	-0.8
Interstate	MP 35.00	MP 40.00	-20.2	-16	-13.5	-10.5	-8.2	-4.9	-2.8	-1.8	-1.1
Interstate	MP 35.00	MP 40.00	-18.6	-15.3	-13.2	-10.6	-8.5	-5.2	-3.2	-2	-1.2

Main Screen

Instruction | Main Screen | FWD Input | TSD Input | Imported Deflection Data | MR

Figure 6.25 TSD Deflections Input Screen

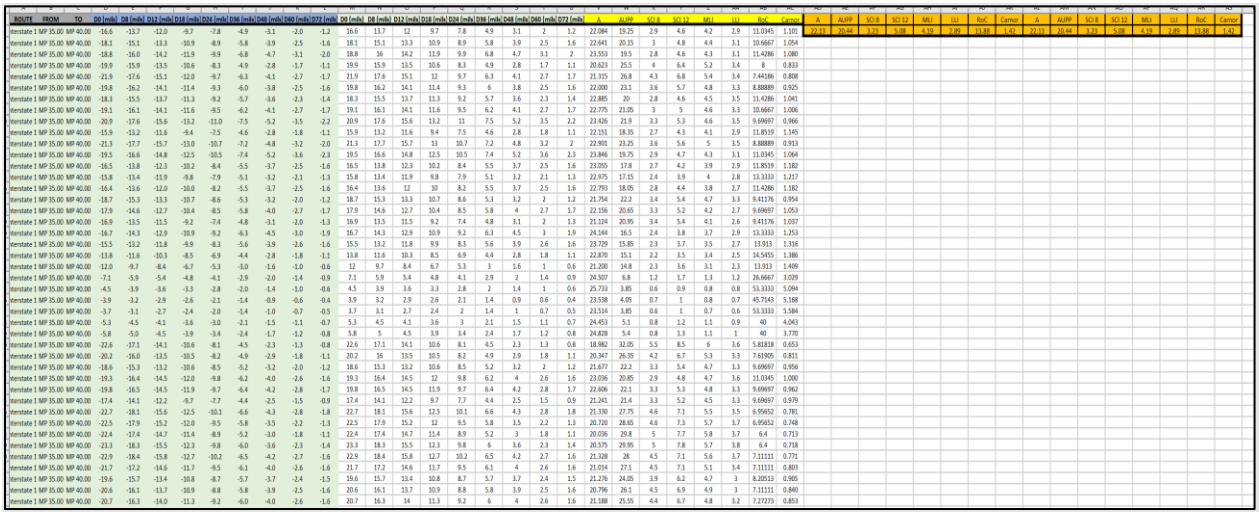

Figure 6.26 Deflection Basin Parameters' Calculations

D0	D60	Subgrade Moduli Min. (psi)	AC Thickness	Base Thickness	Total Pavement Thickness (D) (in.)	Epavement (psi) D (=<12)	Epavement (psi) D (12-15)	Epavement (psi) D (15-18)	Epavement (psi) D (18-21)	Epavement (psi) D (21-24)	Epavement (psi) D (24-27)	Epavement (psi) D (27-30)	Epavement (psi) D (=<12)	Epavement (psi) D (12-15)	Epavement (psi) D (15-18)	Epavement (psi) D (18-21)	Epavement (psi) D (21-24)	Epavement (psi) D (24-27)	Epavement (psi) D (27-30)	Selected $E_{pavement}$ (psi)	Effective Structural Number (SN_{eff})	Effective Structural Number (SN_{eff})
16.6	2	11538.46	4	12	16	174823	121446	97103.7	84002.6	76134.9	71011	67494.2			97103.7					97103.7394	3.29672005	3.546
18.1	2.5	10112.36	4	12	16	202674	136942	107085	91165.2	81673.3	75531.1	71330.7			107085					107085.261	3.40590465	
18.8	3.1	8823.53	4	12	16	253806	166948	127071	105996	93520.7	85501.9	80039.3			127071					127071.181	3.60562179	
19.9	1.7	10843.37	4	12	16	81518.4	61918.4	52534.7	47306.7	44083.3	41937.9	40447.2			52534.7					52534.6516	2.68683481	
21.9	2.7	9278.35	4	12	16	147367	101857	81130.4	69994.6	63316.1	58971.7	55991.8			81130.4					81130.4498	3.10520824	
19.8	2.5	9677.42	4	12	16	161398	110990	88058.5	75759.2	68392.6	63606.3	60325.4			88058.5					88058.5233	3.19110704	
18.3	2.3	9782.61	4	12	16	161623	111251	88332.9	76036.3	68669.5	63882	60599.9			88332.9					88332.87	3.19441426	
19.1	2.7	9473.68	4	12	16	199092	133967	104376	88618.8	79234.3	73167.5	69021			104376					104375.689	3.37696129	
20.9	3.5	8000.00	4	12	16	237462	155916	118409	98597.4	86876.9	79346.9	74218.8			118409					118408.599	3.5218359	
15.9	1.8	12000.00	4	12	16	160047	112789	91130.9	79415.3	72352.8	67738.1	64564.8			91130.9					91130.931	3.22775981	
21.3	3.2	8333.33	4	12	16	198313	132116	101966	85964.8	76459.6	70329.7	66145.8			101966					101966.371	3.35080122	
19.5	3.6	8108.11	4	12	16	293180	190747	142898	117705	102845	93325.8	86853.8			142898					142898.367	3.74935511	
16.5	2.5	10714.29	4	12	16	259426	172607	133044	112056	99593.1	91558.2	86075.1			133044					133044.443	3.66119964	
15.8	2.1	11392.41	4	12	16	211052	143639	113015	96646.7	86869.3	80531.6	76193.3			113015					113015.102	3.46758363	
16.4	2.5	10909.09	4	12	16	267438	177776	136902	115225	102355	94060.5	88400.8			136902					136902.025	3.69621295	
18.7	2	10465.12	4	12	16	124252	88791.8	72440.5	63550.9	58171.4	54645	52215.6			72440.5					72440.474	2.9902415	
17.9	2.7	10344.83	4	12	16	248202	165251	127462	107410	95500.3	87820.9	82580			127462					127461.762	3.60930854	
16.9	2	12162.16	4	12	16	177636	123897	99360.9	86136.5	78186.4	73004.1	69445.2			99360.9					99360.8996	3.3220431	
16.7	3	9523.81	4	12	16	325887	212488	159781	132008	115614	105104	97954.7			159781					159781.22	3.89140619	
15.5	2.6	10714.29	4	12	16	319101	209480	159050	132414	116657	106534	99640.5			159050					159049.64	3.88546393	

Figure 6.27 SN_{eff} Calculations using Deflection Method

- The user can view the required overlay thickness graphically by clicking on the Output Icon. This will generate a profile for the entire pavement section, with the required overlay thickness for each 0.01 mile, as depicted in Figure 6.28. This chart allows the user to compare different required thicknesses, pinpoint weak spots, and assess the overall condition of the pavement section.

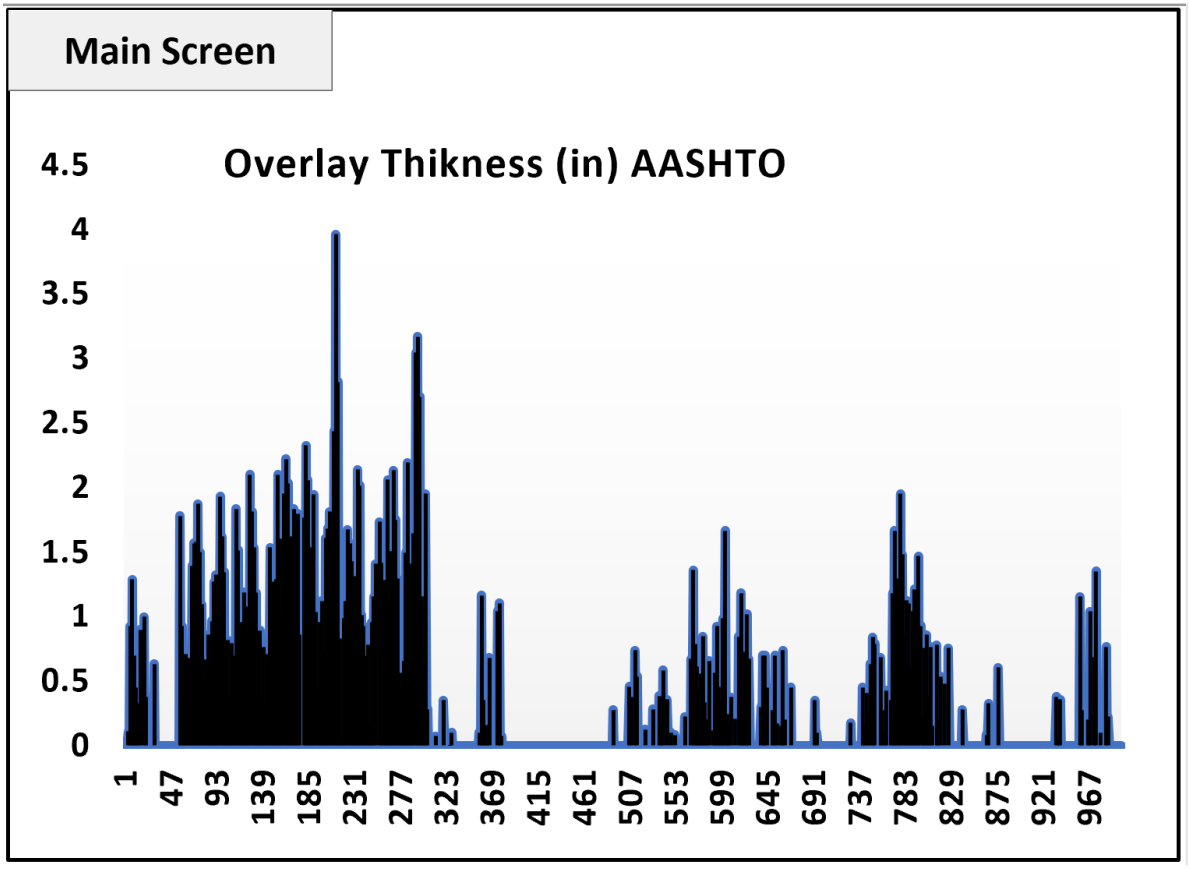

Figure 6.28 Overlay Generated Graph using the AASHTO Iterative Method

Overall, this calculation tool streamlines the processing and analysis of FWD and TSD data. It summarizes all the calculation procedures and provides the user with the required results. The excel sheet analyzes the date for one block of the test section at a time (500 data points). The final deflection data, whether corrected or uncorrected, are copied to the excel sheet by the user to eliminate the error associated with importing raw data with missing information. The user should examine the deflection data and ensure its quality and acceptance before copying the data into the excel sheet. This approach eliminates the risk of errors that could affect the calculations.

7. Artificial Intelligence (AI) utilization for Deflection data

The researchers utilized additional resources that were available outside this project to expand on the analysis and explore the use of Artificial Intelligence (AI) in this study. AI models were developed using the FWD and TSD measurements to predict pavement performance decays as a function of deflection data and traffic level for the parametric study. Furthermore, they developed preliminary models to estimate pavement layers' moduli as a function of layer thickness and FWD deflection data collected in the field. This would enable State Highway Authorities (SHAs) to make informed decisions on maintenance and rehabilitation treatments based on the future condition of pavements. Chapter 7 describes the data and results of the developed AI models to predict pavement performance using the deflection data.

7.1 Introduction

Artificial intelligence (AI) is a branch of computer science that performs tasks and solves problems that would typically require human intelligence (Artificial Intelligence (AI) vs. Machine Learning, 2022). The term was first coined in 1956 by a group of researchers at Dartmouth College (Dick, 2019). Since then, artificial intelligence has advanced and changed immensely. Today, there are many different subsets of AI, and the term AI is often used interchangeably with the term machine learning, although they are not synonymous with one another. Machine learning is a subset of AI where it automatically learns insights and recognizes patterns in data through algorithms and then applies that learning to make increasingly better decisions (Artificial Intelligence vs. Machine Learning, 2022).

There are three groups of machine learning models: supervised learning, unsupervised learning, and reinforcement learning (Justo-Silva et al., 2021). The type of machine learning models investigated in this study are supervised learning. Supervised learning models use input and output data to make predictions for new data and are typically "used for project-level or network-level pavement management" (Justo-Silva et al., 2021).

Most machine learning techniques split data into training and testing sets. The model uses the training data to learn, and the testing set is used to validate that model to see if it can accurately model unseen data. The percentage of data used in each of these sets is dependent on the variability of the data as well as the number of samples available. There are countless different AI and machine learning algorithms including Artificial Neural Networks (ANN), decision trees, random forests, expert systems, genetic algorithms, long term/short term memory (LSTM), intelligent search algorithms, structural equation modeling (SEM), group method of data handling (GMDH), among others. The reader is referred to Natalie (2023) for more information on the various AI and machine learning techniques and application of AI in Civil Engineering. Based on a comprehensive analysis of various AI and machine learning techniques to suit the data considered in this study, the random forest technique was recommended and used in this study (Natalie 2023). This chapter focuses on the analysis and results of various models developed to predict pavement performance using the deflection data and other information.

7.2 Results for Models Predicting Pavement Performance based on Theoretical FWD Data

This section discusses the models developed to predict the pavement performance (e.g., IRI, rutting, cracking) that were trained and tested using the theoretical parametric study. The 3D Move was used to predict the FWD and TSD deflection data as discussed in Chapter 4, while the AASHTOWare Pavement ME was used to predict the pavement performance (e.g., IRI, rutting, cracking) for these sections. The team considered 57,120 total data points (each section had multiple data points taken at different times) to describe the deflection and performance data for 266 pavement sections (additional sections were evaluated and considered for the AI models). The developed models randomly selected sixty percent of the data points to be used in the training and the remaining data to be used for testing. The models used to predict performance based on the data gathered by the FWD using D_0, Car', SCI, AUPP, and cumulative traffic as inputs. Different models were developed to predict total rutting, rutting of the asphalt layer only, top-down fatigue cracking, bottom-up fatigue cracking, and IRI. The python codes for all AI models were written in Google Collaboratory and can be found in Appendix C.

7.2.1 FWD Asphalt Layer Deformation Prediction Results

For the rutting of asphalt layers, the random forests regression model had an R^2 of 0.9999 and 0.9996 for the training and testing data sets, respectively. The difference in these accuracies is negligible since it is so small. Figure 7.1 shows the correlation for the testing set between the predicted rutting of the asphalt layers using the random forests regression model and rutting in asphalt layer calculated using the AASHTOWare Pavement ME software. The high prediction accuracy is partially attributed to the theoretical nature of the data since the rutting in the asphalt layer is not measured but rather calculated based on material properties and pavement structure information using the AASHTOWare Pavement ME software.

This model was also used to examine the increase in deformation of the asphalt layer as a function of traffic. An example of the change in rutting of AC with ESALs is shown in Figure 7.2. Figure 7.2 shows the increase in deformation or rutting of the pavement section over a 20-year span as a function of the traffic with no surface treatments over the service life (i.e., 20 years). As one expects, the rutting increased with traffic. Also, the random forests regression model closely simulated the theoretical rutting data. Such rutting performance curve could be utilized to determine the most economical times to perform treatments on a given section.

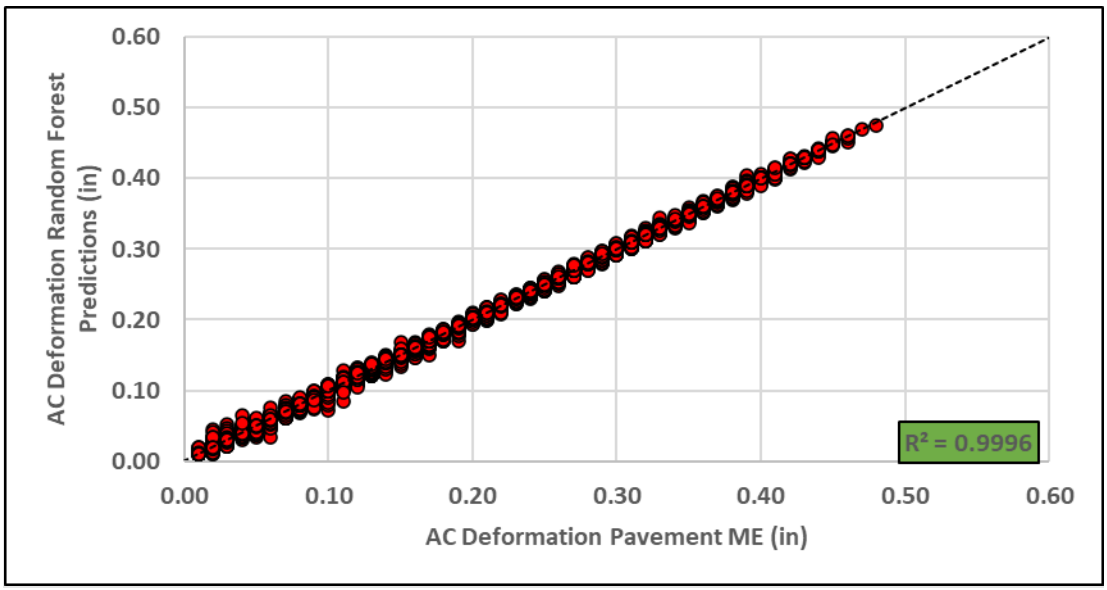

Figure 7.1 Random Forests Predictions vs. Pavement ME AC Deformation

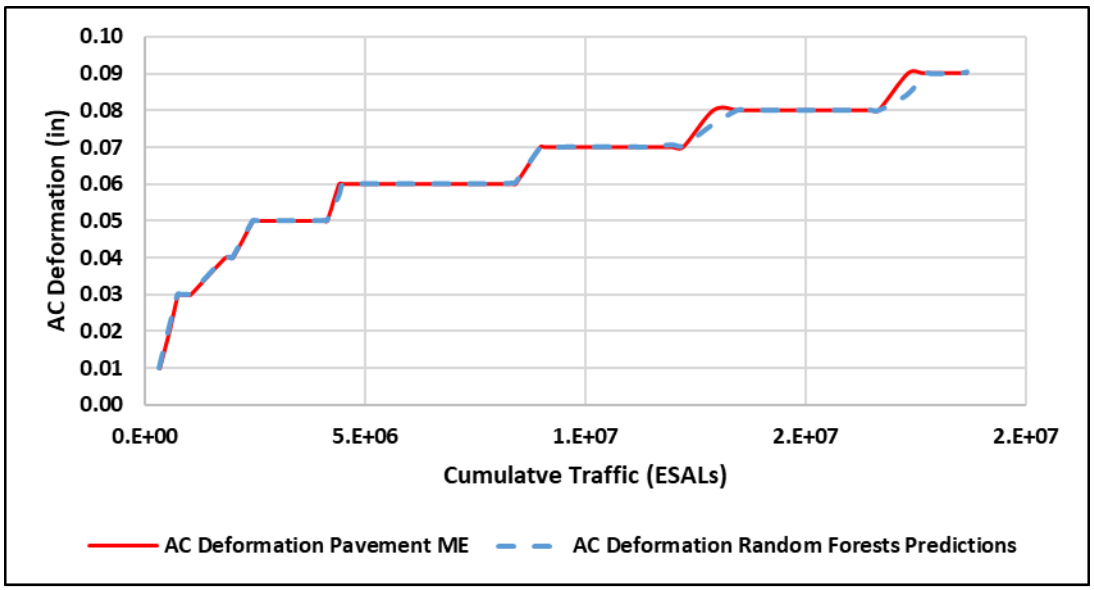

Figure 7.2 AC Deformation Curve with ESALs

7.2.2 FWD Total Deformation Prediction Results

The model developed to predict the total deformation (rutting) of the pavement sections had an R^2 of 0.9999 in both the training and testing data sets. Since there is no change in accuracy from the training set to the testing set, it can be assumed that the model was able to fully capture the full dataset using only the data points used in the training set. Figure 7.3 shows the correlation in the testing set between the predicted total rutting using the random forests regression model and total rutting calculated using the Pavement ME software. Again, this model was able to predict rutting at such a high accuracy due to the theoretical nature of the dataset. However, using the theoretical dataset exemplifies that random forests regression is able to accurately model and predict the relationship between these deflection parameters and rutting. Figure 7.4 shows an example for the change in total rutting as a function of traffic for a given section for both predicted rutting and calculated rutting from AASHTOWare.

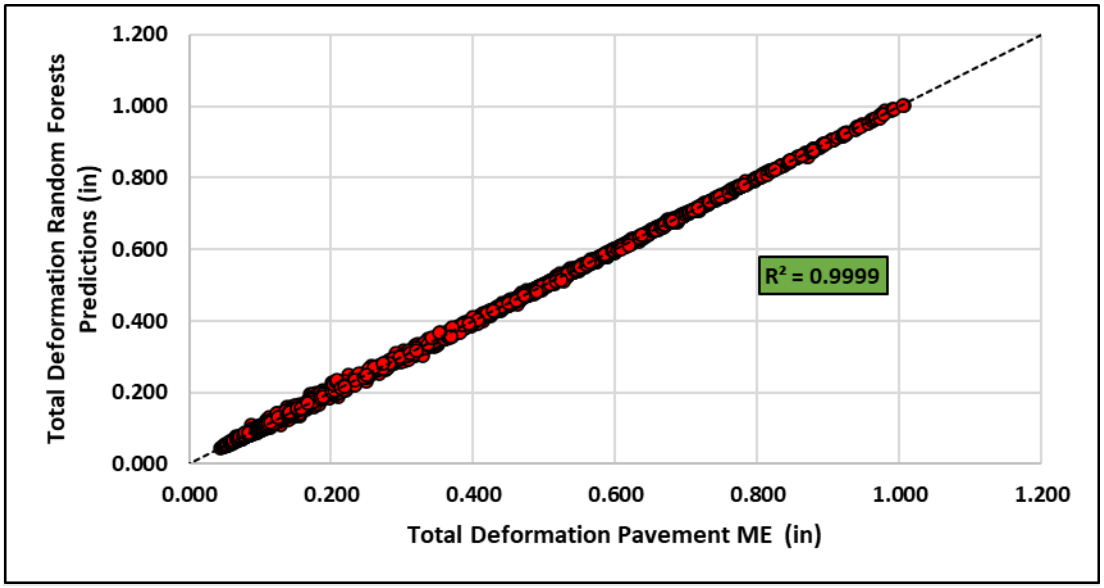

Figure 7.3 Random Forests Predictions vs. Pavement ME Total Deformation

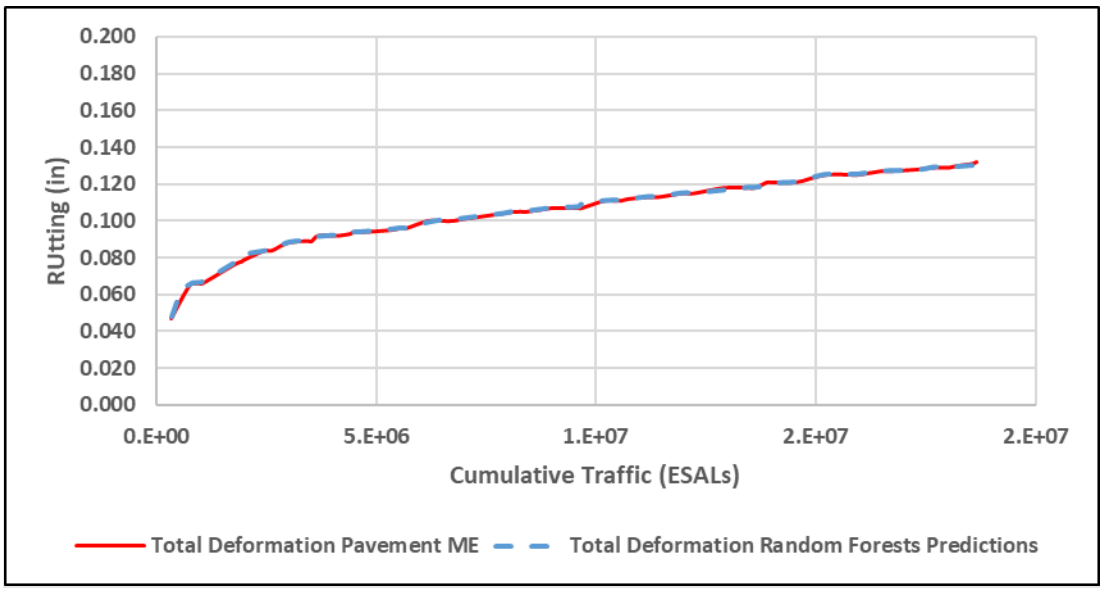

Figure 7.4 Total Deformation Curve with ESALs

7.2.3 FWD IRI Prediction Results

The researchers developed the random forests regression model for the IRI that provided R^2 of 0.9999 and 0.9998 for the training and testing sets, respectively. The minor decrease in accuracy from the training set to the testing set is negligible due to its size. Figure 7.5 shows the correlation for the testing set between the random forest regression model predictions and the calculated IRI values. Figure 7.6. shows an example of the change in IRI as a function of cumulative traffic for a given section. The model was able to predict the change in IRI with high accuracy.

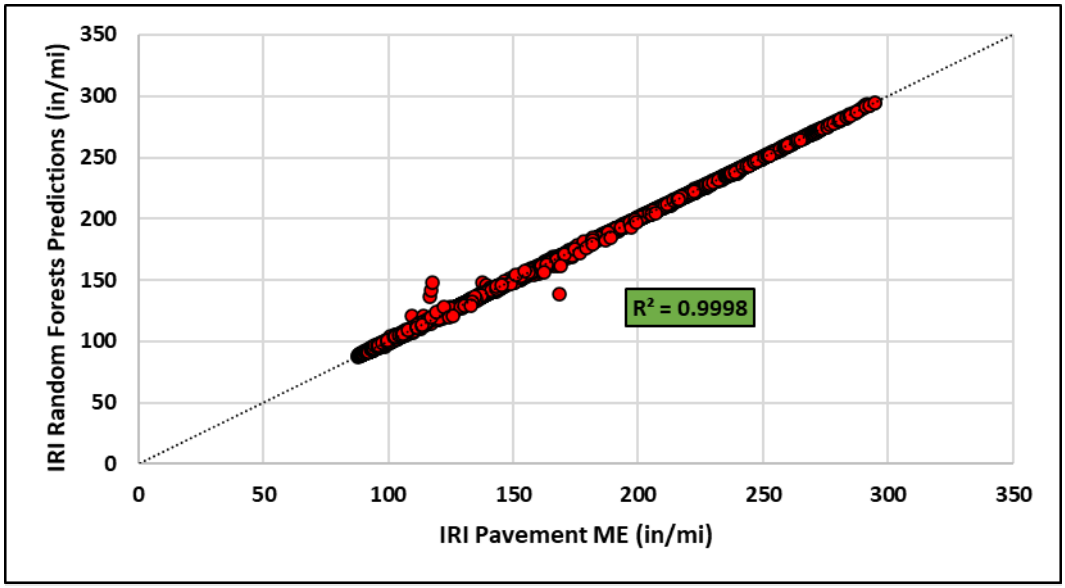

Figure 7.5 Random Forests Predictions vs Pavement ME IRI

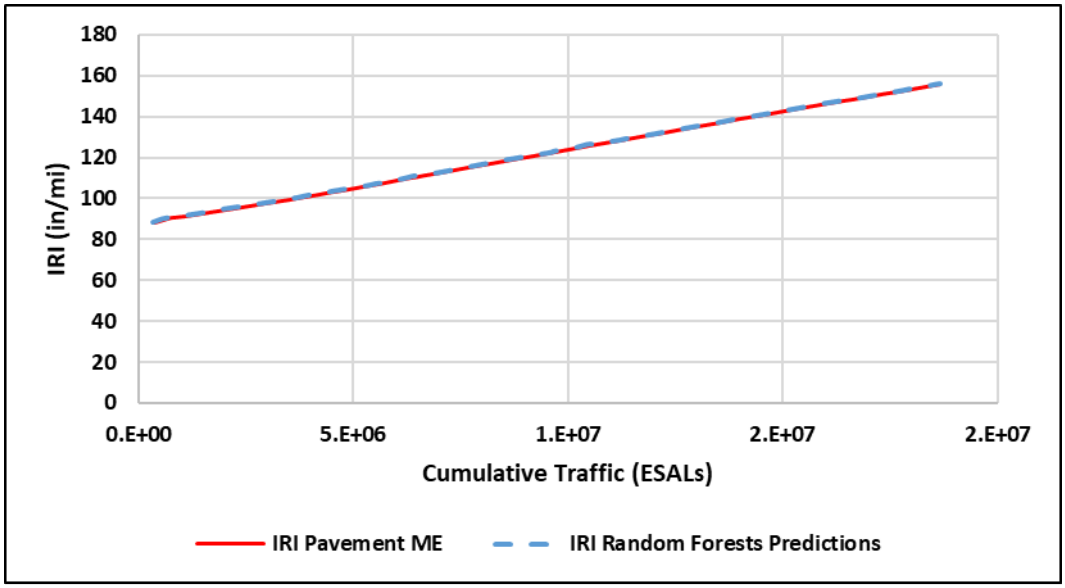

Figure 7.6 IRI Decay Curve

7.2.4 FWD Bottom-Up Cracking Prediction Results

The developed random forests regression model for the bottom-up fatigue cracking provided R^2 of 0.9999 and 0.9998 for the training and testing sets, respectively. Figure 7.7 shows the

correlation for the testing set between the predicted bottom-up fatigue cracking using the random forests regression model and bottom-up fatigue cracking calculated using the Pavement ME software. The high prediction accuracy is partially attributed to the theoretical nature of the data, but the use of theoretical data allows the model to showcase its ability to pinpoint the relationship between cumulative traffic, deflection parameters, and bottom-up fatigue cracking. In Figure 7.7, there are a few data points that do not directly match the correlation line. These points, however, are likely due to the fact that cracking is typically harder to predict than other performance measures such as IRI or rutting. It is clear that due to the large size of the testing set, these points do not have a noticeable effect on the R^2 and thus, do not raise any concerns.

This model was also used to examine the increase bottom-up fatigue cracking as a function of traffic. An example of this decay curve is shown in Figure 7.8. Figure 7.8 shows the increase in percentage of bottom-up fatigue cracking on the pavement section over a 20-year span as a function of the traffic with no surface treatments over the service life (i.e., 20 years). As one expects, the percentage of cracking increased with traffic. It can also be noted that the decay curve generated by the random forests predictions greatly mimics the decay curve generated by the Pavement ME data.

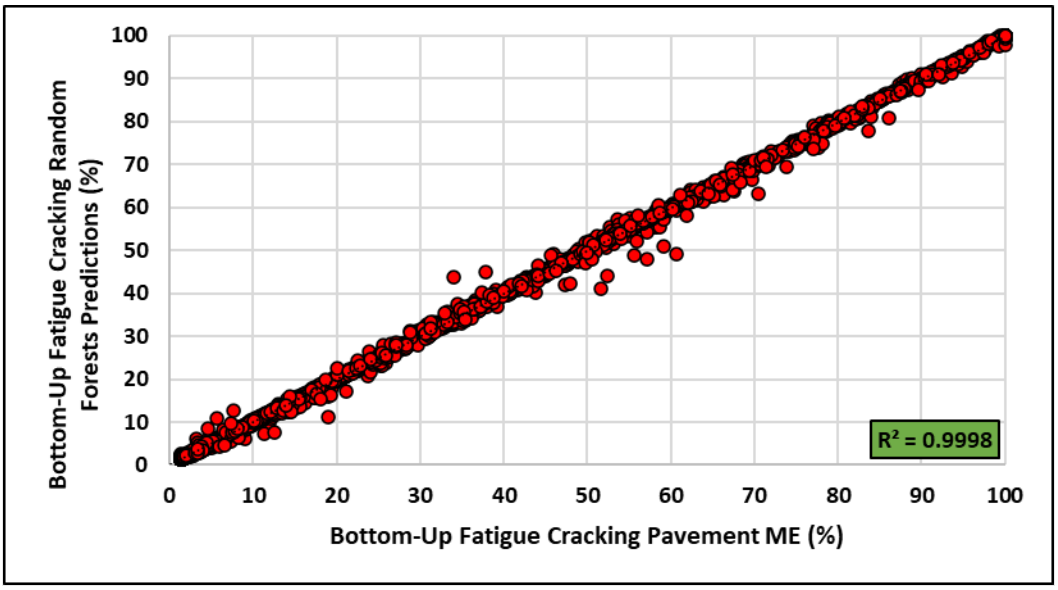

Figure 7.7 Random Forests Predictions vs. Pavement ME Bottom-Up Fatigue Cracking

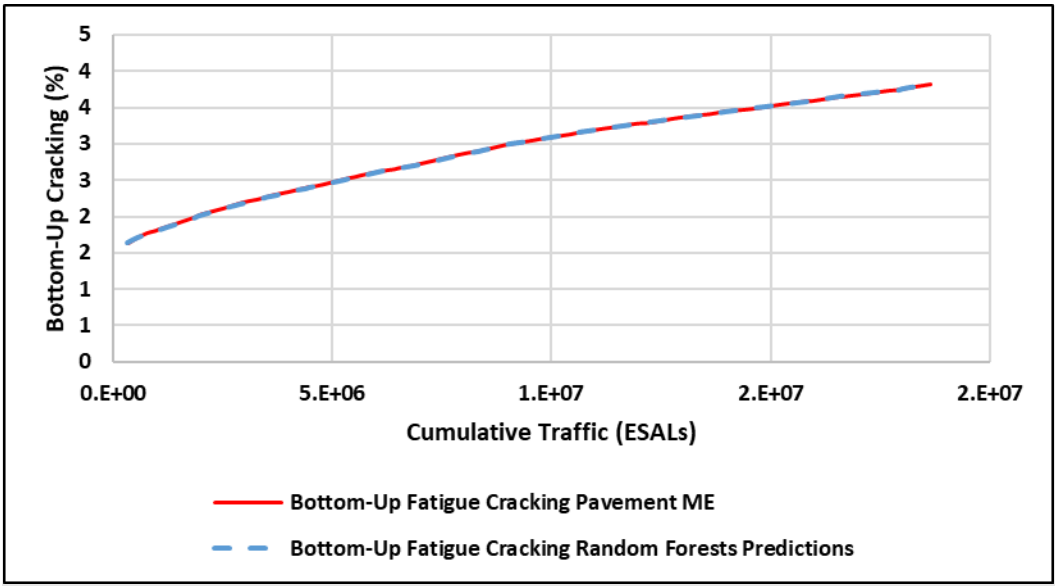

Figure 7.8 Change in Bottom-Up Fatigue Cracking with ESALs

7.2.5 FWD Top-Down Fatigue Cracking Prediction Results

The developed random forests regression model for the top-down fatigue cracking provided R^2 of 0.9997 and 0.9978 for the training and testing sets, respectively. This difference in these accuracies is negligible since it is so small. However, out of all the random forests regression models developed to predict pavement performance based on the theoretical deflection datasets, this model yielded the lowest accuracy in both the training and testing sets. This is believed to be due to both the difficult nature of modeling the top-down cracking as well as a lack of ability in the Pavement ME software to generate top-down fatigue cracking data. It is still important to note, however, that the R^2 for this model is still very high. In Figure 7.9, the correlation is shown for testing set between the predicted top-down fatigue cracking using the random forests regression model and top-down fatigue cracking calculated using the Pavement ME software.

This model was also used to examine the increase top-down fatigue cracking as a function of traffic as shown in Figure 7.10. As one expects, the percentage of cracking increased with traffic. It can also be noted that the decay curve generated by the random forests predictions mimics the decay curve generated by the Pavement ME data.

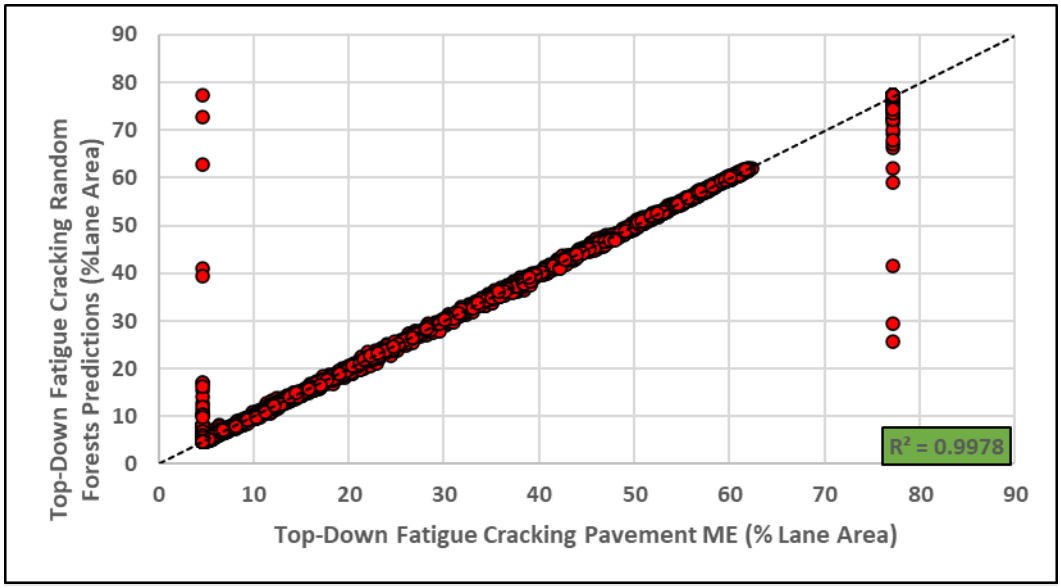

Figure 7.9 Random Forests Predictions vs Pavement ME Top-Down Fatigue Cracking

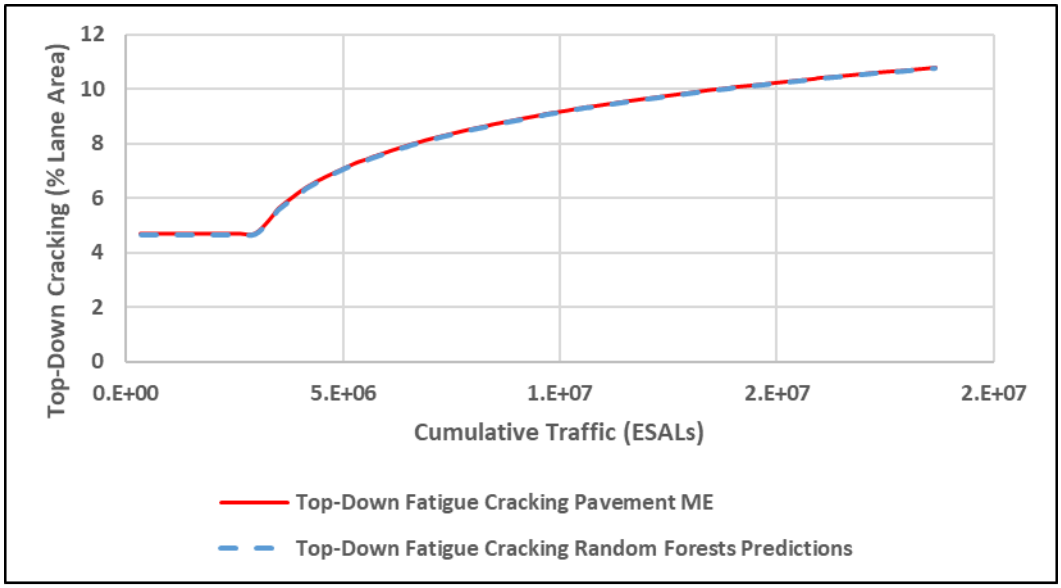

Figure 7.10 Change in Top-Down Fatigue Cracking with ESALs

7.3 Results for Models Predicting Pavement Performance based on Theoretical TSD Data

The researchers repeated the analysis in Section 7.2 for the FWD data set using the TSD data set. Similar to FWD analysis, the 3D Move was used to predict the FWD and TSD deflection data as

discussed in Chapter 4, while the AASHTOWare Pavement ME was used to predict the pavement performance (e.g., IRI, rutting, cracking) for these sections. The team considered 57,120 total data points (each section had multiple data points taken at different times) to describe the deflection and performance data for 266 pavement sections. This section focuses on the models developed to predict pavement performance using the TSD deflection data. The python codes for all AI models using the TSD data were also written in Google Collaboratory and can be found in Appendix C.

7.3.1 TSD Asphalt Layer Deformation Prediction Results

The developed random forests regression model for the deformation of asphalt layers provided R^2 of 0.9999 and 0.9995 for the training and testing sets, respectively. Figure 7.11 shows the correlation for the testing set between the predicted rutting in asphalt layer using the random forests regression model and rutting in asphalt layer calculated using the Pavement ME software. In Figure 7.11, the data points appear in small groups with gaps every 0.01 of an inch. These gaps are because the data generated by the Pavement ME software rounds the asphalt layer deformation to the nearest hundredth whereas the random forests model is predicting asphalt layer deformation to the nearest ten-thousandth.

This model was also used to examine the increase in deformation of the asphalt layer as a function of traffic. An example of the increase in AC rutting with traffic is shown in Figure 7.12. Figure 7.12 shows the increase in rutting of the asphalt layer over a 20-year span as a function of the traffic with no treatments over this span. As one expects, the rutting in the asphalt layer increased with traffic. Also, the random forests regression model closely simulates the theoretical rutting data.

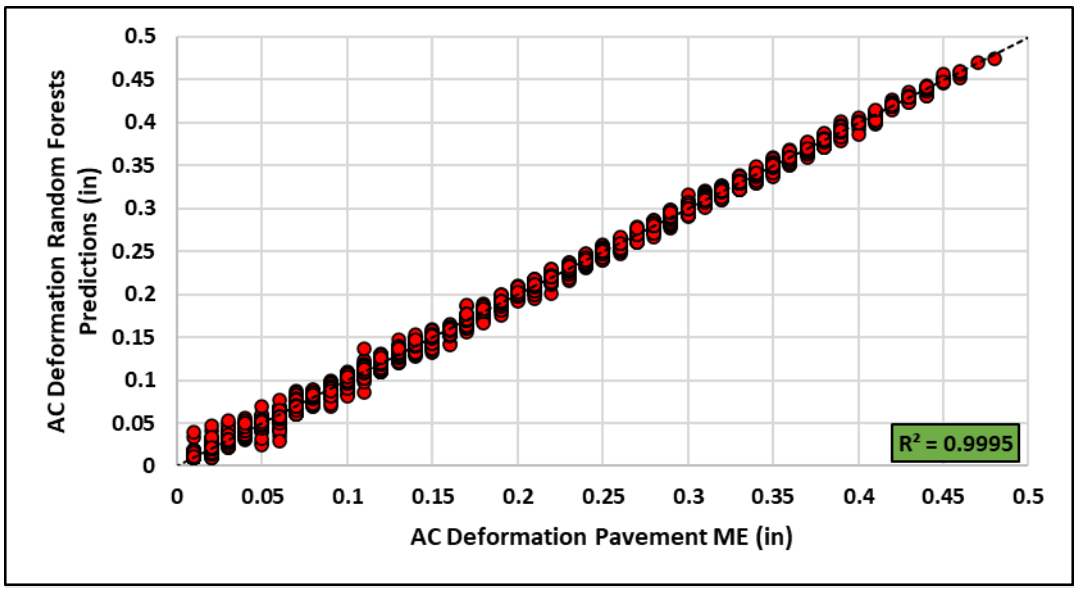

Figure 7.11 Random Forests Predictions vs Pavement ME Asphalt Layer Deformation

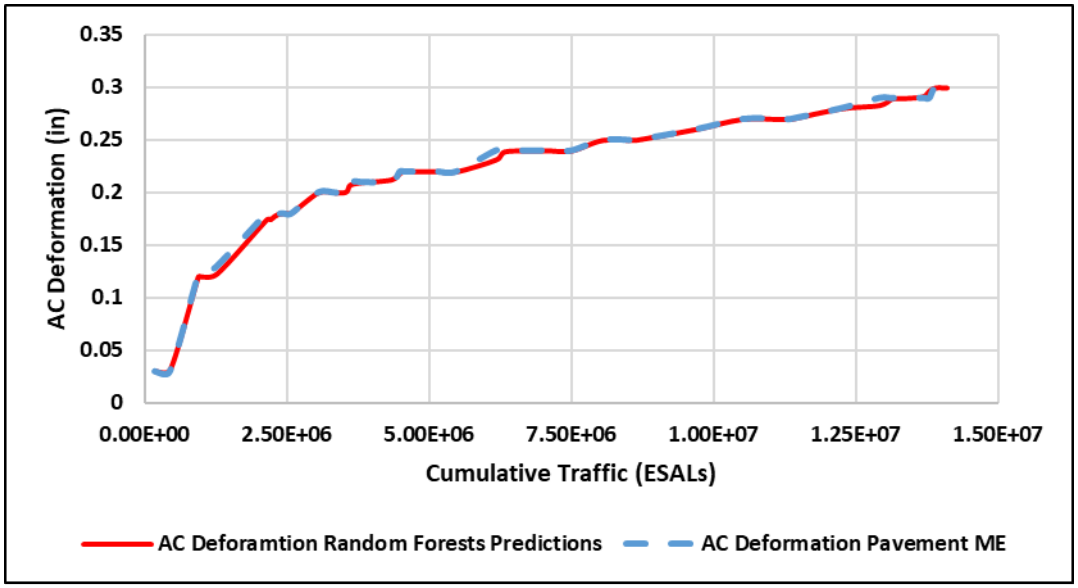

Figure 7.12 Asphalt Layer Deformation vs. ESALs

7.3.2 TSD Total Deformation Prediction Results

The random forests regression model developed to predict total deformation of pavement sections had R^2 of 0.9999 and 0.9996 for the training and testing sets, respectively. Figure 7.13 shows the correlation for the testing set between the predicted rutting using the random forests regression model and rutting calculated using the Pavement ME software. The high prediction

accuracy (R^2) is partially attributed to the theoretical nature of the data since the rutting is not measured but rather calculated based on material properties and pavement structure information. However, the use of theoretical data allows for the exhibition of the random forest regression model's ability to accurately use traffic and deflection data collected by the TSD to predict rutting. Similarly, Figure 7.14 shows an example of the change in total rutting as a function of traffic.

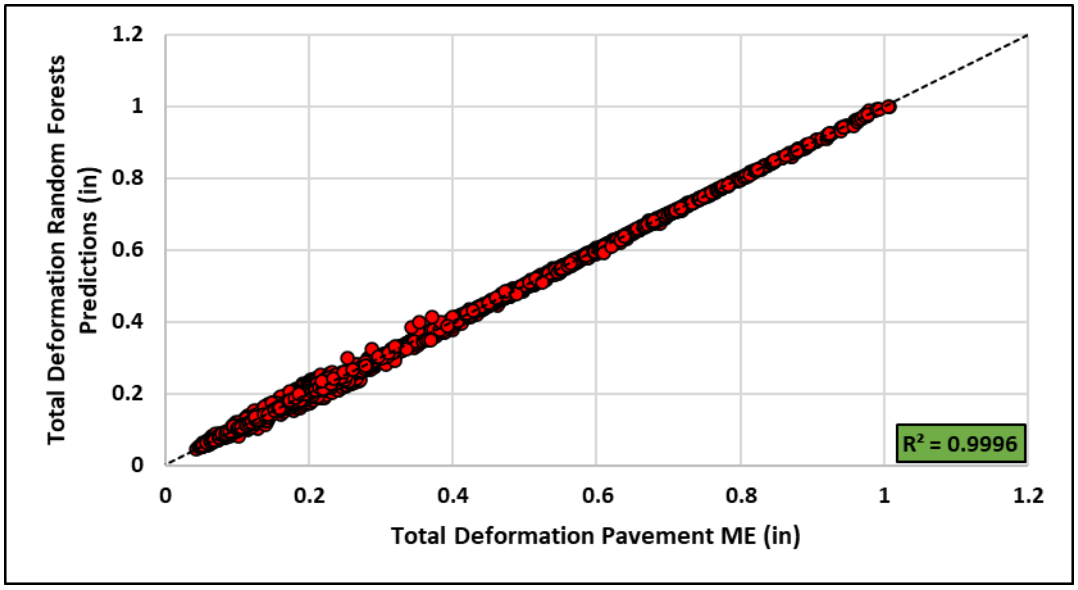

Figure 7.13 Random Forests Predictions vs Pavement ME Total Deformation

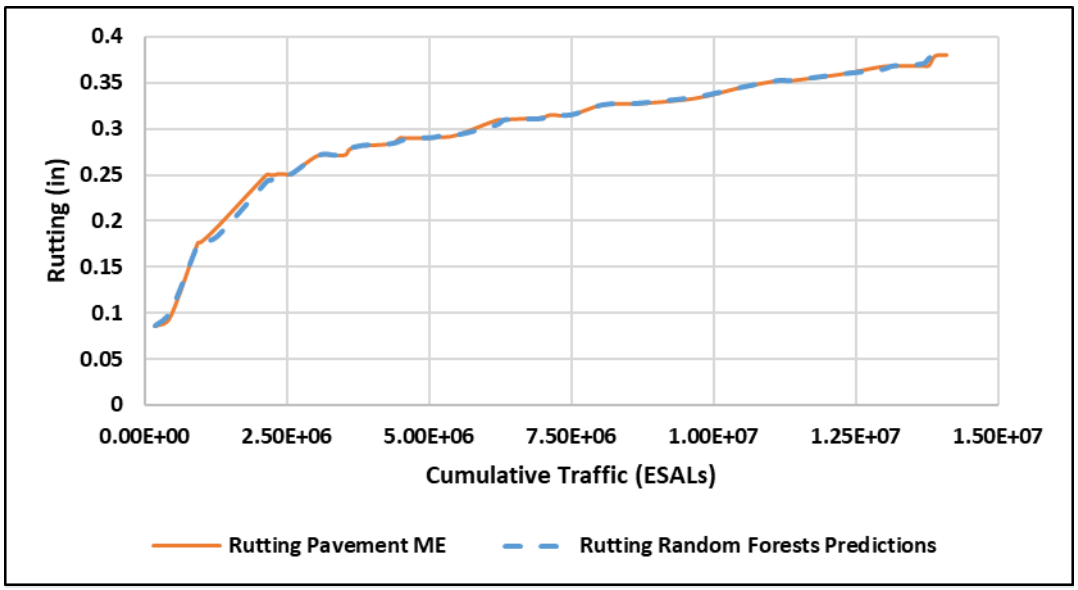

Figure 7.14 Total Deformation vs. ESALs

7.3.3 TSD IRI Prediction Results

The random forests regression model developed to predict IRI of pavement sections had R^2 of 0.9999 and 0.9996 for the training and testing sets, respectively. The decrease in accuracy from the training set to the testing set does not raise concerns since the decrease is small. Figure 7.15 shows the correlation for the testing set between the predicted IRI using the random forests regression model and IRI calculated using the Pavement ME software. This model was also used to create performance decay curves of pavement sections as a function of traffic. An example of this increase of IRI over an increase in cumulative traffic is shown in Figure 7.16. As expected, the IRI increased with traffic. It is also important to note that the decay curve predicted by the model closely mimics the decay curve generated using the Pavement ME data.

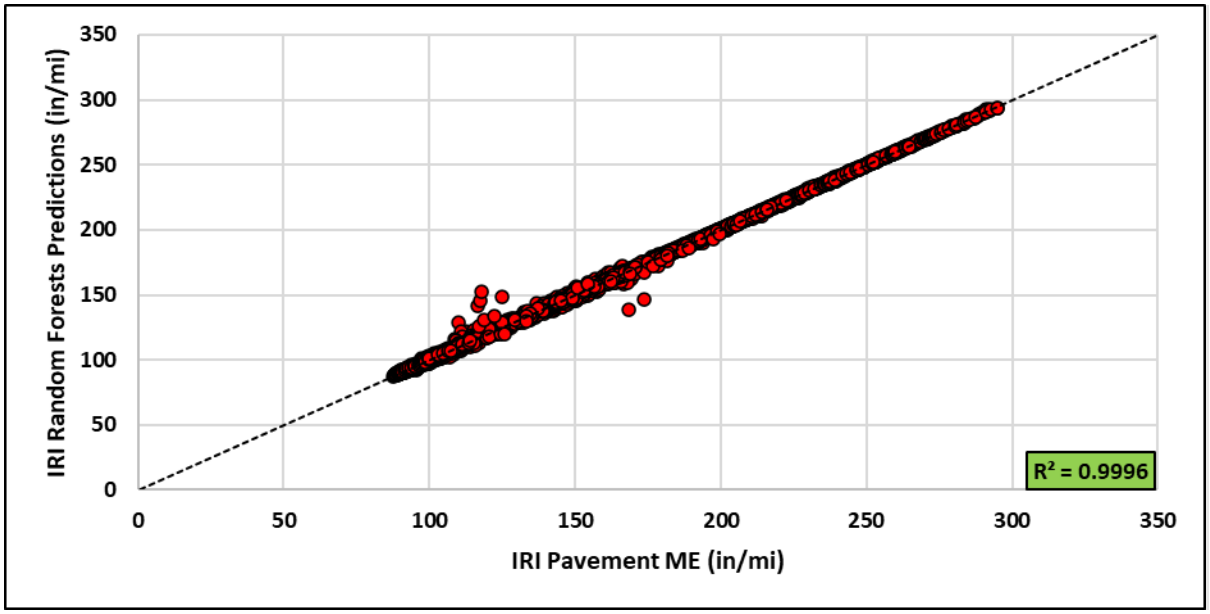

Figure 7.15 Random Forests Predictions vs Pavement ME IRI

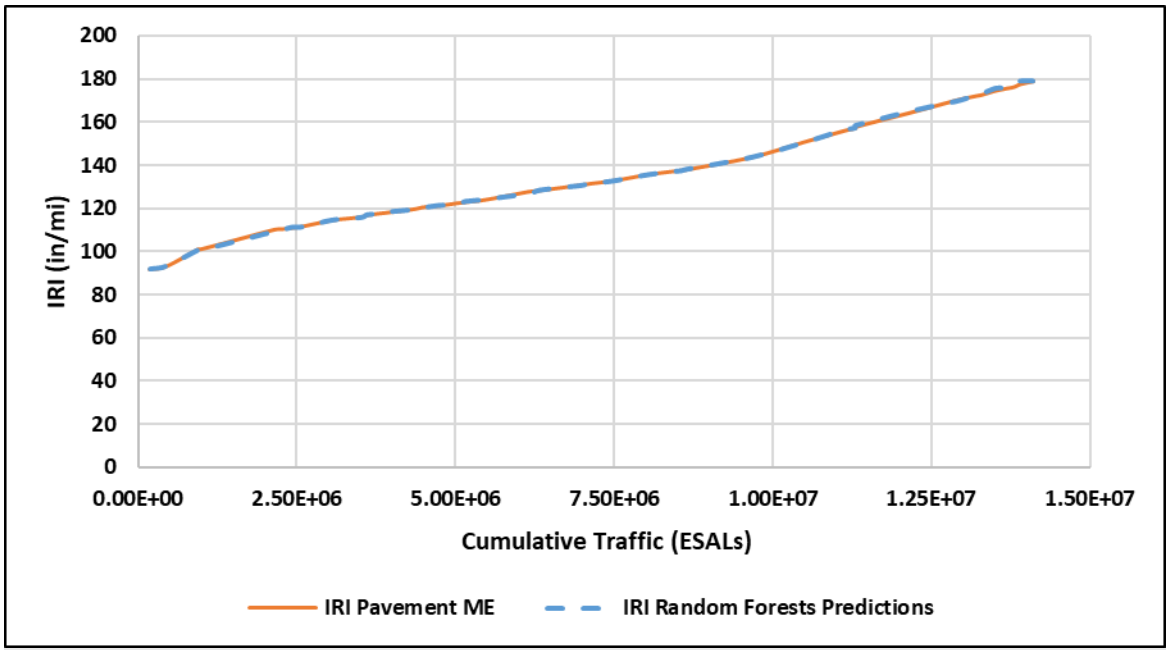

Figure 7.16 IRI Decay Curve

7.3.4 TSD Bottom-Up Fatigue Cracking Prediction Results

The random forests regression model developed to predict bottom-up fatigue cracking of pavement sections had R^2 of 0.9998 and 0.9994 for the training and testing sets, respectively. Figure 7.17 shows the correlation for the testing set between the predicted bottom-up fatigue cracking using the random forests regression model and bottom-up fatigue cracking calculated using the Pavement ME software. As shown in Figure 7.17, not all data points fall directly on the correlation line. However, the R^2 did not seem to be greatly affected by this slight variance. This model was also used to create performance decay curves of pavement sections as a function of traffic. An example of the increase in bottom-up fatigue cracking with cumulative traffic is shown in Figure 7.18. Figure 7.18 depicts the change in percentage of bottom-up fatigue cracking of the pavement section over a 20-year span. In this 20-year span, no treatments were performed on the section. As expected, more cracking occurs with an increase in traffic. It is also important to note that the decay curve predicted by the model closely mimics the decay curve generated using the Pavement ME data.

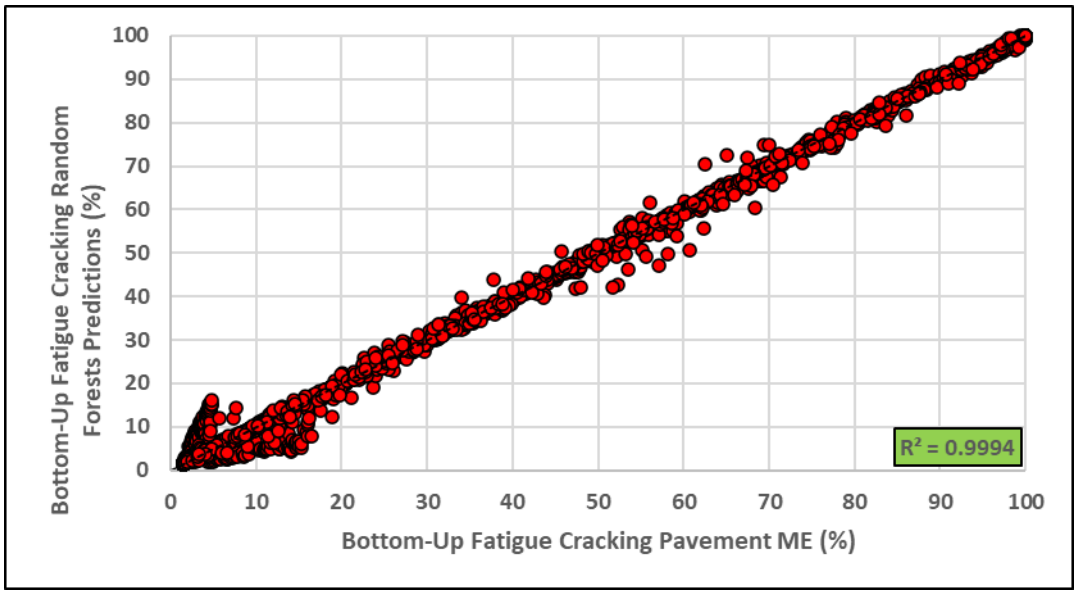

Figure 7.17 Random Forests Predictions vs Pavement ME Bottom-Up Fatigue Cracking

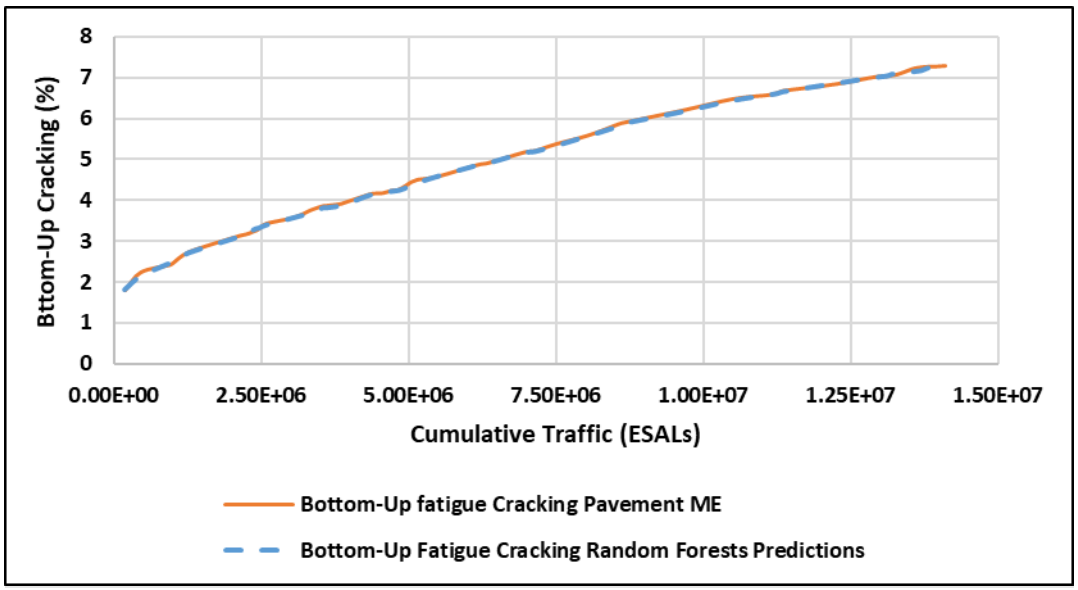

Figure 7.18 Bottom-Up Fatigue Cracking vs. ESALs

7.3.5 TSD Top-Down Fatigue Cracking Prediction Results

The random forests regression model developed to predict top-down fatigue cracking of pavement sections had R^2 of 0.9997 and 0.9979 for the training and testing sets, respectively. This model has the lowest R^2 compared to all other TSD models. Figure 7.19 shows the correlation for the testing set between the predicted top-down fatigue cracking using the random forests regression model and top-down fatigue cracking calculated using the Pavement ME software. As shown in Figure 7.19, there are some outliers near the extremes of values. These outliers are likely due to the limitations of Pavement ME to model top-down fatigue cracking. Figure 7.20 shows an example of the increase in top-down fatigue cracking with cumulative traffic. It is interesting to note that the top-down fatigue cracking starts to propagate at a specific number of ESALs in this example with a shape increase in cracking with traffic.

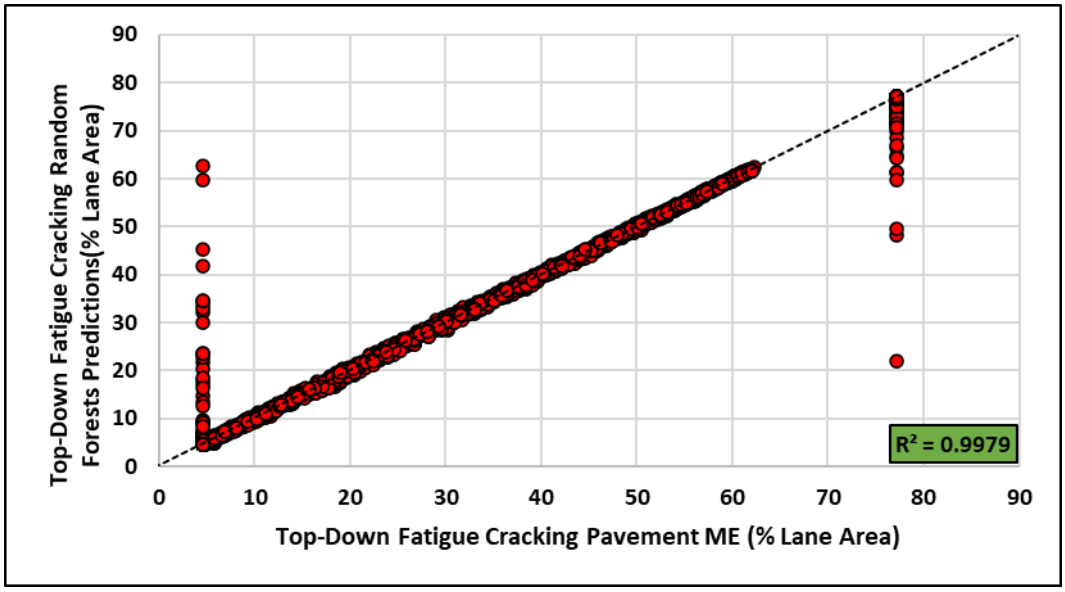

Figure 7.19 Random Forests Predictions vs Pavement ME Top-Down Fatigue Cracking

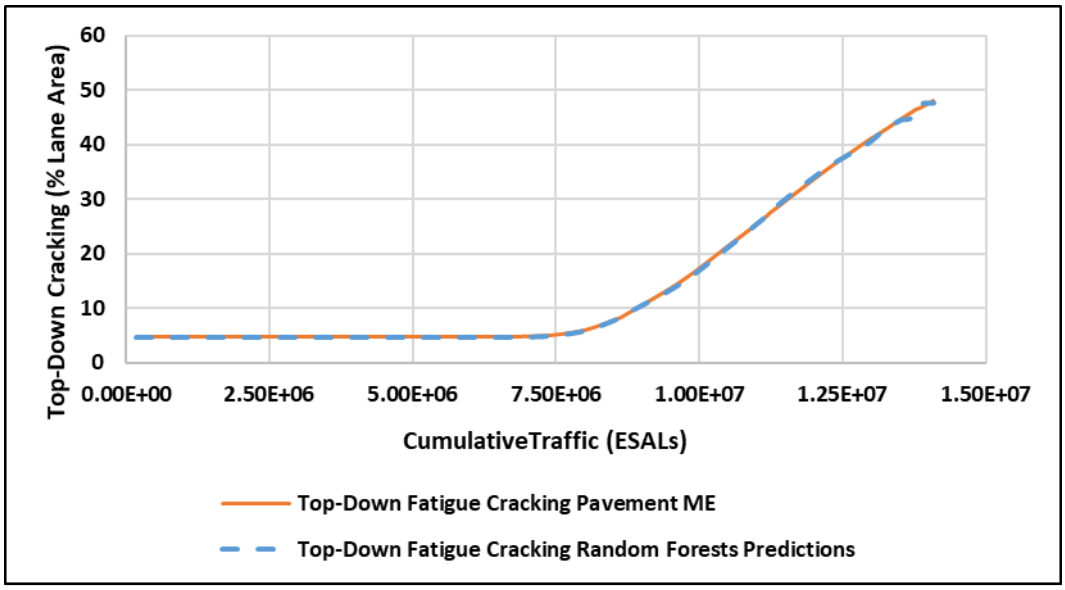

Figure 7.20 Top-Down Fatigue Cracking Decay Curve

7.4 Back-calculating Layer Moduli using Theoretical Deflection Data

The researchers explored the use of random forests regression techniques to backcalculate the layers' modulus of pavement structures as a function of deflection measurements using FWD or

TSD, and layer thickness. First, the team developed models using the deflection data generated from the parametric study. There were 266 data points and all models randomly selected sixty percent of the data points to be used in the training and the remaining data to be used for testing. The models developed based on theoretical FWD data to backcalculate the modulus of different structural layers used deflection measurements at 0, 8, 12, 18, 24, 36 and 60 inches from the center of applied load calculated using the 3D-Move as well as the thicknesses of the HMA and base layers.

The random forests regression model developed to backcalculate the HMA layer modulus had an R^2 of 1 in both the training and testing sets. The correlation between the moduli predicted by the model and the modulus used in the 3D-Move analysis is shown in Figure 7.21. Similar correlations for the predicted models of base layer and subgrade are shown in Figure 7.22 and 7.23, respectively. It should be pointed out that the models used 266 data points in the analysis; however, there were three possible values for the modulus of each layer. The HMA layer had a modulus of 200, 500, or 1000 ksi, the base layer had a modulus of 15, 50, or 200 ksi, while the subgrade had a modulus of 7, 20, and 35 ksi as assigned in the parametric study. The random forests regression model provided a perfect prediction of the modulus of each layer (i.e., three possible values for each layer). Similar results were also obtained using the TSD deflection data ($R^2 = 1$).

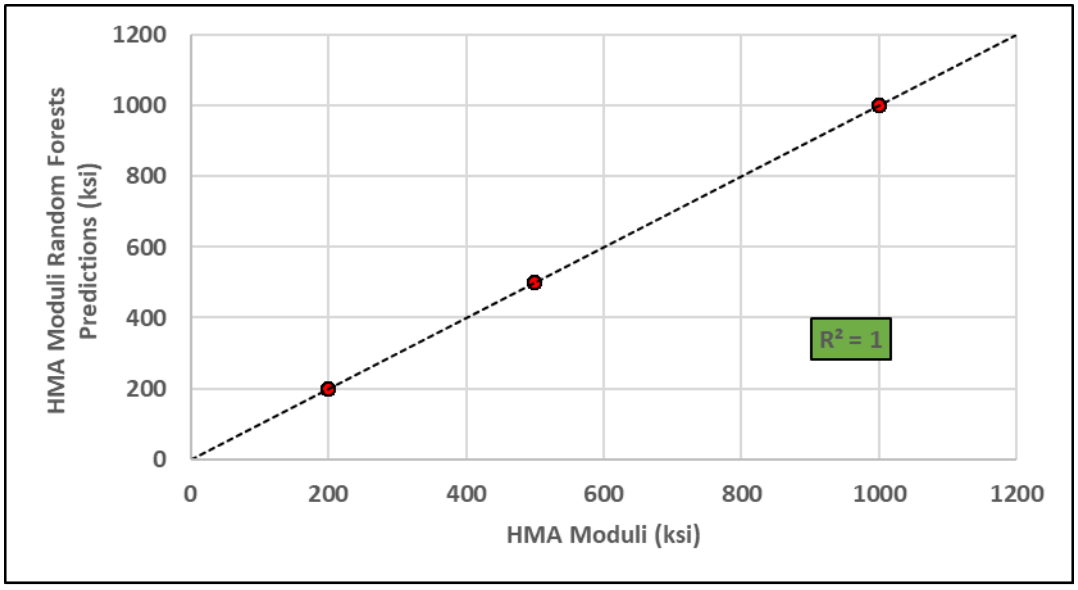

Figure 7.21 Predicted HMA Moduli using the FWD Theoretical Data

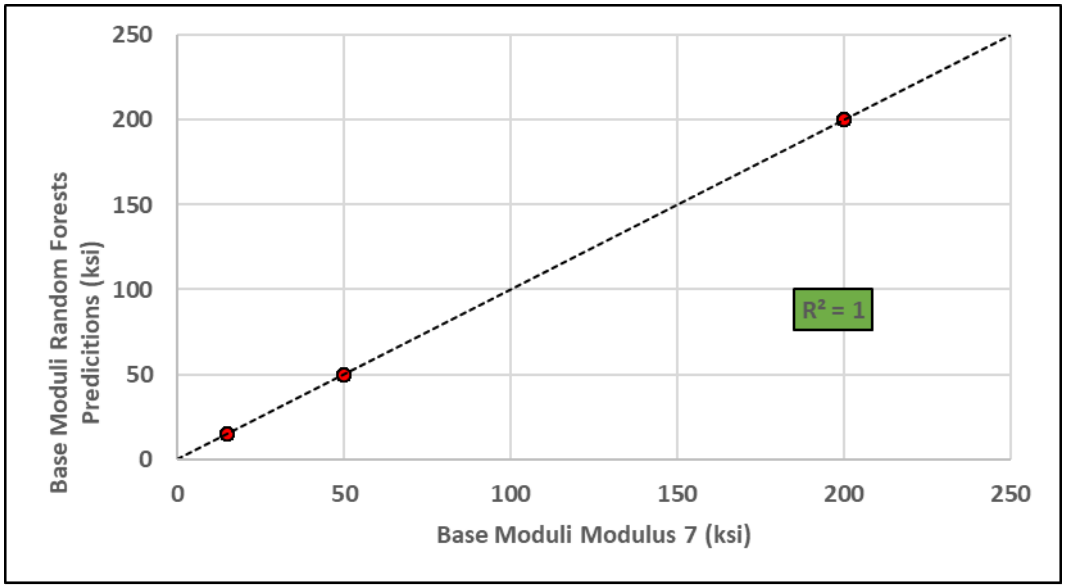

Figure 7.22 Predicted Base Moduli using the FWD Theoretical Data

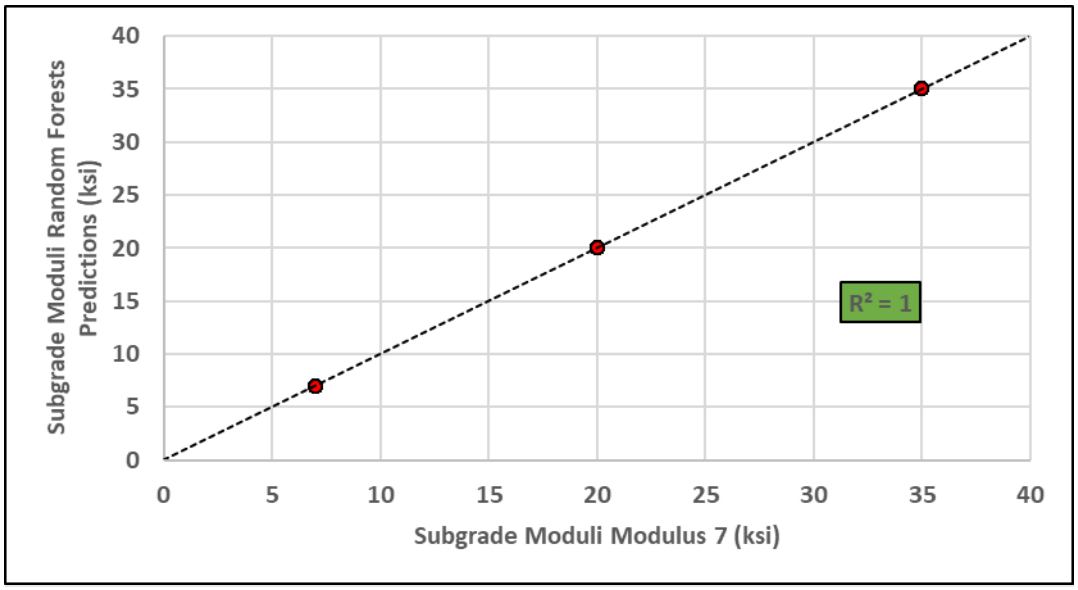

Figure 7.23 Predicted Subgrade Moduli using the FWD Theoretical Data

7.5 Back-calculating Layer Moduli using Combined Field and Theoretical Deflection Data

The research team explored the use of random forests regression techniques to develop models to backcalculate the modulus of pavement layers using both theoretical and field deflection measurements. Modulus 7 was used to analyze the FWD deflection data and backcalculate the modulus of pavement layers for field sections, and these data were added to the ones from the parametric study. The combined dataset had a total number of 766 data points. All models randomly selected sixty percent of the data points to be used in the training and the remaining data to be used for testing.

The random forests regression model developed to backcalculate the HMA layer modulus had R^2 of 0.8541 and 0.5238 in the training and testing sets, respectively. The decrease in accuracy from the training set to the testing set is potentially an indicator of the model overfitting. Figure 7.24 shows the correlation between the predicted HMA layer modulus and modulus from the combined dataset (i.e., parametric study and field sections) and the correlation between predicted HMA layer modulus for the field sections only. The R^2 appears to be more heavily attributed to the theoretical dataset than the field dataset since the R^2 for the field dataset in the testing group is 0.6830 which is higher than the R^2 of 0.5238 for the combined dataset in the testing group.

The random forests regression model developed to back-calculate the base layer modulus had R^2 of 0.9234 and 0.6889 in the training and testing sets, respectively. While the entire combined dataset comprised of over 700 data points, AI models can be improved by introducing more samples into the dataset. Figure 7.25 shows the correlation between the predicted base layer modulus and modulus from the combined dataset (i.e., parametric study and field sections) and the correlation between predicted HMA layer modulus for the field sections only. Also, the decrease in R^2 appears to be evenly affected in the theoretical dataset than the field dataset since the R^2 for the field dataset in the testing group is 0.7050 which is similar to the R^2 of 0.6889 for the combined dataset in the testing group.

The random forests regression model developed to back-calculate the base layer modulus had an R^2 of 0.9945 and 0.9327 in the training and testing sets, respectively. Figure 7.26 shows the results for the subgrade moduli. This model had the highest R^2 of all the models developed for various layers (HMA, base, and subgrade). The results of this section clearly demonstrated the potential of AI in predicting the modulus of pavement layers; however, in order to obtain accurate predictions, a larger data set is required. Therefore, additional research could be

performed to expand the database and improve the accuracy of the models for the HMA and base layers.

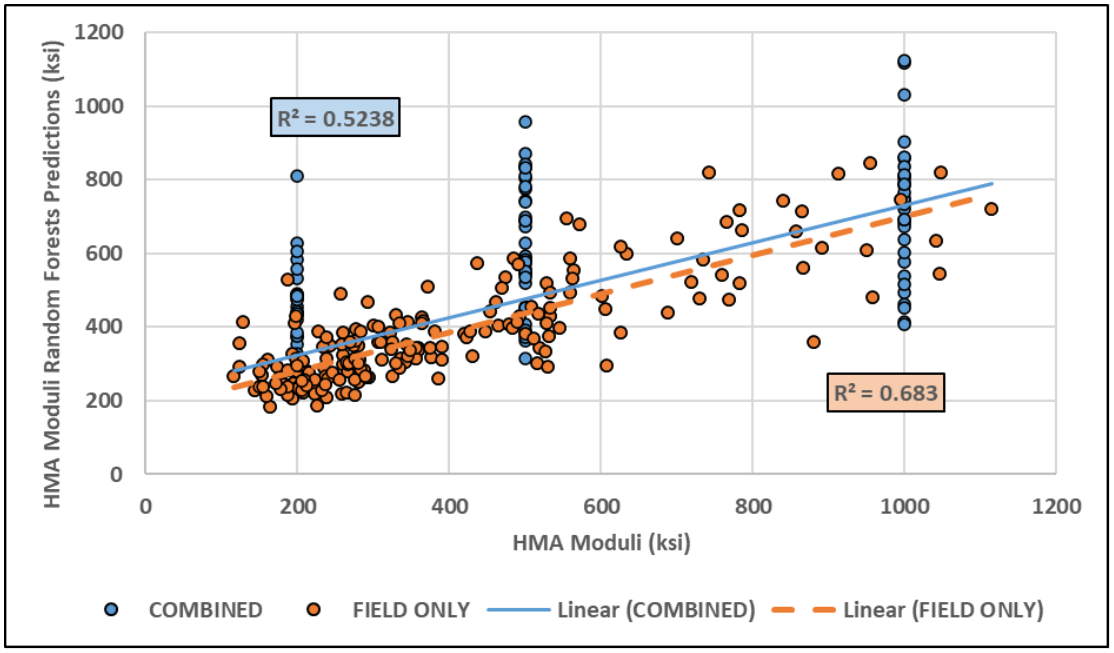

Figure 7.24 Predicted HMA Moduli using the Combined FWD Data

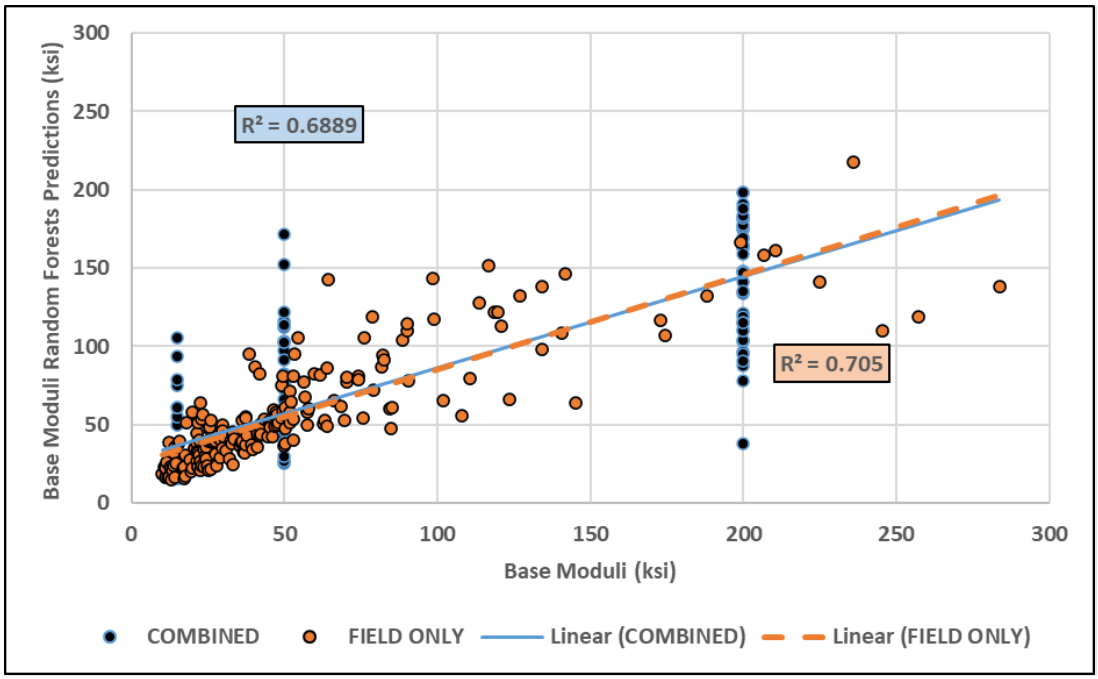

Figure 7.25 Predicted Base Moduli using the Combined FWD Data

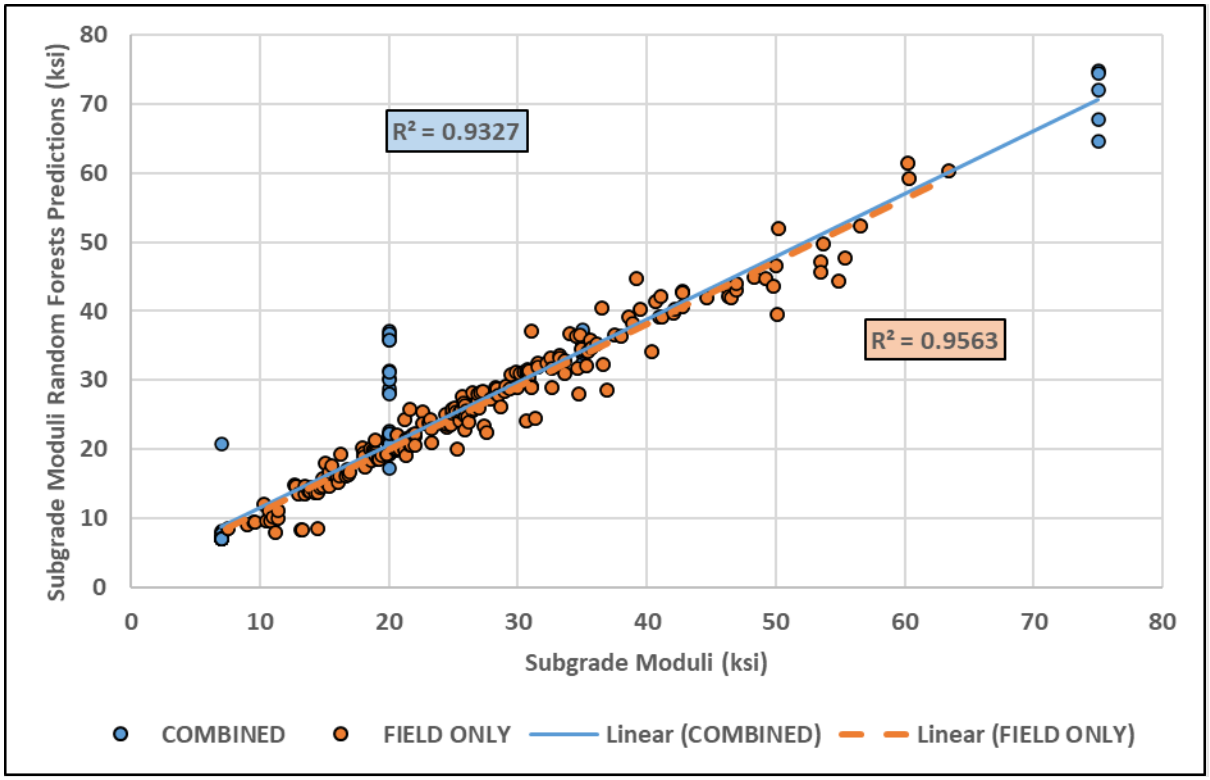

Figure 7.26 Predicted Subgrade Moduli using the Combined FWD Data

8. Summary, Conclusions, and Recommendations

8.1 Summary and Conclusions

Pavement evaluation is critical for determining proper and cost-effective surface treatments and allocation of limited funds and resources to maintain, rehabilitate and reconstruct asphalt pavements. State highway agencies use PMS to make decisions on applying preventive and corrective treatments based on proper assessment of the present status and accurate prediction of pavement future performance. Nondestructive Testing (NDT) is one of most well-recognized tools for evaluating the structural capacity and integrity of highway pavements. The NDT includes FWD and TSD among others. The FWD measures deflection with high accuracy; however, it requires lane closures causing traffic delays and posing safety concerns for both operators and motorists. The drawbacks have limited the use of FWD to project level applications only and paved the way for the introduction of TSD. TSD can measure pavement deflection at traffic speeds, which enables large spatial coverage and can generate continuous deflection profiles rather than only measuring deflection at discrete points.

This study had three phases. In the first phase, the team conducted a theoretical parametric study to simulate the FWD and TSD loading using the 3D Move software. This software is a powerful analytical tool that can accurately simulate pavement responses under complex loading conditions, such as non-uniform tire-pavement contact stress distributions and moving loads. The theoretical parametric study included 243 different pavement structures with different layer thickness and modulus. The 3D-Move software was used to predict the mechanical pavement response including stresses, strains, and deflections. The team used the predicted pavement response to assess the relationship between various DBPs and mechanical response (e.g., horizontal tensile strain on bottom of the asphalt layer and vertical compressive strain at top of subgrade) and layers' moduli. They also examined the correlation between TSD and FWD deflections, obtained using 3D Move. Furthermore, the researchers used the AASHTOWare Pavement ME software to predict the performance of all sections included in the parametric study. The researchers assessed the correlation between FWD and TSD DBPs and predicted stresses at the end of the design life for the examined test sections.

In the second phase of this study, the researchers analyzed the deflection data collected using FWD and TSD for 24 field sections across Idaho. The FWD and TSD deflection data were corrected and normalized to account for the effect of pavement temperature using the same method. In addition, the team considered the deflection data without temperature correction. The team calculated various DBPs and assessed the correlation with pavement layers' moduli and field performance. In addition, they used the deflection data and other information to calculate the Effective Structural Number (SN_{eff}) using three different methods (i.e., deflection value, Rohde's equation, and iterative AASHTO method) and calculated the overlay requirements and remaining service life. Furthermore, the team conducted a comparison between the FWD and TSD results. The comparison included deflection measurements, deflection basin

parameters, and pavement structural conditions (e.g., overlay thickness and remaining service life). In this comparison, the research team considered both corrected and uncorrected FWD and TSD data. Finally, the team developed an Excel-based utility to facilitate the analysis of FWD and TSD deflection data and evaluate the pavement conditions.

In the third phase of this study, with additional resources that were available outside this project, the researchers expanded on the analysis conducted on this study and explored the use of Artificial Intelligence (AI). They developed AI models using the FWD and TSD measurements to predict pavement performance over time as a function of deflection data and traffic level for the parametric study. Furthermore, the team developed preliminary models to estimate pavement layers' moduli as a function of layer thickness and FWD deflection data collected in the field.

The main findings from each stage of this study can be summarized below.

Main Findings of the First Phase

- The 3D-Move software was able to reasonably model the pavement response to FWD and TSD loading. The 3D-Move software was able to simulate the deflection basin of FWD and TSD.
- There was a strong correlation between the FWD deflection of the last sensor (D60) and subgrade modulus which is consistent with the literature.
- The results demonstrated that there was a good correlation between the pavement responses and deflection parameters. Both SCI and AUPP were found to be highly correlated with the tensile strain (ε_t) at the bottom of the asphalt layer. In addition, there was a strong correlation between the vertical compressive strain (ε_v) at top of subgrade and $SN_{eff.}$ The vertical compressive strain (ε_v) at the top of subgrade is a parameter that is used to predict the rutting life of flexible pavements, while the tensile strain (ε_t) at the bottom of the asphalt layer is used to determine the allowable number of load repetitions before cracking for flexible pavement design. These relationships can be used as a simple approach to estimate the pavement response without the need for complicated analysis methods.
- The results demonstrated that there are good correlations between the Structural Condition Index (SCI) and maximum deflection (D_0) from the FWD data with the terminal International Roughness Index (IRI) and rutting calculated from the AASHTOWare. Furthermore, there was a trend between bottom-up cracking and both SCI and D_0. However, there was no correlation with these indices (i.e., SCI and D_0) and top-down cracking.
- Both SCI_8 and SCI_{12} calculated from the TSD data were found to correlate with the tensile strain (ε_t) at the bottom of asphalt layer. In addition, higher vertical compressive strain (ε_v) at top of subgrade was associated with lower SN_{eff} and normalized comprehensive area ratio (CAr') calculated from the TSD data.

- There was a good correlation between the Structural Condition Index (SCI) from the TSD data and the terminal International Roughness Index (IRI) and a fair correlation with rutting. In addition, there was a trend between bottom-up cracking and both TSD SCI and D_0; however, and similar to FWD, there was no correlation with these indices (i.e., SCI and D_0) and top-down cracking.

- There was a strong correlation between the FWD and TSD deflection measurements with an R^2 of 0.88. However, the TSD deflection values appeared to be slightly higher than those of FWD. Furthermore, the results of the parametric study indicated a strong correlation between the maximum deflection (D_o) of FWD and TSD, with an R^2 of 0.80. Meanwhile, there was a trend between the deflection of the last sensor of the FWD and the corresponding sensor of the TSD.

- The deflection basin parameters (DBPs) such as SCI, MLI, LLI calculated from the FWD data were found to correlate well with the ones calculated from the TSD data.

Main Findings of the Second Phase

- The researchers assessed the correlation between various DBPs and the pavement layer moduli (calculated using Modulus 6 software). The results demonstrated that that there is a fair correlation between the deflection of the last sensor (D_{60} or W_7) of FWD and subgrade modulus. Also, there was a trend between SCI and the modulus of asphalt layer. The modulus of asphalt layer increased with the decrease of SCI. Other DBPs didn't provide strong correlations with the pavement layer moduli.

- The research team investigated the correlation between the field performance indicators such as rutting, IRI, and cracking from TAMS with the FWD DBPs. Some pavement sections with lower deflection values showed higher rutting measurements, while others showed lower rutting measurements. A similar trend was observed for the Overall Condition Index (OCI); however, a better correlation was observed between the deflection values and IRI performance, where higher deflection values were associated with poor IRI performance. The results also demonstrated that some sections with higher IRI (poor performance) had relatively higher deflection parameters (e.g., D_0, BLI, MLI), meanwhile there was no consistent trend to make definitive conclusions. It should be noted that surface treatments could improve the overall performance (e.g., improve IRI, rutting, cracking) without improving the structural capacity of the pavements. Pavements with higher deflections (i.e., lower structural capacity) could exhibit less surface distresses due to the surface treatments. This could have affected the correlation between the FWD DBPs and surface distresses.

- The three methods used to calculate the SN_{eff} using the FWD and TSD deflection data provided comparable results; however, the iterative AASHTO method was the most conservative and resulted in lower SN_{eff} compared to other methods for most sections. While the deflection value method was the least conservative and provided higher SN_{eff} compared to the iterative AASHTO method and Rohde's equation for most of the sections.

- The required overlay thickness calculations demonstrated that some sections don't require overlays; however, other sections showed that an overlay is required to accommodate future traffic.

- The TSD trailer is equipped with the capability of measuring pavement surface conditions including cracking (e.g., alligator, longitudinal, transverse) and rutting. The research team investigated the correlation between the surface conditions and TSD DBPs. The results showed that measured distresses (e.g., cracking and rutting) correlated well with the TSD maximum deflection (D_o) measurements for some sections. However, there were some inconsistencies between the TSD maximum deflection (D_o) measurements and pavement distresses in other sections. Similar to FWD, the use of surface treatments could improve the surface conditions while the pavements still exhibit higher TSD deflection (i.e., lower structural capacity).

- The researchers compared the FWD and TSD deflection data before and after temperature correction. The results demonstrated that there was a strong correlation between the FWD and TSD deflections before and after temperature correction. However, the correlation between FWD and TSD based on uncorrected deflection data was better than the one based on temperature-corrected deflection data. In addition, the FWD and TSD deflection measurements were closer to the equality line. Also, the TSD deflections were slightly higher than the FWD. However, an analysis of variance (ANOVA) shows that the difference between the TSD and FWD deflections is statistically not significant. Furthermore, there was a good correlation between the maximum deflection (Do) from both FWD and TSD; however, the deflection data from both FWD and TSD at 60 inches didn't provide good correlation.

- The results of the comparison between the FWD and TSD DBPs demonstrated that here was a fair correlation for LLI and MLI (R^2 of 0.60 and 0.55, respectively) for the FWD and TSD data.

- The researchers compared SN_{eff} calculated using the FWD and TSD. The results demonstrated that there is a strong correlation between FWD SN_{eff} and TSD SN_{eff} with R^2 of 0.91 for the uncorrected deflection data and R^2 of 0.87 for the corrected deflection data. In addition, the SN_{eff} values were close to the quality line with higher R^2 using the uncorrected deflection data.

- The overlay requirements showed that there was good agreement between the two data sets (i.e., FWD and TSD); however, the FWD demonstrated that the eight sections don't need an overlay while the TSD demonstrated that only six of those eight sections would need an overlay. Furthermore, the remaining service life of the examined test sections exhibited a good agreement between both methods (i.e., FWD and TSD); however, there are two sections where there were conflicting calculations in assessing the remaining service life.

- The researchers developed a Microsoft Excel-based tool to streamline the processing of FWD and TSD data. This tool can handle up to 500 deflection measurements in one run and provides

outputs such as the calculation of DBPs, a rating of the pavement conditions based on the DBPs values, the effective and required structural numbers, and the required overlay thickness.

Main Findings of the Third Phase

- The researchers developed models to predict the pavement performance calculated using AASHTOWare Pavement ME as a function of FWD and TSD deflection measurements and traffic level. The results demonstrated a strong correlation between the predicted and calculated performance indicators including IRI, rutting of AC, total rutting, bottom-up cracking, and top-down cracking. Furthermore, AI models were developed to predict layers' moduli as a function of layer thickness and deflection data. The model developed to predict the subgrade moduli provided the highest R^2 of all the models developed for various layers (HMA, base, and subgrade). The results clearly indicate the AI is a very powerful technique to model pavement performance and response.

8.2 Recommendations

Based on the investigation and result analysis in this study, following recommendations can be made for future FWD and TSD research:

- Based on the comprehensive analysis of the three different phases of this study, and the good correlations between the FWD and TSD, the TSD can be effectively used at the network level to identify hot spots or sections with potential structural deficiency for further FWD analysis at the project level. This can optimize the time and resources of employing the FWD crew and reduce traffic interruption and improve the safety of FWD crew and motorists.

- The Artificial Intelligence (AI) models were found to be very powerful and promising tools to predict pavement performance over time. These models produce performance decay curves for flexible pavements based on the FWD or TSD deflection measurements and traffic level. These models have distinct advantages in data analysis and processing over traditional models, leveraging large datasets for greater accuracy and effectiveness. The researchers believe that this is the future in various pavement engineering applications, including TSD data and pavement performance analysis. The researchers recommend further research to populate much larger performance datasets that cover the environmental conditions of all six districts of the state. The performance data generated in this study from 243 sections were based on environmental conditions of one location (i.e., Boise). Also, the AI models should incorporate more test sections with performance data to validate the developed models and gain more confidence before implementation.

- The developed Microsoft Excel-based tool can be used to simplify and standardize the FWD and TSD analysis and eliminate errors and mistakes associated with data processing. This software can be further developed as standalone software with more capabilities to generate performance decay curves at the network level.
- The researchers believe that there is a need for future testing to develop and validate methods to correct the TSD deflection data to account for the effect of pavement temperatures. At the time, the researchers utilized the methods used for the FWD. In addition, the effect of TSD speed and pavement surface irregularities on TSD deflection data should be carefully examined. Furthermore, further research should evaluate the effect of horizontal and vertical curves as well as TSD tire properties and configurations on the TSD measurements.

9. Cited Works

Alavi, Sirous, Jeffrey F. Lecates, and Michael P. Tavares. 2008. *Falling Weight Deflectometer Usage.* National cooperative Highway Research Program (NCHRP) Synthesis 381.

American Association of State Highway and Transportation Officials (AASHTO) resource. 2020. *FWD Calibration Centers with AASHTO-Certified Operators*. Accessed November 6, 2020. http://www.aashtoresource.org/fwd/certified-operators.

American Association of State Highway and Transportation Officials (AASHTO) resource. 2020. *The Importance of FWD Calibration*. Accessed November 7, 2020. http://www.aashtoresource.org/university/newsletters/newsletters/2016/08/04/the-importance-of-fwd-calibration

American Association of State Highway and Transportation Officials (AASHTO). 1993. *AASHTO Guide for Design of Pavement Structures.* Accessed November 7, 2020. https://habib00ugm.files.wordpress.com/2010/05/aashto1993.pdf

American Association of State Highway and Transportation Officials (AASHTO). 1990. *AASHTO Guidelines for Pavement Management Systems*.

American Association of State Highway and Transportation Officials (AASHTO). 2020. *Standard Practice for Calibrating the Load Cell and Deflection Sensors for a Falling Weight Deflectometer*. AASHTO R 32.

American Association of State Highway and Transportation Officials (AASHTO). 2011. *Standard Practice for Calibrating the Reference Load Cell Used for Reference Calibrations for a Falling Weight Deflectometer*. AASHTO R 33.

American Society for Testing and Materials (ASTM). 2015. *Standard Test Method for Deflections with a Falling-Weight-Type Impulse Load Device*. ASTM D4694 – 09.

Bayomy, Fouad, Mostafa, Abo Hashema. 2000. *WINFLEX 2000 Mechanistic-Emperical Overly Design System for Flexible Pavement User Guide.* NIATT Report N01-13, University of Idaho, Moscow, ID.

Březina, Ilja, Josef Stryk, and Jiří Grošek. 2017. "Using Traffic Speed Deflectometer to Measure Deflections and Evaluate Bearing Capacity of Asphalt Pavements at Network Level." Presented at 2017 IOP Conference Series: Materials Science and Engineering, Prague, Czech Republic.

Bryce, James, Samer Katicha, Gerardo Flintsch, and Brian K. Diefenderfer. 2013. "Developing a Network-Level Structural Capacity Index for Composite Pavements." *Journal of Infrastructure Systems*, 23(1): 04016020.

Bush III, Albert J., and Ross A. Bentsen. 1990. “Nondestructive Evaluation Equipment for Airfield Pavements.” *Transportation Research Record: Journal of the Transportation Research Board*, 1260: 192-215.

Cauwelaert, Frans J. Van, Don R. Alexander, Thomas D. White, and Walter R. Barker. 1989. “Multilayer Elastic Program for Backcalculating Layer Moduli in Pavement Evaluation.” American Society for Testing and Materials (ASTM). Nondestructive Testing of Pavements and Backcalculation of Moduli, ASTM STP 1026.

Chatti, Karim, M. Emin Kutay, Nizar Lajnef, Imen Zaabar, Sudhir Varma, and Hyung Suk Lee. 2017. *Enhanced Analysis of Falling Weight Deflectometer Data for Use with Mechanistic-Empirical Flexible Pavement Design and Analysis and Recommendations for Improvements to Falling Weight Deflectometers*. Federal Highway Administration (FHWA). FHWA-HRT-15-063.

Chen, Dar-Hao, John Bilyeu, Huang-Hsiung Lin, and Mike Murphy. 1999. “Temperature Correction on Falling Weight Deflectometer Measurements.” *Transportation Research Record: Journal of the Transportation Research Board*, 1716, 30-39.

Chowdhury, T. 1998. *Bayesian Regression Methodology for Network Level Pavement Project Rating*. Master’s Thesis, Department of Civil Engineering, Kansas State University, Manhattan.

Choubane, Bouzid, Salil Gokhale, and Abdenour Nazef. 2003. *Assessing the Precision of Falling Weight Deflectometers for Field Measurements*. Report No. FL/DOT/SMO/03-468. Florida Department of Transportation.

Chowdhury, Tanveer, and Mustaque Hossain. 1999. Use of Falling Weight Deflectometer Data for Assessing Pavement Structural Evaluation Values. Report No. K-TRAN: KSU-96-4, Kansas State University, Manhattan, KS.

Eagleson, Bary, Scott Heisey, W. Ronald Hudson, Alvin H. Meyer, and Kenneth H. Stokoe. 1983. *Comparison of The Falling Weight Deflectometer and the Dynaflect for Pavement Evaluation*. Summary report 256-1(s), Center for Transportation Research, Bureau of Engineering Research, The University of Texas at Austin, Austin, Texas.

Elbagalati, Omar, Mostafa A. Elseifi, Kevin Gaspard, and Zhongjie Zhang. 2016. “Development of The Pavement Structural Health Index Based on Falling Weight Deflectometer Testing.” *International Journal of Pavement Engineering*, 19(1), 1–8

Elkins, Gary E., Gonzalo R. Rada, Jonathan L. Groeger, and Beth Visintine. 2013. *Pavement Remaining Service Interval Implementation Guidelines*. Report No. FHWA-HRT-13-050. AMEC Environment and Infrastructure, Beltsville, MD.

Elkins, Gary E., Travis M. Thompson, Jonathan L. Groeger, Beth Visintine, and Gonzalo R. Rada. 2013. *Reformulated Pavement Remaining Service Life Framework*. Report No. FHWA-HRT-13-038. AMEC Foster Wheeler Environment & Infrastructure, Inc. Beltsville, MD

Elseifi, Mostafa A., and Zia Uddin Ahmed Zihan. 2018. Assessment of the Traffic Speed Deflectometer in Louisiana for Pavement Structural Evaluation. Report No. FHWA/LA.18/590. Louisiana Transportation Research Center (LTRC), Louisiana State University, Baton Rouge, Louisiana.

Elseifi, Mostafa A., Zia Uddin Ahmed Zihan, and Patrick Icenogle. 2019. A Mechanistic Approach to Utilize Traffic Speed Deflectometer (TSD) Measurements into Backcalculation Analysis. Report No. FHWA/LA.17/612. Louisiana Transportation Research Center (LTRC), Louisiana State University, Baton Rouge, Louisiana.

Federal Highway Administration (FHWA). 2000. *LTPP Manual for Falling Weight Deflectometer Measurements Operational Field Guidelines.* FHWA-LTPP Technical Support Services.

Ferne, Brian W., Peter Langdale, N. Round, and R. Fairclough. 2009. "Development of a Calibration Procedure for the U.K. Highways Agency Traffic-Speed Deflectometer." *Transportation Research Record: Journal of the Transportation Research Board*, 2093 (1), 111-117.

Flintsch, Gerardo W., Brian Ferne, Brian Diefenderfer, Samer Katicha, James Bryce, and Simon Nell. 2012. "Evaluation of Traffic-Speed Deflectometers." *Transportation Research Record: Journal of the Transportation Research Board*, 2304:37-46.

Flora, William Fredrick, Ghim Ping (Raymond) Ong, and Kumares C. Sinha. 2010. Development of a Structural Index as an Integral Part of the Overall Pavement Quality in the INDOT PMS. Federal Highway Administration (FHWA). FHWA/IN/JTRP-2010/11, Joint Transportation Research Program.

Gedafa, Daba Shabara. 2008. *Estimation of Remaining Service Life of Flexible Pavements from Surface Deflections*. PhD Dissertation, Kansas State University, Manhattan, Kansas.

Gedafa, Daba S., Mustaque Hossain, Richard Miller, and Thomas Van. 2010. "Estimation of Remaining Service Life of Flexible Pavements from Surface Deflections." Journal of Transportation Engineering, 136:4.

Graczyk, Miroslaw, Adam Zofka, Jacek Sudyka, and Jozef Rafa. 2014. "Analytical Solution of Pavement Deflections and Its Application to The TSD Measurements." Presented at 26th Australian Pavement Research Board (ARRB) Conference, Sydney, New South Wales, Australia.

Greenwood Engineering. 2018. Greenwood TSD: *Project Level Assessment on The Whole Network*. Greenwood Engineering A/S, Denmark. Accessed November 7, 2020. https://greenwood.dk/wp-content/uploads/2020/05/Brochure-TSD-2018-01.pdf

Hildebrand, Gregers, Soren Rasmussen, and R. Andre´s. 1999. Development of a Laser-Based High Speed Deflectograph. Report 97, Danish Pavement Institute, Roskilde, Denmark.

Horak, Emile, and Stephen Emery. 2006. *Falling Weight Deflectometer Bowl Parameters as Analysis Tool for Pavement Structural Evaluations*. Presented at 22nd Australian Pavement Research Board (ARRB) Conference, Canberra, Australia.

Hossain, A. S. M. Mustaque, and John P. Zaniewski. 1991. "Characterization of Falling Weight Deflectometer Deflection Basin." *Transportation Research Record: Journal of the Transportation Research Board*, 1293, 1-11.

Idaho Transportation Department. 2017. *Idaho Transportation System Pavement Performance Report.* Accessed November 7, 2020. *https://apps.itd.idaho.gov/apps/pm/ITD_2017_Performance_Report.pdf*

Irwin, Lynne H. 1983. User's guide to Modcomp2. Version 2.1. Local Pavements Program, Cornell University, Ithaca, NY.

Irwin, Lynne H., David P. Orr, and Daniel Atkins. 2017. *Falling Weight Deflectometer Calibration Center and Operational Improvements: Redevelopment of the Calibration Protocol and Equipment*. Report No. FHWA-HRT-07-040. Cornell University Local Roads Program, Ithaca, NY

Jameson, G. W. 1993. *Development of Procedures to Predict Structural Number and Subgrade Strength from Falling-Weight Deflectometer Deflections*. ARRB TR, Vermont South, Victoria

Katicha, Samer W., Gerardo W. Flintsch, Brian Ferne, and James Bryce. 2013. "Limits of Agreement Method for Comparing TSD and FWD Measurements." *International Journal of Pavement Engineering*, 15(6), 532-541.

Kannemeyer, Louw, Werner Lategan, and Andrew Mckellar. 2014. "Verification of Traffic Speed Deflectometer measurements using Instrumented Pavements in South Africa." Presented at National Pavement Evaluation Conference 2014, Blacksburg, VA.

Kassem, Emad, Fouad M.S. Bayomy, Christopher Williams, Eric Saasita, Simpson Lamichane, and Dio D. Permadi. 2020. *Development of Pavement Temperature Prediction Model.* Report No. FHWA-ID-20-279, University of Idaho, Moscow, ID.

Katicha, Samer W., Shivesh Shrestha, Gerardo W. Flintsch, and Brian K. Diefenderfer. 2020. *Network Level Pavement Structural Testing with the Traffic Speed Deflectometer*. Report No. VTRC 21-R4, Virginia Transportation Research Council (VTRC), Charlottesville, VA.

Kim, Richard, and Heemun Park. 2002. *Use of FWD Multi-Load Data for Pavement Strength Estimation*. Report No. FHWA/NC/2002-006, North Carolina State University, Raleigh, North Carolina.

Kim, Y. Richard, Bradley O. Hibbs, And Yung-Chien Lee. 1995. "Temperature Correction of Deflections and Backcalculated Asphalt Concrete Moduli." *Transportation Research Record: Journal of the Transportation Research Board*, 1473, 55-62.

Kim, Richard, Ranji Ranjithan, J. D. Troxler, and Bin Xu. 2000. Assessing Pavement Layer Condition Using Deflection Data. National cooperative Highway Research Program (NCHRP) 10-48, North Carolina State University, Raleigh, North Carolina.

Krarup, Jorgen, Soren Rasmussen, Lisbeth Aagaard, and Poul G Hjorth. 2006. "Output from The Greenwood Traffic Speed Deflectometer." Presented at 22nd Australian Pavement Research Board (ARRB) Conference, Canberra, Australia.

Lee, Sang Won, Joe P. Mahoney, and Newton C. Jackson. 1988. "Verification of Backcalculation of Pavement Moduli." *Transportation Research Record: Journal of the Transportation Research Board*, 1196, 85-94.

Lorenzetti, Tommaso Paoletti. 2013. *Characterization of Pavement Bearing Capacity by Traffic Speed Deflectometer*. Master's Thesis, University of Pisa, Italy.

Lukanen, Erland O., Richard Stubstad, and Robert Briggs. 2000. *Temperature Predictions and Adjustment Factors for Asphalt Pavement*. Report No. FHWA-RD-98-085. Braun Intertec Corporation, Minneapolis, MN.

Mikels, Natalie. 2023. *Applications of Artificial Intelligence in Pavement Engineering*. MS Thesis, University of Idaho, Moscow, ID

Mishra, Deb, and Md. Fazle Rabbi. 2017. "Use of Visual Distress Survey and Deflection Data for Rehabilitation Decisions in Idaho." Presented at 57th Idaho Asphalt Conference, Moscow, Idaho.

Muller, Wayne B., and Jon Roberts. 2012. "Revised Approach to Assessing Traffic Speed Deflectometer Data and Field Validation of Deflection Bowl Predictions." International Journal of Pavement Engineering, 14:4, 388–402.

Nasimifar, Mahdi, Sarah Chaudhari, Senthilmurugan Thyagarajan, and Nadarajah Sivaneswaran. 2018. "Temperature Adjustment of Surface Curvature Index Computed from Traffic Speed Deflectometer Measurements." International Journal of Pavement Engineering. 21(11), 1408–1418

Nasimifar, Mahdi, Senthilmurugan Thyagarajan, Sarah Chaudhari, and Nadarajah Sivaneswaran. 2019. "Pavement Structural Capacity from Traffic Speed Deflectometer for Network Level Pavement

Management System Application." Presented at 98th Transportation Research Board (TRB) Annual Meeting, Washington, D.C.

National cooperative Highway Research Program (NCHRP). 1979. Pavement Management System Development. NCHRP 215, National Research Council, Washington, D.C.

Park, Hee Mun, Richard Kim, and Sunwoo Park. 2002. "Temperature Correction of Multiload-Level Falling Weight Deflectometer Deflections." *Transportation Research Record: Journal of the Transportation Research Board*, 1806, 3-8.

Paterson, W.D.O. 1987. *Pavement Deterioration and Maintenance Effects*. Models for Planning and Management. Highway Design and Maintenance Standards Series, The Johns Hopkins University Press, Baltimore and London.

Pavement Interactive. 2021. "Nondestructive Pavement Evaluation Tools." Accessed March 22, 2021. https://pavementinteractive.org/nondestructive-pavement-evaluation-tools/

Pedersen, Louis. 2013. Viscoelastic Modelling of Pavement Deflections for use with the Traffic Speed Deflectometer. PhD Dissertation, Technical University of Denmark, Lyngby, Denmark.

Rabbi, Md. Fazle, and Debakanta Mishra. 2019. "Using FWD Deflection Basin Parameters for Network-Level Assessment of Flexible Pavements." *International Journal of Pavement Engineering,* 22(2), 147–161

Rada, Gonzalo R., Soheil Nazarian, Beth A. Visintine, Raj Siddharthan, and Senthil Thyagarajan. 2016. *Pavement Structural Evaluation at the Network Level*. Report No. FHWA-HRT-15-074. AMEC Foster Wheeler Environment & Infrastructure, Inc. Beltsville, MD

Rada, Gonzalo, Soheil Nazarian, Jerry Daleiden, and Tom Yu. 2012. "Moving Pavement Deflection Testing Devices: State-Of the-Art Technology and Best Uses." Presented at 8th International Conference on Managing Pavement Assets, Santiago, Chile.

Rada, Gonzalo R, Soheil Nazarian, Raj V. Siddharthan, and Nadarajah Sivaneswaran. 2015. "Use of High-Speed Deflection Devices in Network-Level PMS Applications: Are We Ready?" Presented at 9th International Conference on Managing Pavement Assets (ICMPA9), Washington, D.C.

Rohde, Gustav T., and Tom Scullion. 1990*. MODULUS 4.0: Expansion and Validation of the MODULUS Backcalculation System*. Report No. FHWA/TX - 91/1123-3, Texas Transportation Institute, College Station, Texas.

Rohde, Gustav T. 1994. "Determining Pavement Structural Number from FWD Testing." *Transportation Research Record: Journal of the Transportation Research Board*, 1448, 61-68.

Rasmussen, Soren, Lisbeth Aagaard, Susanne Baltzer, and Jorgen Krarup. 2008. “A comparison of two years of network level measurements with the Traffic Speed Deflectometer.” Presented at Transport Research Arena Europe 2008, Ljubljana, Slovenia.

Romanoschi, Stefan, and John B. Metcalf. 1999. “Simple Approach to Estimation of Pavement Structural Capacity.” Transportation Research Record: *Journal of the Transportation Research Board*, 1652, 198-205.

Schmalzer, Peter. 2006. *Long-Term Pavement Performance Program Manual for Falling Weight Deflectometer Measurements*. Report No. FHWA-HRT-06-132. AMEC Environment and Infrastructure, Beltsville, MD.

Scullion, Tom. 1988. Incorporating a Structural Strength Index into the Texas Pavement Evaluation System. Report No. FHWA/TX-88/409-3F, Texas Transportation Institute, The Texas A&M University System, College Station, Texas

Shahin, M.Y. 2005. *Pavement Management for Airports, Pavements, and Parking Lots*. Second Edition, Springer Science, New York.

Shrestha, Shivesh, Samer W. Katicha, Gerardo W. Flintsch, and Senthilmurugan Thyagarajan. 2018. “Application of Traffic Speed Deflectometer for Network-Level Pavement Management.” *Transportation Research Record*, 2672(40), 348-359.

Simonin, J-M, D. Lièvre, Soren Rasmussen, and Gregers Hildebrand. 2005. “Assessment of the Danish High Speed Deflectograph in France.” Presented at Seventh International Conference on the Bearing Capacity of Pavements, Railways and Airfields, Trondheim, Norway.

Smith, Kurt D., James E. Bruinsma, Monty J. Wade, Karim Chatti, Julie M. Vandenbossche, and H. Thomas Yu. 2017. *Using Falling Weight Deflectometer Data with Mechanistic- Empirical Design and Analysis, Volume I: Final Report*. FHWA-HRT-16-009. Applied Pavement Technology Inc. Urbana, IL

Souliman, Mena, Stefan Romanoschi, Samer Dessouky, Karthikeyan Loganathan, Ana Maria Coca, and Mayzan Isied. 2018. *Simplified Approach for Structural Evaluation of Flexible Pavements at the Network Level*. Report No. 17PUTA02, Transportation Consortium of South-Central States (Tran-SET). University Transportation Center for Region 6, Louisiana State University, Baton Rouge, Louisiana.

Steinert, Byran C., Dana N. Humphrey, and Maureen A. Kestler. 2005. Portable Falling Weight Deflectometer Study. New England Transportation Consortium (NETC), NETCR52, University of Maine Orono, ME.

Stubstad, Richard, Regis Carvalho, Robert Briggs, and Olga Selezneva. 2012. *Simplified Techniques for Evaluation and Interpretation of Pavement Deflections for Network-Level Analysis: Guide for*

Assessment of Pavement Structural Performance for PMS Applications. Report No. FHWA-HRT-12-025. Applied Research Associates, Inc. Elkridge, MD

Talvik, Ott, and Andrus Aavik. 2009. Use of FWD Deflection Basin Parameters (SCI, BDI, BCI) For Pavement Condition Assessment. *The Baltic Journal of Pavement and Bridge Engineering*, 4(4):196-202.

Tayabji, Shiraz D., and Erland O. Lukanen. 2000. "Nondestructive Testing of Pavements and Backcalculation of Moduli" American Society for Testing and Materials (ASTM). Third Volume. ASTM STP 1375.

Texas Department of Transportation (TxDOT). 2021. *Pavement Manual*. Accessed March 22, 2021. http://onlinemanuals.txdot.gov/txdotmanuals/pdm/non_destruct_eval_p_struct_prop.htm

University of Nevada, Reno (UNR) Releases 3D-Move Analysis Software. *Asphalt Research Consortium (ARC) Newsletter.* UNR, 2010. Accessed July 29, 2022. http://www.arc.unr.edu/Newsletter/Aug10/UNRReleases3DMoveAnalysis.pdf.

Yavuzturk, Cenk, and Khaled Ksaibati. 2002. *Assessment of Temperature Fluctuations in Asphalt Pavements Due to Thermal Environmental Conditions Using A Two-Dimensional, Transient Finite Difference Approach*. Mountain Plains Consortium (MPC), MPC Report No. 02-136, University of Wyoming, Laramie, WY.

Yoder, Eldon J., and Matthew W. Witczak. 1975. *Principles of Pavement Design*. 2nd Edition, John Wiley and Sons, New York.

Uzan, Jacob. 1994. "Advanced Backcalculation Techniques." American Society for Testing and Materials (ASTM). Nondestructive Testing of Pavements and Backcalculation of Moduli: Second Volume. ASTM STP 1198.

Zhang, Bin, Desh R. Sonyok, and Jie Zhang. 2008. "Temperature Effects on Falling Weight Deflectometer Measurement." GeoCongress 2008: Characterization, Monitoring, and Modeling of GeoSystems. American Society of Civil Engineers (ASCE)

Zhang, Zhanmin, German Claros, Lance Manuel, and Ivan Damnjanovic. 2003. "Evaluation of The Pavement Structural Condition at Network Level Using Falling Weight Deflectometer (FWD) Data." Presented at Transportation Research Board 82nd Annual Meeting, Washington, D.C.

10. Appendices

Appendix A FWD and TSD Deflection Data

Table 10.1 Example of FWD Data (US95-2020)

Pavement Site	BMP-EMP	Plate Radius (in.)	Test Date	Test Time						
US-95	515.000-521.879	5.91	9/24/2020	7:41 - 9:48						
				Distance from Load Center (Inch)						
			0	8	12	18	24	36	60
Location/Milepost	Drop No./Height	Drop Load (lb)	Deflection (Mils)						
			D1	D2	D3	D4	D5	D6	D7
515	1	8984	8.26	7.12	6.42	5.59	4.89	3.77	2.24
515	2	8951	8.26	7.11	6.41	5.59	4.89	3.76	2.25
515	3	11975	11.03	9.52	8.59	7.52	6.59	5.07	3.04
515	4	11964	11.02	9.52	8.58	7.5	6.59	5.06	3.05
515.1	1	8984	7.18	6.13	5.49	4.66	4	2.89	1.52
515.1	2	9006	7.17	6.15	5.5	4.67	4	2.91	1.54
515.1	3	11920	9.55	8.21	7.36	6.27	5.39	3.91	2.06
515.1	4	11964	9.58	8.24	7.38	6.28	5.41	3.94	2.09
515.201	1	8962	7.28	6.3	5.65	4.94	4.3	3.31	2.04
515.201	2	8973	7.29	6.3	5.65	4.94	4.3	3.28	2.02
515.201	3	11910	9.71	8.4	7.58	6.61	5.83	4.44	2.69
515.201	4	11899	9.7	8.39	7.58	6.63	5.84	4.46	2.71
515.3	1	8973	7.11	6.11	5.5	4.75	4.15	3.07	1.59
515.3	2	8951	7.06	6.07	5.48	4.74	4.13	3.06	1.58
515.3	3	11942	9.52	8.24	7.43	6.43	5.62	4.17	2.17
515.3	4	11953	9.54	8.22	7.43	6.46	5.62	4.16	2.18
515.4	1	8940	7.59	6.59	5.87	5.11	4.43	3.3	1.81
515.4	2	8907	7.57	6.58	5.85	5.08	4.42	3.29	1.81
515.4	3	11920	10.23	8.92	7.98	6.96	6.06	4.52	2.48
515.4	4	11931	10.24	8.94	7.99	6.97	6.07	4.53	2.47
515.5	1	8907	10.59	8.62	7.25	5.89	4.85	3.3	1.59
515.5	2	8907	10.57	8.62	7.25	5.88	4.83	3.29	1.57
515.5	3	11899	14.22	11.69	9.91	8.09	6.69	4.56	2.17
515.5	4	11899	14.23	11.7	9.91	8.08	6.67	4.57	2.17
515.6	1	8886	6.91	5.9	5.28	4.52	3.88	3	1.57
515.6	2	8886	6.89	5.9	5.27	4.51	3.88	3	1.59
515.6	3	11822	9.2	7.9	7.06	6.07	5.23	4.01	2.15
515.6	4	11822	9.2	7.9	7.07	6.07	5.23	4.03	2.14
515.7	1	8853	12.44	10.4	8.85	7.15	5.81	3.87	1.78
515.7	2	8809	12.33	10.33	8.8	7.11	5.78	3.85	1.78
515.7	3	11811	16.5	13.91	11.91	9.67	7.9	5.32	2.47
515.7	4	11822	16.47	13.9	11.91	9.66	7.91	5.32	2.48
515.8	1	8710	18.59	15.32	12.93	10.2	8.11	5.22	2.25
515.8	2	8721	18.57	15.32	12.89	10.18	8.12	5.21	2.29
515.8	3	11581	23.94	19.94	16.96	13.51	10.9	7.08	3.16
515.8	4	11592	23.97	20	17.02	13.59	10.96	7.14	3.15
515.901	1	8820	15.37	12.59	10.55	8.1	6.17	3.72	1.54
515.901	2	8787	15.25	12.51	10.45	8.03	6.15	3.71	1.53

Table 10.2 Example of FWD Data (US95-2019)

Pavement Site	BMP-EMP	Plate Radius (in.)	Test Date	Test Time						
US-95	0.0005-8.8005	5.91	6/4/2019	13:58 - 15:23						
				Distance from Load Center (Inch)						
			0	8	12	18	24	36	60
Location/Milepost	Drop No./Height	Drop Load (lb)	Deflection (Mils)						
			D1	D2	D3	D4	D5	D6	D7
0.0005	1	7329	17.48	12.66	8.85	5.9	4.25	2.69	1.61
0.0005	2	7329	17.1	12.51	8.81	5.91	4.28	2.76	1.7
0.0005	3	9892	21.46	15.89	11.41	7.85	5.76	3.72	2.28
0.0005	4	9837	21.21	15.72	11.33	7.82	5.75	3.74	2.28
0.2005	1	7241	9.15	6.41	5.54	4.83	4.13	3.09	1.82
0.2005	2	7274	9.14	6.38	5.54	4.83	4.13	3.09	1.83
0.2005	3	9903	11.85	8.39	7.3	6.35	5.46	4.08	2.4
0.2005	4	9892	11.84	8.37	7.31	6.35	5.46	4.07	2.41
0.4005	1	7329	5.4	3.63	3.23	2.85	2.5	1.93	1.25
0.4005	2	7339	5.37	3.63	3.24	2.87	2.5	1.93	1.27
0.4005	3	10155	6.91	4.71	4.21	3.72	3.28	2.57	1.69
0.4005	4	9881	7.08	4.85	4.33	3.83	3.37	2.61	1.71
0.6005	1	7427	9.52	7.17	6.06	4.94	4.18	3.06	1.83
0.6005	2	7394	9.44	7.12	6.02	4.91	4.15	3.03	1.83
0.6005	3	9969	12.3	9.33	7.93	6.49	5.52	4.06	2.45
0.6005	4	9925	12.24	9.28	7.9	6.47	5.49	4.05	2.44
0.8005	1	7383	13.04	9.91	8.01	6.57	5.29	3.59	2
0.8005	2	7372	12.91	9.83	7.97	6.54	5.27	3.6	2.01
0.8005	3	9892	16.5	12.76	10.5	8.68	7.04	4.83	2.73
0.8005	4	9914	16.48	12.76	10.52	8.69	7.05	4.85	2.74
1.0005	1	7383	9.41	7.1	6.18	5.1	4.24	2.99	1.63
1.0005	2	7361	9.32	7.06	6.18	5.08	4.23	2.99	1.64
1.0005	3	9673	11.94	9.14	8.04	6.67	5.59	3.99	2.23
1.0005	4	9914	12.2	9.31	8.17	6.77	5.66	4.03	2.26
1.2005	1	7329	6.24	4.5	3.93	3.48	3.09	2.45	1.55
1.2005	2	7350	6.2	4.49	3.93	3.48	3.11	2.48	1.56
1.2005	3	9859	8	5.87	5.13	4.54	4	3.14	1.94
1.2005	4	9947	7.9	5.85	5.15	4.59	4.09	3.26	2.07
1.4005	1	7350	8.48	6.37	4.89	3.87	3.02	1.82	0.78
1.4005	2	7318	8.44	6.34	4.85	3.86	3.01	1.83	0.79
1.4005	3	10056	10.93	8.27	6.42	5.13	4.04	2.47	1.11
1.4005	4	10133	10.67	8.11	6.33	5.09	4	2.45	1.1
1.6005	1	7372	8.69	5.87	4.74	3.44	2.61	1.58	0.86
1.6005	2	7361	8.67	5.87	4.73	3.43	2.61	1.57	0.86
1.6005	3	9958	10.87	7.43	6.04	4.44	3.39	2.07	1.14
1.6005	4	9859	10.76	7.35	6	4.44	3.42	2.1	1.17
1.8005	1	7329	14.68	9.6	7.31	5.21	3.93	2.61	1.41
1.8005	2	7296	14.44	9.48	7.24	5.17	3.92	2.61	1.42

Table 10.3 Example of TSD Data (US95-2019)

Location	RDER - MCBRID	Test Date	8/5/2019	Test Duration	11:38	12:46	Day Tempera	85	Temper	108	Weather Statio	Boise, ID	Thickness (t	4.83	α
Direction	R ()														0.00367809
Beginning Chainage	End Chainage	D0 (mils)	D8 (mils)	D12 (mils)	D18 (mils)	D24 (mils)	D36 (mils)	D48 (mils)	D60 (mils	D72 (mils)	ce Temperatur	Temperature	rey Speed (I	Latitude	Longitude
0	0.01	-21.3	-16.2	-14.1	-11.8	-10.1	-7.1	-4.9	-3.2	-1.9	109.8	93.5	53.6	43.25108	-117.02618
0.01	0.02	-24.3	-14.1	-11.3	-8.7	-6.9	-4.3	-2.8	-1.8	-1.1	108.7	93.4	53.7	43.25118	-117.02603
0.02	0.03	-17.4	-9.9	-7.4	-5.2	-3.7	-1.8	-0.9	-0.5	-0.3	106.2	93.4	53.7	43.25127	-117.02588
0.03	0.04	-12.2	-9.2	-8.3	-7.3	-6.6	-5.2	-4.1	-3.1	-2.2	105.3	93.4	53.7	43.25137	-117.02573
0.04	0.05	-9.6	-7.9	-7.2	-6.3	-5.5	-4.1	-2.9	-2.1	-1.4	105.4	93.5	53.7	43.25146	-117.02558
0.05	0.06	-8.8	-6.7	-6.1	-5.3	-4.6	-3.1	-2.1	-1.4	-0.9	105.4	93.5	53.6	43.25156	-117.02543
0.06	0.07	-10.3	-8.7	-8.2	-7.5	-6.6	-4.8	-3.5	-2.7	-2.1	105.4	93.5	53.7	43.25165	-117.02528
0.07	0.08	-7.2	-5.7	-5.2	-4.6	-3.7	-2	-0.9	-0.5	-0.3	105.1	93.5	53.7	43.25175	-117.02513
0.08	0.09	-6	-4.5	-4.1	-3.5	-2.8	-1.4	-0.6	-0.3	-0.2	105.1	93.4	53.7	43.25184	-117.02498
0.09	0.1	-7.7	-5.6	-4.9	-4.1	-3.2	-1.4	-0.5	-0.2	-0.1	105.6	93.4	53.7	43.25194	-117.02483
0.1	0.11	-7.8	-6	-5.3	-4.6	-3.7	-2.1	-1.2	-0.8	-0.5	105.9	93.4	53.6	43.25203	-117.02468
0.11	0.12	-12.5	-10.9	-10.2	-9.4	-8.7	-7.1	-5.7	-4.4	-3.3	105.9	93.3	53.6	43.25213	-117.02453
0.12	0.13	-10.4	-8.4	-7.7	-6.9	-6	-4.1	-2.8	-1.9	-1.3	106	93.4	53.7	43.25222	-117.02438
0.13	0.14	-11.8	-10.4	-10	-9.5	-8.7	-7	-5.6	-4.4	-3.4	106	93.5	53.7	43.25231	-117.02423
0.14	0.15	-10.6	-8.3	-7.5	-6.4	-5.3	-3.3	-1.9	-1.2	-0.8	106.1	93.5	53.7	43.25241	-117.02407
0.15	0.16	-10	-8.6	-8	-7.5	-6.8	-5.4	-4.2	-3.3	-2.5	105.9	93.5	53.7	43.2525	-117.02392
0.16	0.17	-9	-7.3	-6.7	-6	-5	-3.2	-1.9	-1.2	-0.7	105.7	93.5	53.6	43.25259	-117.02377
0.17	0.18	-10	-7.8	-7.1	-6.4	-5.4	-3.4	-2	-1.2	-0.8	105.8	93.4	53.6	43.25269	-117.02362
0.18	0.19	-15.4	-13.8	-13.2	-12.6	-11.6	-9.5	-7.7	-6	-4.5	106.2	93.4	53.6	43.25278	-117.02346
0.19	0.2	-10.6	-8.6	-7.7	-6.6	-5.5	-3.4	-2	-1.2	-0.8	106.2	93.5	53.6	43.25287	-117.02331
0.2	0.21	-13.7	-11	-9.9	-8.5	-7.2	-4.8	-3.2	-2.1	-1.4	106.3	93.6	53.7	43.25296	-117.02316
0.21	0.22	-11.1	-8.4	-7.5	-6.5	-5.4	-3.5	-2.2	-1.5	-1.1	106.1	93.5	53.7	43.25305	-117.023
0.22	0.23	-12.4	-9.5	-8.4	-7.2	-5.9	-3.5	-2	-1.2	-0.8	106.2	93.5	53.7	43.25315	-117.02285
0.23	0.24	-8.8	-6.5	-5.7	-4.6	-3.6	-1.8	-0.8	-0.5	-0.3	106.1	93.5	53.7	43.25324	-117.0227
0.24	0.25	-12.6	-10.8	-10.1	-9.2	-8.2	-6.3	-4.8	-3.6	-2.6	106.3	93.5	53.7	43.25333	-117.02254
0.25	0.26	-10.9	-8.6	-7.7	-6.6	-5.5	-3.4	-2.1	-1.4	-1	106.3	93.5	53.6	43.25342	-117.02239
0.26	0.27	-22.1	-19.5	-18.6	-17.4	-16.2	-13.6	-11.2	-8.9	-6.8	105.9	93.6	53.6	43.25351	-117.02223
0.27	0.28	-12.6	-9.8	-8.6	-7.3	-6	-3.6	-2.2	-1.5	-1	106	93.6	53.6	43.2536	-117.02208
0.28	0.29	-9.9	-7.8	-6.9	-5.8	-4.6	-2.5	-1.2	-0.7	-0.4	105.8	93.5	53.7	43.25369	-117.02193
0.29	0.3	-9.5	-7.9	-7.2	-6.3	-5.3	-3.3	-1.9	-1.2	-0.7	105.9	93.5	53.7	43.25379	-117.02178
0.3	0.31	-7	-5.6	-5.1	-4.3	-3.5	-1.9	-0.9	-0.5	-0.3	105.7	93.5	53.6	43.25388	-117.02162
0.31	0.32	-8.3	-6.5	-6.1	-5.4	-4.5	-2.6	-1.3	-0.8	-0.5	105.7	93.5	53.7	43.25397	-117.02147
0.32	0.33	-23.2	-20.6	-19.6	-18.3	-17	-14.4	-11.9	-9.4	-7.1	106	93.5	53.5	43.25406	-117.02132
0.33	0.34	-12.6	-10.2	-9.2	-8.2	-7.3	-5.4	-3.9	-2.8	-2	106.5	93.6	53.7	43.25416	-117.02116
0.34	0.35	-7.4	-5.2	-4.6	-4	-3.4	-2.2	-1.4	-0.9	-0.6	106.5	93.6	53.8	43.25425	-117.02101
0.35	0.36	-11	-9.1	-8.6	-8.1	-7.5	-6.3	-5.2	-4.2	-3.2	107	93.6	53.9	43.25434	-117.02086
0.36	0.37	-8.6	-7.1	-6.5	-5.9	-5.3	-4	-2.9	-2.2	-1.5	107.3	93.7	53.9	43.25443	-117.02071
0.37	0.38	-6.6	-5.1	-4.5	-4	-3.4	-2.1	-1.2	-0.8	-0.5	107.2	93.6	53.9	43.25453	-117.02055
0.38	0.39	-8.6	-7	-6.5	-6	-5.5	-4.3	-3.4	-2.6	-2	106.9	93.6	53.8	43.25462	-117.0204
0.39	0.4	-13.3	-12	-11.6	-11.1	-10.4	-8.9	-7.5	-6	-4.7	107	93.6	53.7	43.25471	-117.02025
0.4	0.41	-16.9	-14.2	-13.5	-12.6	-11.7	-9.6	-7.8	-6.1	-4.6	107.1	93.6	53.7	43.2548	-117.02009
0.41	0.42	-18.5	-15.7	-14.9	-13.9	-12.8	-10.6	-8.6	-6.7	-5.1	107.2	93.7	53.6	43.25489	-117.01994
0.42	0.43	-6.6	-4.5	-3.9	-3.3	-2.8	-1.7	-1.1	-0.7	-0.4	107.5	93.8	53.6	43.25498	-117.01979
0.43	0.44	-10.3	-7.6	-6.7	-5.5	-4.4	-2.4	-1.2	-0.7	-0.4	107.4	93.8	53.4	43.25508	-117.01963
0.44	0.45	-10.7	-8.2	-7.3	-6.2	-5.1	-3.1	-1.8	-1.1	-0.7	107.6	93.7	53.4	43.25517	-117.01948
0.45	0.46	-14.3	-11.4	-10.3	-8.9	-7.5	-4.8	-3	-2	-1.4	107.9	93.7	53.4	43.25526	-117.01932
0.46	0.47	-11.6	-9.3	-8.5	-7.4	-6.3	-4.2	-2.7	-1.9	-1.3	108	93.6	53.5	43.25535	-117.01917
0.47	0.48	-13.6	-11.2	-10.3	-9.2	-8.1	-6.1	-4.6	-3.5	-2.6	108.1	93.6	53.5	43.25544	-117.01902
0.48	0.49	-10.6	-8.4	-7.6	-6.6	-5.6	-3.7	-2.4	-1.7	-1.2	108.3	93.7	53.5	43.25554	-117.01886
0.49	0.5	-10.7	-8.2	-7.2	-6.2	-5.3	-3.8	-2.7	-2	-1.4	108.3	93.7	53.5	43.25563	-117.01871
0.5	0.51	-16.1	-13.7	-12.8	-11.7	-10.7	-8.7	-6.9	-5.4	-4.1	108.7	93.7	53.5	43.25572	-117.01856
0.51	0.52	-11.4	-9.2	-8.3	-7.3	-6.4	-4.8	-3.6	-2.7	-1.9	108.7	93.6	53.5	43.25581	-117.0184
0.52	0.53	-14	-11	-9.8	-8.4	-7	-4.7	-3.1	-2.2	-1.5	108.5	93.7	53.5	43.2559	-117.01825
0.53	0.54	-12.6	-10	-8.8	-7.4	-6.2	-4.2	-2.8	-1.8	-1.2	108.5	93.7	53.6	43.256	-117.0181
0.54	0.55	-11.4	-8.8	-7.6	-6.3	-5.1	-2.9	-1.7	-1	-0.6	108.6	93.6	53.6	43.25609	-117.01795
0.55	0.56	-10.4	-7.7	-6.7	-5.5	-4.3	-2.1	-0.8	-0.4	-0.3	108.9	93.7	53.6	43.25618	-117.0178
0.56	0.57	-9.5	-7	-6.1	-4.9	-3.8	-1.7	-0.6	-0.3	-0.2	109	93.8	53.6	43.25628	-117.01764
0.57	0.58	-8.9	-6.8	-6	-5.1	-4.2	-2.4	-1.2	-0.7	-0.5	109.3	93.7	53.6	43.25637	-117.01749
0.58	0.59	-11.5	-8.5	-7.4	-6	-4.7	-2.4	-1.1	-0.6	-0.4	109.1	93.6	53.7	43.25646	-117.01734
0.59	0.6	-9.6	-7.4	-6.6	-5.5	-4.3	-2.1	-0.8	-0.4	-0.3	109.3	93.7	53.8	43.25655	-117.01718
0.6	0.61	-16.7	-14.6	-13.6	-12.4	-11.1	-8.5	-6.4	-4.8	-3.4	109.6	93.7	53.8	43.25664	-117.01703
0.61	0.62	-12.8	-10.5	-9.6	-8.5	-7.3	-5.1	-3.6	-2.5	-1.8	109.5	93.7	54	43.25674	-117.01688
0.62	0.63	-10	-7.9	-7	-6.1	-5.2	-3.5	-2.3	-1.5	-0.9	109.7	93.7	54.1	43.25683	-117.01672
0.63	0.64	-9.4	-7.4	-6.7	-5.8	-4.7	-2.6	-1.4	-0.8	-0.5	109.7	93.6	54.3	43.25692	-117.01657
0.64	0.65	-9.9	-8	-7.3	-6.4	-5.3	-3	-1.6	-1	-0.6	110.1	93.6	54.5	43.25701	-117.01642
0.65	0.66	-10.7	-8.1	-7.4	-6.5	-5.5	-3.6	-2.2	-1.4	-0.9	110.3	93.6	54.6	43.2571	-117.01626
0.66	0.67	-9.5	-6.9	-6.2	-5.4	-4.5	-2.8	-1.6	-1	-0.6	110.3	93.7	54.8	43.2572	-117.01611
0.67	0.68	-11.7	-9	-8	-6.9	-5.7	-3.5	-2	-1.3	-0.8	110.6	93.7	54.9	43.25729	-117.01596
0.68	0.69	-10.6	-7.8	-6.8	-5.8	-4.8	-3.3	-2.2	-1.4	-0.9	110.6	93.7	54.9	43.25738	-117.01581

Table 10.4 Example of TSD Data (SH55-2019)

Location	HAMPTON DR - I-84 I	Test Date	7/31/2019	Test Duration	14:21	14:41	s Day Temperat	53	)epth Temperatur	61	Weather Statio	Meridian	Thickness (t), in.		α
Direction	F (South)														0
Beginning Chainage	End Chainage	D0 (mils)	D8 (mils)	D12 (mils)	D18 (mils)	D24 (mils)	D36 (mils)	D48 (mils)	D60 (mils)	D72 (mils)	ice Temperatur	Temperature (	rey Speed (r	Latitude	Longitude
0	0.01	-11	-6.6	-4.9	-3	-1.8	-0.6	-0.2	-0.1	-0.1	101.2	90.5	18.7	43.6694487	-116.35447
0.01	0.02	-9.3	-5.5	-4	-2.4	-1.6	-0.8	-0.5	-0.3	-0.2	100.9	90.4	17.4	43.6693041	-116.3544717
0.02	0.03	-9.4	-6.3	-5	-3.6	-2.8	-2	-1.5	-1.1	-0.8	100.9	90.4	17.1	43.6691591	-116.354475
0.03	0.04	-8.3	-5	-3.6	-2.3	-1.5	-0.7	-0.4	-0.3	-0.1	100.8	90.3	16.5	43.6690142	-116.3544782
0.04	0.05	-9.5	-6.1	-4.6	-2.9	-1.9	-1	-0.6	-0.4	-0.2	100.8	90.3	15.7	43.6688696	-116.3544815
0.05	0.06										100.8	90.4	7.1	43.6687252	-116.3544847
0.06	0.07	-8.4	-4.4	-3	-1.6	-0.8	-0.2	-0.2	-0.1	-0.1	101	90.3	11.2	43.6685821	-116.3544879
0.07	0.08	-8.9	-5.8	-4.5	-3.1	-2.3	-1.5	-1	-0.6	-0.3	101	90.3	14	43.6684349	-116.354491
0.08	0.09	-7.9	-5	-3.7	-2.1	-1.1	-0.4	-0.3	-0.2	-0.1	101	90.3	19.4	43.6682914	-116.3544929
0.09	0.1	-8.6	-5.9	-4.6	-3	-1.9	-0.9	-0.6	-0.4	-0.2	101	90.4	19.4	43.6681475	-116.3544969
0.1	0.11	-9.2	-6.6	-5.2	-3.4	-2.2	-1	-0.6	-0.3	-0.2	100.8	90.4	17.9	43.6680028	-116.3545013
0.11	0.12	-10.8	-8	-6.7	-5.2	-4.3	-3	-2	-1.2	-0.7	100.7	90.4	10.5	43.6678583	-116.3545054
0.12	0.13	-7.1	-4.7	-3.5	-1.9	-0.8	-0.1	-0.1	-0.1	0	101.3	90.3	0.9	43.6677146	-116.3545088
0.13	0.14	-7.3	-4.7	-3.5	-1.9	-0.9	-0.2	-0.1	-0.1	0	101.4	90.3	12.5	43.6675705	-116.3545116
0.14	0.15	-8.5	-5.8	-4.4	-2.7	-1.5	-0.4	-0.1	0	0	101.4	90.4	12.8	43.6674272	-116.3545159
0.15	0.16	-6.9	-4.6	-3.4	-2	-1	-0.3	-0.2	-0.1	-0.1	101.2	90.3	0.5	43.6672807	-116.3545382
0.16	0.17	-9.5	-7.1	-5.9	-4.3	-3.3	-2.1	-1.4	-0.9	-0.5	101.5	90.3	10.9	43.6671183	-116.3545194
0.17	0.18	-7.2	-5.1	-3.8	-2.3	-1.3	-0.5	-0.3	-0.2	-0.1	101.5	90.3	13.3	43.6669932	-116.3545162
0.18	0.19	-7.6	-5.4	-4.2	-2.8	-2	-1.2	-0.8	-0.5	-0.3	101.4	90.3	16.1	43.6668494	-116.354526
0.19	0.2	-7.9	-5.5	-4.2	-2.8	-1.9	-1.1	-0.7	-0.4	-0.3	101.4	90.4	17.7	43.6667053	-116.3545293
0.2	0.21	-8.7	-6.5	-5.3	-3.9	-3.1	-2.1	-1.4	-0.9	-0.5	101.3	90.4	19.6	43.6665604	-116.3545314
0.21	0.22	-7.3	-5.3	-4.2	-2.8	-2.1	-1.4	-0.9	-0.5	-0.3	101.1	90.3	22.5	43.6664159	-116.3545336
0.22	0.23	-7.8	-5.5	-4.2	-2.6	-1.6	-0.8	-0.5	-0.3	-0.2	101.1	90.3	24.3	43.6662711	-116.3545361
0.23	0.24	-9.4	-6.6	-5.2	-3.5	-2.3	-1.1	-0.7	-0.5	-0.3	101	90.3	24.8	43.6661267	-116.3545386
0.24	0.25	-11.2	-7.9	-6.3	-4.4	-3.1	-1.8	-1.2	-0.7	-0.4	101.1	90.4	24.6	43.6659822	-116.3545409
0.25	0.26	-11.2	-7.5	-5.8	-3.9	-2.6	-1.4	-0.9	-0.6	-0.4	101.2	90.4	23.2	43.6658376	-116.354544
0.26	0.27	-12.4	-8.1	-6.3	-4.3	-2.9	-1.5	-1	-0.6	-0.4	101.4	90.3	20.1	43.6656931	-116.354548
0.27	0.28	-12.3	-8.2	-6.4	-4.3	-3	-1.7	-1.1	-0.7	-0.4	101.4	90.4	14.4	43.6655485	-116.3545553
0.28	0.29	-9.1	-6.3	-5.1	-3.3	-2.1	-1.1	-0.7	-0.4	-0.2	100.3	90.2	0.2	43.6654053	-116.3545755
0.29	0.3	-11.2	-5.9	-4.6	-3.1	-2.1	-1.2	-0.8	-0.5	-0.3	100.8	90.2	11	43.6652626	-116.3545155
0.3	0.31	-9.8	-6.1	-4.6	-2.9	-1.8	-0.9	-0.6	-0.4	-0.2	99.1	90.2	14.8	43.6651176	-116.354584
0.31	0.32	-11.1	-7.3	-5.6	-3.5	-2.2	-0.9	-0.5	-0.3	-0.2	98.3	90.2	17.2	43.6649722	-116.354569
0.32	0.33	-10.4	-6.9	-5.3	-3.3	-2	-0.8	-0.4	-0.2	-0.1	99.2	90.3	19.6	43.6648307	-116.354577
0.33	0.34	-9.5	-6.2	-4.6	-2.8	-1.7	-0.9	-0.6	-0.3	-0.2	101.5	90.2	20.5	43.6646886	-116.3545821
0.34	0.35	-9.4	-6.1	-4.6	-2.8	-1.6	-0.8	-0.5	-0.3	-0.2	102.1	90.2	24.2	43.6645449	-116.354584
0.35	0.36	-10.1	-6.8	-5.2	-3.3	-2.1	-1.1	-0.7	-0.5	-0.3	102	90.2	25	43.6644013	-116.3545845
0.36	0.37	-8.4	-5.1	-3.7	-2.1	-1.1	-0.4	-0.3	-0.2	-0.1	101.4	90.3	25.5	43.6642578	-116.354584
0.37	0.38	-11.2	-7.3	-5.7	-3.7	-2.3	-1.1	-0.7	-0.5	-0.3	101.8	90.3	26.8	43.6641112	-116.3545837
0.38	0.39	-11.7	-7.7	-6	-3.7	-2.2	-1	-0.7	-0.4	-0.2	102.1	90.3	29.4	43.6639641	-116.3545845
0.39	0.4	-12.2	-8.2	-6.3	-4.2	-2.7	-1.1	-0.5	-0.3	-0.2	101.8	90.3	28.9	43.6638171	-116.3545859
0.4	0.41	-12.2	-7.8	-6	-3.8	-2.4	-1.1	-0.7	-0.4	-0.2	100.8	90.4	25.3	43.6636701	-116.3545879
0.41	0.42	-13.6	-9	-7.1	-5	-3.4	-1.9	-1.2	-0.8	-0.4	100.2	90.3	13.1	43.6635231	-116.3545906
0.42	0.43	-13.7	-8	-6.3	-4.3	-3	-1.8	-1.2	-0.7	-0.4	101.4	90.2	6.2	43.6633761	-116.3545939
0.43	0.44	-11.5	-7.4	-6.1	-4.4	-3.2	-1.8	-1.2	-0.7	-0.4	102.4	90.2	12.2	43.663219	-116.3545917
0.44	0.45	-8.3	-5.1	-4	-2.6	-1.6	-0.8	-0.5	-0.3	-0.2	102.2	90.2	15.8	43.6630789	-116.3545921
0.45	0.46	-9.4	-6.9	-5.8	-4.3	-3.2	-2	-1.3	-0.8	-0.5	102.1	90.2	19.6	43.6629376	-116.3545895
0.46	0.47	-12.2	-8.8	-7.1	-5.3	-4.2	-2.8	-1.8	-1.1	-0.7	101.8	90.2	24.5	43.6627964	-116.3545886
0.47	0.48	-11	-7.3	-5.6	-3.7	-2.5	-1.3	-0.9	-0.5	-0.3	101.7	90.2	25.8	43.6626553	-116.3545859
0.48	0.49	-9	-5.7	-4.3	-2.5	-1.3	-0.4	-0.3	-0.2	-0.1	101.6	90.1	27.2	43.6625142	-116.3545797
0.49	0.5	-8.2	-5.1	-3.6	-2	-1	-0.3	-0.2	-0.1	-0.1	101.6	90.1	30	43.6623711	-116.3545752
0.5	0.51	-10	-6.4	-4.7	-2.8	-1.7	-0.9	-0.6	-0.4	-0.2	101.4	90.3	31.3	43.6622265	-116.3545711
0.51	0.52	-11.3	-7.4	-5.6	-3.5	-2.2	-0.9	-0.4	-0.2	-0.1	101.4	90.3	33.8	43.662082	-116.3545663
0.52	0.53	-13.6	-9.4	-7.5	-5.1	-3.5	-1.9	-1.1	-0.7	-0.4	101.4	90.2	35.9	43.6619373	-116.3545604
0.53	0.54	-18.1	-13.3	-10.9	-7.7	-5.5	-3.1	-2.1	-1.3	-0.8	101.3	90.1	36.3	43.6617926	-116.3545527
0.54	0.55	-13.9	-9.9	-7.8	-5.2	-3.6	-2	-1.3	-0.8	-0.5	101	90.2	36.4	43.661648	-116.3545438

Table 10.5 Example of TSD Data (I-5-2020)

Location	MP 35.00 - MP 40.0	Test Date	5/1/2020	Test Time	11:34	Previous Day Temperature (° F)		Mid Depth Temperature (° F)			Weather Station	Pocatello, ID	AC Thickness (t), in.		α
Direction	F														0
Beginning Chainage	End Chainage	D0 (mils)	D8 (mils)	D12 (mils)	D18 (mils)	D24 (mils)	D36 (mils)	D48 (mils)	D60 (mils)	D72 (mils)	Surface Temperature (°	Air Temperature (°	Survey Speed (mpl	Latitude	Longitude
0	0.01	-8.2	-7.4	-6.9	-6.2	-5.3	-3.8	-2.9	-2.1	-1.5	51.4	56.6	53.4	42.4882761	-112.16935
0.01	0.02	-8.8	-7.9	-7.6	-6.9	-6	-4.5	-3.6	-2.8	-2	51.4	56.7	53.3	42.4884209	-112.16935
0.02	0.03	-10.4	-9.2	-8.5	-7.5	-6.3	-4.4	-3.2	-2.2	-1.5	51.4	56.6	53.3	42.4885657	-112.16935
0.03	0.04	-9.8	-8.8	-8.2	-7.2	-6.2	-4.4	-3.2	-2.3	-1.5	51.4	56.6	53.3	42.4887105	-112.16935
0.04	0.05	-11.9	-10.6	-9.8	-8.5	-7.2	-5.1	-4	-3	-2.2	51.5	56.5	53.3	42.4888554	-112.16935
0.05	0.06	-11.8	-10.5	-9.7	-8.5	-7.2	-5	-3.6	-2.5	-1.7	51.4	56.6	53.4	42.4890003	-112.16935
0.06	0.07	-11.9	-10.7	-10	-8.9	-7.7	-5.6	-4.3	-3.2	-2.3	51.4	56.7	53.4	42.4891452	-112.16935
0.07	0.08	-11.4	-10.2	-9.4	-8.3	-7	-4.9	-3.6	-2.5	-1.7	51.4	56.7	53.4	42.48929	-112.16935
0.08	0.09	-8.9	-7.9	-7.3	-6.4	-5.4	-3.5	-2.3	-1.6	-1	51.4	56.6	53.4	42.4894348	-112.16935
0.09	0.1	-7.3	-6.7	-6.3	-5.6	-4.8	-3.4	-2.4	-1.7	-1.1	51.4	56.6	53.4	42.4895796	-112.16934
0.1	0.11	-8.3	-7.5	-6.9	-6.1	-5.3	-3.7	-2.7	-1.9	-1.3	51.4	56.6	53.4	42.4897244	-112.16934
0.11	0.12	-10	-9.1	-8.5	-7.7	-6.6	-4.9	-3.8	-2.8	-2	51.4	56.6	53.4	42.4898692	-112.16934
0.12	0.13	-8.7	-7.8	-7.4	-6.8	-5.9	-4.3	-3.2	-2.3	-1.6	51.4	56.5	53.4	42.490014	-112.16934
0.13	0.14	-9.4	-8.5	-7.9	-7.2	-6.2	-4.3	-3.1	-2.1	-1.4	51.5	56.5	53.4	42.4901588	-112.16935
0.14	0.15	-8.6	-7.6	-7.1	-6.3	-5.3	-3.7	-2.8	-2	-1.3	51.5	56.5	53.4	42.4903036	-112.16935
0.15	0.16	-6.7	-5.8	-5.4	-4.7	-3.8	-2.3	-1.5	-1	-0.6	51.5	56.5	53.3	42.4904485	-112.16935
0.16	0.17	-7.9	-7	-6.6	-6	-5.2	-4	-3.2	-2.5	-1.9	51.6	56.5	53.3	42.4905934	-112.16935
0.17	0.18	-9.4	-8.5	-7.9	-6.9	-6	-4.3	-3.3	-2.4	-1.6	51.6	56.6	53.3	42.4907383	-112.16935
0.18	0.19	-10	-9.1	-8.6	-7.7	-6.6	-4.9	-3.8	-2.8	-2	51.6	56.6	53.3	42.4908832	-112.16934
0.19	0.2	-10.2	-9.3	-8.8	-7.9	-6.8	-5	-4	-3	-2.2	51.6	56.5	53.4	42.4910281	-112.16934
0.2	0.21	-10	-9.1	-8.5	-7.7	-6.6	-4.6	-3.4	-2.3	-1.5	51.6	56.6	53.4	42.491173	-112.16934
0.21	0.22	-12	-10.9	-10.2	-9.2	-7.9	-5.6	-4.1	-2.8	-1.9	51.6	56.5	53.4	42.4913178	-112.16934
0.22	0.23	-10.1	-9.1	-8.5	-7.6	-6.5	-4.6	-3.3	-2.3	-1.5	51.6	56.4	53.5	42.4914626	-112.16934
0.23	0.24	-8.8	-8	-7.5	-6.7	-5.8	-4.3	-3.3	-2.5	-1.8	51.6	56.4	53.7	42.4916074	-112.16934
0.24	0.25	-9.4	-8.4	-7.8	-6.9	-5.9	-4.1	-2.9	-2	-1.3	51.6	56.4	54.1	42.4917522	-112.16934
0.25	0.26	-10.4	-9.4	-8.7	-7.8	-6.7	-4.6	-3.3	-2.3	-1.5	51.6	56.5	54.6	42.491897	-112.16934
0.26	0.27	-8.9	-8	-7.5	-6.8	-5.9	-4.2	-3.2	-2.3	-1.6	51.5	56.6	54.9	42.4920419	-112.16934
0.27	0.28	-11.4	-10	-9.1	-7.8	-6.5	-4.3	-2.9	-1.9	-1.3	51.4	56.6	55.1	42.4921868	-112.16935
0.28	0.29	-10.4	-9.4	-8.8	-7.8	-6.7	-4.8	-3.7	-2.7	-1.9	51.4	56.5	55.2	42.4923316	-112.16935
0.29	0.3	-9	-8	-7.4	-6.5	-5.5	-3.8	-2.8	-1.9	-1.3	51.4	56.5	55.4	42.4924766	-112.16935
0.3	0.31	-8.1	-7.2	-6.7	-5.8	-4.8	-3	-1.9	-1.3	-0.8	51.4	56.6	55.4	42.4926214	-112.16935
0.31	0.32	-10.5	-9.3	-8.5	-7.3	-6	-3.9	-2.7	-1.8	-1.1	51.4	56.5	55.5	42.4927663	-112.16935
0.32	0.33	-9.8	-8.9	-8.4	-7.5	-6.4	-4.5	-3.3	-2.3	-1.5	51.4	56.5	55.5	42.4929112	-112.16935
0.33	0.34	-9.8	-8.8	-8.2	-7.2	-6.2	-4.4	-3.1	-2.2	-1.4	51.4	56.5	55.4	42.4930561	-112.16934
0.34	0.35	-10.7	-9.6	-9	-7.9	-6.8	-4.7	-3.4	-2.3	-1.5	51.4	56.6	55.4	42.493201	-112.16934
0.35	0.36	-11.2	-9.8	-9	-7.8	-6.6	-4.6	-3.4	-2.5	-1.7	51.4	56.7	55.3	42.4933461	-112.16934
0.36	0.37	-11.2	-9.9	-9.1	-8	-6.7	-5	-4.1	-3.3	-2.5	51.4	56.7	55.1	42.4934911	-112.16934
0.37	0.38	-6.6	-5.5	-4.9	-4.1	-3.4	-2.1	-1.4	-0.9	-0.5	51.3	56.5	55.3	42.4936362	-112.16934
0.38	0.39	-8.6	-7.8	-7.3	-6.6	-5.8	-4.4	-3.3	-2.4	-1.7	51.2	56.4	55.3	42.4937813	-112.16934
0.39	0.4	-13.9	-13	-12.6	-11.7	-10.7	-8.8	-7.3	-5.7	-4.4	51	56.4	55.2	42.4939261	-112.16934
0.4	0.41	-8.3	-7.4	-7	-6.3	-5.4	-3.9	-3	-2.2	-1.5	51.3	56.3	55.2	42.4940709	-112.16934
0.41	0.42	-10.7	-9.4	-8.7	-7.7	-6.5	-4.6	-3.4	-2.4	-1.7	51.3	56.3	55.1	42.4942157	-112.16934
0.42	0.43	-6.2	-5.3	-4.9	-4.4	-3.6	-2.2	-1.4	-0.9	-0.5	51.2	56.4	55.1	42.4943605	-112.16934
0.43	0.44	-5.4	-4.7	-4.3	-3.7	-2.9	-1.7	-1.2	-0.8	-0.5	51.2	56.4	54.9	42.4945053	-112.16934
0.44	0.45	-8.4	-7.5	-7	-6.3	-5.5	-4.1	-3.2	-2.4	-1.8	51.2	56.5	55.1	42.4946501	-112.16934
0.45	0.46	-7.7	-6.8	-6.3	-5.5	-4.6	-3	-2.1	-1.4	-0.9	51.2	56.4	55.1	42.4947951	-112.16934
0.46	0.47	-10.2	-9.1	-8.4	-7.2	-6.1	-4	-2.8	-1.9	-1.2	51.3	56.4	55.1	42.49494	-112.16934
0.47	0.48	-8.2	-7.2	-6.6	-5.8	-4.9	-3.3	-2.4	-1.7	-1.2	51.2	56.4	55.1	42.495085	-112.16934
0.48	0.49	-7.3	-6.6	-6.2	-5.5	-4.7	-3.5	-2.9	-2.3	-1.8	51.2	56.5	55.1	42.4952298	-112.16934
0.49	0.5	-8.1	-7.2	-6.7	-5.9	-5	-3.5	-2.6	-1.8	-1.2	51.2	56.4	55.1	42.4953746	-112.16934
0.5	0.51	-9.8	-8.8	-8.1	-7.2	-6.2	-4.4	-3.3	-2.3	-1.6	51.2	56.4	55.1	42.4955195	-112.16934
0.51	0.52	-7	-6.3	-5.8	-5.1	-4.4	-3.2	-2.4	-1.7	-1.2	51.3	56.5	55.1	42.4956643	-112.16934
0.52	0.53	-9.7	-9	-8.5	-7.8	-6.8	-4.9	-3.7	-2.7	-1.8	51.3	56.5	55.1	42.4958091	-112.16934
0.53	0.54	-9.3	-8.3	-7.7	-6.9	-5.8	-4.1	-3.1	-2.2	-1.5	51.3	56.5	55.1	42.495954	-112.16934
0.54	0.55	-9.3	-8.5	-8	-7.1	-6.1	-4.2	-3	-2	-1.3	51.3	56.4	55.1	42.4960988	-112.16934

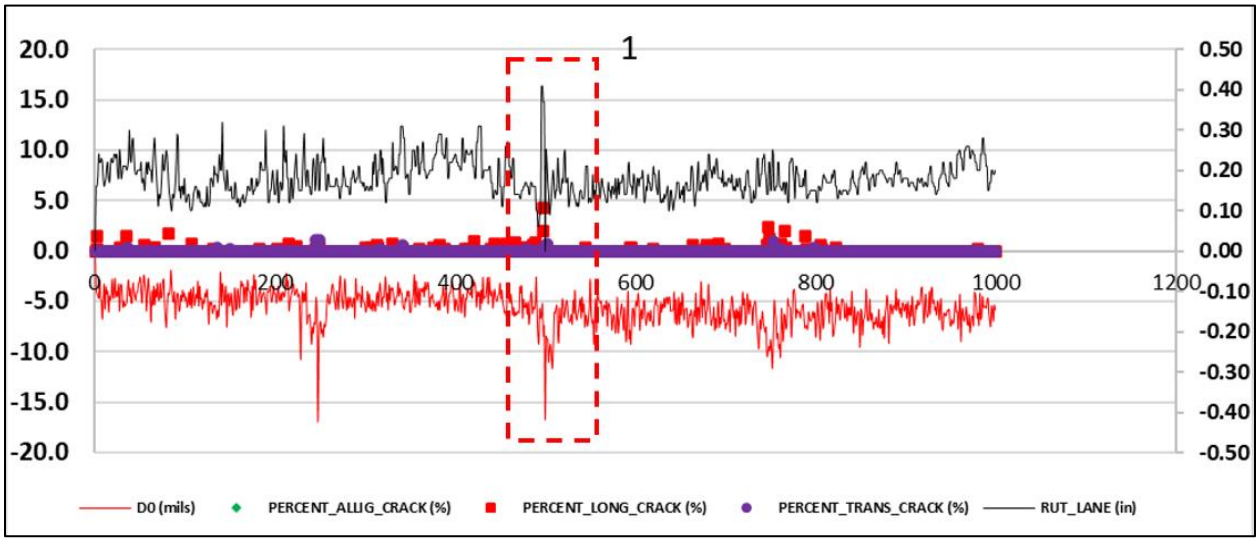

Figure 10.1 I-15 TSD Deflection (D0) Vs. Pavement Distresses

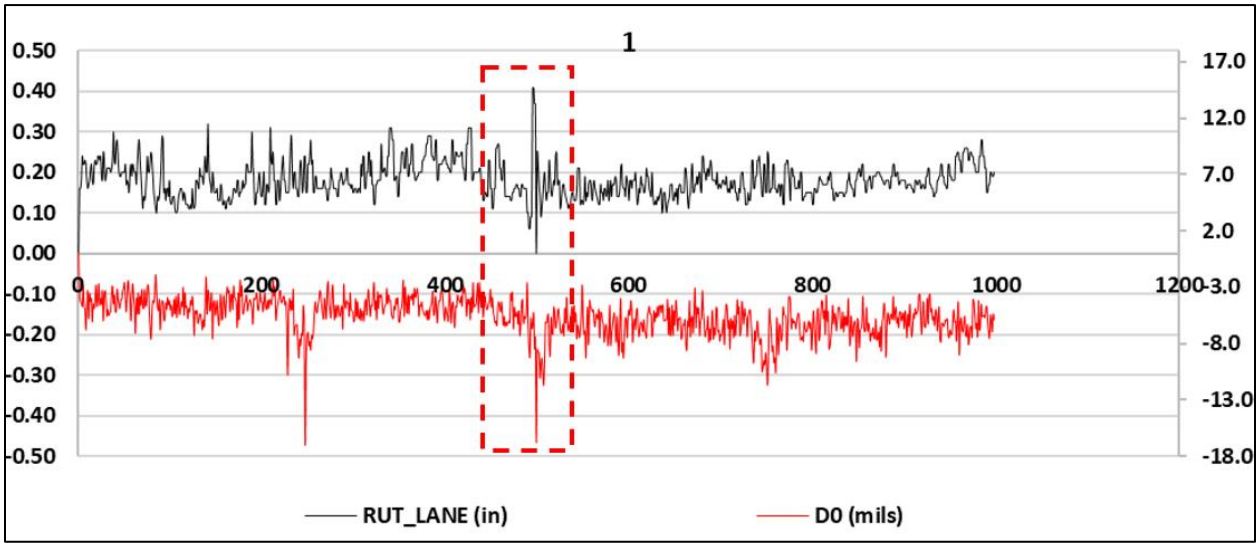

Figure 10.2 I-15 TSD Deflection (D0) Vs. Rutting

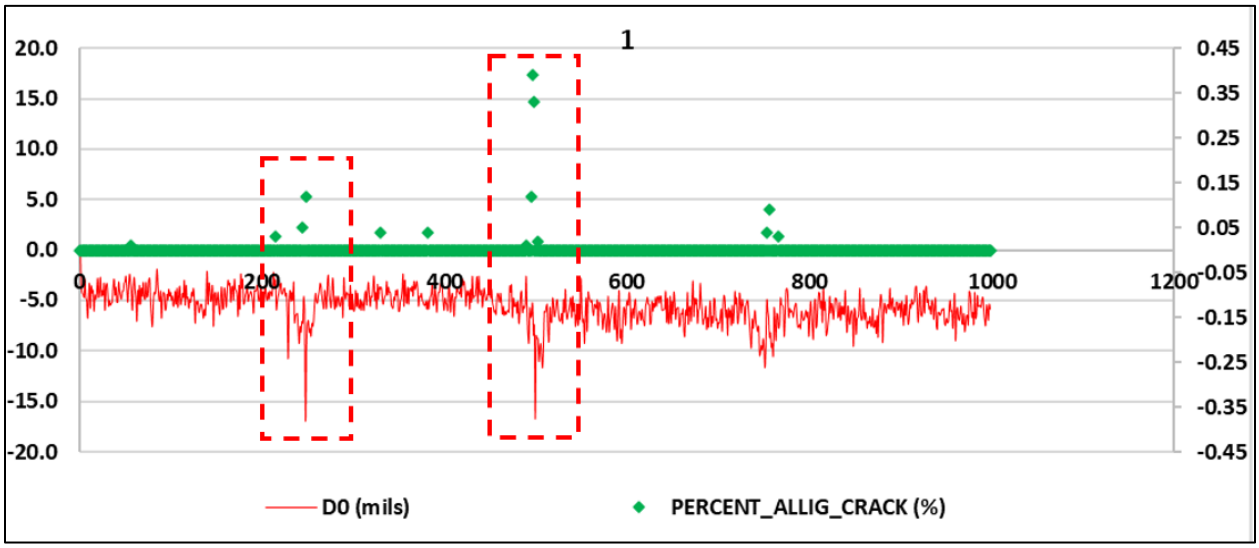

Figure 10.3 I-15 TSD Deflection (D0) Vs. Alligator Cracking

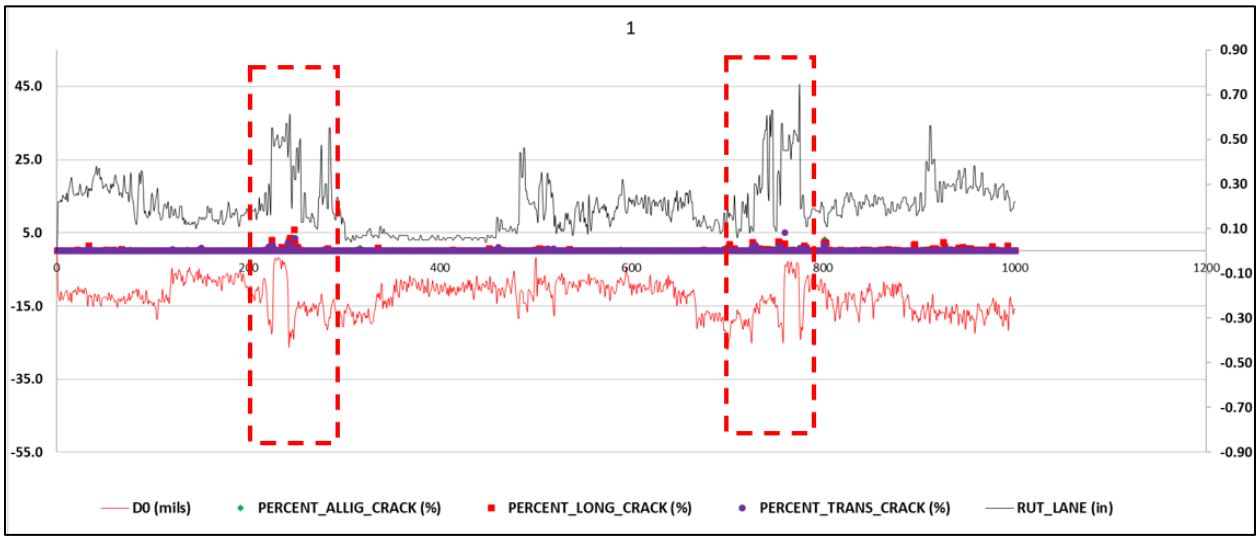

Figure 10.4 SH-55 TSD Deflection (D0) Vs. Pavement Distresses

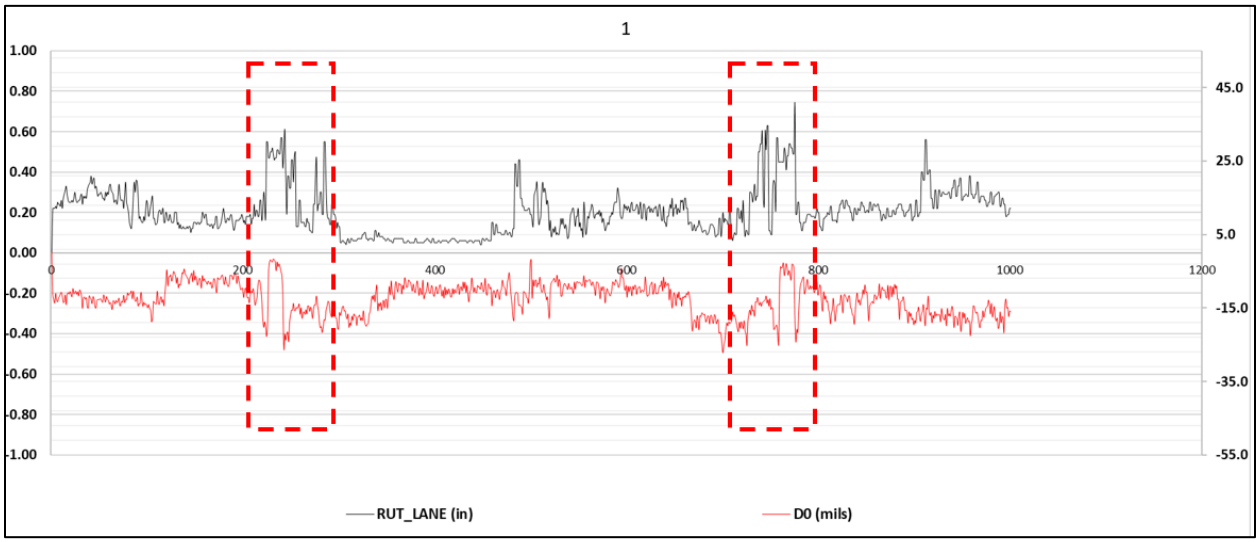

Figure 10.5 SH55 TSD Deflection (D0) Vs. Rutting

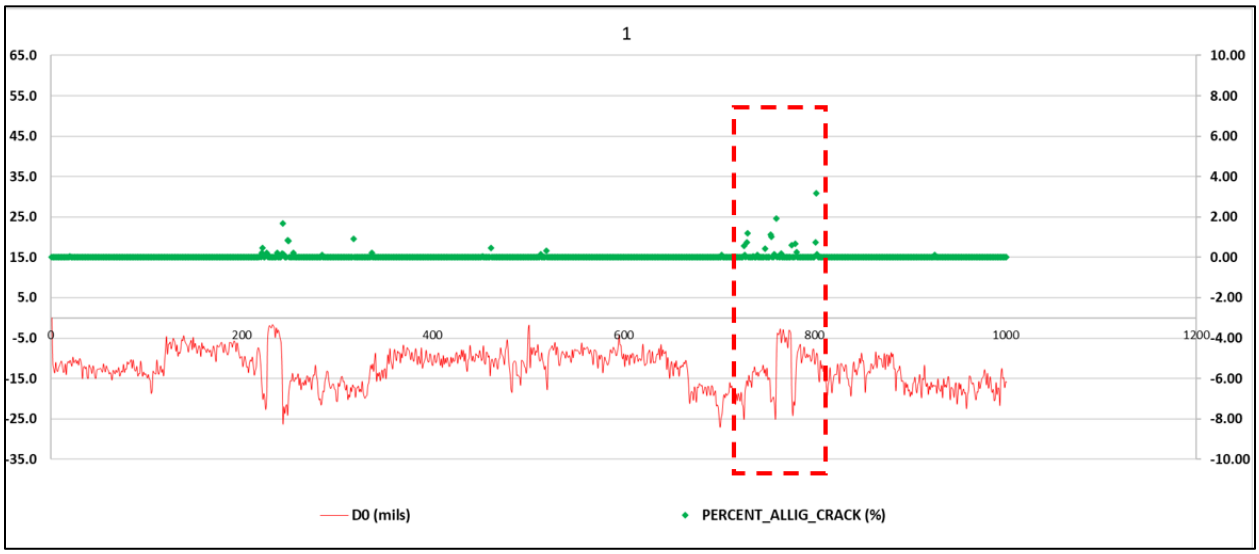

Figure 10.6 SH55 TSD Deflection (D0) Vs. Alligator Cracking

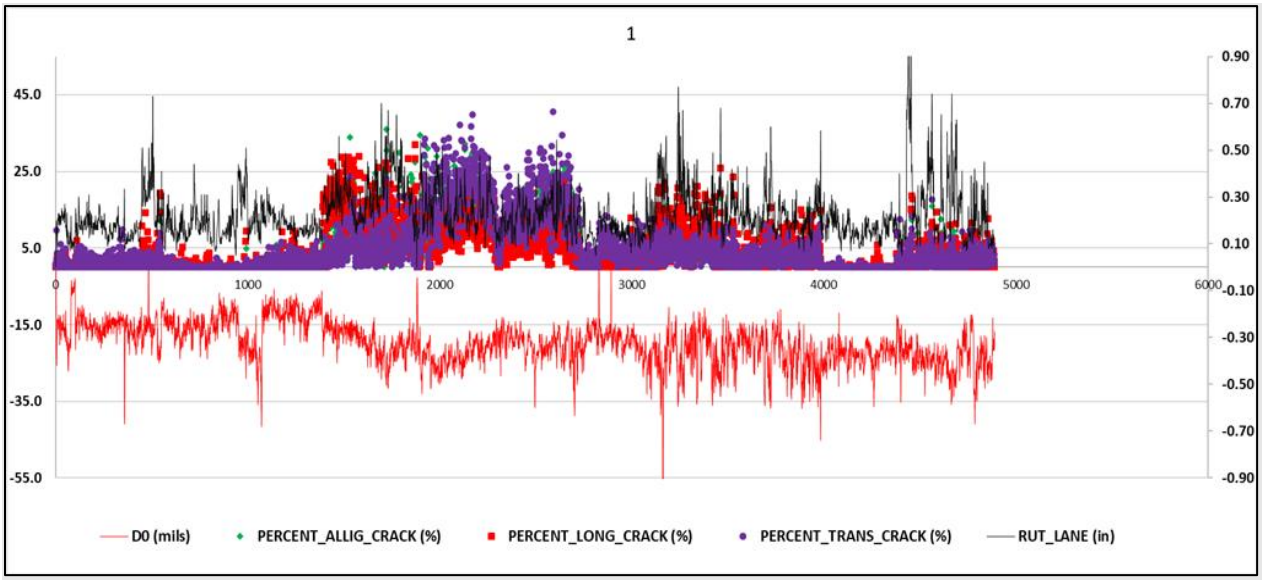

Figure 10.7 SH25 TSD Deflection (D0) Vs. Pavement Distresses

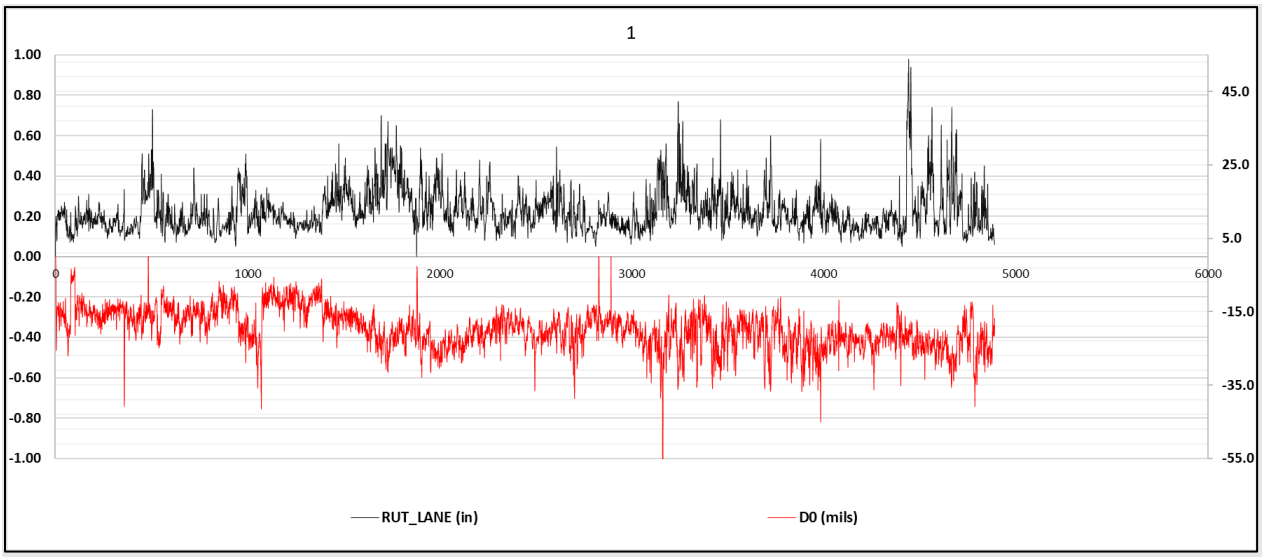

Figure 10.8 SH25 TSD Deflection (D0) Vs. Rutting

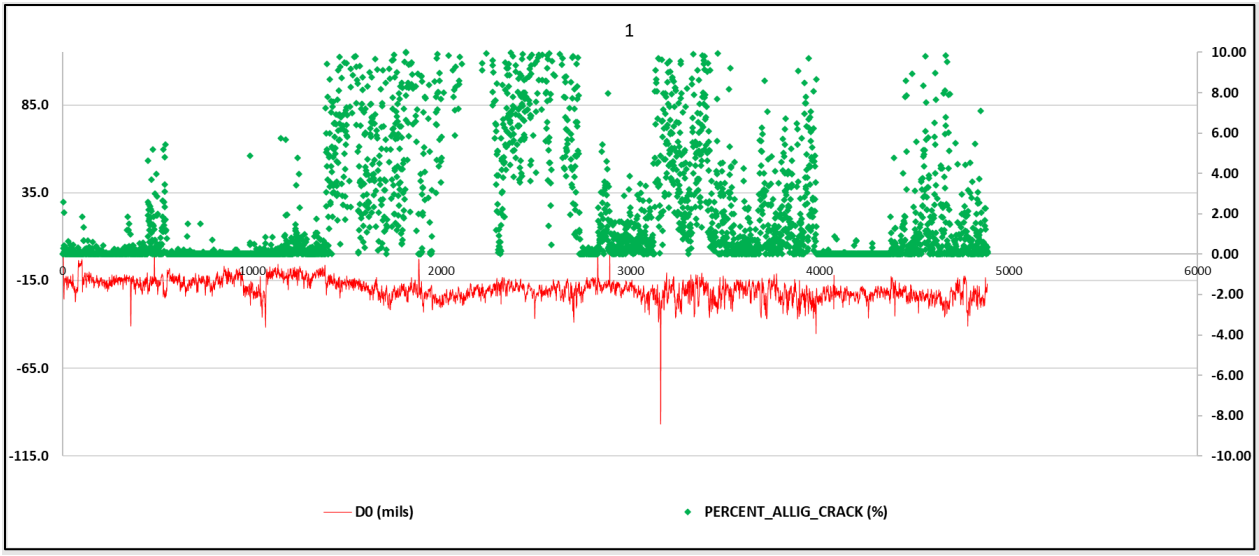

Figure 10.9 SH25 TSD Deflection (D0) Vs. Alligator Cracking

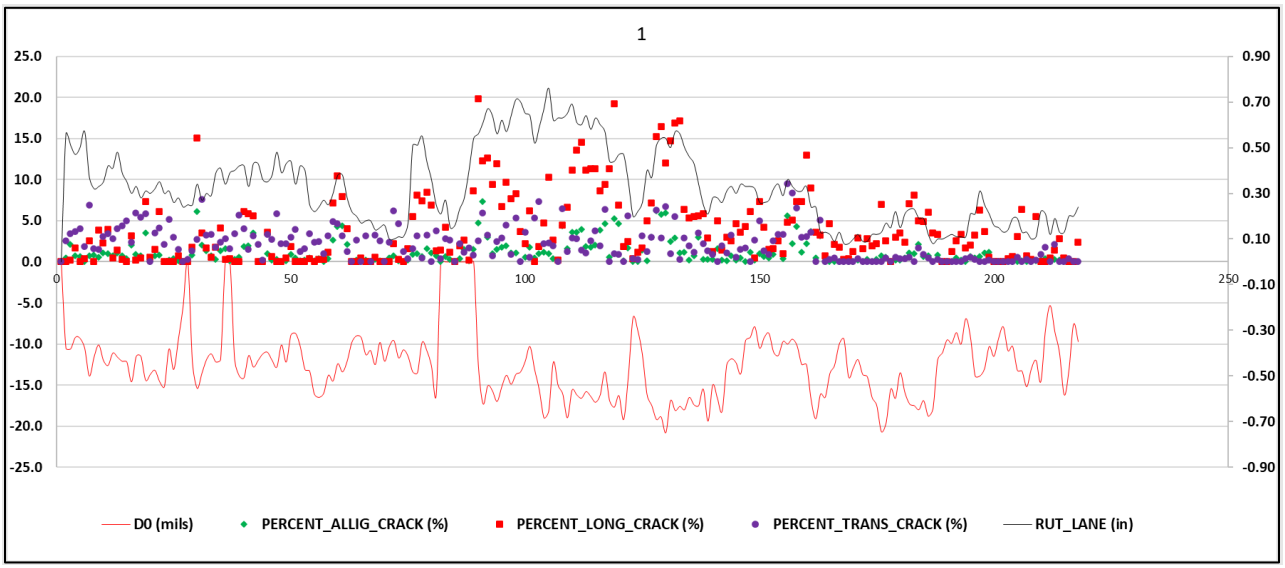

Figure 10.10 I-86 TSD Deflection (D0) Vs. Pavement Distresses

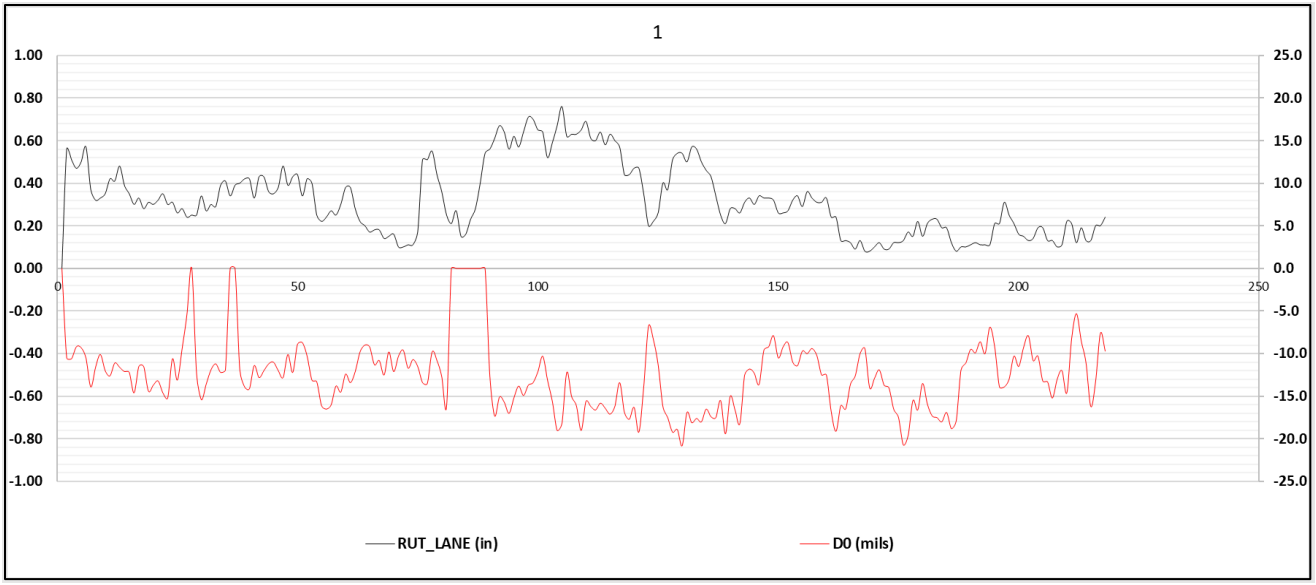

Figure 10.11 I-86 TSD Deflection (D0) Vs. Rutting

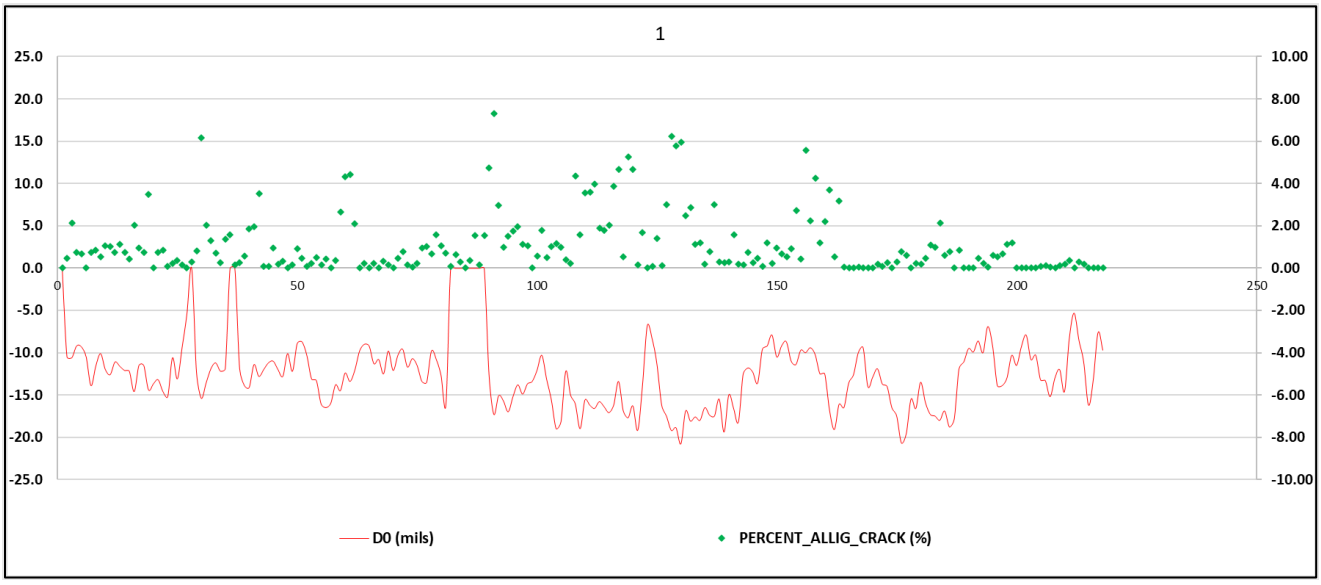

Figure 10.12 I-86 TSD Deflection (D0) Vs. Alligator Cracking

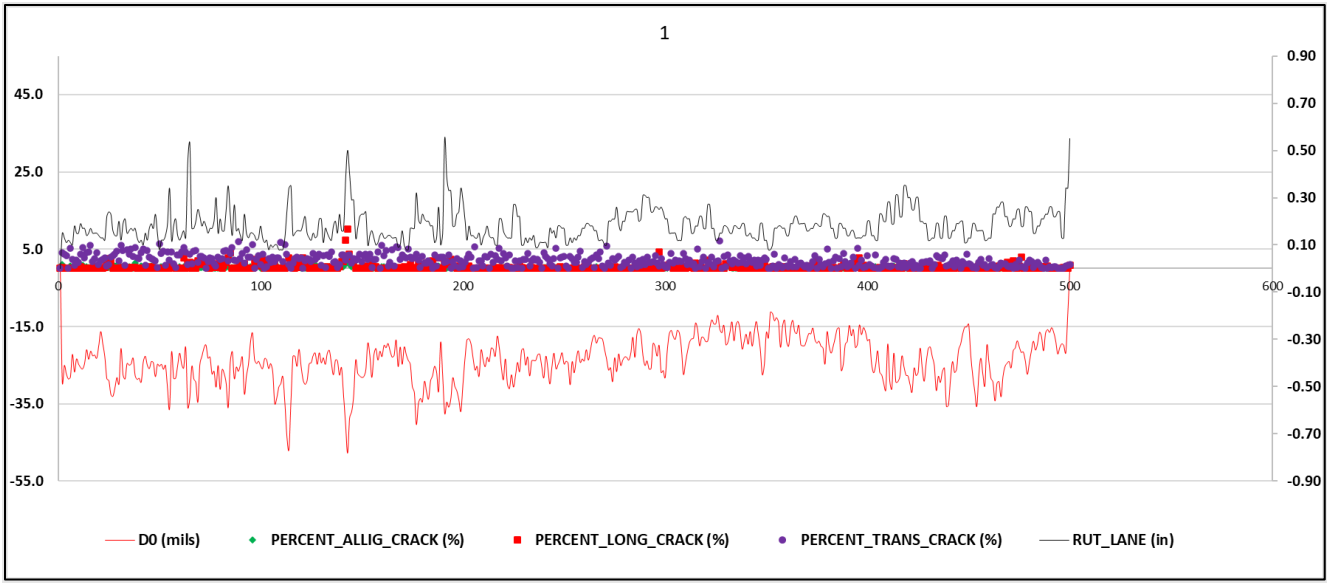

Figure 10.13 SH-27 TSD Deflection (D0) Vs. Pavement Distresses

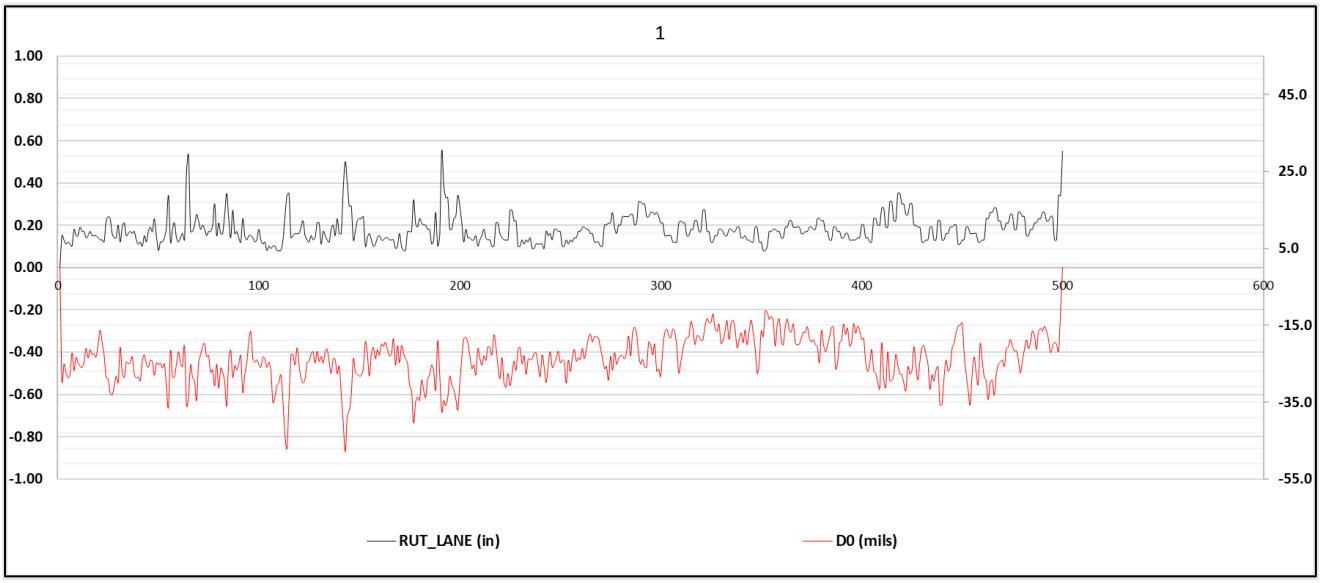

Figure 10.14 SH-27 TSD Deflection (D0) Vs. Rutting

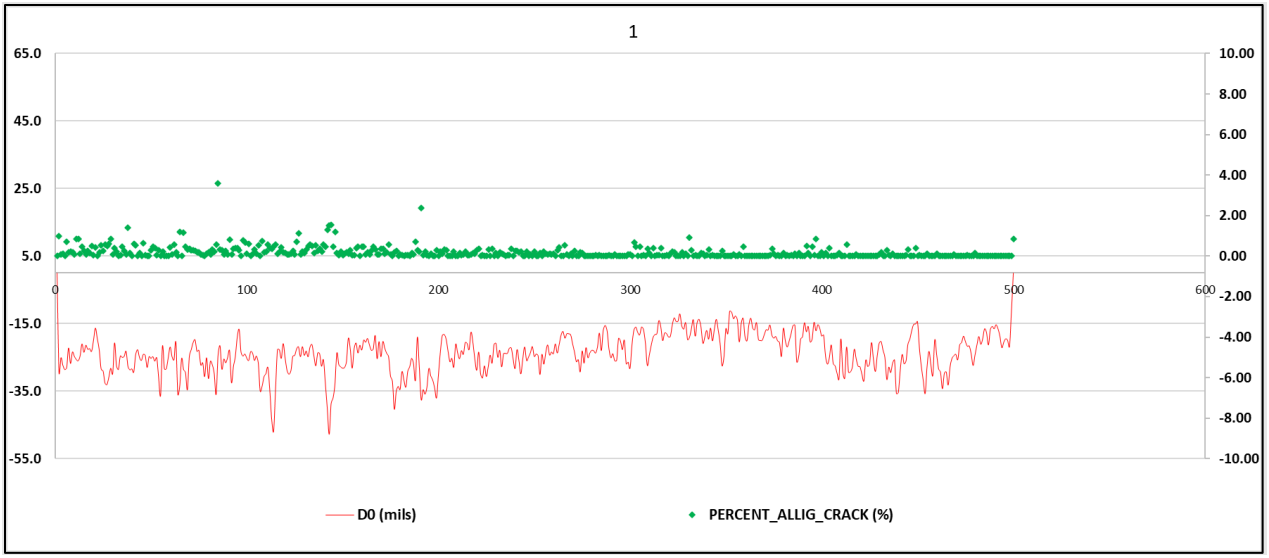

Figure 10.15 SH-27 TSD Deflection (D0) Vs. Alligator Cracking

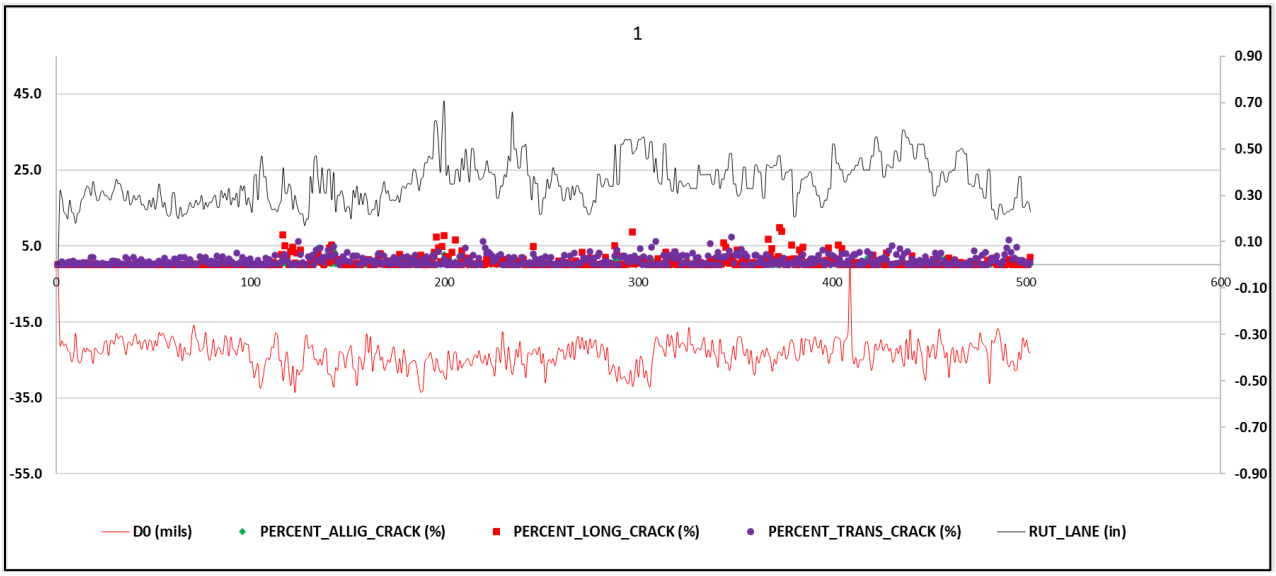

Figure 10.16 SH-26 TSD Deflection (D0) Vs. Pavement Distresses

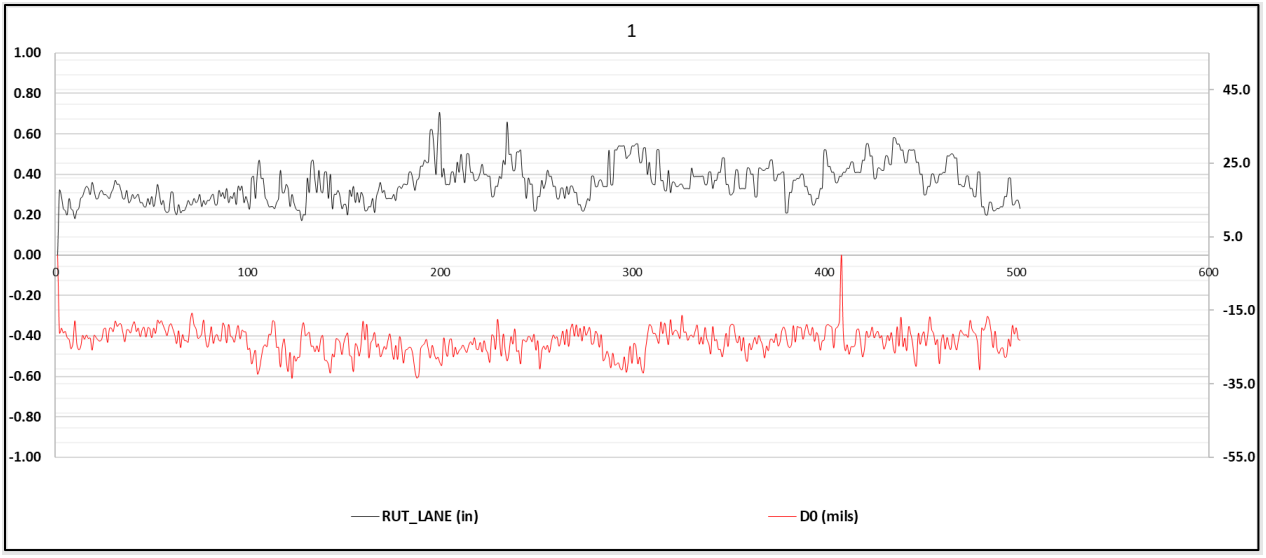

Figure 10.17 SH-26 TSD Deflection (D0) Vs. Rutting

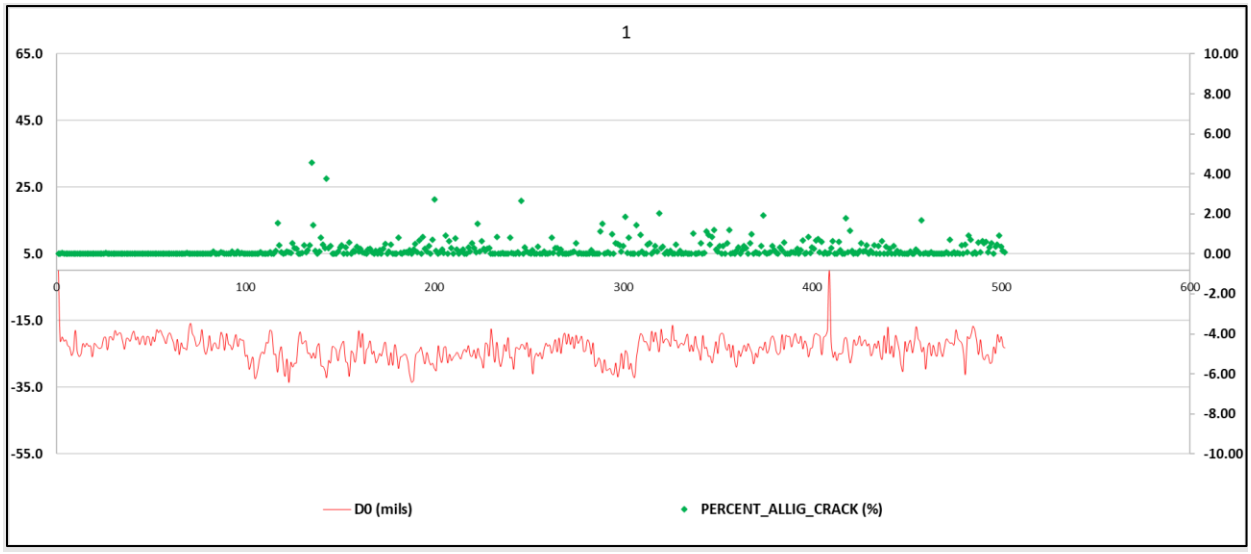

Figure 10.18 SH-26 TSD Deflection (D0) Vs. Alligator Cracking

Table 10.6 D0 vs. Pavement Performance

Pavement Site	D0 (mils)	OCI	IRI (inch/mile)	Rutting (in.)	Base Layer Condition	OCI Condition	IRI Condition	Rutting Condition
D-5 I-15 40.70-43.80 2020 9K	9.67	97.3	37	0.13	Sound	Good	Good	Good
D-5 I-15 89.412-92.191 2020 9K	9.2	94.82	62	0.3	Sound	Good	Good	Fair
D-5 I-15 99.00-104.001 2020 9K	9.9	89.28	56	0.29	Sound	Good	Good	Fair
D-5 SH-39 49.80-44.50 2020 9K	14.16	89.52	73	0.19	Sound	Good	Good	Good
D-4 SH-27 0.000-10.000 2020 9K	23.84	88.52	107	0.17	Sound	Good	Fair	Good
D-4 SH-27 19.445-22.000 2020 9K	22.35	89.82	95	0.2	Sound	Good	Good	Good
D-4 SH-27 MP 0.000 - MP 5.000 2020 9K	23.84	87.13	113	0.16	Sound	Good	Fair	Good
D-4 SH-27 MP 5.000 - MP 10.000 2020 9K	25.85	89.94	101	0.19	Warning	Good	Fair	Good
D-4 US-30 MP 249.000 - MP 253.101 2020 9K	16.69	82.88	84	0.25	Sound	Good	Good	Fair
D-4 US-93 MP 203.000 - MP 208.000 2020 9K	16.96	100	193	0.27	Sound	Good	Poor	Fair
D-4 US-93 MP 208.000 - MP 211.201 2020 9K	18.65	100	193	0.27	Sound	Good	Poor	Fair
D-4 US-93 MP 211.300 - MP 216.201 2020 9K	19.33	100	201	0.25	Sound	Good	Poor	Fair
D-4 US-93 MP 216.300 - MP 221.201 2020 9K	11.5	100	151	0.24	Sound	Good	Fair	Fair
D-3 SH-55 MP 101.50 - MP 105.20 2020 9K	19.95	97.63	74	0.3	Sound	Good	Good	Fair
D-3 SH-55 MP 105.30 - MP 110.20 2020 9K	16.04	93.19	80	0.18	Sound	Good	Good	Good
D-3 SH-55 MP 110.30 - MP 114.00 2020 9K	12.96	98.51	56	0.17	Sound	Good	Good	Good

Table 10.7 BLI vs. Pavement Performance

Pavement Site	BLI (mils)	OCI	IRI (inch/mile)	Rutting (in.)	Asphalt Layer Condition	OCI Condition	IRI Condition	Rutting Condition
D-5 I-15 40.70-43.80 2020 9K	2.6	97.3	37	0.13	Very Good	Good	Good	Good
D-5 I-15 89.412-92.191 2020 9K	3.07	94.82	62	0.3	Very Good	Good	Good	Fair
D-5 I-15 99.00-104.001 2020 9K	2.95	89.28	56	0.29	Very Good	Good	Good	Fair
D-5 SH-39 49.80-44.50 2020 9K	4.18	89.52	73	0.19	Good	Good	Good	Good
D-4 SH-27 0.000-10.000 2020 9K	7.68	88.52	107	0.17	Fair	Good	Fair	Good
D-4 SH-27 19.445-22.000 2020 9K	7.97	89.82	95	0.2	Fair	Good	Good	Good
D-4 SH-27 MP 0.000 - MP 5.000 2020 9K	7.68	87.13	113	0.16	Fair	Good	Fair	Good
D-4 SH-27 MP 5.000 - MP 10.000 2020 9K	8.07	89.94	101	0.19	Poor	Good	Fair	Good
D-4 US-30 MP 249.000 - MP 253.101 2020 9K	5.62	82.88	84	0.25	Good	Good	Good	Fair
D-4 US-93 MP 203.000 - MP 208.000 2020 9K	6.52	100	193	0.27	Fair	Good	Poor	Fair
D-4 US-93 MP 208.000 - MP 211.201 2020 9K	7.42	100	193	0.27	Fair	Good	Poor	Fair
D-4 US-93 MP 211.300 - MP 216.201 2020 9K	7.86	100	201	0.25	Fair	Good	Poor	Fair
D-4 US-93 MP 216.300 - MP 221.201 2020 9K	4.3	100	151	0.24	Good	Good	Fair	Fair
D-3 SH-55 MP 101.50 - MP 105.20 2020 9K	6.03	97.63	74	0.3	Poor	Good	Good	Fair
D-3 SH-55 MP 105.30 - MP 110.20 2020 9K	4.05	93.19	80	0.18	Good	Good	Good	Good
D-3 SH-55 MP 110.30 - MP 114.00 2020 9K	3.23	98.51	56	0.17	Very Good	Good	Good	Good

Table 10.8 MLI vs. Pavement Performance

Pavement Site	MLI (mils)	OCI	IRI (inch/mile)	Rutting (in.)	Base Layer Condition	OCI Condition	IRI Condition	Rutting Condition
D-5 I-15 40.70-43.80 2020 9K	2.45	97.3	37	0.13	Good	Good	Good	Good
D-5 I-15 89.412-92.191 2020 9K	2.35	94.82	62	0.3	Good	Good	Good	Fair
D-5 I-15 99.00-104.001 2020 9K	2.35	89.28	56	0.29	Good	Good	Good	Fair
D-5 SH-39 49.80-44.50 2020 9K	3.59	89.52	73	0.19	Fair	Good	Good	Good
D-4 SH-27 0.000-10.000 2020 9K	6.5	88.52	107	0.17	Very Poor	Good	Fair	Good
D-4 SH-27 19.445-22.000 2020 9K	6.04	89.82	95	0.2	Very Poor	Good	Good	Good
D-4 SH-27 MP 0.000 - MP 5.000 2020 9K	6.5	87.13	113	0.16	Very Poor	Good	Fair	Good
D-4 SH-27 MP 5.000 - MP 10.000 2020 9K	6.8	89.94	101	0.19	Very Poor	Good	Fair	Good
D-4 US-30 MP 249.000 - MP 253.101 2020 9K	4.48	82.88	84	0.25	Poor	Good	Good	Fair
D-4 US-93 MP 203.000 - MP 208.000 2020 9K	4.32	100	193	0.27	Poor	Good	Poor	Fair
D-4 US-93 MP 208.000 - MP 211.201 2020 9K	4.66	100	193	0.27	Poor	Good	Poor	Fair
D-4 US-93 MP 211.300 - MP 216.201 2020 9K	4.93	100	201	0.25	Poor	Good	Poor	Fair
D-4 US-93 MP 216.300 - MP 221.201 2020 9K	3.21	100	151	0.24	Fair	Good	Fair	Fair
D-3 SH-55 MP 101.50 - MP 105.20 2020 9K	4.83	97.63	74	0.3	Fair	Good	Good	Fair
D-3 SH-55 MP 105.30 - MP 110.20 2020 9K	3.61	93.19	80	0.18	Fair	Good	Good	Good
D-3 SH-55 MP 110.30 - MP 114.00 2020 9K	2.89	98.51	56	0.17	Good	Good	Good	Good

Table 10.9 LLI vs. Pavement Performance

Pavement Site	LLI (mils)	OCI	IRI (inch/mile)	Rutting (in.)	Base/Lower Layer Condition	OCI Condition	IRI Condition	Rutting Condition
D-5 I-15 40.70-43.80 2020 9K	1.61	97.3	37	0.13	Sound	Good	Good	Good
D-5 I-15 89.412-92.191 2020 9K	1.24	94.82	62	0.3	Sound	Good	Good	Fair
D-5 I-15 99.00-104.001 2020 9K	1.46	89.28	56	0.29	Sound	Good	Good	Fair
D-5 SH-39 49.80-44.50 2020 9K	2.04	89.52	73	0.19	Sound	Good	Good	Good
D-4 SH-27 0.000-10.000 2020 9K	3.95	88.52	107	0.17	Warning	Good	Fair	Good
D-4 SH-27 19.445-22.000 2020 9K	3.4	89.82	95	0.2	Warning	Good	Good	Good
D-4 SH-27 MP 0.000 - MP 5.000 2020 9K	3.95	87.13	113	0.16	Warning	Good	Fair	Good
D-4 SH-27 MP 5.000 - MP 10.000 2020 9K	4.18	89.94	101	0.19	Warning	Good	Fair	Good
D-4 US-30 MP 249.000 - MP 253.101 2020 9K	2.22	82.88	84	0.25	Sound	Good	Good	Fair
D-4 US-93 MP 203.000 - MP 208.000 2020 9K	2.06	100	193	0.27	Sound	Good	Poor	Fair
D-4 US-93 MP 208.000 - MP 211.201 2020 9K	2.34	100	193	0.27	Sound	Good	Poor	Fair
D-4 US-93 MP 211.300 - MP 216.201 2020 9K	2.46	100	201	0.25	Sound	Good	Poor	Fair
D-4 US-93 MP 216.300 - MP 221.201 2020 9K	1.74	100	151	0.24	Sound	Good	Fair	Fair
D-3 SH-55 MP 101.50 - MP 105.20 2020 9K	3.16	97.63	74	0.3	Warning	Good	Good	Fair
D-3 SH-55 MP 105.30 - MP 110.20 2020 9K	2.65	93.19	80	0.18	Warning	Good	Good	Good
D-3 SH-55 MP 110.30 - MP 114.00 2020 9K	2.13	98.51	56	0.17	Sound	Good	Good	Good

Table 10.10 W7 vs. Pavement Performance

Pavement Site	W7 (mils)	OCI	IRI (inch/mile)	Rutting (in.)	Subgrade Layer Condition	OCI Condition	IRI Condition	Rutting Condition
D-5 I-15 40.70-43.80 2020 9K	1.56	97.3	37	0.13	Fair	Good	Good	Good
D-5 I-15 89.412-92.191 2020 9K	1.35	94.82	62	0.3	Good	Good	Good	Fair
D-5 I-15 99.00-104.001 2020 9K	1.55	89.28	56	0.29	Fair	Good	Good	Fair
D-5 SH-39 49.80-44.50 2020 9K	2.53	89.52	73	0.19	Very Poor	Good	Good	Good
D-4 SH-27 0.000-10.000 2020 9K	2.41	88.52	107	0.17	Very Poor	Good	Fair	Good
D-4 SH-27 19.445-22.000 2020 9K	2.12	89.82	95	0.2	Poor	Good	Good	Good
D-4 SH-27 MP 0.000 - MP 5.000 2020 9K	2.41	87.13	113	0.16	Very Poor	Good	Fair	Good
D-4 SH-27 MP 5.000 - MP 10.000 2020 9K	2.95	89.94	101	0.19	Very Poor	Good	Fair	Good
D-4 US-30 MP 249.000 - MP 253.101 2020 9K	2.57	82.88	84	0.25	Very Poor	Good	Good	Fair
D-4 US-93 MP 203.000 - MP 208.000 2020 9K	2.2	100	193	0.27	Poor	Good	Poor	Fair
D-4 US-93 MP 208.000 - MP 211.201 2020 9K	2.12	100	193	0.27	Poor	Good	Poor	Fair
D-4 US-93 MP 211.300 - MP 216.201 2020 9K	1.91	100	201	0.25	Poor	Good	Poor	Fair
D-4 US-93 MP 216.300 - MP 221.201 2020 9K	1.03	100	151	0.24	Very Poor	Good	Fair	Fair
D-3 SH-55 MP 101.50 - MP 105.20 2020 9K	2.77	97.63	74	0.3	Very Poor	Good	Good	Fair
D-3 SH-55 MP 105.30 - MP 110.20 2020 9K	2.83	93.19	80	0.18	Very Poor	Good	Good	Good
D-3 SH-55 MP 110.30 - MP 114.00 2020 9K	2.31	98.51	56	0.17	Very Poor	Good	Good	Good

Appendix B FWD and TSD Correlations

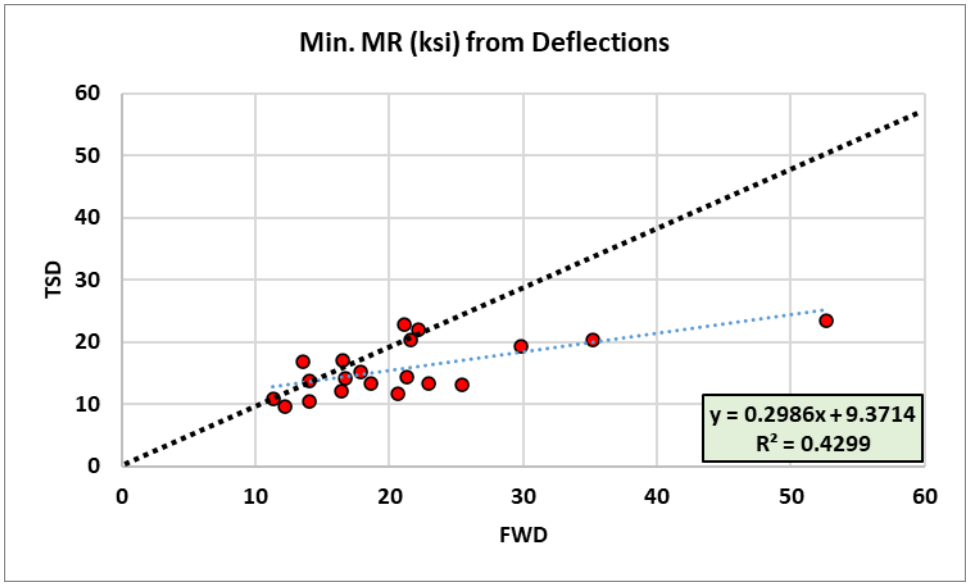

Figure 10.19 FWD vs. TSD Minimum MR values from Field Data (Uncorrected)

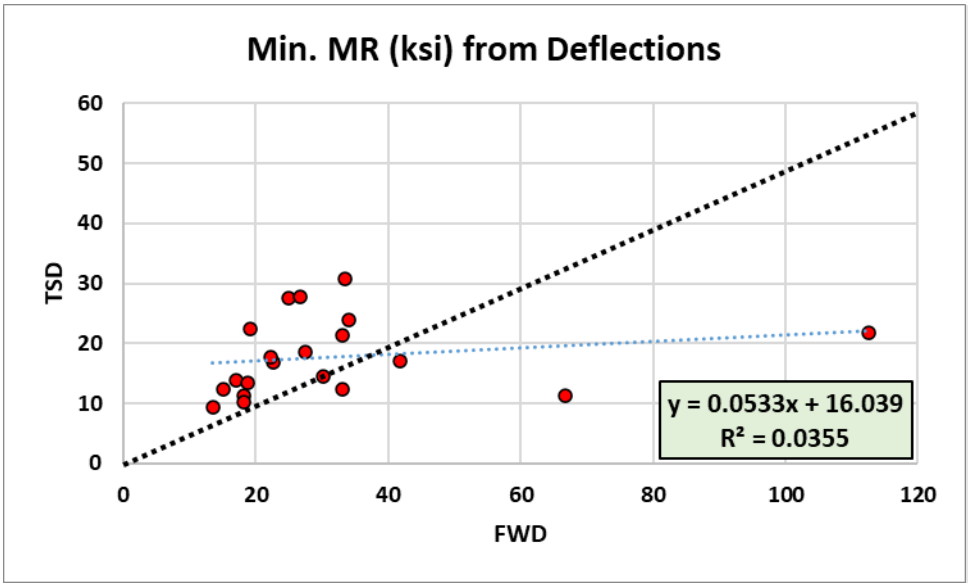

Figure 10.20 FWD vs. TSD Minimum MR values from Field Data (Corrected)

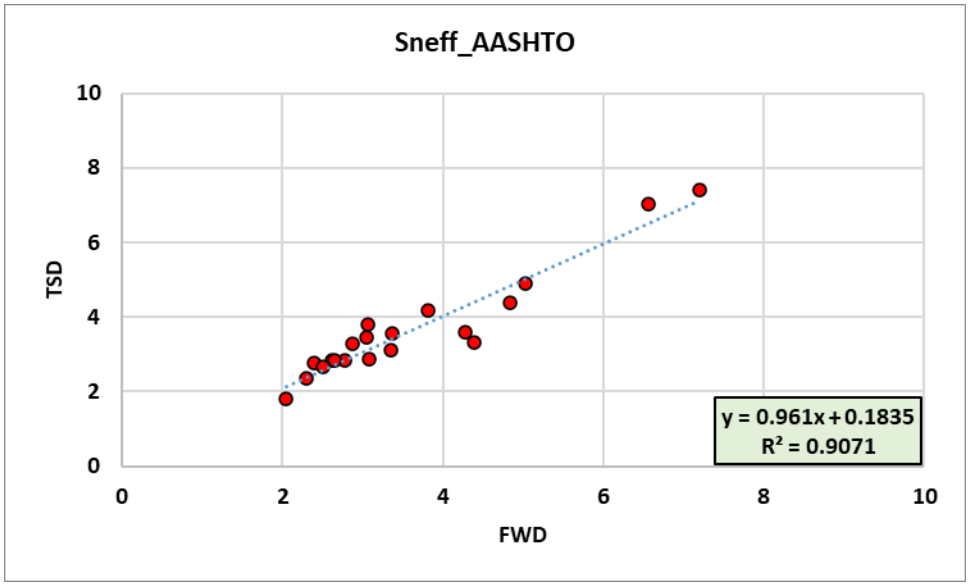

Figure 10.21 FWD vs. TSD SNeff (AASHTO) from Field Data (Uncorrected)

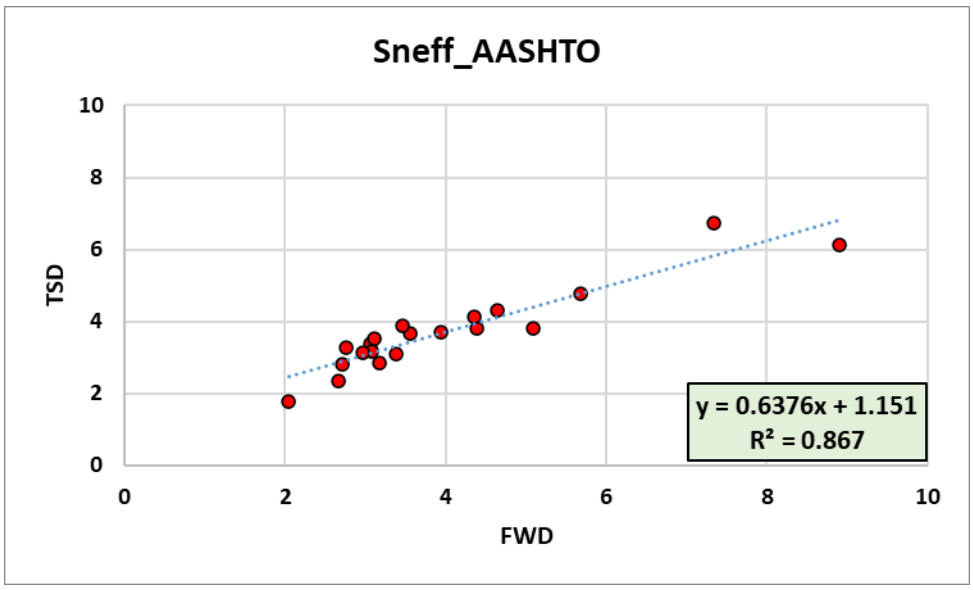

Figure 10.22 FWD vs. TSD SNeff (AASHTO) from Field Data (Corrected)

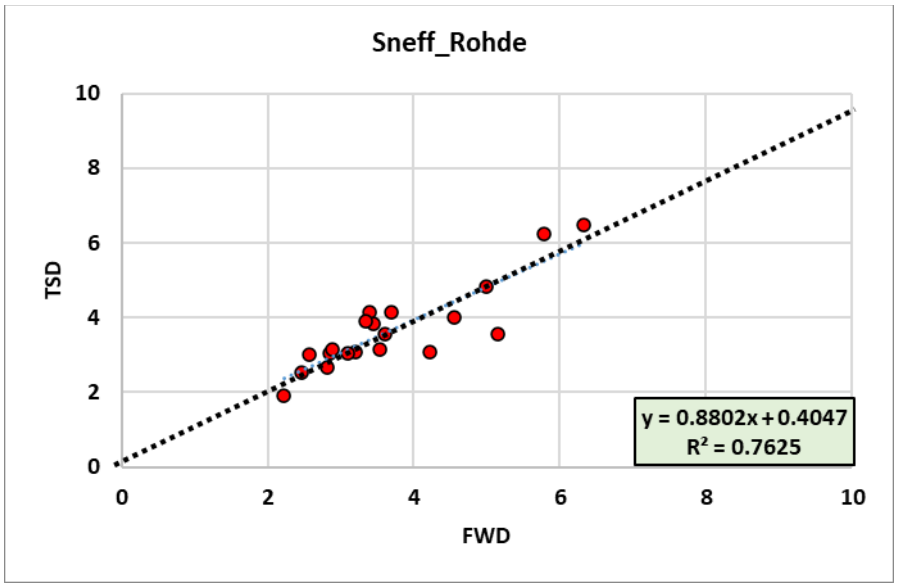

Figure 10.23 FWD vs. TSD SNeff (Rohde) from Field Data (Uncorrected)

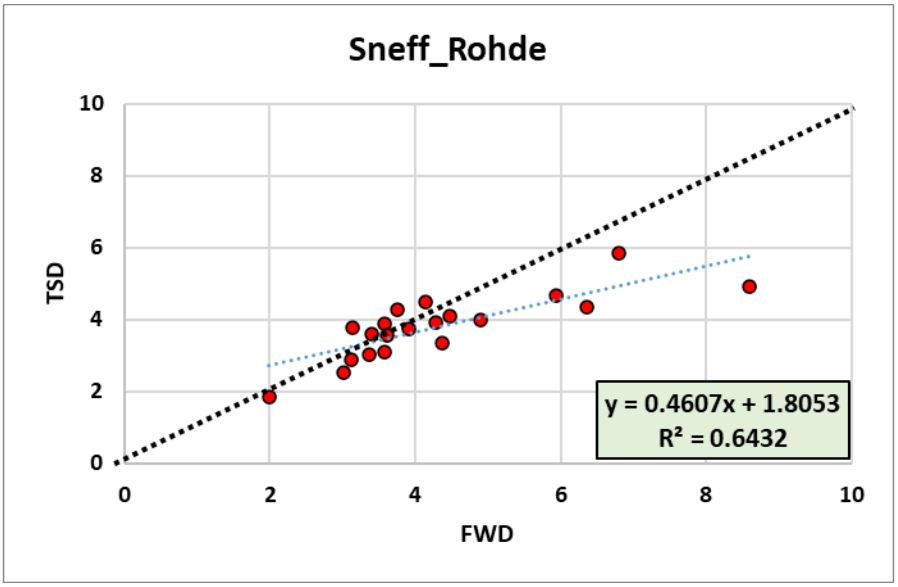

Figure 10.24 FWD vs. TSD SNeff (Rohde) from Field Data (Corrected)

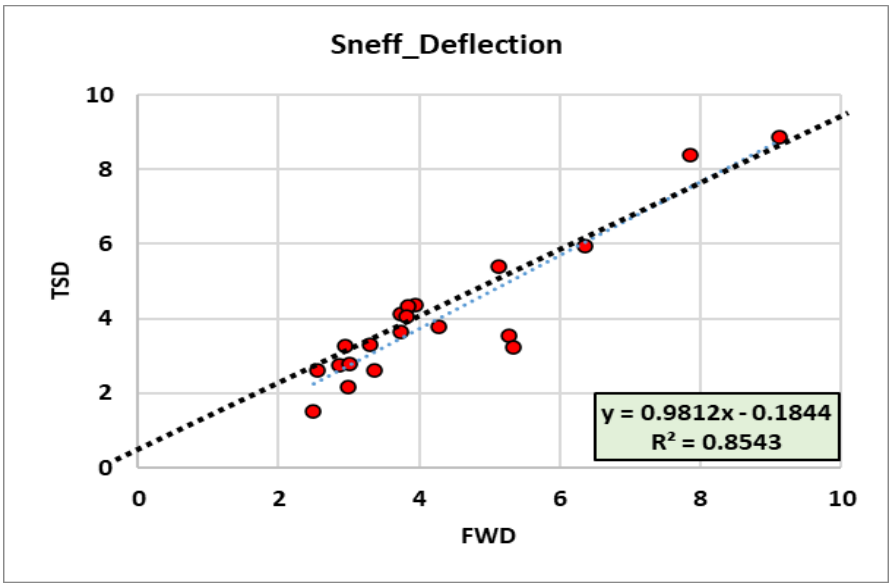

Figure 10.25 FWD vs. TSD SNeff (Defelction) from Field Data (Uncorrected)

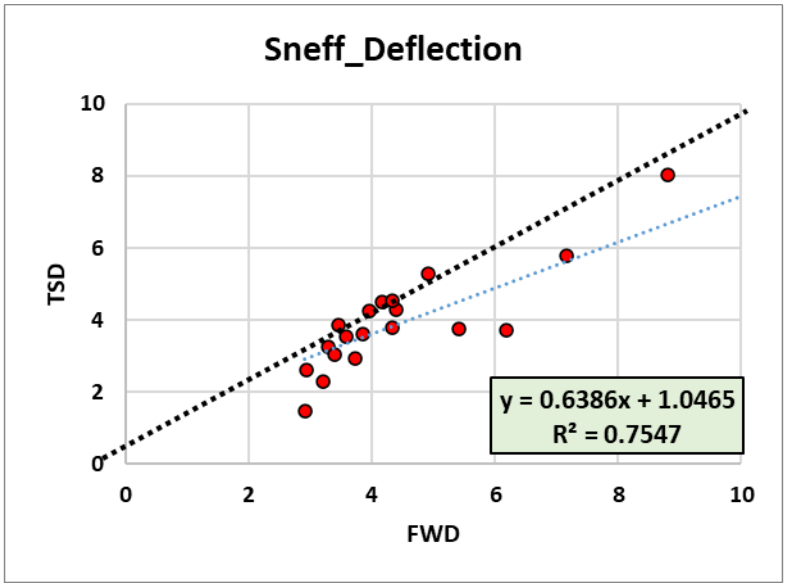

Figure 10.26 FWD vs. TSD SNeff (Defelction) from Field Data (Corrected)

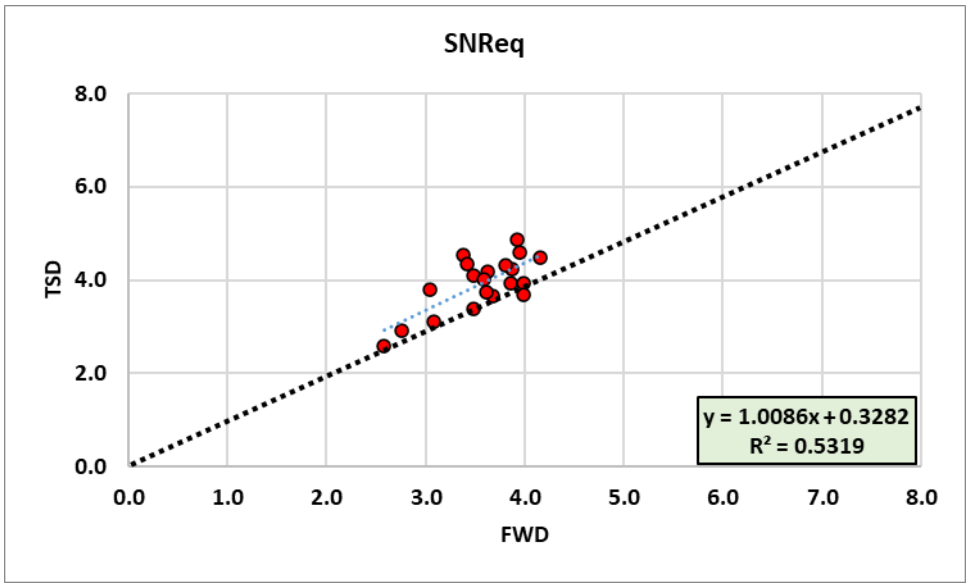

Figure 10.27 FWD vs. TSD SNReq from Field Data (Uncorrected)

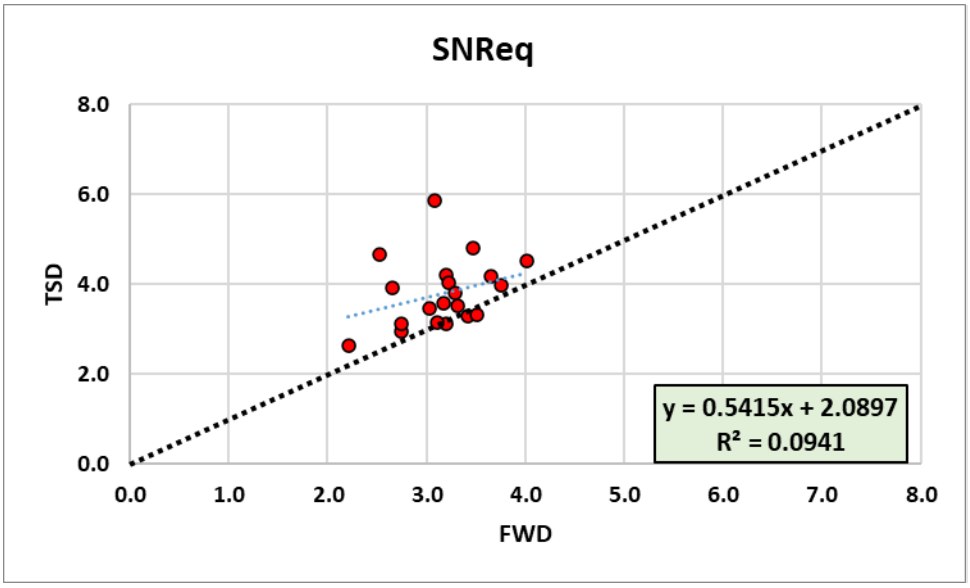

Figure 10.28 FWD vs. TSD SNReq from Field Data (Corrected)

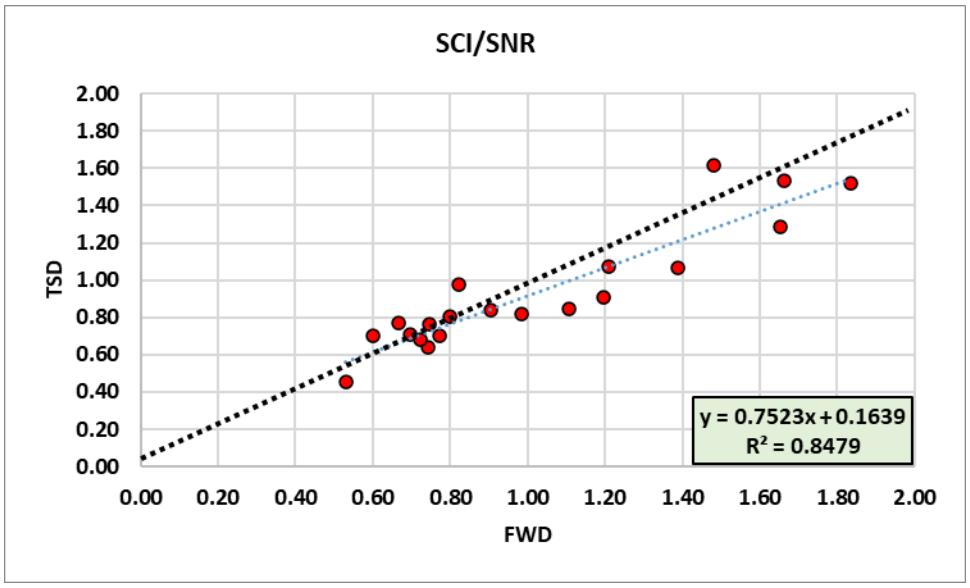

Figure 10.29 FWD vs. TSD SCI/SNR from Field Data (Uncorrected)

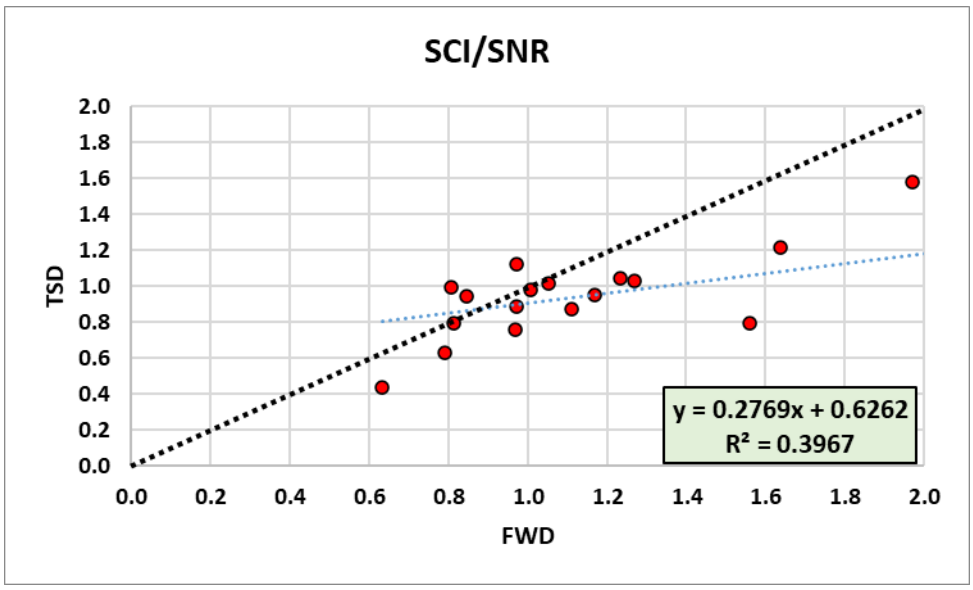

Figure 10.30 FWD vs. TSD SCI/SNR from Field Data (Corrected)

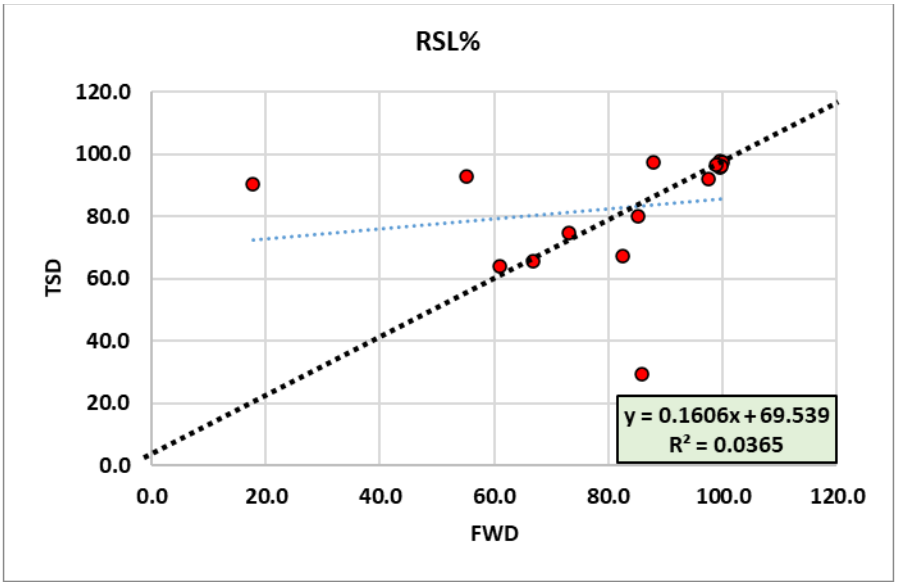

Figure 10.31 FWD vs. TSD RSL% from Field Data (Uncorrected)

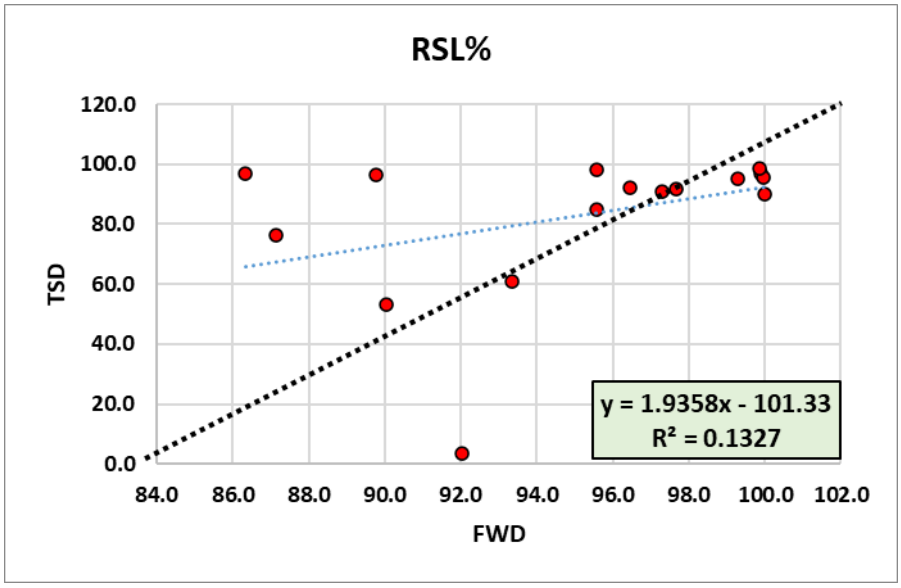

Figure 10.32 FWD vs. TSD RSL% from Field Data (Corrected)

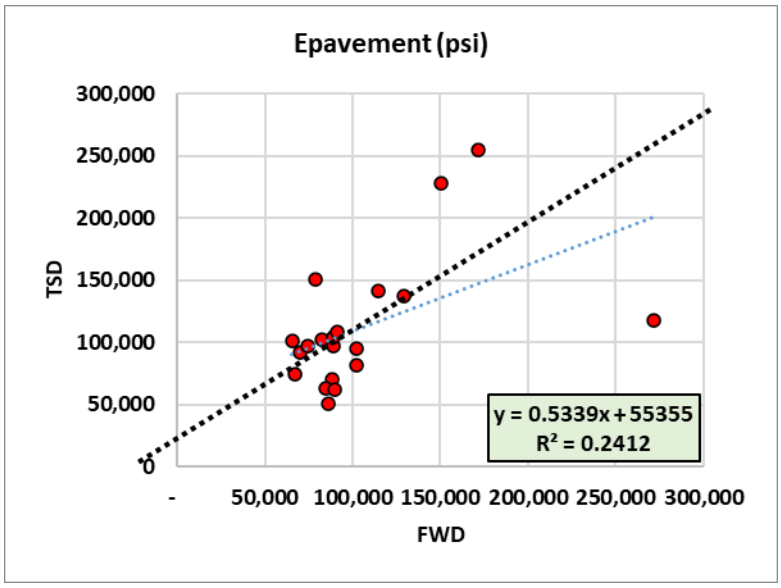

Figure 10.33 FWD vs. TSD EPavement from Field Data (Uncorrected)

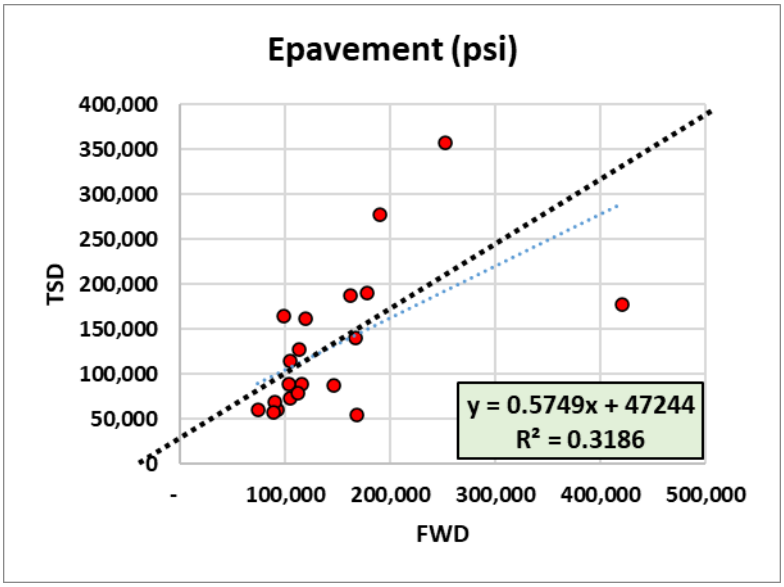

Figure 10.34 FWD vs. TSD EPavement from Field Data (Corrected)

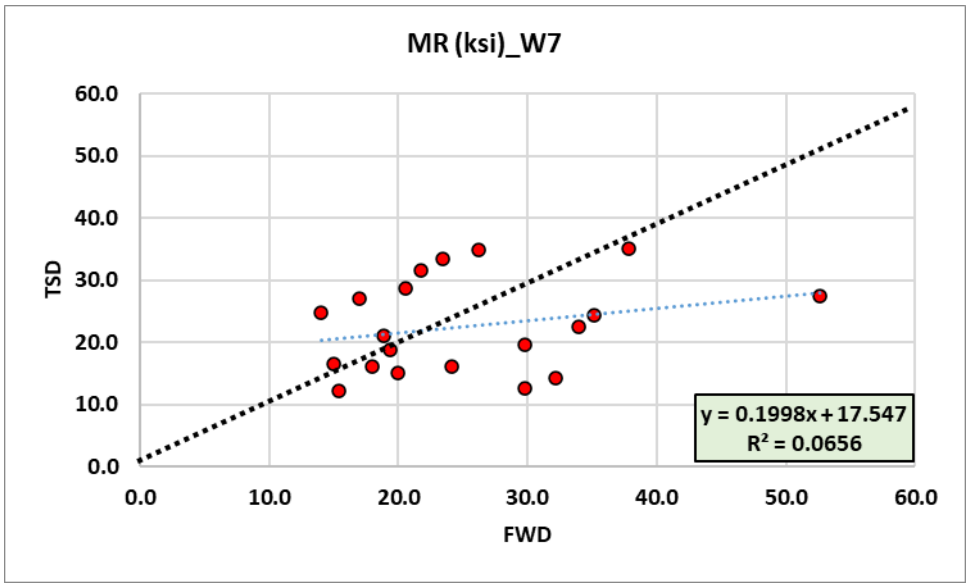

Figure 10.35 FWD vs. TSD MR based on W7 from Field Data (Uncorrected)

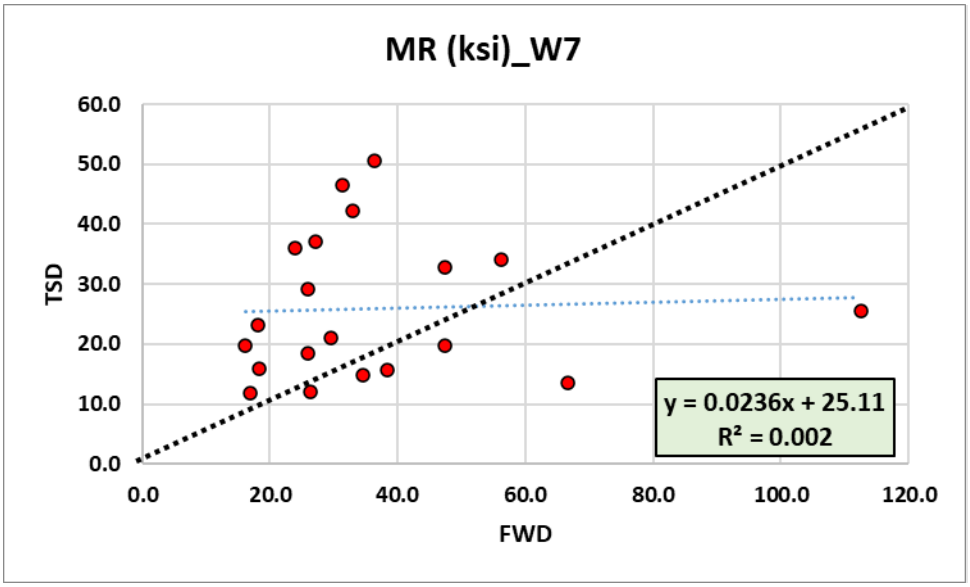

Figure 10.36 FWD vs. TSD MR based on W7 from Field Data (Corrected)

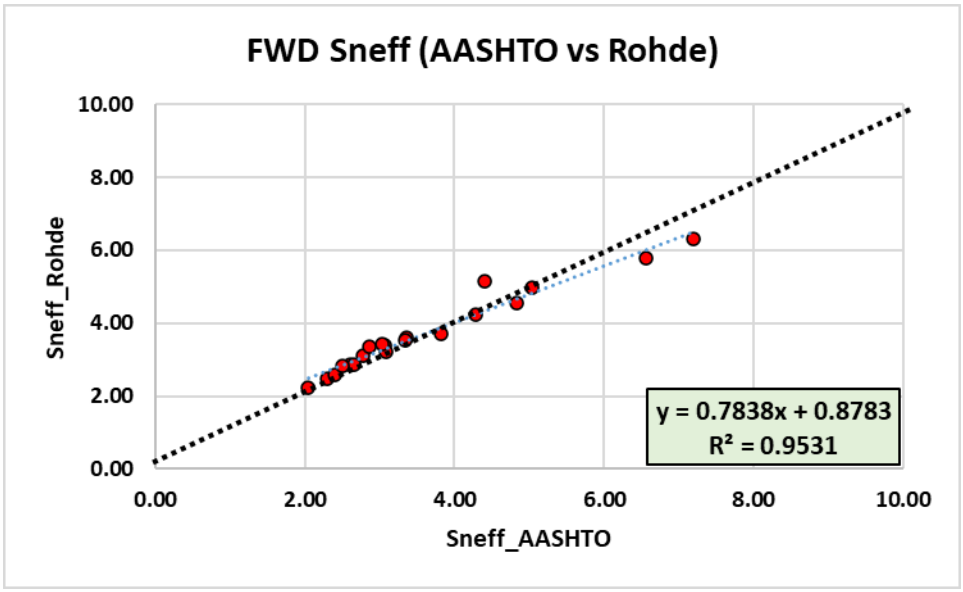

Figure 10.37 FWD SNeff (AASHTO vs. Rohde) from Field Data (Uncorrected)

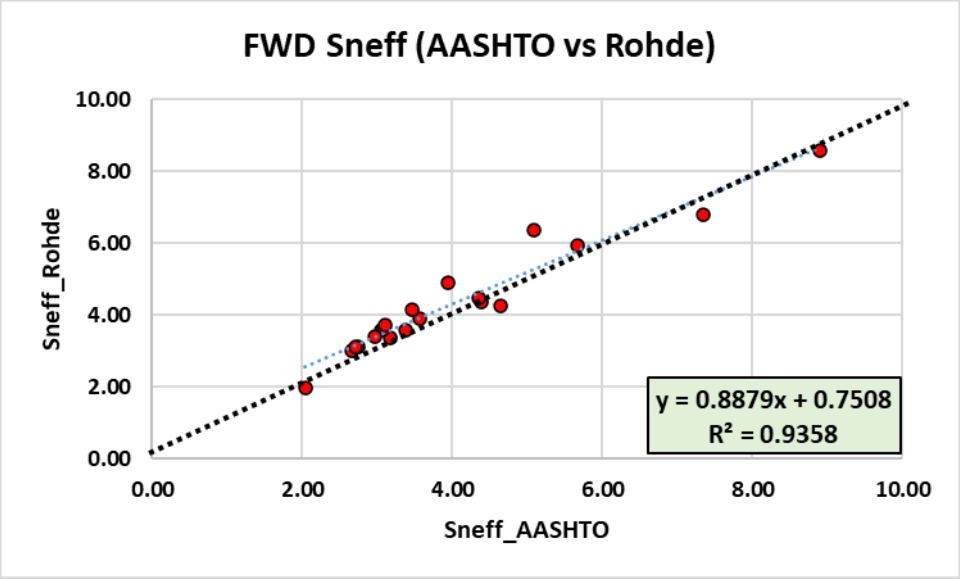

Figure 10.38 FWD SNeff (AASHTO vs. Rohde) from Field Data (Corrected)

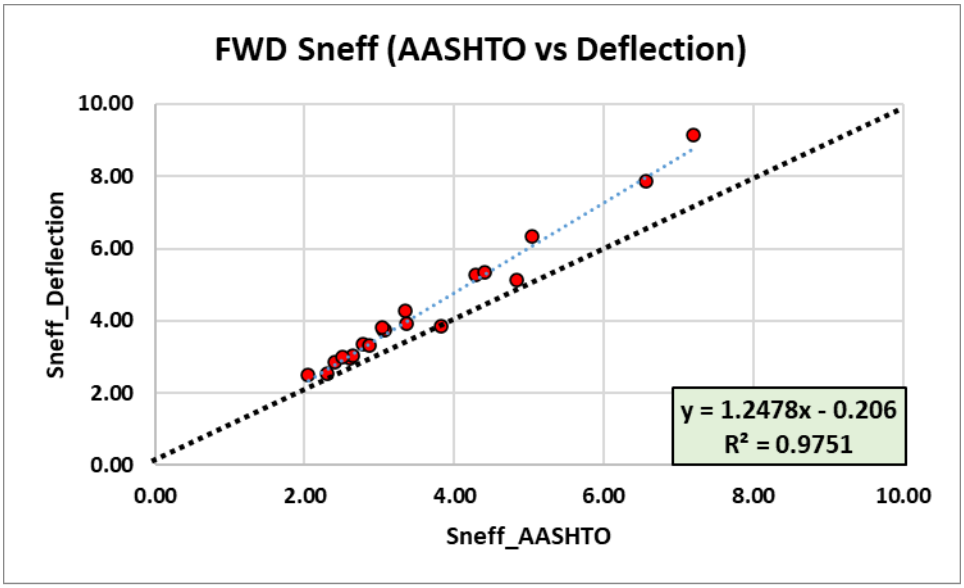

Figure 10.39 FWD SNeff (AASHTO vs. Deflection) from Field Data (Uncorrected)

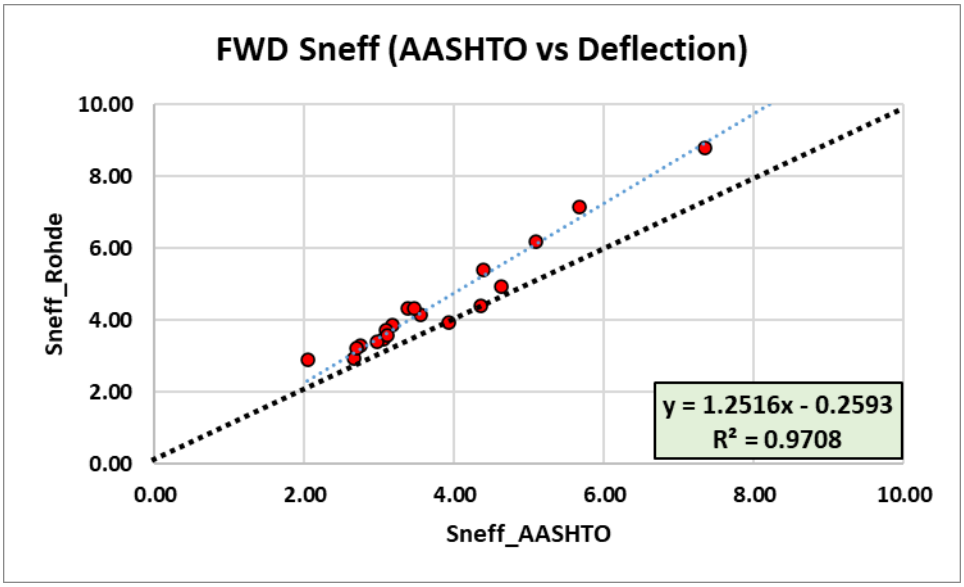

Figure 10.40 FWD SNeff (AASHTO vs. Deflection) from Field Data (Corrected)

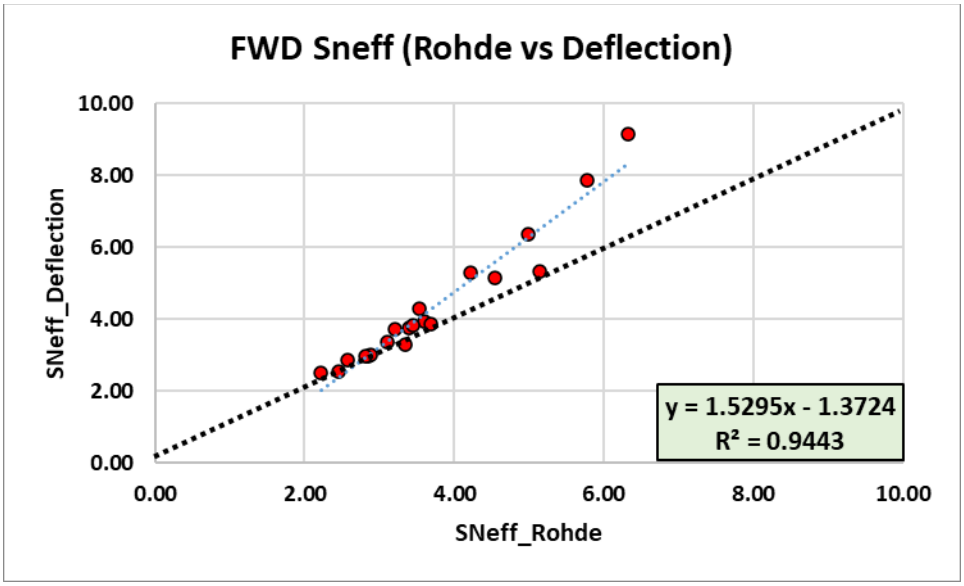

Figure 10.41 FWD SNeff (Rohde vs. Deflection) from Field Data (Uncorrected)

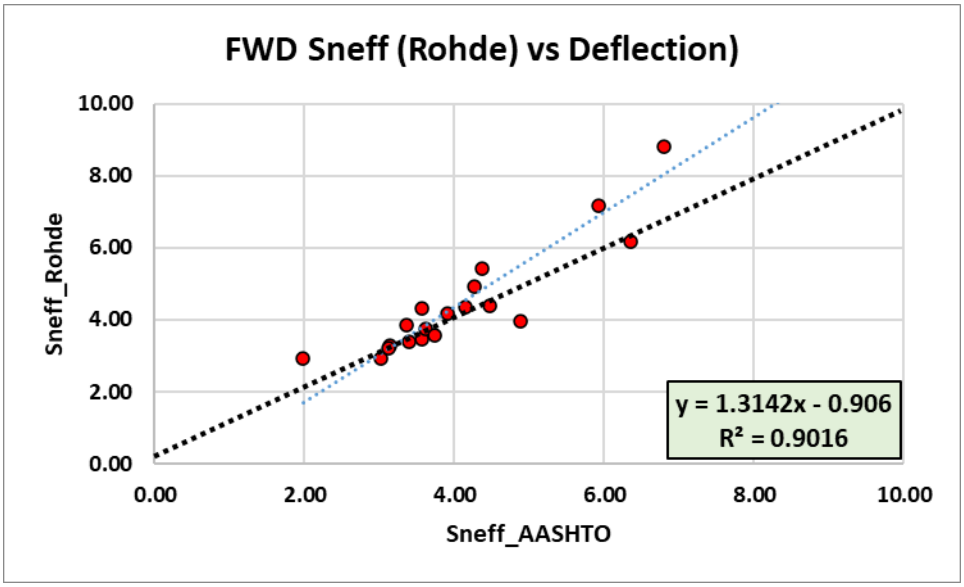

Figure 10.42 FWD SNeff (Rohde vs. Deflection) from Field Data (Corrected)

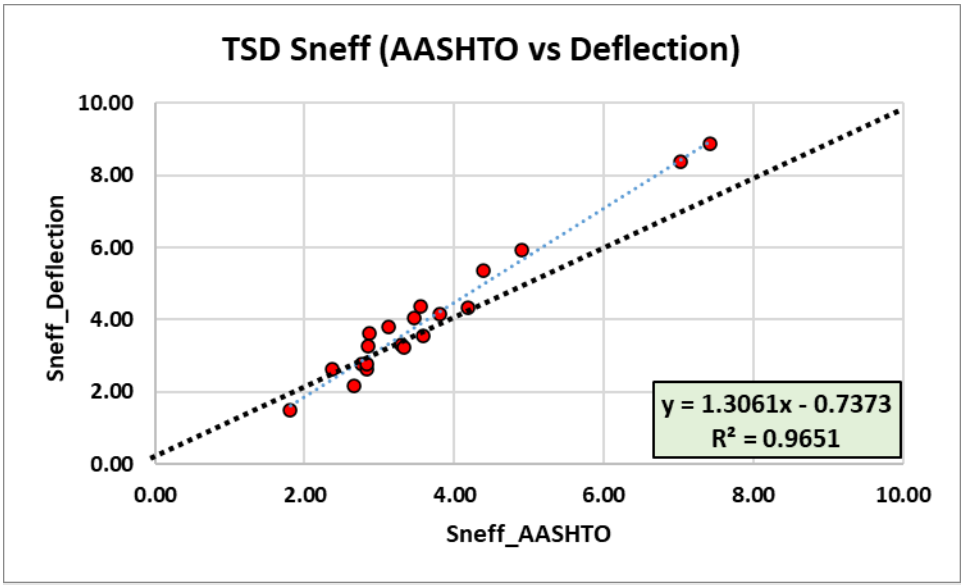

Figure 10.43 TSD SNeff (AASHTO vs. Deflection) from Field Data (Uncorrected)

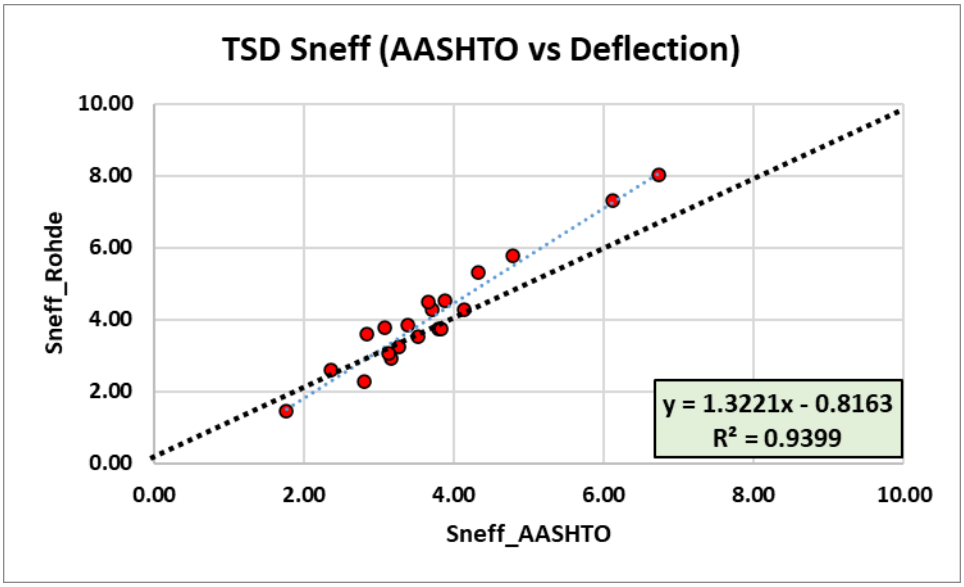

Figure 10.44 TSD SNeff (AASHTO vs. Deflection) from Field Data (Corrected)

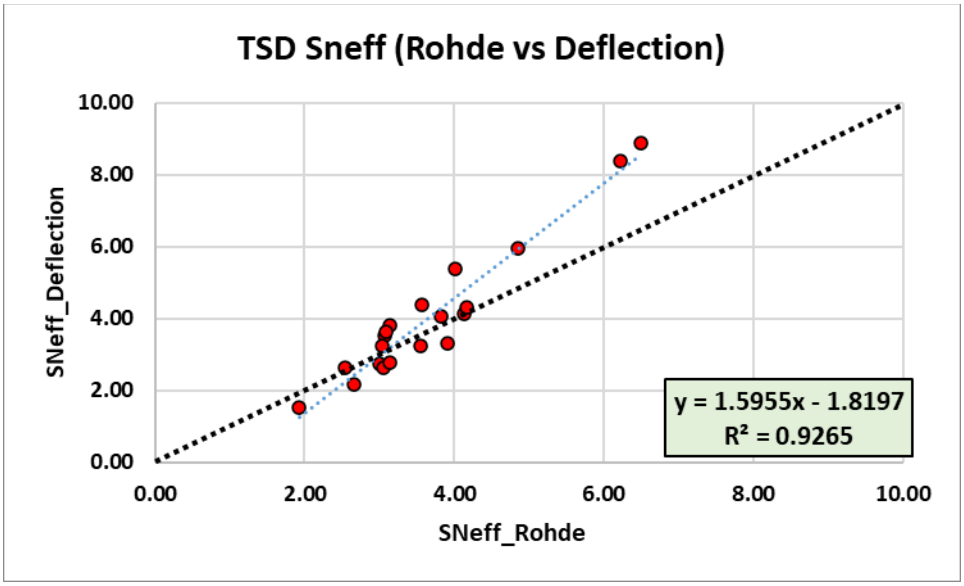

Figure 10.45 TSD SNeff (Rohde vs Deflection) from Field Data (Uncorrected)

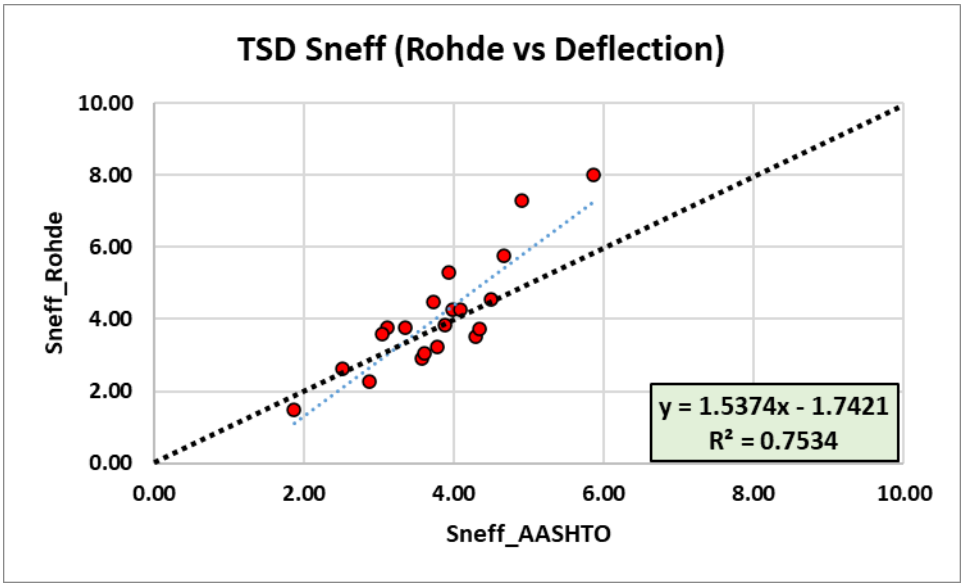

Figure 10.46 TSD SNeff (Rohde vs Deflection) from Field Data (Corrected)

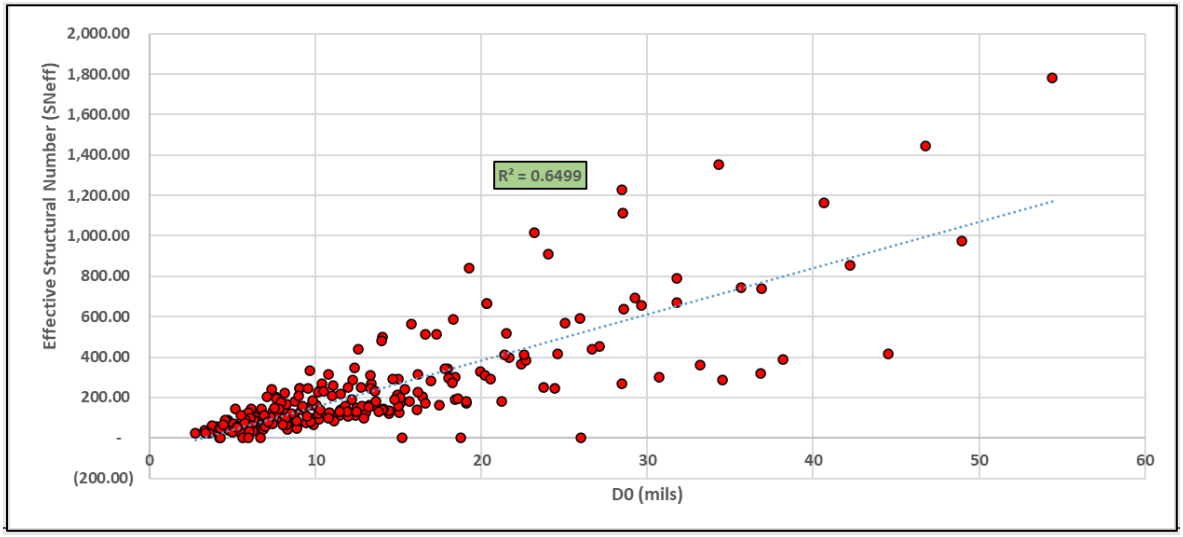

Figure 10.47 Effective Structural Number (SNeff) vs. Do (Parametric Study)

Appendix C Python Code Deflection Based Models

Random Forests Asphalt Layer Deformation Prediction Model Using Pavement ME FWD Deflection Data

```
import numpy as np

import matplotlib.pyplot as plt

import pandas as pd

import sklearn

from sklearn.ensemble import RandomForestRegressor

from sklearn.datasets import load_boston

from sklearn.datasets import make_regression

from sklearn.metrics import mean_squared_error

from sklearn.model_selection import train_test_split
```

```
from sklearn.preprocessing import scale

import matplotlib.pyplot as plt

from sklearn import set_config

from google.colab import files

uploaded = files.upload()

df =
pd.read_excel('/content/PavementME_FWD_RFResults.xlsx',sheet_name='Input_ACDeformatio
n')

#Importing the data

#If you edit the file and reupload make sure to erase the original file from the library

print(df.shape)

print(df)

df.dtypes

df.isnull().values.any()

#if true, make sure excel file has no formulas (copy as values)

target_column = ['AC_Deform']

traffic_column = ['Heavy_Trucks']

predictors = list(set(list(df.columns))-set(target_column))

unnormal = df.copy()

print(df[predictors])

df[predictors] = df[predictors]/df[predictors].max()

print(df[predictors])

#df.describe()
```

```
X = df[predictors].values

y = df[target_column].values

X_train, X_test, y_train, y_test = train_test_split(X, y, test_size=0.40, random_state=40)

print(X_test) #added this in

print(X_train.shape); print(X_test.shape)

set_config(print_changed_only=False)

 rfr = RandomForestRegressor()

print(rfr)

rfr.fit(X_train, y_train)

score = rfr.score(X_train, y_train)

print("R-squared:", score)

# Creating heat map for correlation study which will give us idea about study variables and their inter relationships

#color is correlation

import seaborn as sns

corr = df.corr()

sns.heatmap(corr,

        xticklabels=corr.columns.values,

        yticklabels=corr.columns.values)

y_pred = rfr.predict(X_test)

plt.figure(figsize=(10,10))

plt.scatter(y_test, y_pred, c='crimson')

plt.yscale('log')
```

```
plt.xscale('log')

p1 = max(max(y_pred), max(y_test))

p2 = min(min(y_pred), min(y_test))

plt.plot([p1, p2], [p1, p2], 'b-')

plt.xlabel('Pavement ME', fontsize=15)

plt.ylabel('Predictions', fontsize=15)

plt.axis('equal')

plt.show()

#make sure labels match with columns...should be same as initial randomization but double check by multiplying a number by the max value of that column in excel and see if it exists

dfr = pd.DataFrame(X_test)

dfr.columns = ['D0', 'Heavy_Trucks', 'Carnor', 'AUPP', 'SCI']

print(dfr)

dfr[predictors] = dfr[predictors]*unnormal[predictors].max()

dfr["AC Deform Pavement ME"] = y_test

dfr["AC Deform Predicted"] = y_pred

print(dfr)

dfr.to_csv('Deflection_FWD_ACDeform_Export_RF.csv')
```

Random Forests Total Deformation Prediction Model Using Pavement ME FWD Deflection Data

```
import numpy as np

import matplotlib.pyplot as plt

import pandas as pd
```

```
import sklearn
from sklearn.ensemble import RandomForestRegressor
from sklearn.datasets import load_boston
from sklearn.datasets import make_regression
from sklearn.metrics import mean_squared_error
from sklearn.model_selection import train_test_split
from sklearn.preprocessing import scale
import matplotlib.pyplot as plt
from sklearn import set_config
from google.colab import files
uploaded = files.upload()
df = pd.read_excel('/content/PavementME_FWD_RFResults.xlsx',sheet_name='Input_Rutting')
#Importing the data
#If you edit the file and reupload make sure to erase the original file from the library
print(df.shape)
print(df)
df.dtypes
df.isnull().values.any()
#if true, make sure excel file has no formulas (copy as values)
target_column = ['Rutting']
traffic_column = ['Heavy_Trucks']
predictors = list(set(list(df.columns))-set(target_column))
unnormal = df.copy()
```

```
print(df[predictors])

df[predictors] = df[predictors]/df[predictors].max()

print(df[predictors])

#df.describe()

X = df[predictors].values

y = df[target_column].values

X_train, X_test, y_train, y_test = train_test_split(X, y, test_size=0.40, random_state=40)

print(X_test) #added this in

print(X_train.shape); print(X_test.shape)

set_config(print_changed_only=False)

 rfr = RandomForestRegressor()

print(rfr)

rfr.fit(X_train, y_train)

score = rfr.score(X_train, y_train)

print("R-squared:", score)

# Creating heat map for correlation study which will give us idea about study variables and their inter relationships

#color is correlation

import seaborn as sns

corr = df.corr()

sns.heatmap(corr,

        xticklabels=corr.columns.values,

        yticklabels=corr.columns.values)
```

```
y_pred = rfr.predict(X_test)

plt.figure(figsize=(10,10))

plt.scatter(y_test, y_pred, c='crimson')

plt.yscale('log')

plt.xscale('log')

p1 = max(max(y_pred), max(y_test))

p2 = min(min(y_pred), min(y_test))

plt.plot([p1, p2], [p1, p2], 'b-')

plt.xlabel('Pavement ME', fontsize=15)

plt.ylabel('Predictions', fontsize=15)

plt.axis('equal')

plt.show()

#make sure labels match with columns...should be same as initial randomization but double check by multiplying a number by the max value of that column in excel and see if it exists

dfr = pd.DataFrame(X_test)

dfr.columns = ['Carnor', 'SCI', 'D0', 'Heavy_Trucks', 'AUPP']

print(dfr)

dfr[predictors] = dfr[predictors]*unnormal[predictors].max()

dfr["IRI Pavement ME"] = y_test

dfr["IRI Predicted"] = y_pred

print(dfr)

dfr.to_csv('Deflection_FWD_Rutting_Export_RF.csv')
```

Random Forests IRI Prediction Model Using Pavement ME FWD Deflection Data

```
import numpy as np
import matplotlib.pyplot as plt
import pandas as pd
import sklearn
from sklearn.ensemble import RandomForestRegressor
from sklearn.datasets import load_boston
from sklearn.datasets import make_regression
from sklearn.metrics import mean_squared_error
from sklearn.model_selection import train_test_split
from sklearn.preprocessing import scale
import matplotlib.pyplot as plt
from sklearn import set_config
from google.colab import files
uploaded = files.upload()
df = pd.read_excel('/content/PavementME_FWD.xlsx',sheet_name='Input3_Test')
#Importing the data
#If you edit the file and reupload make sure to erase the original file from the library
print(df.shape)
print(df)
df.dtypes
df.isnull().values.any()
#if true, make sure excel file has no formulas (copy as values)
```

```
target_column = ['IRI']

traffic_column = ['Heavy_Trucks']

predictors = list(set(list(df.columns))-set(target_column))

unnormal = df.copy()

print(df[predictors])

df[predictors] = df[predictors]/df[predictors].max()

print(df[predictors])

#df.describe()

X = df[predictors].values

y = df[target_column].values

X_train, X_test, y_train, y_test = train_test_split(X, y, test_size=0.40, random_state=40)

print(X_test) #added this in

print(X_train.shape); print(X_test.shape)

set_config(print_changed_only=False)

 rfr = RandomForestRegressor()

print(rfr)

rfr.fit(X_train, y_train)

score = rfr.score(X_train, y_train)

print("R-squared:", score)

# Creating heat map for correlation study which will give us idea about study variables and their inter relationships

#color is correlation

import seaborn as sns
```

```
corr = df.corr()
sns.heatmap(corr,
        xticklabels=corr.columns.values,
        yticklabels=corr.columns.values)
y_pred = rfr.predict(X_test)
plt.figure(figsize=(10,10))
plt.scatter(y_test, y_pred, c='crimson')
plt.yscale('log')
plt.xscale('log')
p1 = max(max(y_pred), max(y_test))
p2 = min(min(y_pred), min(y_test))
plt.plot([p1, p2], [p1, p2], 'b-')
plt.xlabel('Pavement ME', fontsize=15)
plt.ylabel('Predictions', fontsize=15)
plt.axis('equal')
plt.show()
#make sure labels match with columns...should be same as initial randomization but double check by multiplying a number by the max value of that column in excel and see if it exists
dfr = pd.DataFrame(X_test)
dfr.columns = ['Heavy_Trucks', 'SCI', 'AUPP', 'Carnor', 'D0']
print(dfr)
dfr[predictors] = dfr[predictors]*unnormal[predictors].max()
dfr["IRI Pavement ME"] = y_test
```

```
dfr["IRI Predicted"] = y_pred

print(dfr)

dfr.to_csv('Deflection_FWD_IRI_Output3_Test_RF.csv')
```

Random Forests Bottom-Up Fatigue Cracking Prediction Model Using Pavement ME FWD Deflection Data

```
import numpy as np

import matplotlib.pyplot as plt

import pandas as pd

import sklearn

from sklearn.ensemble import RandomForestRegressor

from sklearn.datasets import load_boston

from sklearn.datasets import make_regression

from sklearn.metrics import mean_squared_error

from sklearn.model_selection import train_test_split

from sklearn.preprocessing import scale

import matplotlib.pyplot as plt

from sklearn import set_config

from google.colab import files

uploaded = files.upload()

df =
pd.read_excel('/content/PavementME_FWD_RFResults.xlsx',sheet_name='Input_BottomUpCracking')

#Importing the data

#If you edit the file and reupload make sure to erase the original file from the library
```

```
print(df.shape)

print(df)

df.dtypes

df.isnull().values.any()

#if true, make sure excel file has no formulas (copy as values)

target_column = ['Bottom-Up Cracking (%)']

traffic_column = ['Heavy_Trucks']

predictors = list(set(list(df.columns))-set(target_column))

unnormal = df.copy()

print(df[predictors])

df[predictors] = df[predictors]/df[predictors].max()

print(df[predictors])

#df.describe()

X = df[predictors].values

y = df[target_column].values

X_train, X_test, y_train, y_test = train_test_split(X, y, test_size=0.40, random_state=40)

print(X_test) #added this in

print(X_train.shape); print(X_test.shape)

set_config(print_changed_only=False)

 rfr = RandomForestRegressor()

print(rfr)

rfr.fit(X_train, y_train)

score = rfr.score(X_train, y_train)
```

```
print("R-squared:", score)

# Creating heat map for correlation study which will give us idea about study variables and their inter relationships

#color is correlation

import seaborn as sns

corr = df.corr()

sns.heatmap(corr,

        xticklabels=corr.columns.values,

        yticklabels=corr.columns.values)

y_pred = rfr.predict(X_test)

plt.figure(figsize=(10,10))

plt.scatter(y_test, y_pred, c='crimson')

plt.yscale('log')

plt.xscale('log')

p1 = max(max(y_pred), max(y_test))

p2 = min(min(y_pred), min(y_test))

plt.plot([p1, p2], [p1, p2], 'b-')

plt.xlabel('Pavement ME', fontsize=15)

plt.ylabel('Predictions', fontsize=15)

plt.axis('equal')

plt.show()

#make sure labels match with columns...should be same as initial randomization but double check by multiplying a number by the max value of that column in excel and see if it exists
```

```
dfr = pd.DataFrame(X_test)

dfr.columns = ['SCI', 'Carnor', 'D0', 'Heavy_Trucks', 'AUPP']

print(dfr)

dfr[predictors] = dfr[predictors]*unnormal[predictors].max()

dfr["Bottom-Up Cracking Pavement ME"] = y_test

dfr["Bottom-Up Cracking RF Predicted"] = y_pred

print(dfr)

dfr.to_csv('Deflection_FWD_BottomUpCracking_Export_RF.csv')
```

Random Forests Top-Down Fatigue Cracking Prediction Model Using Pavement ME FWD Deflection Data

```
import numpy as np

import matplotlib.pyplot as plt

import pandas as pd

import sklearn

from sklearn.ensemble import RandomForestRegressor

from sklearn.datasets import load_boston

from sklearn.datasets import make_regression

from sklearn.metrics import mean_squared_error

from sklearn.model_selection import train_test_split

from sklearn.preprocessing import scale

import matplotlib.pyplot as plt

from sklearn import set_config

from google.colab import files
```

```
uploaded = files.upload()

df =
pd.read_excel('/content/PavementME_FWD_RFResults.xlsx',sheet_name='Input_TopDownCracking')

#Importing the data

#If you edit the file and reupload make sure to erase the original file from the library

print(df.shape)

print(df)

df.dtypes

df.isnull().values.any()

#if true, make sure excel file has no formulas (copy as values)

target_column = ['TopDownCracking']

traffic_column = ['Heavy_Trucks']

predictors = list(set(list(df.columns))-set(target_column))

unnormal = df.copy()

print(df[predictors])

df[predictors] = df[predictors]/df[predictors].max()

print(df[predictors])

#df.describe()

X = df[predictors].values

y = df[target_column].values

X_train, X_test, y_train, y_test = train_test_split(X, y, test_size=0.40, random_state=40)

print(X_test) #added this in
```

```
print(X_train.shape); print(X_test.shape)

set_config(print_changed_only=False)

 rfr = RandomForestRegressor()

print(rfr)

rfr.fit(X_train, y_train)

score = rfr.score(X_train, y_train)

print("R-squared:", score)

# Creating heat map for correlation study which will give us idea about study variables and their inter relationships

#color is correlation

import seaborn as sns

corr = df.corr()

sns.heatmap(corr,

        xticklabels=corr.columns.values,

        yticklabels=corr.columns.values)

y_pred = rfr.predict(X_test)

plt.figure(figsize=(10,10))

plt.scatter(y_test, y_pred, c='crimson')

plt.yscale('log')

plt.xscale('log')

p1 = max(max(y_pred), max(y_test))

p2 = min(min(y_pred), min(y_test))

plt.plot([p1, p2], [p1, p2], 'b-')
```

```
plt.xlabel('Pavement ME', fontsize=15)

plt.ylabel('Predictions', fontsize=15)

plt.axis('equal')

plt.show()

#make sure labels match with columns...should be same as initial randomization but double check by multiplying a number by the max value of that column in excel and see if it exists

dfr = pd.DataFrame(X_test)

dfr.columns = ['Heavy_Trucks', 'SCI', 'AUPP', 'D0', 'Carnor']

print(dfr)

dfr[predictors] = dfr[predictors]*unnormal[predictors].max()

dfr["Top-Down Cracking Pavement ME"] = y_test

dfr["Top-Down Cracking RF Predicted"] = y_pred

print(dfr)

dfr.to_csv('Deflection_FWD_TopDownCracking_Export_RF.csv')
```

Random Forests Asphalt Layer Deformation Prediction Model Using Pavement ME TSD Deflection Data

```
import numpy as np

import matplotlib.pyplot as plt

import pandas as pd

import sklearn

from sklearn.ensemble import RandomForestRegressor

from sklearn.datasets import load_boston

from sklearn.datasets import make_regression
```

```
from sklearn.metrics import mean_squared_error

from sklearn.model_selection import train_test_split

from sklearn.preprocessing import scale

import matplotlib.pyplot as plt

from sklearn import set_config

from google.colab import files

uploaded = files.upload()

df =
pd.read_excel('/content/PavementME_TSD_RFResults.xlsx',sheet_name='Input_ACDeformatio
n')

#Importing the data

#If you edit the file and reupload make sure to erase the original file from the library

print(df.shape)

print(df)

df.dtypes

df.isnull().values.any()

#if true, make sure excel file has no formulas (copy as values)

target_column = ['ACDeformation']

traffic_column = ['Heavy_Trucks']

predictors = list(set(list(df.columns))-set(target_column))

unnormal = df.copy()

print(df[predictors])

df[predictors] = df[predictors]/df[predictors].max()
```

```
print(df[predictors])

#df.describe()

X = df[predictors].values

y = df[target_column].values

X_train, X_test, y_train, y_test = train_test_split(X, y, test_size=0.40, random_state=40)

print(X_test) #added this in

print(X_train.shape); print(X_test.shape)

set_config(print_changed_only=False)

rfr = RandomForestRegressor()

print(rfr)

rfr.fit(X_train, y_train)

score = rfr.score(X_train, y_train)

print("R-squared:", score)

y_pred = rfr.predict(X_test)

# Creating heat map for correlation study which will give us idea about study variables and their inter relationships

#color is correlation

import seaborn as sns

corr = df.corr()

sns.heatmap(corr,

        xticklabels=corr.columns.values,

        yticklabels=corr.columns.values)

plt.figure(figsize=(10,10))
```

```
plt.scatter(y_test, y_pred, c='crimson')

plt.yscale('log')

plt.xscale('log')

p1 = max(max(y_pred), max(y_test))

p2 = min(min(y_pred), min(y_test))

plt.plot([p1, p2], [p1, p2], 'b-')

plt.xlabel('Pavement ME', fontsize=15)

plt.ylabel('Predictions', fontsize=15)

plt.axis('equal')

plt.show()

#make sure labels match with columns...should be same as initial randomization but double check by multiplying a number by the max value of that column in excel and see if it exists

dfr = pd.DataFrame(X_test)

dfr.columns = ['SCI12',          'Heavy_Trucks',          'SCI8',  'AUPP', 'D0']

print(dfr)

dfr[predictors] = dfr[predictors]*unnormal[predictors].max()

dfr["AC Rutting Pavement ME"] = y_test

dfr["AC Rutting Predicted"] = y_pred

print(dfr)

dfr.to_csv('Deflection_TSD_ACRutting_Export_RF.csv')
```

Random Forests Total Deformation Prediction Model Using Pavement ME TSD Deflection Data

```
import numpy as np
```

```
import matplotlib.pyplot as plt
import pandas as pd
import sklearn
from sklearn.ensemble import RandomForestRegressor
from sklearn.datasets import load_boston
from sklearn.datasets import make_regression
from sklearn.metrics import mean_squared_error
from sklearn.model_selection import train_test_split
from sklearn.preprocessing import scale
import matplotlib.pyplot as plt
from sklearn import set_config
from google.colab import files
uploaded = files.upload()
df = pd.read_excel('/content/PavementME_TSD_RFResults.xlsx',sheet_name='Input_Rutting')
#Importing the data
#If you edit the file and reupload make sure to erase the original file from the library
print(df.shape)
print(df)
df.dtypes
df.isnull().values.any()
#if true, make sure excel file has no formulas (copy as values)
target_column = ['Rutting']
traffic_column = ['Heavy_Trucks']
```

```
predictors = list(set(list(df.columns))-set(target_column))

unnormal = df.copy()

print(df[predictors])

df[predictors] = df[predictors]/df[predictors].max()

print(df[predictors])

#df.describe()

X = df[predictors].values

y = df[target_column].values

X_train, X_test, y_train, y_test = train_test_split(X, y, test_size=0.40, random_state=40)

print(X_test) #added this in

print(X_train.shape); print(X_test.shape)

set_config(print_changed_only=False)

 rfr = RandomForestRegressor()

print(rfr)

rfr.fit(X_train, y_train)

score = rfr.score(X_train, y_train)

print("R-squared:", score)

y_pred = rfr.predict(X_test)

# Creating heat map for correlation study which will give us idea about study variables and their inter relationships

#color is correlation

import seaborn as sns

corr = df.corr()
```

```
sns.heatmap(corr,
        xticklabels=corr.columns.values,
        yticklabels=corr.columns.values)
plt.figure(figsize=(10,10))
plt.scatter(y_test, y_pred, c='crimson')
plt.yscale('log')
plt.xscale('log')
p1 = max(max(y_pred), max(y_test))
p2 = min(min(y_pred), min(y_test))
plt.plot([p1, p2], [p1, p2], 'b-')
plt.xlabel('Pavement ME', fontsize=15)
plt.ylabel('Predictions', fontsize=15)
plt.axis('equal')
plt.show()
#make sure labels match with columns...should be same as initial randomization but double check by multiplying a number by the max value of that column in excel and see if it exists
dfr = pd.DataFrame(X_test)
dfr.columns = ['SCI12',          'Heavy_Trucks',          'SCI8',  'AUPP', 'D0']
print(dfr)
dfr[predictors] = dfr[predictors]*unnormal[predictors].max()
dfr["Rutting Pavement ME"] = y_test
dfr["Rutting Predicted"] = y_pred
print(dfr)
```

```
dfr.to_csv('Deflection_TSD_Rutting_Export_RF.csv')
```

Random Forests IRI Prediction Model Using Pavement ME TSD Deflection Data

```
import numpy as np
import matplotlib.pyplot as plt
import pandas as pd
import sklearn
from sklearn.ensemble import RandomForestRegressor
from sklearn.datasets import load_boston
from sklearn.datasets import make_regression
from sklearn.metrics import mean_squared_error
from sklearn.model_selection import train_test_split
from sklearn.preprocessing import scale
import matplotlib.pyplot as plt
from sklearn import set_config
from google.colab import files
uploaded = files.upload()
df = pd.read_excel('/content/PavementME_TSD.xlsx',sheet_name='Input6_IRI')
#Importing the data
#If you edit the file and reupload make sure to erase the original file from the library
print(df.shape)
print(df)
df.dtypes
```

```
df.isnull().values.any()

#if true, make sure excel file has no formulas (copy as values)

target_column = ['IRI']

traffic_column = ['Heavy_Trucks']

predictors = list(set(list(df.columns))-set(target_column))

unnormal = df.copy()

print(df[predictors])

df[predictors] = df[predictors]/df[predictors].max()

print(df[predictors])

#df.describe()

X = df[predictors].values

y = df[target_column].values

X_train, X_test, y_train, y_test = train_test_split(X, y, test_size=0.40, random_state=40)

print(X_test) #added this in

print(X_train.shape); print(X_test.shape)

set_config(print_changed_only=False)

 rfr = RandomForestRegressor()

print(rfr)

rfr.fit(X_train, y_train)

score = rfr.score(X_train, y_train)

print("R-squared:", score)

y_pred = rfr.predict(X_test)
```

```
# Creating heat map for correlation study which will give us idea about study variables and their inter relationships

#color is correlation

import seaborn as sns

corr = df.corr()

sns.heatmap(corr,

        xticklabels=corr.columns.values,

        yticklabels=corr.columns.values)

plt.figure(figsize=(10,10))

plt.scatter(y_test, y_pred, c='crimson')

plt.yscale('log')

plt.xscale('log')

p1 = max(max(y_pred), max(y_test))

p2 = min(min(y_pred), min(y_test))

plt.plot([p1, p2], [p1, p2], 'b-')

plt.xlabel('Pavement ME', fontsize=15)

plt.ylabel('Predictions', fontsize=15)

plt.axis('equal')

plt.show()

#make sure labels match with columns...should be same as initial randomization but double check by multiplying a number by the max value of that column in excel and see if it exists

dfr = pd.DataFrame(X_test)

dfr.columns = ['SCI8',  'AUPP','Heavy_Trucks',          'D0', 'SCI12']
```

```
print(dfr)

dfr[predictors] = dfr[predictors]*unnormal[predictors].max()

dfr["IRI Pavement ME"] = y_test

dfr["IRI Predicted"] = y_pred

print(dfr)

dfr.to_csv('Deflection_TSD_IRI_Export6_RF.csv')
```

Random Forests Bottom-Up Fatigue Cracking Prediction Model Using Pavement ME TSD Deflection Data

```
import numpy as np

import matplotlib.pyplot as plt

import pandas as pd

import sklearn

from sklearn.ensemble import RandomForestRegressor

from sklearn.datasets import load_boston

from sklearn.datasets import make_regression

from sklearn.metrics import mean_squared_error

from sklearn.model_selection import train_test_split

from sklearn.preprocessing import scale

import matplotlib.pyplot as plt

from sklearn import set_config

from google.colab import files

uploaded = files.upload()
```

```
df =
pd.read_excel('/content/PavementME_TSD_RFResults.xlsx',sheet_name='Input_BottomUpCracking')

#Importing the data

#If you edit the file and reupload make sure to erase the original file from the library

print(df.shape)

print(df)

df.dtypes

df.isnull().values.any()

#if true, make sure excel file has no formulas (copy as values)

target_column = ['BottomUpCracking']

traffic_column = ['Heavy_Trucks']

predictors = list(set(list(df.columns))-set(target_column))

unnormal = df.copy()

print(df[predictors])

df[predictors] = df[predictors]/df[predictors].max()

print(df[predictors])

#df.describe()

X = df[predictors].values

y = df[target_column].values

X_train, X_test, y_train, y_test = train_test_split(X, y, test_size=0.40, random_state=40)

print(X_test) #added this in

print(X_train.shape); print(X_test.shape)
```

```
set_config(print_changed_only=False)

 rfr = RandomForestRegressor()

print(rfr)

rfr.fit(X_train, y_train)

score = rfr.score(X_train, y_train)

print("R-squared:", score)

y_pred = rfr.predict(X_test)

# Creating heat map for correlation study which will give us idea about study variables and their inter relationships

#color is correlation

import seaborn as sns

corr = df.corr()

sns.heatmap(corr,

        xticklabels=corr.columns.values,

        yticklabels=corr.columns.values)

plt.figure(figsize=(10,10))

plt.scatter(y_test, y_pred, c='crimson')

plt.yscale('log')

plt.xscale('log')

p1 = max(max(y_pred), max(y_test))

p2 = min(min(y_pred), min(y_test))

plt.plot([p1, p2], [p1, p2], 'b-')

plt.xlabel('Pavement ME', fontsize=15)
```

```
plt.ylabel('Predictions', fontsize=15)

plt.axis('equal')

plt.show()

#make sure labels match with columns...should be same as initial randomization but double check by multiplying a number by the max value of that column in excel and see if it exists

dfr = pd.DataFrame(X_test)

dfr.columns = ['Heavy_Trucks',          'SCI8',  'SCI12','AUPP', 'D0']

print(dfr)

dfr[predictors] = dfr[predictors]*unnormal[predictors].max()

dfr["Bottom Up Cracking Pavement ME"] = y_test

dfr["Bottom Up Cracking RF Predicted"] = y_pred

print(dfr)

dfr.to_csv('Deflection_TSD_BottomUpCracking_Export_RF.csv')
```

Random Forests Top-Down Fatigue Cracking Prediction Model Using Pavement ME TSD Deflection Data

```
import numpy as np

import matplotlib.pyplot as plt

import pandas as pd

import sklearn

from sklearn.ensemble import RandomForestRegressor

from sklearn.datasets import load_boston

from sklearn.datasets import make_regression

from sklearn.metrics import mean_squared_error
```

```
from sklearn.model_selection import train_test_split

from sklearn.preprocessing import scale

import matplotlib.pyplot as plt

from sklearn import set_config

from google.colab import files

uploaded = files.upload()

df =
pd.read_excel('/content/PavementME_TSD_RFResults.xlsx',sheet_name='Input_TopDownCrack
ing')

#Importing the data

#If you edit the file and reupload make sure to erase the original file from the library

print(df.shape)

print(df)

df.dtypes

df.isnull().values.any()

#if true, make sure excel file has no formulas (copy as values)

target_column = ['TopDownCracking']

traffic_column = ['Heavy_Trucks']

predictors = list(set(list(df.columns))-set(target_column))

unnormal = df.copy()

print(df[predictors])

df[predictors] = df[predictors]/df[predictors].max()

print(df[predictors])
```

```
#df.describe()

X = df[predictors].values

y = df[target_column].values

X_train, X_test, y_train, y_test = train_test_split(X, y, test_size=0.40, random_state=40)

print(X_test) #added this in

print(X_train.shape); print(X_test.shape)

set_config(print_changed_only=False)

 rfr = RandomForestRegressor()

print(rfr)

rfr.fit(X_train, y_train)

score = rfr.score(X_train, y_train)

print("R-squared:", score)

y_pred = rfr.predict(X_test)

# Creating heat map for correlation study which will give us idea about study variables and their inter relationships

#color is correlation

import seaborn as sns

corr = df.corr()

sns.heatmap(corr,

        xticklabels=corr.columns.values,

        yticklabels=corr.columns.values)

plt.figure(figsize=(10,10))

plt.scatter(y_test, y_pred, c='crimson')
```

```
plt.yscale('log')

plt.xscale('log')

p1 = max(max(y_pred), max(y_test))

p2 = min(min(y_pred), min(y_test))

plt.plot([p1, p2], [p1, p2], 'b-')

plt.xlabel('Pavement ME', fontsize=15)

plt.ylabel('Predictions', fontsize=15)

plt.axis('equal')

plt.show()

#make sure labels match with columns...should be same as initial randomization but double check by multiplying a number by the max value of that column in excel and see if it exists

dfr = pd.DataFrame(X_test)

dfr.columns = ['AUPP',          'Heavy_Trucks',          'D0',     'SCI8', 'SCI12']

print(dfr)

dfr[predictors] = dfr[predictors]*unnormal[predictors].max()

dfr["Top Down Cracking Pavement ME"] = y_test

dfr["Top Down Cracking RF Predicted"] = y_pred

print(dfr)

dfr.to_csv('Deflection_TSD_TopDownCracking_Export_RF.csv')
```

Random Forests HMA Modulus Back-Calculation Model Using Modulus 7 FWD Deflection Data

```
import numpy as np

import matplotlib.pyplot as plt
```

```
import pandas as pd

import sklearn

from sklearn.ensemble import RandomForestRegressor

from sklearn.datasets import load_boston

from sklearn.datasets import make_regression

from sklearn.metrics import mean_squared_error

from sklearn.model_selection import train_test_split

from sklearn.preprocessing import scale

import matplotlib.pyplot as plt

from sklearn import set_config

from google.colab import files

uploaded = files.upload()

df =
pd.read_excel('/content/PavementME_FWD_ModuliPrediction.xlsx',sheet_name='Input2_ACM
oduli')

#Importing the data

#If you edit the file and reupload make sure to erase the original file from the library

print(df.shape)

print(df)

df.dtypes

df.isnull().values.any()

#if true, make sure excel file has no formulas (copy as values)

target_column = ['AC_Moduli']
```

```
traffic_column = ['Heavy_Trucks']

predictors = list(set(list(df.columns))-set(target_column))

unnormal = df.copy()

print(df[predictors])

df[predictors] = df[predictors]/df[predictors].max()

print(df[predictors])

#df.describe()

X = df[predictors].values

y = df[target_column].values

X_train, X_test, y_train, y_test = train_test_split(X, y, test_size=0.40, random_state=40)

print(X_test) #added this in

print(X_train.shape); print(X_test.shape)

set_config(print_changed_only=False)

 rfr = RandomForestRegressor()

print(rfr)

rfr.fit(X_train, y_train)

score = rfr.score(X_train, y_train)

print("R-squared:", score)

# Creating heat map for correlation study which will give us idea about study variables and their inter relationships

#color is correlation

import seaborn as sns

corr = df.corr()
```

```
sns.heatmap(corr,
        xticklabels=corr.columns.values,
        yticklabels=corr.columns.values)
y_pred = rfr.predict(X_test)
plt.figure(figsize=(10,10))
plt.scatter(y_test, y_pred, c='crimson')
plt.yscale('log')
plt.xscale('log')
p1 = max(max(y_pred), max(y_test))
p2 = min(min(y_pred), min(y_test))
plt.plot([p1, p2], [p1, p2], 'b-')
plt.xlabel('Pavement ME', fontsize=15)
plt.ylabel('Predictions', fontsize=15)
plt.axis('equal')
plt.show()
#make sure labels match with columns...should be same as intitial randomization but double check by mutliplying a number by the max value of that column in excel and see if it exists
dfr = pd.DataFrame(X_test)
dfr.columns = ['D60', 'D36', 'AC_Thickness', 'D24', 'D12', 'D0']
print(dfr)
dfr[predictors] = dfr[predictors]*unnormal[predictors].max()
dfr["AC Moduli Pavement ME"] = y_test
dfr["AC Moduli RF Predicted"] = y_pred
```

```
print(dfr)

dfr.to_csv('Deflection_FWD_ACModuli_Test2_Export_RF.csv')
```

Random Forests Base Modulus Back-Calculation Model Using Modulus 7 FWD Deflection Data

```
import numpy as np

import matplotlib.pyplot as plt

import pandas as pd

import sklearn

from sklearn.ensemble import RandomForestRegressor

from sklearn.datasets import load_boston

from sklearn.datasets import make_regression

from sklearn.metrics import mean_squared_error

from sklearn.model_selection import train_test_split

from sklearn.preprocessing import scale

import matplotlib.pyplot as plt

from sklearn import set_config

from google.colab import files

uploaded = files.upload()

df =
pd.read_excel('/content/PavementME_FWD_ModuliPrediction.xlsx',sheet_name='Input2_Base
Moduli')

#Importing the data

#If you edit the file and reupload make sure to erase the original file from the library

print(df.shape)
```

```
print(df)

df.dtypes

df.isnull().values.any()

#if true, make sure excel file has no formulas (copy as values)

target_column = ['Base Moduli']

predictors = list(set(list(df.columns))-set(target_column))

unnormal = df.copy()

print(df[predictors])

df[predictors] = df[predictors]/df[predictors].max()

print(df[predictors])

#df.describe()

X = df[predictors].values

y = df[target_column].values

X_train, X_test, y_train, y_test = train_test_split(X, y, test_size=0.40, random_state=40)

print(X_test) #added this in

print(X_train.shape); print(X_test.shape)


set_config(print_changed_only=False)

 rfr = RandomForestRegressor()

print(rfr)

rfr.fit(X_train, y_train)

score = rfr.score(X_train, y_train)

print("R-squared:", score)
```

```
# Creating heat map for correlation study which will give us idea about study variables and their inter relationships

#color is correlation

import seaborn as sns

corr = df.corr()

sns.heatmap(corr,

        xticklabels=corr.columns.values,

        yticklabels=corr.columns.values)

y_pred = rfr.predict(X_test)

plt.figure(figsize=(10,10))

plt.scatter(y_test, y_pred, c='crimson')

plt.yscale('log')

plt.xscale('log')

p1 = max(max(y_pred), max(y_test))

p2 = min(min(y_pred), min(y_test))

plt.plot([p1, p2], [p1, p2], 'b-')

plt.xlabel('Pavement ME', fontsize=15)

plt.ylabel('Predictions', fontsize=15)

plt.axis('equal')

plt.show()

#make sure labels match with columns...should be same as intitial randomization but double check by mutliplying a number by the max value of that column in excel and see if it exists

dfr = pd.DataFrame(X_test)
```

```
dfr.columns = ['D0', 'D60', 'AC_Thickness', 'D36', 'Base_Thickness']

print(dfr)

dfr[predictors] = dfr[predictors]*unnormal[predictors].max()

dfr["Base Moduli Pavement ME"] = y_test

dfr["Base Moduli RF Predicted"] = y_pred

print(dfr)

dfr.to_csv('Deflection_FWD_BaseModuli_Test2_Export_RF.csv')
```

Random Forests Subgrade Modulus Back-Calculation Model Using Modulus 7 FWD Deflection Data

```
import numpy as np

import matplotlib.pyplot as plt

import pandas as pd

import sklearn

from sklearn.ensemble import RandomForestRegressor

from sklearn.datasets import load_boston

from sklearn.datasets import make_regression

from sklearn.metrics import mean_squared_error

from sklearn.model_selection import train_test_split

from sklearn.preprocessing import scale

import matplotlib.pyplot as plt

from sklearn import set_config

from google.colab import files
```

```
uploaded = files.upload()

df =
pd.read_excel('/content/PavementME_FWD_ModuliPrediction.xlsx',sheet_name='Input2_Subg
radeModuli')

#Importing the data

#If you edit the file and reupload make sure to erase the original file from the library

print(df.shape)

print(df)

df.dtypes

df.isnull().values.any()

#if true, make sure excel file has no formulas (copy as values)

target_column = ['Subgrade Moduli']

predictors = list(set(list(df.columns))-set(target_column))

unnormal = df.copy()

print(df[predictors])

df[predictors] = df[predictors]/df[predictors].max()

print(df[predictors])

#df.describe()

X = df[predictors].values

y = df[target_column].values

X_train, X_test, y_train, y_test = train_test_split(X, y, test_size=0.40, random_state=40)

print(X_test) #added this in

print(X_train.shape); print(X_test.shape)
```

```
set_config(print_changed_only=False)

 rfr = RandomForestRegressor()

print(rfr)

rfr.fit(X_train, y_train)

score = rfr.score(X_train, y_train)

print("R-squared:", score)

# Creating heat map for correlation study which will give us idea about study variables and their inter relationships

#color is correlation

import seaborn as sns

corr = df.corr()

sns.heatmap(corr,

        xticklabels=corr.columns.values,

        yticklabels=corr.columns.values)

y_pred = rfr.predict(X_test)


plt.figure(figsize=(10,10))

plt.scatter(y_test, y_pred, c='crimson')

plt.yscale('log')

plt.xscale('log')

p1 = max(max(y_pred), max(y_test))

p2 = min(min(y_pred), min(y_test))

plt.plot([p1, p2], [p1, p2], 'b-')
```

```
plt.xlabel('Pavement ME', fontsize=15)

plt.ylabel('Predictions', fontsize=15)

plt.axis('equal')

plt.show()

#make sure labels match with columns...should be same as initial randomization but double check by multiplying a number by the max value of that column in excel and see if it exists

dfr = pd.DataFrame(X_test)

dfr.columns = ['D0', 'D60', 'AC_Thickness', 'D36', 'Base_Thickness']

print(dfr)

dfr[predictors] = dfr[predictors]*unnormal[predictors].max()

dfr["Subgrade Moduli Pavement ME"] = y_test

dfr["Subgrade Moduli RF Predicted"] = y_pred

print(dfr)

dfr.to_csv('Deflection_FWD_SubgradeModuli_Test2_Export_RF.csv')
```

Random Forests HMA Modulus Back-Calculation Model Using Modulus 7 TSD Deflection Data

```
import numpy as np

import matplotlib.pyplot as plt

import pandas as pd

import sklearn

from sklearn.ensemble import RandomForestRegressor

from sklearn.datasets import load_boston
```

```
from sklearn.datasets import make_regression

from sklearn.metrics import mean_squared_error

from sklearn.model_selection import train_test_split

from sklearn.preprocessing import scale

import matplotlib.pyplot as plt

from sklearn import set_config

from google.colab import files

uploaded = files.upload()

df =
pd.read_excel('/content/COMBINED_3_FWD_MODULIPREDICTION.xlsx',sheet_name='INPUT_ALL_AC')

#Importing the data

#If you edit the file and reupload make sure to erase the original file from the library

print(df.shape)

print(df)

df.dtypes

df.isnull().values.any()

#if true, make sure excel file has no formulas (copy as values)

target_column = ['AC Moduli']

predictors = list(set(list(df.columns))-set(target_column))

unnormal = df.copy()

print(df[predictors])

df[predictors] = df[predictors]/df[predictors].max()
```

```
print(df[predictors])

#df.describe()

X = df[predictors].values

y = df[target_column].values

X_train, X_test, y_train, y_test = train_test_split(X, y, test_size=0.4, random_state=40)

print(X_test) #added this in

print(X_train.shape); print(X_test.shape)

set_config(print_changed_only=False)

 rfr = RandomForestRegressor()

print(rfr)

rfr.fit(X_train, y_train)

score = rfr.score(X_train, y_train)

print("R-squared:", score)

# Creating heat map for correlation study which will give us idea about study variables and their inter relationships

#color is correlation

import seaborn as sns

corr = df.corr()

sns.heatmap(corr,

        xticklabels=corr.columns.values,

        yticklabels=corr.columns.values)

y_pred = rfr.predict(X_test)

plt.figure(figsize=(10,10))
```

```
plt.scatter(y_test, y_pred, c='crimson')

plt.yscale('log')

plt.xscale('log')

p1 = max(max(y_pred), max(y_test))

p2 = min(min(y_pred), min(y_test))

plt.plot([p1, p2], [p1, p2], 'b-')

plt.xlabel('Pavement ME', fontsize=15)

plt.ylabel('Predictions', fontsize=15)

plt.axis('equal')

plt.show()

#make sure labels match with columns...should be same as intitial randomization but double check by mutliplying a number by the max value of that column in excel and see if it exists

dfr = pd.DataFrame(X_test)

dfr.columns = ['AC Thickness', 'D18', 'D24', 'D8', 'D0', 'Base Thickness', 'D12', 'D60', 'D36']

print(dfr)

dfr[predictors] = dfr[predictors]*unnormal[predictors].max()

dfr["AC Moduli Combined"] = y_test

dfr["AC Moduli RF Predicted"] = y_pred

print(dfr)

dfr.to_csv('FWDCOMBINED_3_ALL_ACModuli_Export_RF.csv')
```

Random Forests Base Modulus Back-Calculation Model Using Modulus 7 TSD Deflection Data

```
import numpy as np

import matplotlib.pyplot as plt

import pandas as pd

import sklearn

from sklearn.ensemble import RandomForestRegressor

from sklearn.datasets import load_boston

from sklearn.datasets import make_regression

from sklearn.metrics import mean_squared_error

from sklearn.model_selection import train_test_split

from sklearn.preprocessing import scale

import matplotlib.pyplot as plt

from sklearn import set_config

from google.colab import files

uploaded = files.upload()

df =
pd.read_excel('/content/COMBINED_3_FWD_MODULIPREDICTION.xlsx',sheet_name='INPUT_A
LL_BASE')

#Importing the data

#If you edit the file and reupload make sure to erase the original file from the library

print(df.shape)

print(df)

df.dtypes
```

```
df.isnull().values.any()

#if true, make sure excel file has no formulas (copy as values)

target_column = ['Base Moduli']

predictors = list(set(list(df.columns))-set(target_column))

unnormal = df.copy()

print(df[predictors])

df[predictors] = df[predictors]/df[predictors].max()

print(df[predictors])

#df.describe()

X = df[predictors].values

y = df[target_column].values

X_train, X_test, y_train, y_test = train_test_split(X, y, test_size=0.4, random_state=40)

print(X_test) #added this in

print(X_train.shape); print(X_test.shape)

set_config(print_changed_only=False)

 rfr = RandomForestRegressor()

print(rfr)

rfr.fit(X_train, y_train)

score = rfr.score(X_train, y_train)

print("R-squared:", score)

# Creating heat map for correlation study which will give us idea about study variables and their inter relationships

#color is correlation
```

```
import seaborn as sns

corr = df.corr()

sns.heatmap(corr,

        xticklabels=corr.columns.values,

        yticklabels=corr.columns.values)

y_pred = rfr.predict(X_test)

plt.figure(figsize=(10,10))

plt.scatter(y_test, y_pred, c='crimson')

plt.yscale('log')

plt.xscale('log')

p1 = max(max(y_pred), max(y_test))

p2 = min(min(y_pred), min(y_test))

plt.plot([p1, p2], [p1, p2], 'b-')

plt.xlabel('Pavement ME', fontsize=15)

plt.ylabel('Predictions', fontsize=15)

plt.axis('equal')

plt.show()

#make sure labels match with columns...should be same as intitial randomization but double check by mutliplying a number by the max value of that column in excel and see if it exists

dfr = pd.DataFrame(X_test)

dfr.columns = ['D18', 'Base Thickness', 'D12', 'D24', 'D0', 'AC Thickness', 'D36', 'D8', 'D60']

print(dfr)

dfr[predictors] = dfr[predictors]*unnormal[predictors].max()
```

```
dfr["Base Moduli Combined"] = y_test

dfr["Base Moduli RF Predicted"] = y_pred

print(dfr)

dfr.to_csv('FWDCOMBINED_3_ALL_BaseModuli_Export_RF.csv')
```

Random Forests Subgrade Modulus Back-Calculation Model Using Modulus 7 TSD Deflection Data

```
import numpy as np

import matplotlib.pyplot as plt

import pandas as pd

import sklearn

from sklearn.ensemble import RandomForestRegressor

from sklearn.datasets import load_boston

from sklearn.datasets import make_regression

from sklearn.metrics import mean_squared_error

from sklearn.model_selection import train_test_split

from sklearn.preprocessing import scale

import matplotlib.pyplot as plt

from sklearn import set_config

from google.colab import files

uploaded = files.upload()

df =
pd.read_excel('/content/COMBINED_3_FWD_MODULIPREDICTION.xlsx',sheet_name='INPUT_ALL_SUBGRADE')
```

```
#Importing the data
#If you edit the file and reupload make sure to erase the original file from the library
print(df.shape)
print(df)
df.dtypes
df.isnull().values.any()
#if true, make sure excel file has no formulas (copy as values)
target_column = ['Subgrade Moduli']
predictors = list(set(list(df.columns))-set(target_column))
unnormal = df.copy()
print(df[predictors])
df[predictors] = df[predictors]/df[predictors].max()
print(df[predictors])
#df.describe()
X = df[predictors].values
y = df[target_column].values
X_train, X_test, y_train, y_test = train_test_split(X, y, test_size=0.65, random_state=40)
print(X_test) #added this in
print(X_train.shape); print(X_test.shape)
set_config(print_changed_only=False)
 rfr = RandomForestRegressor()
print(rfr)
rfr.fit(X_train, y_train)
```

```
score = rfr.score(X_train, y_train)

print("R-squared:", score)

# Creating heat map for correlation study which will give us idea about study variables and their inter relationships

#color is correlation

import seaborn as sns

corr = df.corr()

sns.heatmap(corr,

        xticklabels=corr.columns.values,

        yticklabels=corr.columns.values)

y_pred = rfr.predict(X_test)

plt.figure(figsize=(10,10))

plt.scatter(y_test, y_pred, c='crimson')

plt.yscale('log')

plt.xscale('log')

p1 = max(max(y_pred), max(y_test))

p2 = min(min(y_pred), min(y_test))

plt.plot([p1, p2], [p1, p2], 'b-')

plt.xlabel('Pavement ME', fontsize=15)

plt.ylabel('Predictions', fontsize=15)

plt.axis('equal')

plt.show()
```

```
#make sure labels match with columns...should be same as intitial randomization but double check by mutliplying a number by the max value of that column in excel and see if it exists

dfr = pd.DataFrame(X_test)

dfr.columns = ['AC Thickness', 'D8', 'D18', 'D12', 'D36', 'Base Thickness', 'D0', 'D60', 'D24']

print(dfr)

dfr[predictors] = dfr[predictors]*unnormal[predictors].max()

dfr["Subgrade Moduli Combined"] = y_test

dfr["Subgrade Moduli RF Predicted"] = y_pred

print(dfr)

dfr.to_csv('FWDCOMBINED_3_ALL_SubgradeModuli_Export_RF.csv')
```